

55 11/30/85

ANALYTICA CHIMICA ACTA

International journal devoted to all branches of analytical chemistry

EDITORS

A. M. G. MACDONALD (Birmingham, Great Britain)

HARRY L. PARDUE (West Lafayette, IN, U.S.A.)

ALAN TOWNSHEND (Hull, Great Britain)

J. T. CLERC (Bern, Switzerland)

Editorial Advisers

F. C. Adams, Antwerp
H. Bergamin F², Piracicaba
G. den Boef, Amsterdam
A. M. Bond, Waurin Ponds
D. Dyrssen, Göteborg
J. W. Frazer, Livermore, CA
S. Gomisček, Ljubljana
S. R. Heller, Beltsville, MD
G. M. Hieftje, Bloomington, IN
J. Hoste, Ghent
A. Hulanicki, Warsaw
G. Johansson, Lund
D. C. Johnson, Ames, IA
P. C. Jurs, University Park, PA
J. Kragten, Amsterdam
D. E. Leyden, Fort Collins, CO
F. E. Lytle, West Lafayette, IN
D. L. Massart, Brussels
A. Mizuike, Nagoya
E. Munk, Tempe, AZ

M. Otto, Freiberg
E. Pungor, Budapest
J. P. Riley, Liverpool
J. Růžička, Copenhagen
D. E. Ryan, Halifax, N.S.
S. Sasaki, Toyohashi
J. Savory, Charlottesville, VA
W. D. Shults, Oak Ridge, TN
W. I. Stephen, Birmingham
M. Thompson, Toronto
G. Tölg, Schwäbisch Gmünd
W. E. van der Linden, Enschede
A. Walsh, Melbourne
H. Weisz, Freiburg i. Br.
P. W. West, Baton Rouge, LA
T. S. West, Aberdeen
J. B. Willis, Melbourne
E. Ziegler, Mülheim
Yu. A. Zolotov, Moscow

ANALYTICA CHIMICA ACTA

*International journal devoted to all branches of analytical chemistry
Revue internationale consacrée à tous les domaines de la chimie analytique
Internationale Zeitschrift für alle Gebiete der analytischen Chemie*

PUBLICATION SCHEDULE FOR 1985

	J	F	M	A	M	J	J	A	S	O	N	D
Analytica Chimica Acta	167	168	169	170/1 170/2	171	172	173	174	175	176	177	178/1 178/2

Scope. *Analytica Chimica Acta* publishes original papers, short communications, and reviews dealing with every aspect of modern chemical analysis both fundamental and applied.

Submission of Papers. Manuscripts (three copies) should be submitted as designated below for rapid and efficient handling:

Papers from the Americas to: Professor Harry L. Pardue, Department of Chemistry, Purdue University, West Lafayette IN 47907, U.S.A.

Papers from all other countries to: Dr. A. M. G. Macdonald, Department of Chemistry, The University, P.O. Box 363 Birmingham B15 2TT, England. Papers dealing particularly with computer techniques to: Professor J. T. Clerc Universität Bern, Pharmazeutisches Institut, Baltzerstrasse 5, CH-3012 Bern, Switzerland.

Submission of an article is understood to imply that the article is original and unpublished and is not being considered for publication elsewhere. Upon acceptance of an article by the journal, authors will be asked to transfer the copyright of the article to the publisher. This transfer will ensure the widest possible dissemination of information.

Information for Authors. Papers in English, French and German are published. There are no page charges. Manuscripts should conform in layout and style to the papers published in this Volume. Authors should consult Vol. 170 for detailed information. Reprints of this information are available from the Editors or from: Elsevier Editoria Services Ltd., Mayfield House, 256 Banbury Road, Oxford OX2 7DH (Great Britain).

Reprints. Fifty reprints will be supplied free of charge. Additional reprints (minimum 100) can be ordered. An order form containing price quotations will be sent to the authors together with the proofs of their article.

Advertisements. Advertisement rates are available from the publisher.

Subscriptions. Subscriptions should be sent to: Elsevier Science Publishers B.V., Journals Department, P.O. Box 211, 1000 AE Amsterdam, The Netherlands. Tel: 5803 911, Telex: 18582.

Publication. *Analytica Chimica Acta* appears in 12 volumes in 1985. The subscription for 1985 (Vols. 167–178) is Dfl. 2400.00 plus Dfl. 264.00 (p.p.h.) (total approx. US \$986.70). All earlier volumes (Vols. 1–166) except Vols. 23 and 28 are available at Dfl. 231.00 (US \$85.56), plus Dfl. 15.00 (US \$5.56) p.p.h., per volume.

Our p.p.h. (postage, packing and handling) charge includes surface delivery of all issues, except to subscribers in the U.S.A., Canada, Japan, Australia, New Zealand, P.R. China, India, Israel, South Africa, Malaysia, Singapore, South Korea, Taiwan, Pakistan, Hong Kong and Brazil who receive all issues by air delivery (S.A.L. — Surface Air Lifted) at no extra cost. For the rest of the world, airmail and S.A.L. charges are available upon request.

Claims for issues not received should be made within three months of publication of the issues. If not they cannot be honoured free of charge.

For further information, or a free sample copy of this or any other Elsevier Science Publishers journal, readers in the U.S.A. and Canada can contact the following address: Elsevier Science Publishing Co. Inc., Journal Information Center, 52 Vanderbilt Avenue, New York, NY 10017, U.S.A., Tel: (212) 916-1250.

© 1985, ELSEVIER SCIENCE PUBLISHERS B.V.

0003-2670/85/\$03.30

All rights reserved. No part of this publication may be reproduced, stored in a retrieval system or transmitted in any form or by any means, electronic, mechanical, photocopying, recording or otherwise, without the prior written permission of the publisher, Elsevier Science Publishers B.V., P.O. Box 330 1000 AH Amsterdam, The Netherlands. Upon acceptance of an article by the journal, the author(s) will be asked to transfer copyright of the article to the publisher. The transfer will ensure the widest possible dissemination of information.

Submission of an article for publication entails the author(s) irrevocable and exclusive authorization of the publisher to collect any sums or considerations for copying or reproduction payable by third parties (as mentioned in article 17 paragraph 2 of the Dutch Copyright Act of 1912 and in the Royal Decree of June 20, 1974 (S. 351) pursuant to article 16b of the Dutch Copyright Act of 1912) and/or to act in or out of Court in connection therewith.

Special regulations for readers in the U.S.A. — This journal has been registered with the Copyright Clearance Center, Inc. Consent is given for copying of articles for personal or internal use, or for the personal use of specific clients. This consent is given on the condition that the copier pays through the Center the per-copy fee for copying beyond that permitted by Sections 107 or 108 of the U.S. Copyright Law. The per-copy fee is stated in the code-line at the bottom of the first page of each article. The appropriate fee, together with a copy of the first page of the article, should be forwarded to the Copyright Clearance Center, Inc., 27 Congress Street, Salem, MA 01970, U.S.A. If no code-line appears, broad consent to copy has not been given and permission to copy must be obtained directly from the author(s). All articles published prior to 1980 may be copied for a per-copy fee of US \$ 2.25, also payable through the Center. This consent does not extend to other kinds of copying, such as for general distribution, resale, advertising and promotion purposes, or for creating new collective works. Special written permission must be obtained from the publisher for such copying.

ANALYTICA CHIMICA ACTA
VOL. 177 (1985)



ANALYTICA CHIMICA ACTA

International journal devoted to all branches of analytical chemistry

EDITORS

A. M. G. MACDONALD (Birmingham, Great Britain)

HARRY L. PARDUE (West Lafayette, IN, U.S.A.)

ALAN TOWNSHEND (Hull, Great Britain)

J. T. CLERC (Bern, Switzerland)

Editorial Advisers

F. C. Adams, Antwerp
H. Bergamin F², Piracicaba
G. den Boef, Amsterdam
A. M. Bond, Waurin Ponds
D. Dyrssen, Göteborg
J. W. Frazer, Livermore, CA
S. Gomisček, Ljubljana
S. R. Heller, Beltsville, MD
G. M. Hieftje, Bloomington, IN
J. Hoste, Ghent
A. Hulanicki, Warsaw
G. Johansson, Lund
D. C. Johnson, Ames, IA
P. C. Jurs, University Park, PA
J. Kragten, Amsterdam
D. E. Leyden, Fort Collins, CO
F. E. Lytle, West Lafayette, IN
D. L. Massart, Brussels
A. Mizuike, Nagoya
E. Munk, Tempe, AZ

M. Otto, Freiberg
E. Pungor, Budapest
J. P. Riley, Liverpool
J. Růžička, Copenhagen
D. E. Ryan, Halifax, N.S.
S. Sasaki, Toyohashi
J. Savory, Charlottesville, VA
W. D. Shults, Oak Ridge, TN
W. I. Stephen, Birmingham
M. Thompson, Toronto
G. Tölg, Schwäbisch Gmünd
W. E. van der Linden, Enschede
A. Walsh, Melbourne
H. Weisz, Freiburg i. Br.
P. W. West, Baton Rouge, LA
T. S. West, Aberdeen
J. B. Willis, Melbourne
E. Ziegler, Mülheim
Yu. A. Zolotov, Moscow



ELSEVIER Amsterdam-Oxford-New York-Tokyo

Anal. Chim. Acta, Vol. 177 (1985)

All rights reserved. No part of this publication may be reproduced, stored in a retrieval system or transmitted in any form or by any means, electronic, mechanical, photocopying, recording or otherwise, without the prior written permission of the publisher, Elsevier Science Publishers B.V., P.O. Box 330, 1000 AH Amsterdam, The Netherlands. Upon acceptance of an article by the journal, the author(s) will be asked to transfer copyright of the article to the publisher. The transfer will ensure the widest possible dissemination of information.

Submission of an article for publication entails the author(s) irrevocable and exclusive authorization of the publisher to collect any sums or considerations for copying or reproduction payable by third parties (as mentioned in article 17 paragraph 2 of the Dutch Copyright Act of 1912 and in the Royal Decree of June 20, 1974 (S. 351) pursuant to article 16b of the Dutch Copyright Act of 1912) and/or to act in or out of Court in connection therewith.

Special regulations for readers in the U.S.A. — This journal has been registered with the Copyright Clearance Center, Inc. Consent is given for copying of articles for personal or internal use, or for the personal use of specific clients. This consent is given on the condition that the copier pays through the Center the per-copy fee for copying beyond that permitted by Sections 107 or 108 of the U.S. Copyright Law. The per-copy fee is stated in the code-line at the bottom of the first page of each article. The appropriate fee together with a copy of the first page of the article, should be forwarded to the Copyright Clearance Center, Inc., 27 Congress Street, Salem, MA 01970, U.S.A. If no code-line appears, broad consent to copy has not been given and permission to copy must be obtained directly from the author(s). All articles published prior to 1980 may be copied for a per-copy fee of US \$ 2.25, also payable through the Center. This consent does not extend to other kinds of copying, such as for general distribution, resale, advertising and promotional purposes, or for creating new collective works. Special written permission must be obtained from the publisher for such copying.

PREDICTION OF PARTITION COEFFICIENTS IN TERNARY LIQUID-LIQUID SYSTEMS AS A FUNCTION OF THE PHASE SYSTEM COMPOSITION BY FACTOR ANALYSIS FOR CHROMATOGRAPHY

J. F. K. HUBER*, S. WELTE and G. REICH

Institute of Analytical Chemistry, University of Vienna, Waehringerstr. 38, A-1090 Vienna (Austria)

(Received 6th May 1985)

SUMMARY

The measured partition data of 26 steroids for six different compositions of ternary liquid-liquid systems consisting of 2,2,4-trimethylpentane, ethanol and water are used in calculations of partition data for new phase system compositions. It was possible to reproduce the original data and to verify new experimental data by this calculation with high accuracy. Calculations were done in three ways. In the first, non-linear regression of the partition coefficients as a function of the phase system composition was examined. With this classical approach it is possible to calculate the values of the partition coefficients, solute by solute, with good accuracy. In the second approach, principal component factor analysis was used. The phase system-specific factors for further phase system compositions were calculated with a non-linear regression of these factors on the phase system composition. In combination with the solute-specific factors, the values of the partition coefficients for all solutes in any phase system composition could be predicted with excellent accuracy. In the third approach, target transformation factor analysis was applied. A relationship between the partition coefficient and the phase system composition was established on the basis of either the phase system composition itself or a simple function of it. This method also gave very accurate predictions of known and unknown partition coefficients.

For optimization of the chromatographic separation of a given sample, it is necessary to know the dependence of the retention data of all constituents of the sample on the composition of the phase system. The measurement of this relationship for all solutes of the sample for all solvent systems of interest is not feasible in practice because of the high costs and time involved. Therefore, a method for the accurate prediction of partition coefficients, from which retention data can be easily derived, would be very helpful. A classical approach for prediction of partition coefficients is the curve fitting of known partition coefficients with the phase system composition. This must be done, however, for each solute of interest.

The application of factor analysis also enables the number of measurements of retention data to be reduced because it is possible to predict partition coefficients for various quantitative compositions of a phase system of given qualitative composition starting from a few measured values. The

information which is included in the liquid-liquid partition coefficient, can be divided into two parts, one of which depends on the phase system composition while the other part characterizes the nature of the solute. A growing number of applications of factor analysis in analytical chemistry have been presented in recent years. The applications are mainly to chromatography and spectroscopic methods, such as n.m.r. and mass spectroscopy. Factor analysis has also proved its usefulness for the analysis of mixtures. Several overviews of the theoretical background and analytical applications are available [1-4].

Factor analysis makes it possible to calculate the partition coefficients from additive terms. Each term is the product of two cofactors, one of which describes the phase system composition and the other the chemical nature of the solute. Partition coefficients for new phase system compositions can be predicted either by curve fitting of factors specific for the phase system composition (PCFA) or by rotating characteristic factors of the phase system to physically significant test vectors (TFA) [5]. The compound specific factors remain unchanged (PCFA) or must be rotated in agreement with the rotation of the factors specific for the phase system (TFA).

Factor analysis is a multivariate statistical method, which is used to reduce the dimensionality of multidimensional data and to show interdependences in the data set. In the execution of factor analysis, three steps are involved: (1) extraction of factors, (2) reduction of dimensionality, and (3) rotation of factors for interpretation. The flow chart in Fig. 1 shows the details of this method. The main equation in factor analysis is

$$z_{ik} = a_{i1}p_{k1} + a_{i2}p_{k2} + \dots + a_{ir}p_{kr} \quad (1)$$

or written as a matrix equation $Z = AP$. In Eqn. 1, z_{ik} is the partition coefficient of the solute, i , in the phase system, k , a_{in} is a cofactor depending on the solute, p_{kn} is a cofactor depending on the solvent system, $n = 1, 2, \dots, r$, r is the running number of factors, and r is the total number of factors needed to reproduce the original data with sufficient accuracy.

The values of one cofactor are called the factor loadings, the values of the other cofactor are called factor scores. The factor loadings and the factor scores should not be confused. In this work, the specific cofactors of the phase system are chosen as factor loadings, and the solute-dependent cofactors as the factor scores. Whether the factor loadings are chosen as solvent-specific and the factor scores as solute-specific or vice versa depends on the definition of the problem and is not of fundamental significance, because the main equation is invariant to a change of A and P . In the calculation, however, these two terms should not be confused. Once the assignment has been made, it cannot be changed without complete recalculation.

The use of factor analysis in the prediction of partition coefficients is physically justified by the theory of regular solutions from which an equation for the partition coefficients can be derived [6]. The logarithm of the

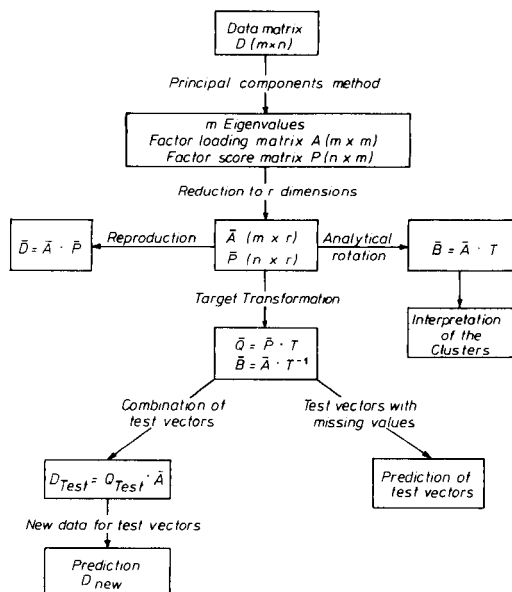


Fig. 1. Flow chart for calculations with factor analysis.

partition coefficient, K_{i0} , of a solute, i , at infinite dilution is given by

$$\ln(K_{i0}) = a_{i1}a_{k1} + a_{i2}a_{k2} \quad (2)$$

This expression is formally identical with Eqn. 1, setting $r = 2$. For nonregular solutions it must be expected that r must be made > 2 , in order to achieve the required accuracy.

The rotation of the factors is an important step for discovering interdependences in the data and is necessary for interpretation of the purely mathematical factors in terms of physical properties. Strictly mathematical approaches often fail in chemistry, because the hidden real properties (factors) are correlated, and the best rotation methods for obtaining interpretable factors are nonorthogonal rotations. Target transformation factor analysis can indicate some directions in space (test vectors) to which the rotation should go. By careful selection of these test vectors, it is possible to replace the abstract factors by physical data. In the present case, the physical data are the phase system compositions. The flow chart for the calculation of TFA is shown in Fig. 1.

EXPERIMENTAL

An experimental data set of partition coefficients of 26 steroids for six different compositions of a ternary liquid-liquid system consisting of water, ethanol and 2,2,4-trimethylpentane was used [7, 8]. The steroids are listed in Table 1; the phase system compositions are given in Table 2.

TABLE 1

List of solutes

1 Progesterone	16 14 α -Hydroxyandrost-4-ene-3,17-dione
2 20 β -Hydroxypregn-4-ene-3-one	17 16 α -Hydroxypregn-4-ene-3,20-dione
3 Androstenedione	18 17 α ,21-Dihydroxypregn-4-ene-3,20-dione
4 Androstadiene-(4,9(11))-3,17-dione	19 19-Hydroxyandrost-4-ene-3,17-dione
5 Methyltestosterone	20 Corticosterone
6 20 α -Hydroxypregn-4-ene-3-one	21 3,16 α ,17 α -Trihydroxyestratri-(1,3,5(10))-ene
7 Epitestosterone	22 11-Dehydrocorticosterone
8 Estrone	23 3,16 β ,17 β -Trihydroxyestratri-(1,3,5(10))-ene
9 Testosterone	24 Cortisone
10 17 α -Hydroxypregn-4-ene-3,20-dione	25 17 β ,21-Dihydroxypregn-4-ene-3,11,20-trione
11 11-Desoxycorticosterone	26 Cortisol
12 Andrenosterone	
13 11 β -Hydroxyandrost-4-ene-3,17-dione	
14 17 β -Hydroxyandrosta-1,4-diene-3-one	
15 Estratri-(1,3,5,(10))ene-3,17 β -diol	

TABLE 2

Phase system compositions

Phase system code number	Mole fractions					
	Water-rich phase			Water-poor phase		
	Water	Ethanol	2,2,4-Tri-methylpentane	Water	Ethanol	2,2,4-Tri-methylpentane
1	0.167	0.700	0.133	0.025	0.317	0.658
2	0.278	0.671	0.051	0.011	0.142	0.847
3	0.378	0.601	0.021	0.009	0.126	0.865
4	0.462	0.529	0.009	0.007	0.093	0.900
5	0.581	0.416	0.003	0.006	0.059	0.935
6	0.702	0.296	0.002	0.002	0.037	0.961

The calculations were done on the mainframe computer at the computing center of the University of Vienna. The computer is a Control Data CYBER 170-720 with 256K words of 60 bits, disk and tape storage. Access to this computer was established in a time-sharing mode through a dial-up telephone line.

For the nonlinear regression, programs were taken from the literature [9]; second-degree and third-degree polynomials were used. For the principal components factor analysis the SPSS program package was used [10]; the FAKTANAL program [11] was applied for the calculations in the target transformation factor analysis. A few additional programs for transforming the data formats, for transportation of results from one program to another, for displaying the results and for the calculation of the prediction errors were written in FORTRAN.

TABLE 3

Least-squares regression of the logarithm of the partition coefficients on the mole fraction of water in the more polar phase. Relative error for the prediction of the logarithm of the partition coefficient and the partition coefficient

Solute	Multiple correlation coefficient	Relative error (%)								
		Logarithm of partition coefficient			Partition coefficient					
		Mean value	RMS value	Mean value	RMS value	Mean value	RMS value			
Degree of polynomial										
		2	3	2	3	2	3			
1 Progesterone	0.994	0.999	1.95	0.48	2.21	0.58	3.59	1.01	4.11	1.29
2 20 β -Hydroxypregn-4-ene-3-one	0.965	0.994	4.15	1.40	4.79	1.74	10.92	4.07	13.14	5.19
3 Androstenedione	0.980	0.997	2.99	1.02	3.43	1.23	8.03	2.87	9.64	3.62
4 Androstadiene-(4,9(11))-3,17-dione	0.995	0.998	1.88	0.82	2.05	0.99	4.99	2.46	5.48	3.13
5 Methyltestosterone	0.992	0.998	2.48	1.24	2.96	1.35	6.76	3.79	7.78	4.27
6 20 α -Hydroxypregn-4-ene-3-one	0.988	0.999	3.24	0.64	3.58	0.68	9.16	1.96	9.62	2.13
7 Epitestosterone	0.998	0.998	0.98	0.97	1.21	1.22	3.22	3.10	4.01	3.96
8 Estrone	0.994	0.999	1.98	0.61	2.47	0.77	6.10	2.06	7.46	2.71
9 Testosterone	0.999	0.999	0.90	0.70	1.22	0.75	2.76	2.45	3.66	2.66
10 17 α -Hydroxypregn-4-ene-3,20-dione	0.999	1.000	0.90	0.53	1.15	0.59	2.92	1.90	3.54	2.14
11 11-Desoxycorticosterone	0.995	0.999	1.87	0.67	1.99	0.84	6.82	2.79	7.24	3.65
12 Androstosterone	0.999	1.000	1.02	0.36	1.12	0.42	3.84	1.53	4.08	1.91
13 11 β -Hydroxyandrost-4-ene-3,17-dione	0.997	0.999	1.51	0.57	1.72	0.64	6.12	2.40	7.38	2.77
14 17 β -Hydroxyandrost-1,4-diene-3-one	0.998	1.000	1.35	0.27	1.48	0.29	5.16	1.11	5.38	1.25
15 Estratri-(1,3,5,(10))ene-3,17 β -diol	0.992	1.000	2.43	0.41	2.79	0.50	9.62	1.86	10.97	2.33
16 14 α -Hydroxyandrost-4-ene-3,17-dione	0.999	0.999	1.06	0.87	1.45	1.09	4.15	3.87	5.50	4.90
17 16 α -Hydroxypregn-4-ene-3,20-dione	0.997	0.998	1.80	1.38	2.25	1.57	7.74	6.76	9.68	8.09
18 17 α ,21-Dihydroxypregn-4-ene-3,20-dione	0.996	0.999	2.27	0.76	2.41	0.97	10.81	4.30	11.36	5.68
19 19-Hydroxyandrost-4-ene-3,17-dione	0.995	0.999	2.57	0.71	2.77	0.87	11.84	3.95	12.26	5.12
20 Corticosterone	0.997	1.000	1.85	0.55	1.92	0.71	9.58	2.79	9.97	3.70
21 3,16 α ,17 α -Trihydroxyestratri-(1,3,5(10))-ene	0.995	1.000	2.44	0.39	2.83	0.49	11.86	1.99	12.93	2.53
22 11-Dehydrocorticosterone	0.998	1.000	1.70	0.28	1.99	0.34	8.26	1.54	9.34	1.96
23 3,16 β ,17 β -Trihydroxyestratri-(1,3,5(10))-ene	0.993	0.999	2.74	0.61	3.26	0.77	13.48	3.22	15.11	4.13
24 Cortisone	0.998	0.998	1.25	1.36	1.44	1.51	8.24	8.19	9.77	9.46
25 17 β ,21-Dihydroxypregn-4-ene-3,11,20-trione	0.998	0.999	1.15	1.23	1.40	1.41	7.57	7.13	9.44	7.97
26 Cortisol	0.999	1.000	1.20	0.41	1.28	0.52	7.68	2.48	8.29	3.08
Average error			1.91	0.74	2.20	0.88	7.35	3.14	8.35	3.83

TABLE 4

Least-squares regression of the partition coefficients on the mole fraction of water in the more polar phase

Solute	Multiple correlation coefficient		Partition coefficient				
			Relative error (%)				
			Mean value		RMS value		
	Degree of polynomial						
		2	3	2	3	2	3
1 Progesterone	0.987	0.997	5.41	2.30	6.51	2.49	
2 20 β -Hydroxypregn-4-ene-3-one	0.955	0.964	7.62	7.74	9.85	8.88	
3 Androstenedione	0.973	0.975	6.54	7.21	7.31	7.88	
4 Androstadiene-(4,9(11))-3,17-dione	0.991	0.995	6.15	3.28	8.10	4.05	
5 Methyltestosterone	0.992	0.999	6.61	1.40	9.27	1.59	
6 20 α -Hydroxypregn-4-ene-3-one	0.995	0.996	5.55	4.11	8.04	4.73	
7 Epitestosterone	0.964	0.997	14.88	3.02	17.51	3.73	
8 Estrone	0.991	0.996	8.87	3.17	12.14	3.46	
9 Testosterone	0.974	1.000	15.88	0.15	21.26	0.18	
10 17 α -Hydroxypregn-4-ene-3,20-dione	0.973	1.000	18.84	0.58	26.05	0.69	
11 11-Desoxycorticosterone	0.981	0.996	14.23	4.35	21.41	5.56	
12 Andrenosterone	0.971	1.000	23.90	1.29	35.94	1.62	
13 11 β -Hydroxyandrost-4-ene-3,17-dione	0.985	0.994	17.83	7.28	27.90	9.01	
14 17 β -Hydroxyandrost-1,4-diene-3-one	0.980	1.000	20.03	1.77	30.05	2.22	
15 Estratri-(1,3,5,(10))ene-3,17 β -diol	0.978	0.989	19.95	8.24	32.43	10.38	
16 14 α -Hydroxyandrost-4-ene-3,17-dione	0.944	0.998	71.32	11.29	125.0	16.91	
17 16 α -Hydroxypregn-4-ene-3,20-dione	0.938	0.989	64.14	17.08	114.6	25.26	
18 17 α ,21-Dihydroxypregn-4-ene-3,20-dione	0.974	0.996	51.23	4.98	94.6	5.70	
19 19-Hydroxyandrost-4-ene-3,17-dione	0.981	0.998	47.97	3.75	89.7	4.30	
20 Corticosterone	0.978	0.999	65.48	8.86	122.0	13.83	
21 3,16 α ,17 α -Trihydroxyestratri-(1,3,5(10))-ene	0.982	0.999	56.32	5.65	105.7	8.15	
22 11-Dehydrocorticosterone	0.962	0.997	86.06	6.10	162.4	8.33	
23 3,16 β ,17 β -Trihydroxyestratri-(1,3,5(10))-ene	0.983	0.997	50.18	6.89	94.28	9.70	
24 Cortisone	0.847	0.975	198.0	59.10	389.5	99.04	
25 17 β ,21-Dihydroxypregn-4-ene-3,11,20-trione	0.878	0.983	195.8	64.49	381.9	106.1	
26 Cortisol	0.881	0.986	323.9	93.17	656.3	160.0	
Average error			53.95	12.97	100.4	20.15	

The partition coefficients were measured as described in the literature [7, 8].

RESULTS AND DISCUSSION

Nonlinear regression of the partition coefficients with the phase system composition

The nonlinear regression of partition coefficients can be done with the partition coefficients themselves, or with their logarithms. The phase system composition was described by the mole fraction of water in the more polar phase. The results of this regression are given in Tables 3 and 4. Typical examples are shown in Figs. 2 and 3. It can be concluded that the fitting of the partition coefficients themselves is preferable to the fitting of the logarithms because the logarithm is a nonlinear transformation.

Regression of the factor loadings

With the principal components factor analysis, it is possible to extract simple factors from the data set. The eigenvectors of the data matrix are the factor loadings. The information content of the factor loadings decreases with the number of the factor. This is a property of the eigenvectors. Four factors were found to be sufficient to describe the given data matrix with the required accuracy. The flow chart for this calculation is shown in Fig. 4. The results of the regression of the four factors with the mole fraction of water in the more polar phase are given in Table 5. The regression curves are

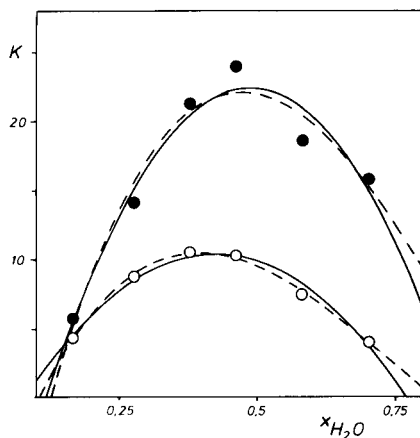
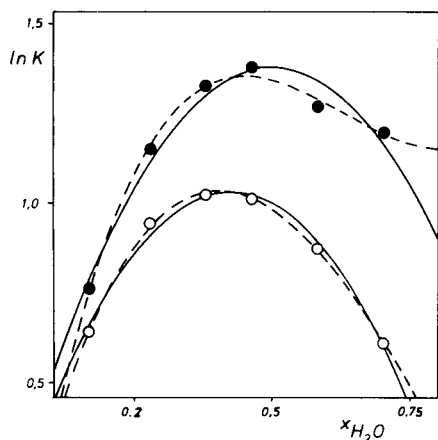


Fig. 2. Nonlinear regression of the logarithm of the partition coefficient for progesterone (\circ) and androstenedione (\bullet): (—) with a second-degree polynomial; (---) with a third-degree polynomial.

Fig. 3. Nonlinear regression of the partition coefficient for progesterone (\circ) and androstenedione (\bullet): (—) with a second-degree polynomial; (---) with a third-degree polynomial.

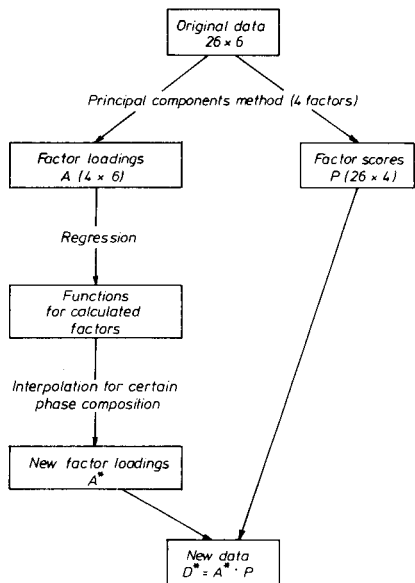


Fig. 4. Flow chart for the prediction of partition coefficients with curve fitting of the factor loadings.

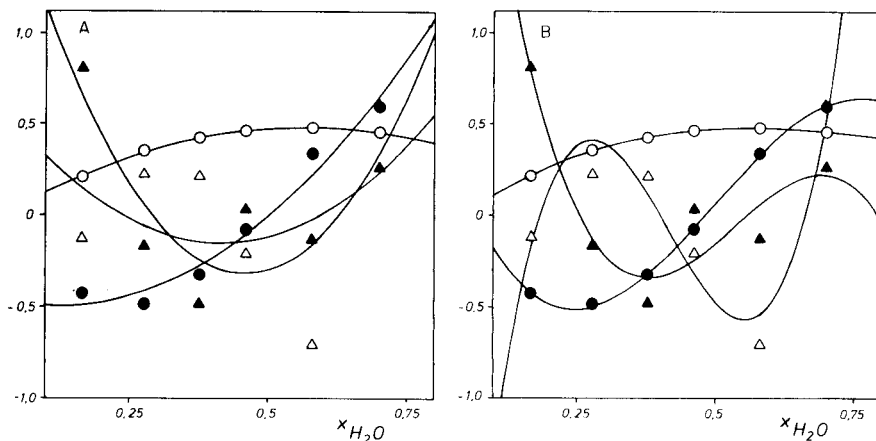


Fig. 5. Nonlinear regression of four factors: (○) 1, (●) 2, (△) 3, (▲) 4. (A) Second-degree polynomial; (B) third-degree polynomial.

shown in Fig. 5. The prediction errors are of the same order of magnitude as for the regression of the partition coefficients. The main advantage of fitting the factor loadings is that only as many regressions as the number of factors are required, independently of the number of solutes.

TABLE 5

Least-squares regressions of the factor loadings on the mole fraction of water in the more polar phase

Factor	Multiple correlation coefficient		Relative error (%)			
			Mean value		RMS value	
	Degree of polynomial		2	3	2	3
1	0.998	1.00	1.28	0.48	1.52	0.52
2	0.985	0.999	15.73	9.81	18.12	18.32
3	0.349	0.949	117.63	45.62	134.45	51.55
4	0.857	0.936	196.35	149.41	380.81	287.98

Calculation with the target transformation factor analysis

The first step in the target transformation factor analysis is the principal component factor analysis. The next step is the selection of test vectors for guiding the rotation. In this application, the test vectors consist of the phase system compositions or simple functions of these compositions, e.g., square, reciprocal or logarithmic. In the first step, single test vectors are chosen; in the second step, several selected test vectors are combined to form a group

TABLE 6

Error of the rotated vectors, related to the test vectors^a

Test vector	Relative error (%)		
	Mean value	RMS value	Exner value
x H ₂ O	1.1	1.3	0.053
x EtOH	6.6	8.8	0.539
x TMP	154.3	226.0	0.541
RE H ₂ O	18.3	25.6	0.615
RE EtOH	5.8	7.4	0.364
RE TMP	65.9	95.0	0.320
SQ H ₂ O	3.8	4.9	0.067
SQ EtOH	11.3	15.0	0.444
SQ TMP	4389.7	7010.9	0.538
LN H ₂ O	15.3	20.9	0.548
LN EtOH	4.6	5.8	0.206
LN TMP	1.7	2.1	0.105
EX H ₂ O	4.9	6.4	366.0
EX EtOH	4.9	6.4	461.0
EX TMP	4.9	6.4	1420.0

^aEtOH, ethanol; TMP, 2,2,4-trimethylpentane; x , mole fraction; RE, $1/x$; SQ, $(x)^2$; LN, $\ln(x)$; EX, $\exp(-x/RT)$.

of test vectors. By comparison of the predicted and the experimental values for the test vectors the best combination of test vectors can be selected. An additional criterion for the goodness of the prediction ability is the so-called Exner function [1, 12, 13]. It is a measure of the correlation between the given and the predicted test vectors and hence for the fit of the data. The value of the function can vary from zero to infinity, with the best fit approaching zero. It is useful when a good measure of the experimental error is not available. The errors of the reproduced test vectors in comparison with the phase system composition are given in Table 6. The complete results for the selected test vectors are given in Table 7. Then combinations of four vectors from this group of possible test vectors are selected, giving the best reproduction of the data. These calculations are done in the following way:

TABLE 7

Comparison of the predicted vectors and the test vectors^a

System	Test vector	Predicted vector	Absolute error	Relative error (%)	System	Test vector	Predicted vector	Absolute error	Relative error (%)
<i>x H₂O</i>					<i>LN TMP</i>				
1	0.167	0.1645	-0.0025	-1.52	1	-2.017	-1.971	0.0461	-2.28
2	0.278	0.2745	-0.0035	-1.25	2	-2.976	-2.932	0.0442	-1.48
3	0.378	0.3766	-0.0014	-0.37	3	-3.863	-3.828	0.0349	-0.90
4	0.473	0.4846	0.0115	2.44	4	-4.710	-4.901	-0.1905	4.04
5	0.581	0.5757	-0.0053	-0.91	5	-5.809	-5.724	0.0851	-1.47
6	0.702	0.7011	-0.00092	-0.13	6	-6.215	-6.200	0.0149	-0.24
<i>x EtOH</i>					<i>EX H₂O</i>				
1	0.700	0.6766	-0.0234	-3.34	1	0.99972	0.9650	-0.0347	-3.47
2	0.671	0.6520	-0.0190	-2.84	2	0.99953	0.9750	-0.0245	-2.45
3	0.601	0.5816	-0.0194	-3.23	3	0.99936	0.9687	-0.0307	-3.07
4	0.518	0.6115	0.0934	18.04	4	0.99920	1.1343	0.1350	13.52
5	0.416	0.3746	-0.0414	-9.95	5	0.99902	0.9396	-0.0594	-5.95
6	0.296	0.2888	-0.0072	-2.44	6	0.99882	0.9885	-0.0103	-1.03
<i>RE EtOH</i>					<i>EX EtOH</i>				
1	1.429	1.362	-0.0665	-4.65	1	0.99882	0.9641	-0.0347	-3.47
2	1.490	1.403	-0.0875	-5.87	2	0.99887	0.9744	-0.0245	-2.45
3	1.664	1.625	-0.0386	-2.32	3	0.99899	0.9683	-0.0307	-3.07
4	1.931	2.229	0.2980	15.43	4	0.99913	1.1340	0.1349	13.50
5	2.404	2.268	-0.1357	-5.65	5	0.99930	0.9400	-0.0593	-5.94
6	3.378	3.355	-0.0239	-0.71	6	0.99950	0.9892	-0.0103	-1.03
<i>SQ H₂O</i>					<i>EX TMP</i>				
1	0.0279	0.0262	-0.0017	6.16	1	0.99978	0.9650	-0.0347	-3.47
2	0.0773	0.0706	-0.0067	-8.65	2	0.99991	0.9754	-0.0245	-2.45
3	0.1429	0.1441	0.0012	0.84	3	0.99996	0.9693	-0.0307	-3.07
4	0.2237	0.2358	0.0120	5.37	4	0.99998	1.1350	0.1350	13.50
5	0.3376	0.3317	-0.0059	-1.75	5	0.99999	0.9406	-0.0594	-5.94
6	0.4928	0.4917	-0.0011	-0.22	6	1.0000	0.9897	-0.0103	-1.03
<i>LN EtOH</i>									
1	-0.357	-0.3394	0.0173	-4.85					
2	-0.399	-0.3789	0.0201	-5.04					
3	-0.509	-0.4978	0.0113	-2.23					
4	-0.658	-0.7327	-0.0749	11.39					
5	-0.877	-0.8432	0.0339	-3.86					
6	-1.217	-1.2115	0.0059	-0.49					

^aFor abbreviations, see Table 6.

the calculated eigenvectors (factor loadings) are rotated in space to those directions which are given by the selected test vectors. Then the factor scores are rotated in accordance with the rotation of the factor loadings. With these new factor loadings and scores, the partition coefficients can be calculated. The prediction errors for some combinations of test vectors are given in Table 8.

A final comparison of the accuracy of different methods for prediction of the partition coefficients of some steroids was conducted by using the methods to predict these coefficients for new phase system compositions; the values were then compared with experimental data. The compositions of

TABLE 8

Results of the calculations with a combination of four test vectors^a

Combination of test vectors	Mean error	RMS error	Exner function	Combination of test vectors	Mean error	RMS error	Exner function
1,2,3,5	0.64	0.91	0.008	1,2,3,7	0.76	1.09	0.010
1,2,3,8	0.76	1.09	0.010	1,2,3,9	0.76	1.09	0.010
1,2,5,6	0.64	0.90	0.009	1,2,5,7	0.74	1.08	0.010
1,2,5,8	0.74	1.08	0.010	1,2,5,9	0.74	1.08	0.010
1,3,4,5	0.72	1.01	0.010	1,3,5,7	0.64	0.91	0.008
1,3,5,8	0.64	0.91	0.008	1,3,5,9	0.64	0.91	0.008
1,3,7,8	0.77	1.10	0.010	1,3,7,9	0.76	1.09	0.010
1,3,8,9	0.76	1.10	0.010	1,5,7,8	0.75	1.09	0.010
1,5,7,9	0.74	1.08	0.010	1,5,8,9	0.75	1.08	0.010
2,3,7,8	0.75	1.08	0.010	2,3,7,9	0.76	1.09	0.010
2,3,8,9	0.77	1.10	0.010	2,5,7,8	0.74	1.07	0.010
2,5,7,9	0.74	1.08	0.010	2,5,8,9	0.75	1.09	0.010
3,4,7,9	0.62	0.86	0.008	3,5,7,8	0.75	1.02	0.010
3,5,7,9	0.68	0.97	0.009	3,6,7,9	0.61	0.84	0.008
3,7,8,9	0.76	1.09	0.010	4,6,7,9	0.62	0.83	0.008
5,6,7,9	0.64	0.86	0.009	5,7,8,9	0.75	1.08	0.010

^aDefinition for the test vector symbols: (1) *x* H₂O, (2) *x* EtOH, (3) *RE* EtOH, (4) *SQ* H₂O, (5) *LN* EtOH, (6) *LN* TMP, (7) *EX* H₂O, (8) *EX* EtOH, (9) *EX* TMP.

TABLE 9

Composition of additional phase systems for experimental verification of the prediction of partition coefficients

Phase system code number	Mole fraction		
	2,2,4-Tri-methylpentane	Ethanol	Water
7	0.053	0.698	0.249
8	0.035	0.634	0.331
9	0.009	0.581	0.410
10	0.009	0.518	0.473
11	0.006	0.467	0.527

TABLE 10

Comparison of calculated and experimental partition coefficients^a

Solute ^b	Target vector factor analysis			Fitting of logarithm of partition coefficients		Fitting of partition coefficients		Fitting of factor loadings		Exp. values ^c
	Set 1	Set 2	Set 3	Degree of polynomial						
				2	3	2	3	2	3	
<i>System 7</i>										
1	8.9	8.8	7.9	7.3	7.6	7.8	8.1	7.3	7.6	8.4
3	14.7	14.7	12.4	11.1	12.2	13.1	14.2	11.2	12.3	13.0
5	16.5	16.4	15.7	12.9	13.8	16.7	15.5	12.9	13.8	18.1
8	20.4	20.3	18.4	16.1	17.3	20.7	18.9	16.1	17.3	20.8
11	32.9	32.6	29.3	25.1	26.8	35.1	30.6	24.9	26.7	29.9
12	33.9	33.6	32.2	27.2	28.3	39.3	29.4	27.1	28.2	36.0
15	49.9	49.6	41.7	34.7	38.8	54.3	46.8	34.8	39.0	57.7
<i>System 8</i>										
1	10.3	10.2	8.7	8.3	8.7	8.6	9.1	8.3	8.7	9.6
3	18.2	18.1	14.1	13.3	14.8	15.4	15.9	13.3	14.9	17.0
5	21.6	21.5	18.1	16.3	17.7	20.4	18.9	16.3	17.6	23.9
8	26.6	26.4	22.6	20.3	22.2	25.7	23.5	20.3	22.1	28.4
11	44.7	44.3	37.3	32.8	35.6	44.3	38.9	32.8	35.6	40.7
12	46.4	45.9	42.4	36.3	38.1	51.3	39.5	36.3	38.1	49.7
15	71.2	70.8	54.1	47.4	54.3	70.4	61.4	47.4	54.4	71.2
<i>System 9</i>										
1	11.4	11.5	9.2	10.8	10.9	10.4	10.5	10.8	10.9	10.1
2	23.6	23.6	16.9	21.7	22.3	21.4	21.6	21.6	22.2	21.3
5	34.7	34.7	27.2	31.6	32.2	30.8	30.5	31.7	32.3	30.8
8	45.2	45.3	36.2	42.0	42.9	42.0	41.5	42.6	42.9	37.6
11	78.8	79.0	61.4	71.5	72.9	70.5	69.2	72.1	73.6	57.9
12	93.8	94.1	81.9	87.6	88.6	89.3	86.5	88.1	89.2	80.8
15	134	134	92.3	119	124	119	117	119	123	135
<i>System 10</i>										
1	10.3	10.4	10.6	10.7	10.6	10.4	10.3	10.7	10.6	9.1
3	22.0	22.1	23.0	23.3	22.7	22.2	22.1	23.1	22.5	21.2
5	33.9	34.0	34.8	35.0	34.3	32.4	32.7	35.1	34.5	32.9
8	46.4	46.5	47.5	48.5	47.5	45.6	46.1	48.5	47.6	42.4
11	78.3	78.6	80.4	81.2	79.8	74.7	75.9	82.1	80.6	65.3
12	99.9	100	101	104	103	97.2	99.8	104	103	87.1
15	132	133	138	141	137	127	129	140	136	140
<i>System 11</i>										
1	9.7	9.7	10.4	10.1	9.8	10.0	9.7	10.1	9.7	8.8
3	21.7	21.8	24.2	24.0	22.2	22.4	22.1	23.8	22.0	21.5
5	35.1	35.2	37.6	36.9	34.8	33.1	34.1	37.1	35.1	33.1
11	82.7	82.9	88.7	87.6	82.9	77.0	80.7	88.4	83.6	64.8

^aTest vectors: Set 1, x_{H_2O} , $1/x_{EtOH}$, x_{EtOH} , $\ln(x_{EtOH})$; Set 2, x_{H_2O} , $1/x_{EtOH}$, $\ln(x_{EtOH})$, $\exp(-x_{EtOH}/RT)$; Set 3, $1/x_{EtOH}$, $\ln(x_{TMP})$, $\exp(-x_{H_2O}/RT)$, $\exp(-x_{TMP}/RT)$.

^bSolutes numbered as in Table 1. ^cExperimental values.

TABLE 11

Comparison of the results of the different methods of calculation with experimental partition coefficients

Solute ^a	T.f.a. ^b	Fit ln <i>K</i>	Fit <i>K</i>	Fit Factor	<i>K</i> _{EXP}
<i>System 1</i>					
1	8.9	7.6	8.1	7.6	8.4
3	14.7	12.2	14.2	12.3	13.0
5	16.5	13.8	15.5	13.8	18.1
8	20.4	17.3	18.9	17.3	20.8
11	32.9	26.8	30.6	26.7	29.9
12	33.9	28.3	29.4	28.2	36.0
15	49.9	38.8	46.8	39.0	57.7
MRE	8.5	17	11	17	
<i>System 2</i>					
1	10.3	8.7	9.1	8.7	9.6
3	18.2	14.8	15.9	14.9	17.0
5	21.6	17.7	18.9	17.6	23.9
8	26.6	22.2	23.5	22.1	28.4
11	44.7	35.6	38.9	35.6	40.7
12	46.4	38.1	39.5	38.1	49.7
15	71.2	54.3	61.4	54.4	71.2
MRE	6.7	19	13	19	
<i>System 3</i>					
1	11.4	10.9	10.5	10.9	10.1
2	23.6	22.3	21.6	22.2	21.3
5	34.7	32.2	30.5	32.3	30.8
8	45.2	42.9	41.5	42.9	37.6
11	78.8	72.9	69.2	73.6	57.9
12	93.8	88.6	86.5	89.2	80.8
15	134	124	117	123	135
MRE	16	11	8.1	11	
<i>System 4</i>					
1	10.3	10.6	10.3	10.6	9.1
3	22.0	22.7	22.1	22.5	21.2
5	33.9	34.3	32.7	34.5	32.9
8	46.4	47.5	46.1	47.6	42.4
11	78.3	79.8	75.9	80.6	65.3
12	99.9	103	99.8	103	87.1
15	132	137	129	136	140
MRE	10	12	9.4	12	
<i>System 5</i>					
1	9.7	9.8	9.7	9.7	8.8
3	21.7	22.2	22.1	22.0	21.5
5	35.1	34.8	34.1	35.1	33.1
11	82.7	82.9	80.7	83.6	64.8
MRE ^c	11	12	10	12	
MRE total	10	14	10	14	

^aSolutes numbered as in Table 1. ^b $x_{\text{H}_2\text{O}}, 1/x_{\text{EtOH}}, x_{\text{EtOH}}, \ln(x_{\text{EtOH}})$ as test vectors. ^cMean relative error (%).

these new phase systems are given in Table 9, and the experimental results are compared with the predicted values in Table 10. The prediction accuracy of the partition coefficients with all three methods is satisfactory. The prediction error is in the same order of magnitude as the experimental error. The methods used are the fitting of the logarithm of the partition coefficient, fitting of the partition coefficient, the fitting of the factor loadings and the target vector factor analysis. Target factor analysis and fitting of the factor loadings are preferable to the fitting of the partition coefficients, because the information from the entire data set is extracted by these methods, and individual errors do not have a great influence.

All these methods offer the possibility of optimizing chromatographic separations by precalculation of partition coefficients for new compositions of the phase system.

Conclusion

The results of the prediction of liquid-liquid partition coefficients and the experimental values for selected solutes are given in Table 11. The mean of the relative errors, $RE = (K_{\text{Calc}} - K_{\text{Exp}})/K_{\text{Exp}}$, for the single phase systems is also included. From the total mean relative error for all five phase systems, it can be concluded that the various methods used have nearly equal accuracy. The best two methods are target factor analysis (t.f.a.) and fitting of the partition coefficient (Fit K) with 10% relative accuracy. Slightly less good, with 14% relative accuracy, are fitting the logarithm of the partition coefficient (Fit ln K) and fitting of the factors (Fit Factor).

This paper was presented in part at the 9th International Symposium on Microchemical Techniques, Amsterdam, 1983.

REFERENCES

- 1 E. R. Malinowski and D. G. Howery, *Factor Analysis in Chemistry*, Wiley, New York, 1980.
- 2 I. E. Frank and B. R. Kowalski, *Anal. Chem.*, 54 (1982) 232R.
- 3 M. F. Delaney, *Anal. Chem.*, 56 (1984) 261R.
- 4 E. R. Malinowski and D. G. Howery, in B. R. Kowalski (Ed.), *Chemometrics: Theory and Applications*, ACS Symposium Series 52, 1977, pp. 53, 73.
- 5 P. H. Weiner, E. R. Malinowski and A. R. Levinstone, *J. Phys. Chem.*, 74 (1970) 4537.
- 6 J. F. K. Huber, *J. Chromatogr. Sci.*, 9 (1971) 72.
- 7 J. F. K. Huber, E. T. Alderlieste, H. Harren and H. Poppe, *Anal. Chem.*, 45 (1973) 1337.
- 8 J. F. K. Huber, C. A. M. Meijers and J. A. R. J. Hulsman, *Anal. Chem.*, 44 (1972) 111.
- 9 W. W. Cooley and P. R. Lohnes, *Multivariate Data Analysis*, Wiley, New York, 1971.
- 10 N. H. Nie, C. H. Hull, J. G. Jenkins, K. Steinbrenner and D. H. Bent, *SPSS — Statistical Package for the Social Sciences*, McGraw-Hill, New York, 1975.
- 11 E. R. Malinowski, D. G. Howery, P. H. Weiner, J. M. Soroka, P. T. Funke, R. B. Selzer and A. Levinstone, *FAKTANAL*, Quantum Chemistry Program Exchange, Program No. 320.
- 12 J. H. Kindsvater, P. H. Weiner and T. J. Klingen, *Anal. Chem.*, 46 (1974) 982.
- 13 O. Exner, *Collect. Czech. Chem. Commun.*, 31 (1966) 3222.

EXTRACTION OF NONSTATIONARITY INFORMATION FROM CORRELATION NOISE

SCOTT FRAZER and MICHAEL F. BURKE*

Department of Chemistry, University of Arizona, Tucson, AZ 85721 (U.S.A.)

(Received 24th June 1985)

SUMMARY

A gas chromatograph is used as a model of a monitored process stream, and a method is developed to detect fixed-amplitude changes either in component concentration or system response to a perturbation. The multiple injection input and its advantages are based on the principles of correlation chromatography. The deconvolution of the aperiodic input pattern from the output results in a signal peak representing average system response and correlation "noise" which, when calibrated, gives the direction and magnitude of the change which has occurred. Because of the signal-averaging effect of the multiple inputs and deconvolution process, the effects of random fluctuations and noise are reduced.

In most analyses, the assumption is made that certain factors, such as sample concentrations, are at a steady state and will remain constant during data collection. However, in many continuous analytical procedures, including kinetic studies and process stream analysis, this assumption is not valid and, in fact, it is the extent of this nonstationarity that is of interest. If random fluctuations are of the same magnitude as the fixed-amplitude change that is occurring, it becomes difficult to evaluate accurately the direction and magnitude of the nonstationarity by simple observation of the output.

To develop a data evaluation method for monitoring concentrations or establishing process dynamics, a gas chromatograph was used as a small model of a process stream. Single-component samples were injected to simulate, in effect, the input of a tracer, voltage or temperature pulse, etc. to characterize a system by determining its transient response [1]. The input, or "forcing", imposed upon the chromatograph and the advantages that result from it are based on correlation chromatography, a method which uses multiple inputs and a correlation operation. Specifically, a unique input pattern, which may be a stream-switching type [2] or, as in this case, a set of multiple injections [3] is continuously fed into a gas chromatograph at a rate that will generally overlap the fronts or peaks in the output to some extent. When the input pattern representation is deconvolved from this output, the result, or correlogram, will represent the average of all the peaks

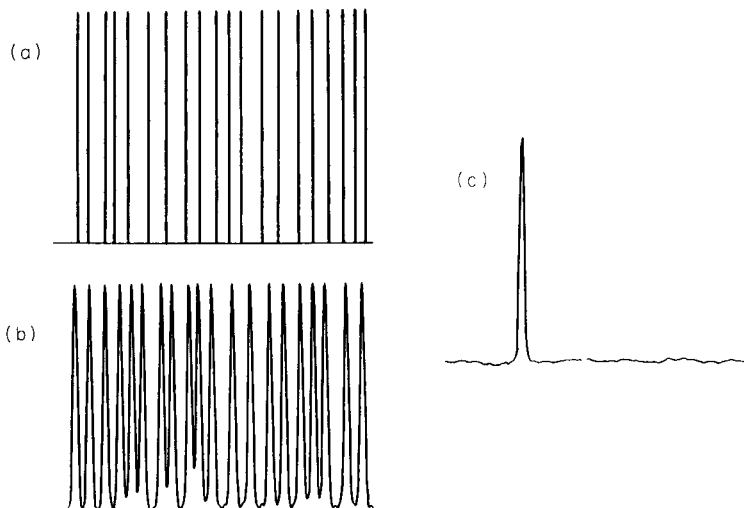


Fig. 1. Typical (a) input pattern, $x(t)$, (b) output, $y(t)$, and (c) correlation function $h(t)$ in correlation chromatography.

present in the output file and will appear as a single injection chromatogram (Fig. 1). The inherent averaging effect of this correlation process reduces the amplitude of the random noise in the raw data to give a correlogram with an improved S/N ratio. Because one does not wait for one injection to elute before making another, this S/N enhancement occurs without requiring the time commitment of ensemble averaging. Considering these properties, it is not surprising that correlation chromatography has found application in trace analysis [4, 5]. However, just as the technique might be used quickly to detect small signal peaks buried in noise, it can also be used to detect small changes in that signal that occur during the course of the injection sequence.

Because the multiple injection process is continuous, the possibility of using it to monitor process streams has been suggested before [5]. The problem encountered in attempting this application is that the deconvolution operation assumes a stationary system and any nonstationarity, such as a fluctuation in input concentration or system response during data collection, causes the appearance of correlation noise in the final results [6, 7]. This noise decreases the reliability of quantitative information and, if severe enough, can lead to a complete breakdown of the correlogram [8]. In this study, it was found that this correlation "noise" contains information on the type and magnitude of changes in system response and can be used to monitor these changes. Random fluctuations and noise are diminished through the same processes which allow S/N enhancement and an accurate evaluation of the constant concentration or response changes that occur during data collection can be made. In addition, however, by finding the

magnitude of the noise under the principal peaks in the correlogram and removing it, reliable quantitation of the average input concentration or system response can also be achieved.

As stated earlier, this study was done with single-component samples to simulate a flowing system which is monitored without a chromatographic separation. The multiple signal or input aspect of the technique may be realized by truly injecting sample into the system (e.g., as in flow injection analysis) or in process dynamics studied by simply taking multiple readings from the monitoring device (e.g., a spectrometer) at set times. Multiple-component samples requiring a separation will show the same type of correlation noise behavior though, as the number of sample components that have changing concentrations increases, so must the sophistication of the procedure for the data analysis.

THEORY

As mentioned before, a correlogram (i.e., the information of interest, $h(\tau)$) can be calculated by deconvolving the input pattern representation $x(t)$ from the output data, $y(t)$. When done in the Fourier domain, this deconvolution is a simple division of the two files [9],

$$h(\tau) = \text{IFT} [Y(f)/X(f)] \quad (1)$$

where IFT indicates the inverse Fourier transform.

The appearance of a system nonstationarity (e.g., a continual concentration increase) may be thought of as a function $NS(t)$ which is added upon $y(t)$ to give a new output (Fig. 2a). Because of the linear addition property of the Fourier transform [9], Eqn. 1 becomes

$$h(\tau) = \text{IFT} [Y(f)/X(f) + NS(f)/X(f)] \quad (2)$$

The result of this operation is the sum of the deconvolution of $x(t)$ from $y(t)$ and $x(t)$ from $NS(t)$; the latter of these provides the correlation noise (Fig. 2b).

With this explanation, the correlation noise in $h(\tau)$ is expected to be consistent with the function $NS(t)$. If the nonstationarity is increased or decreased by some factor (e.g., if the concentration increase is halved), the correlation noise peaks and valleys, while remaining in the same position, will increase or decrease in amplitude by that same factor (Fig. 3a). When the nonstationarity trend is reversed (e.g., if the solute concentration from file start to finish is allowed to decrease), the correlation noise follows the change and one sees the mirror image of the original noise as peaks become valleys and valleys become peaks (Fig. 3b). Both of these facts may be thought of as being due to the deconvolution process linearly converting nonstationarity changes in the output $y(t)$ to correlation noise in the correlogram $h(\tau)$.

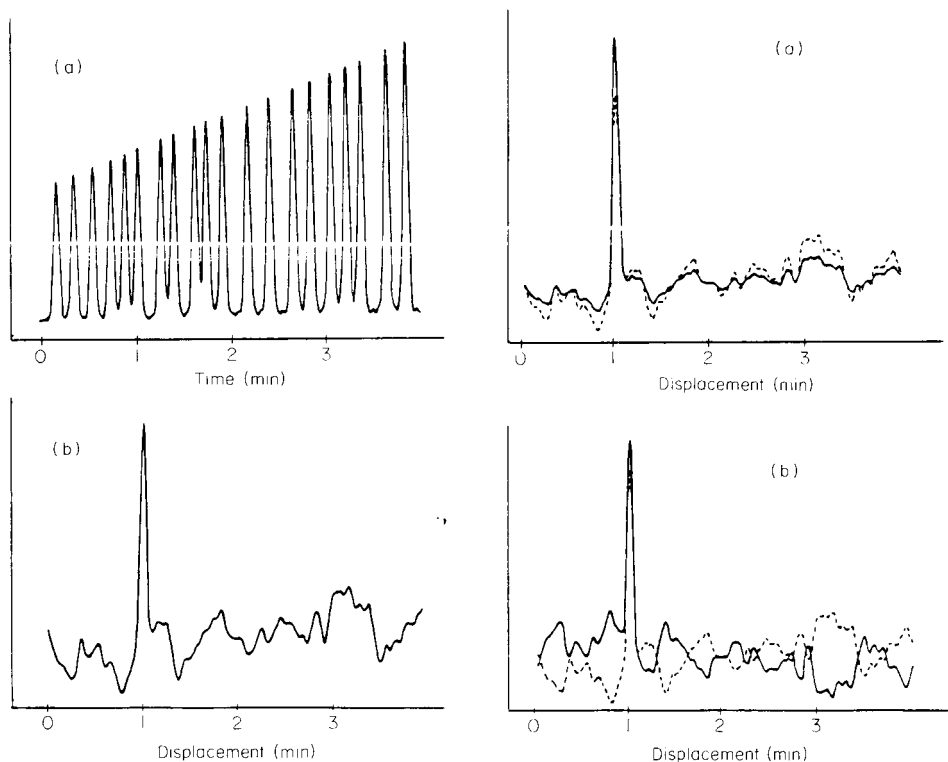


Fig. 2. Output and the correlation function resulting from a nonstationary response to the same input of Fig. 1.

Fig. 3. Comparison of correlation noise patterns: (—) correlation functions of (a) one half the concentration increase of Fig. 2, and (b) a concentration decrease of the same magnitude as the increase of Fig. 2; (···) correlogram of Fig. 2 for comparison.

EXPERIMENTAL

Very few modifications are necessary to convert a gas chromatograph to one with multiple injection capabilities. A Becker model 1452D gas chromatograph oven with a Varian flame ionization detector was used in this study. A computer-controlled autoinjector provided the multiple injections. Though other sampling systems have been suggested and used in multiple injection work [10], the Seiscor model VIII valve used in this study is quite reliable, readily available and has a switching time of only 10 ms.

Injection control, data acquisition, and the deconvolution operation are all done on an IBM 9000 computer. The internal high-resolution timer which controls injection timing and data collection provides an accuracy of $30.5 \mu\text{s}$. At set times, an injection pulse is provided by the computer via a single bit transfer through the parallel port in a nonstrobed mode to a

hardwired pulse-width controller. This, in turn, fires a Clippard Minimatic model EO-3 nitrogen-powered solenoid which opens the Seiscor valve for the set length of time. The computer takes data from a Keithley model 417 high-speed picoammeter, using an internal A/D converter card. This A/D board allows sample rates up to 30 points per second and is set at ± 10 V full scale.

Because this was basically a data-processing investigation, columns, temperatures, flow rates and solutions were chosen to give certain retention times and peak widths. The principal solute used was heptane which had a retention time of 64 s at a temperature of 91°C and flow rate of 20 ml min^{-1} in a Durapak C8 column ($1/8\text{ in.} \times 24\text{ in.}$).

Calibration files can be simulated either experimentally or on the computer. To effect concentration changes experimentally, the resistance of the RC time constant which controlled pulse width was gradually increased or decreased allowing more or less solute to enter the chromatograph and thereby simulating a concentration change. Computer simulations of concentration changes were done by using an output data file with no concentration change and then modifying that data to simulate a nonstationarity effect. All programs were written in FORTRAN-77, using several library subprograms for input/output operations.

RESULTS AND DISCUSSION

This experiment necessarily consists of first establishing a set of simulation files with known concentration changes. From the resulting correlograms, several points are chosen and calibrated for the effect that these concentration changes have had. The points chosen should be at the tops of noise peaks (or the bottoms of noise valleys) to allow better resolution and relative accuracy. As explained, a plot of concentration change vs. point value for each point should be linear. While it is possible to use only one point for calibration and monitoring nonstationary effects, it is probably best to average the results of a number of points to minimize random noise effects.

Linear concentration changes are the easiest fluctuations to calibrate and detect (Fig. 4A). In this case, only the magnitude of the change will affect

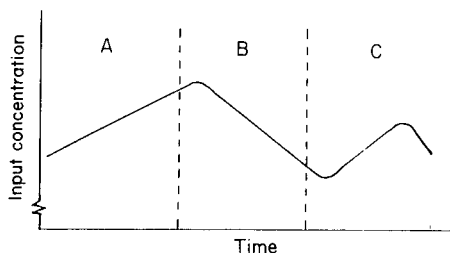


Fig. 4. Plot of possible input concentration change. For explanation, see text.

the correlation noise, so that only a few calibrations are needed. The evaluation process is quite straightforward.

If concentration maxima or minima are present in the file (Fig. 4B), the calibration and evaluation become more complex as the position of a maximum, for example, will greatly affect the correlation noise pattern. In the calibration process, several files with a concentration maximum in various locations of the file will need to be simulated and calibrated. In the evaluation process of an unknown concentration change, the locations of any maxima must first be established. Then, from the appropriate calibration plot, the magnitude of the change can be calculated.

To illustrate how this might be done, the data for a very simple evaluation process are given in Table 1. The calibration points used were chosen for the purpose of differentiating between files that have linear changes or a single concentration maximum (or minimum) and then quantifying that change. The first decision to be made is if there is a concentration maximum present and, if present, where in the data file it is located. This question was answered by noting that while both the position of a concentration maximum and its magnitude affect point values, only the maximum position (or, more generally, output pattern) governs where each calibration point from a group of simulation files crosses zero. For example, point 92 is near zero only when there is no concentration maximum or minimum in the file. Point 203 crosses zero when the turnaround point is at 50% of the file length, no matter what the magnitude of the concentration change at that time. By determining the near-zero values of a correlogram and comparing them to the calibration files, the position of a concentration turnaround can be approximated. Because the correlation noise changes only gradually with turnaround location, an approximation will still allow good accuracy though the higher the frequency change, the more accurate the approximation must be. The values of points 67, 352, and 462 would then be compared to the appropriate calibration to characterize fully the nonstationarity. The number of points to use and the sophistication of their analysis depends

TABLE 1

Simulation results to illustrate evaluation procedure

Conc. change (%) ^a	Conc. maximum location ^b	Point values					
		67	92	203	352	462	803
-25	—	1354	1	1803	1371	-879	-1668
+25	—	-1355	-2	-1802	-1370	880	1668
+50	—	-2710	-3	-3605	-2740	1760	3335
+10, -40	0.25	1491	-269	2417	2355	-840	-2147
+25, -25	0.50	-760	-997	6	525	1198	-139
+40, -10	0.75	-2245	-670	-2358	-1594	1485	2266

^aPercent of largest peak in file. ^bFraction of file length.

on the accuracy desired and the random noise present, and is limited only by the number of points in the file. Fortunately, once a calibration is complete for a certain input pattern, it should require few modifications.

If there is more than one maximum or minimum present in the file (Fig. 4C), very extensive calibration becomes necessary. To avoid this, files of shorter length, though still long enough to include the longest retained eluent, can be collected.

Once the nonstationarity has been identified, the noise directly under the principal peaks can be evaluated and removed. The calibration of this "hidden" noise was accomplished by affecting two simulations of output data, one possessing a certain concentration change and the other a change of equal magnitude but opposite direction. If negligible random noise can be assumed, then, subtracting one of these files from the other leaves only twice the noise of the first file as the principal peaks subtract out but the noise contributions add together (see Fig. 5). When the concentration change has been calibrated, the noise under the principal peaks can be calculated and removed. If one is concerned only with peak height, this is a one-point process; to integrate the peak, noise must be removed over the entire peak width. The adjusted peak should then represent the average peak height or area of the peaks present in the output file.

Ultimately, the resolution and accuracy of this analysis is limited by the random noise (including random nonstationarity) of the system. To establish the effects of this randomness on the technique, the simple evaluation process described was applied to data files which showed various levels of random deviation from linear concentration changes. The results are shown in Table 2. Obviously, random deviations will increase error, but because these fluctuations are averaged in the correlation process, their effect is diminished.

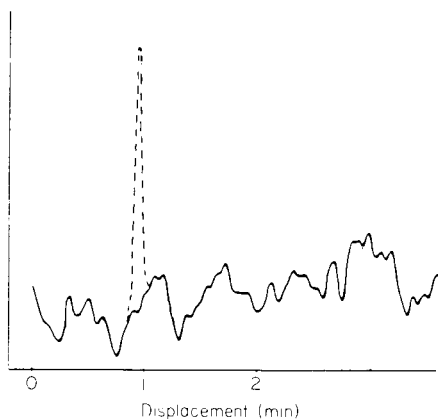


Fig. 5. Correlation noise isolated from peak by subtracting correlograms of opposing concentration changes. Dotted line represents the former peak position.

TABLE 2

Effect on results of random deviations from linear changes (Values are given as percent of initial concentration and those in parentheses are expected averages)

Conc. change (%)	Random deviation (%)	Calculated conc. change (%)	Calculated conc. average (%)
-5	0	-5.7	97.5 (97.5)
	1	-5.2	97.4
	2	-4.7	96.8
-25	0	-25.3	87.3 (87.5)
	2	-25.5	87.3
	5	-23.6	88.2
-50	0	-50.4	74.8 (75.0)
	2	-51.5	74.3
	5	-52.1	73.5

Thus, small changes in system response to a given input which might be difficult to detect and quantify because of random fluctuations and noise, can be evaluated by using multiple inputs and a deconvolution process which effectively averages the results of the multiple signals. Points in a correlation noise pattern directly quantify changes that occur over the length of an entire data file, making the change much more amenable to computer analysis. Finally, the analysis is very fast and continuous, constantly updating old data and giving new values for response changes and averages. It is a data-handling method applicable to a variety of signals and its application to process-stream control, flow-injection analysis and other continuous monitoring devices is direct and viable.

REFERENCES

- 1 J. O. Hougen, *Measurement and Control Applications*, 2nd edn., Instrument Society of America, Pittsburgh, 1979.
- 2 H. C. Smit, *Trends Anal. Chem.*, 2(1) (1983) 1.
- 3 J. B. Phillips and M. F. Burke, *J. Chromatogr. Sci.*, 14 (1976) 495.
- 4 J. B. Phillips, *Anal. Chem.*, 52 (1980) 468A.
- 5 R. Annino and E. J. Grushka, *Chromatogr. Sci.*, 14 (1976) 255.
- 6 R. Annino and L. E. Bullock, *Anal. Chem.*, 45 (1983) 1221.
- 7 T. T. Lub and H. C. Smit, *Anal. Chim. Acta*, 112 (1979) 341.
- 8 K. R. Godfrey and M. Devenish, *Meas. Control*, 2 (1969) 228.
- 9 E. O. Brigham, *The Fast Fourier Transform*, Prentice-Hall, 1974.
- 10 R. Annino, M. F. Gonnard and G. Guoichon, *Anal. Chem.*, 51 (1979) 379.

HIERARCHICAL CLUSTERING OF CARBON-13 NUCLEAR MAGNETIC RESONANCE SPECTRA

M. NOVIČ and J. ZUPAN*

Boris Kidrič Institute of Chemistry, P.O. Box 380 Yu-61001, Ljubljana (Yugoslavia)

(Received 19th March 1985)

SUMMARY

The problems of preprocessing of ^{13}C -n.m.r. spectra for hierarchical clustering are discussed. Encoding of the spectra in nonequidistant intervals is proposed. To establish the optimal intervals, a Simplex method with variable-sized movements is used. The optimized parameter is the amount of information contained in the first two coordinates of the transforms, obtained by the application of principal component analysis to the ^{13}C -n.m.r. spectra. The spectra encoded in optimized intervals are used for automated structure elucidation, based on a hierarchical organization of a collection of more than 2000 assigned ^{13}C -n.m.r. spectra. The hierarchical trees needed for the library search and prediction of some structural features were generated by a 3-distances clustering method. The retrieval and predictive abilities of the system are discussed.

In many laboratories, computer-readable data collections of different kinds of spectra (mass, infrared, ultraviolet, n.m.r., etc.) are available [1–3]. It is generally accepted that ^{13}C -n.m.r. spectroscopy is a powerful tool for the determination of organic structures and structural fragments [4]; computerized analysis of ^{13}C -n.m.r. spectra [5–8] has been investigated for a number of years. This research is usually linked to the development of information systems, which are intended to aid chemists in identifying the structures of unknown compounds from information obtained from complex chemical and spectroscopic data.

The choice of representation of spectra is one of the most important decisions that has to be made at an early stage in the development of any chemical information system based on different spectroscopies. Difficulties in data handling and interpretation can be diminished by using effective representation. It has been shown [9] that for infrared spectra, Fourier transformation with the omission of high-order Fourier coefficients is very suitable for reducing the data with little loss of information. The truncated sets of Fourier coefficients are convenient for storage, and the spectra reproduced from the truncated sets are still very similar to the originals.

A new approach to automated information systems, namely, the 3-distances clustering (3-DC) method [10–13] has recently been introduced for infrared spectra. The same approach is now under examination for ^{13}C -n.m.r. spectra.

Because of the discrete nature of ^{13}C -n.m.r. spectra, the method of compression for their representation must differ from the method used for continuous infrared spectral curves. The peaks in ^{13}C -n.m.r. spectra can be encoded into binary vectors, indicating the presence or absence of the peaks in intervals covering the spectral range from -4 to 277 ppm relative to TMS. Different frequency distributions in equidistant intervals suggested the use of intervals having different widths.

In the present work, the combined use of principal component analysis (p.c.a.) and Simplex optimization is shown to be very useful for determining the optimal interval widths for a selected number of spectral intervals. The spectra encoded in the optimized manner are used for the generation of two large hierarchical trees based on the 3-DC method.

DATA

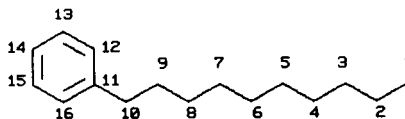
A proton-decoupled ^{13}C -n.m.r. spectrum consists of sharp peaks representing the resonance frequencies of carbon atoms in different molecular environments in the applied magnetic field. The chemical shifts are characteristic for carbon atoms in a given environment, and so the peaks can be assigned to each carbon atom in the structure considered. Usually, the chemical shifts of a compound are coded into the N -component vector, each component representing one of N intervals over the whole spectral region. Because peaks are more frequent in some regions than in others (e.g., around 30 and 130 ppm, corresponding to sp^3 and sp^2 hybridized carbon atoms, respectively), it was decided to choose different widths and a considerably smaller number of intervals for the representation of spectra in the present collection.

The data base for this study consisted of about 2200 ^{13}C -n.m.r. spectra of organic compounds gathered from the Arizona State University collection [14]. All spectra are assigned and each structure is stored in a form of a connection table. Chemical shifts for carbon atoms are stored at the end of corresponding entries in the connection table (Fig. 1).

The master file of connection tables and chemical shifts is linked to a file containing Wiswesser line-formula chemical notations (WLN) of all structures in the data base. The WLN can be accessed via identification numbers, which allows quick sorting of the compounds, or a search for a specific structural fragment. The WLN are particularly useful for analyzing clusters of chemical structures in the hierarchical generated trees where manual inspection is mandatory.

Two problems have to be solved. First, the criterion for the information content conveyed by an arbitrary representation has to be defined; secondly, the optimal representation (for a given number of intervals) on the basis of the selected criterion has to be established.

16 C ₁₆ H ₂₆							
1	C	2	0	0	0	0	14.1
2	C	1	3	0	0	0	22.0
3	C	2	4	0	0	0	32.0
4	C	3	5	0	0	0	29.5
5	C	4	6	0	0	0	29.7
6	C	5	7	0	0	0	29.7
7	C	6	8	0	0	0	29.7
8	C	7	9	0	0	0	29.5
9	C	8	10	0	0	0	31.6
10	C	9	11	0	0	0	36.1
11	C	10	12	16	16	0	142.8
12	C	11	13	13	0	0	128.4
13	C	12	12	14	0	0	128.4
14	C	13	15	15	0	0	125.6
15	C	14	14	16	0	0	128.4
16	C	15	11	11	0	0	128.4



a

b

Fig. 1. The connection table for one compound from the collection (a) and its structure (b). The atoms of each structure are numbered sequentially. The following items are stored: number of the atom; type of the atom; up to 6 neighbours of the atom (for double or triple bonds the corresponding atom number is entered twice or three times, respectively); and for C atoms the chemical shift in ppm from TMS.

RESULTS

The first goal of the investigation was to establish the interval distribution which would provide fast handling and good hierarchical grouping of encoded spectra. Grouping in this context means clustering of similar chemical structures or structural fragments on the basis of their ^{13}C -n.m.r. spectra. The use of the 3-DC method for generation of a complete hierarchical tree of 1000 objects (spectra represented by 281 dimensional vectors) requires a large amount of computer time and storage [13, 15]. The largest proportion of the computer time is required for calculation of the distances between the 281-dimensional vectors. If the representation of the vectors could be shortened, the efficiency of the tree generation would obviously be improved. In the search for a new (shorter) representation, two conflicting requirements were considered: the smaller number of intervals over the entire region and the unambiguity of the representation. In order to evaluate the most appropriate number of intervals, the ratios between the percentages of unambiguously coded spectra and the corresponding number of intervals were inspected. It was found that the maximum of this ratio was very close to 20 intervals with 70% of unambiguously coded spectra. It should be emphasized that, even if the number of intervals is 200, there are still about 20 duplicates in the collection.

After the decision had been taken to represent spectra in 20-dimensional space, the Simplex optimization method was applied to find the optimal interval widths. The simplex technique is widely used for optimization of parameters in many different fields of chemistry [16–21]. The advantage of the Simplex method in the present application lies in the possibility of an easy choice of different starting simplexes. If all starting simplexes yield the same optimal vector, the global character of this optimum is confirmed within a large confidence interval.

TABLE 1

The coordinates (interval widths in ppm) and the OPTIM criterion (sum of the two largest eigenvalues) of the resulting optimized vector

No.	20 components									
1	9.1	17.4	4.1	15.7	1.8	16.9	11.4	8.1	1.1	7.1
2	14.0	17.1	12.3	8.9	13.7	2.2	14.4	13.3	3.6	8.1
3	7.8	18.0	15.7	21.7	11.8	10.9	3.6	14.0	6.3	5.1
4	9.2	11.5	10.0	4.3	7.0	3.7	6.6	6.0	0.5	20.1
.										
.										
20	13.1	13.8	14.9	15.5	9.2	15.9	12.2	13.6	5.7	12.1
21	15.2	24.0	7.3	12.3	7.6	14.5	18.3	5.7	0.8	6.1
	14.5	6.7	2.9	4.1	3.1	2.6	2.1	2.6	2.3	4.1

The criterion for the optimization was the sum of the first two eigenvalues calculated by the p.c.a. [22, 23]. The correlation matrix was obtained by standard procedures [23] from all 2200 ^{13}C -n.m.r. spectra which were encoded each time according to the new interval widths. Initially 21 different vectors represented by 20 coordinates (interval widths) had to be established. The starting coordinates (interval widths) were chosen at random in the spectral range from -4 to 277 ppm. After several Simplex movements, the optimal interval widths were determined.

Table 1 lists the resulting optimized vector for a few of the 21 starting vectors. The optimized percentage of information content in the first two components (OPTIM), obtained by p.c.a. for a given interval distribution, was 32.8%, while the best for any of the starting randomly chosen vectors was 26.2%. The same final information content (32.8%) was also obtained when all starting vectors except one were lying near one of the 20 axes far from the origin (all coordinates small except one) while the last one was placed near the origin equally spaced from all axes. Because different sets of starting simplexes led to the same optimum in the optimization process, it was assumed that the optimum obtained was global.

The improvement of the optimized spectral representation is illustrated in Fig. 2, where normalized frequency distributions of chemical shifts for all 2200 ^{13}C -n.m.r. spectra represented with 20 intervals are shown. The shifts were encoded in 20 equidistant (Fig. 2A) and 20 optimized intervals (Table 1, Fig. 2B), respectively. The main improvement in the proposed spectral representation is better clustering of encoded spectra. To prove this assertion, two small trees were generated by identical procedures based on the 3-DC method and the same set of 20 spectra clustered for both trees in the same sequence order. The only difference was the representation of spectra: the spectra forming tree A (Fig. 3A) were encoded in 20 equidistant intervals, whereas

ained by p.c.a.) of a few starting Simplex vectors. The last row lists the interval widths of the

										OPTIM
.8	0.5	8.7	11.2	7.1	15.9	13.1	9.0	9.7	13.8	22.4
.6	12.6	5.8	10.6	11.3	8.1	0.4	0.4	16.8	8.4	22.1
.4	11.0	8.2	17.6	9.5	11.1	4.1	14.2	3.8	7.1	22.1
.8	4.7	4.6	8.8	11.6	13.9	3.1	12.1	20.9	17.0	26.2
										∴
										.
.7	2.2	4.3	5.6	11.8	3.4	14.4	5.8	5.8	15.9	22.8
.9	15.8	16.2	7.5	4.4	11.7	3.9	23.6	0.5	1.7	23.0
.3	12.1	24.2	18.0	12.4	9.1	7.4	12.5	19.2	13.2	32.8

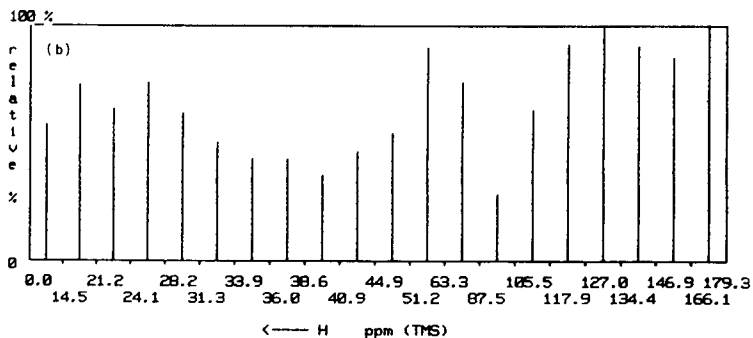
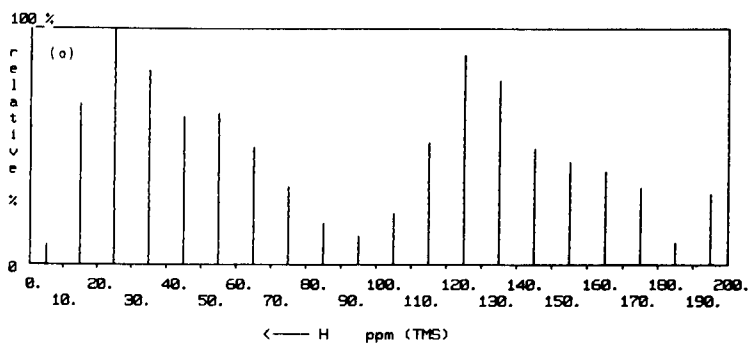


Fig. 2. Two normalized frequency distributions of chemical shifts for 2200 spectra from the collection, represented with 20 equidistant intervals (a) and with 20 optimized intervals (b). The ordinates are normalized to the intensity in the interval over which the chemical shifts of the greatest number of spectra are present.

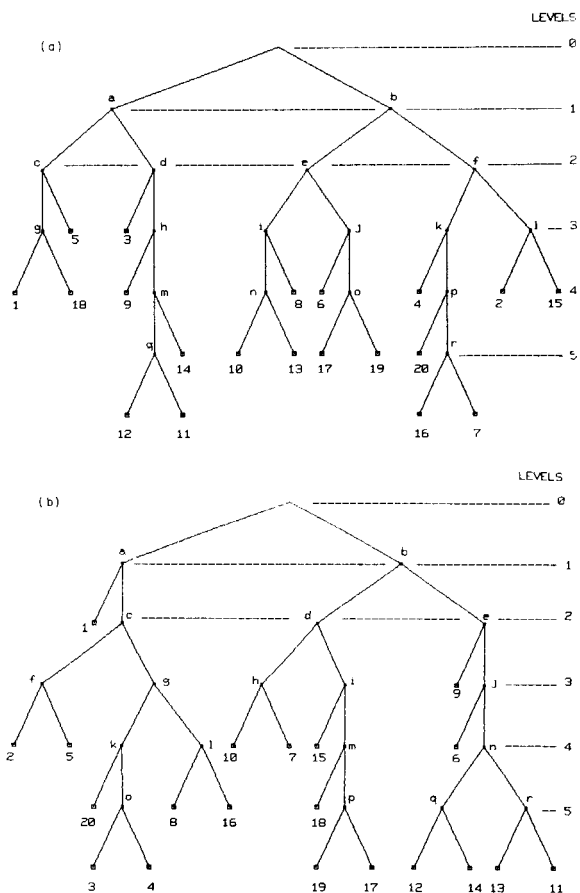


Fig. 3. Two trees of 20 compounds for which the ^{13}C -n.m.r. spectra are clustered by the 3-DC method. The spectra are encoded in 20 equidistant intervals (A) and in 20 optimized intervals (B). For further explanation, see text.

the spectra of the same compounds in tree B (Fig. 3B) were encoded in the 20 optimized intervals. The decision levels in each tree are indicated by the numbers 0–5, while the clusters at different levels are labelled a to r. The numbers 1–20 at the branch ends correspond to the structural formulae of the compounds or fragments listed in Fig. 4. Comparison of the two trees shows that the chemical structures of the compounds are clustered better in tree B. The compounds with saturated carbon atoms are gathered in cluster a, while the aromatic and heterocyclic compounds are in cluster b at the first decision level. Compound 1 (aromatic ring with a chain of 10 carbon atoms as a substituent) is in cluster a together with the aliphatics, but because of the aromatic ring it is quite different from the other compounds of the same group and is, therefore, separated from them at the second decision level. In tree A, the compounds of similar structure are more spread out among the

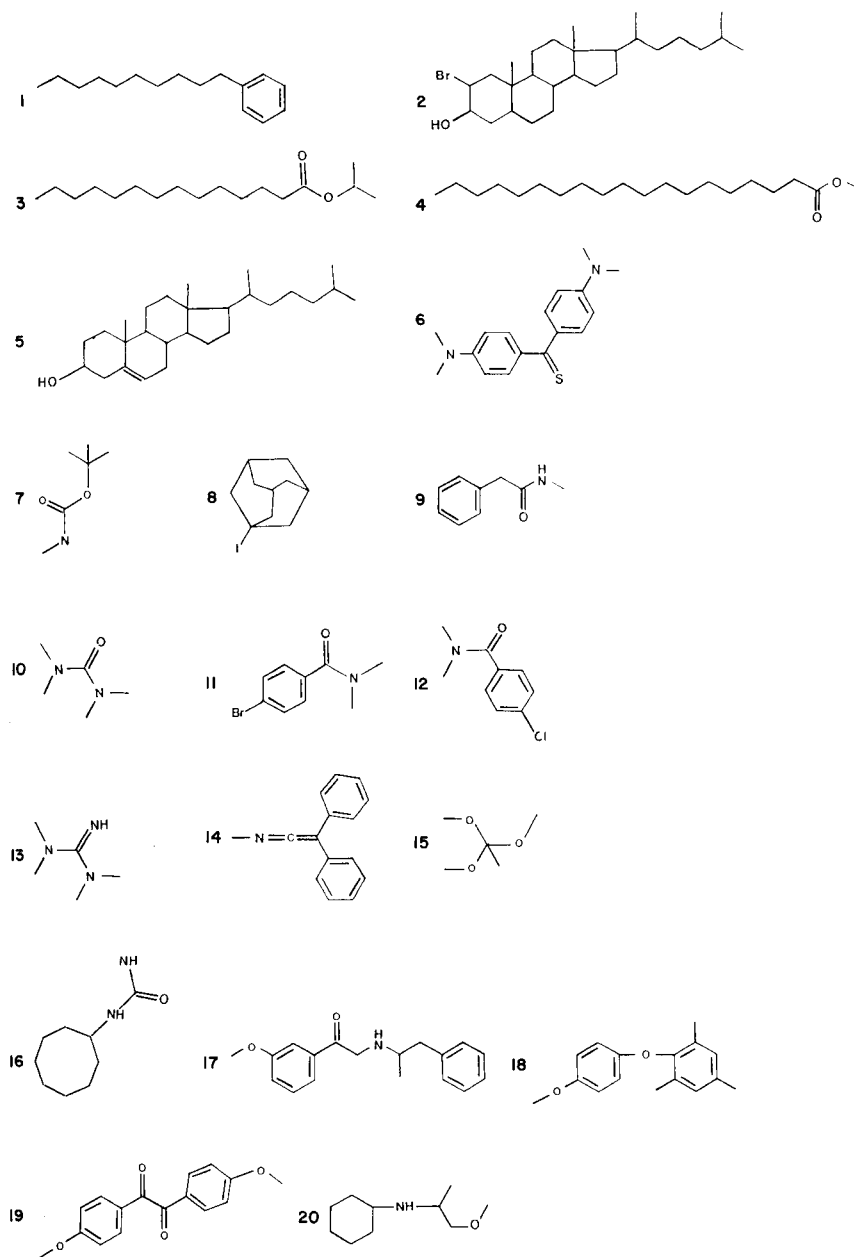


Fig. 4. The structural formulae corresponding to the numbers 1–20 at the branch ends in Fig. 3.

clusters. For example, compounds 3 and 4, which are structurally very similar (Fig. 4), are separated even at the first decision level: compound 3 is in cluster a, and compound 4 is in cluster b. In tree B, the two compounds are in the same cluster, o, up to the fifth decision level.

Among the 2200 spectra encoded in 20 equidistant intervals, 702 spectra (32%) were not unambiguously defined. When the spectra were encoded in 20 optimized intervals obtained by the described method, the number of such spectra was smaller (579 or 26%); this is one reason for preferring the optimized intervals. Because objects with identical representation are always clustered together, handling of duplicates is simplified. Even if there are many of the same kind, they can be detected in a straightforward manner; representation of the cluster is identical for all objects in the cluster. After the duplicate has been detected, it can be treated separately by recalling the extended representations of objects in the particular cluster.

The new 20-dimensional representation of 2200 ^{13}C -n.m.r. spectra were used to generate two hierarchical trees, each consisting of 1000 spectra (Fig. 5). The trees are linked sequentially so that for any query spectrum the search can be made through all 2000 compounds. If one of the compounds clustered in the trees is sought, there is always an exact match to the query spectrum at the end of the path. In other words, the recognition ability of the combined hierarchical retrieval system (two sequentially linked decision trees) is 100%. The longest retrieval path consists of 45 three-way decisions (23 and 22 for each tree, respectively). On average, however, only 25.1 (12.5 + 12.6) decisions are necessary to retrieve any of 2000 spectra from the collection.

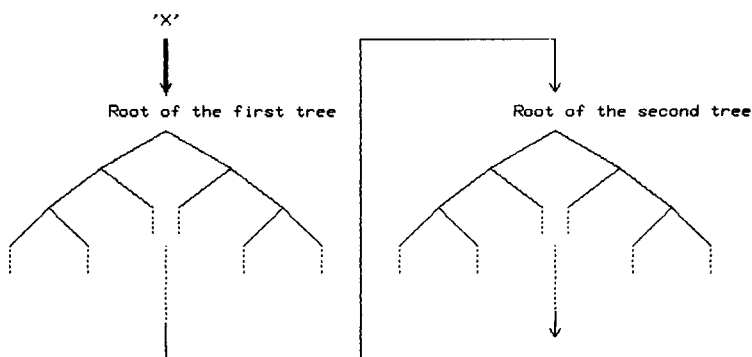


Fig. 5. Two sequentially linked hierarchical trees for the described retrieval scheme. Each tree consists of 1000 spectra. The query spectrum "X" enters at the root of the first tree and continues its path, after leaving the first tree, at the root of the second one. Because of duplicates, it is worthwhile to continue the search through the second tree even if an exact match is found in the first tree.

DISCUSSION

Not only does this hierarchically organized data base provide an efficient means of retrieving an identical query spectrum but there is an additional advantage if the spectrum sought is not in the data base. In Fig. 6 the last part of the retrieval of a test spectrum (labelled X) for such a case is explained in detail. Because an exact match was not found, two clusters, both close to the end of the retrieval path in each tree (three to four levels back depending on the similarity of the objects), were inspected further (Fig. 6A). The compounds from these two clusters were ranked on the basis of the distances between their spectra and spectrum X (Fig. 6B). According to the decision-making process of the retrieval system based on the hierarchically organized data, the structure at the top of the ranking list is the most similar to the structure of the unknown compound X. It is possible in some cases that the most similar compound does not appear on the ranking list because it was overlooked in the retrieval procedure at the point where the decision on the subsequent path was made on the basis of two almost equal distances. For the hierarchical retrieval system based on infrared spectra [13], it was found that "feed-back" searches [24] significantly diminished the possibility of missing the spectrum most similar to that of the unknown compound. The proposed system enables the query spectrum to be re-entered at any vertex, not just at the root, thus offering the repeat searches at vertices branched off of the main retrieval path.

Additional information about the unknown structures of compound X can be obtained from consideration of the common structural fragments assigned to the clusters encountered by the query object X on its path through the two decision trees. Actually, for real cognition of the predictive ability of such hierarchical retrieval systems, common structural features should be extracted and evaluated at each decision point (vertex). This means that for the present scheme of two 1000-object trees, almost 2000 clusters have to be inspected and assigned. Because no assignment can be fixed until

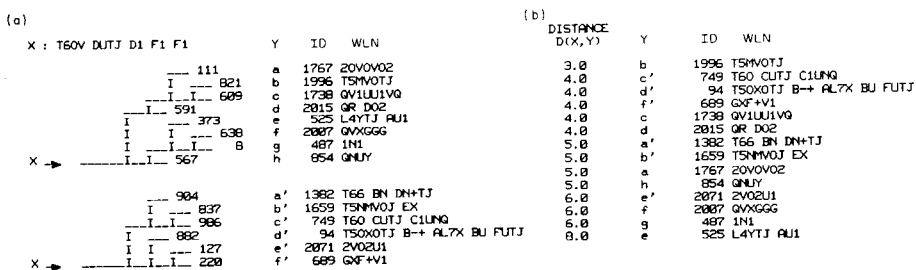


Fig. 6. (A) Two clusters on the retrieval path through two hierarchical trees of 1000 spectra, close to the end of each tree, when an unknown compound X is sought. (B) Ranking of the upper compounds with respect to the distance d between the compounds' spectra and the spectrum of X.

it has been thoroughly tested [13], the predictive abilities of all vertices are the subject of continuing investigation. For testing the predictive ability of the hierarchical retrieval system, 200 spectra from the original collection were omitted before the two trees were generated. The outcomes at each vertex on all 200 retrieval paths have to be evaluated before further conclusions about the predictive ability can be reached.

Conclusion

A hierarchical retrieval system of two sequentially linked trees, each containing 1000 ^{13}C -n.m.r. spectra encoded in optimized intervals, was generated. Because the 100% recognition ability of the retrieval system with an average of 25.1 decisions is a good result (even in the worst case, only 45 decisions are needed), these two trees were not combined into one big tree of 2000 spectra, although this would result in a slightly smaller number of decisions necessary to retrieve a spectrum. The system of two small trees instead of one large tree decreases the demands on program memory and has the important advantage that it is possible to compare two retrieval paths and the decisions made on them, especially if both trees consist of spectra of structurally similar compounds. Even more complete information can be obtained by feed-back searches through both trees; this has been already described for infrared spectra [24] and is also possible in the proposed system.

The authors gratefully acknowledge the financial support of this study by the Research Community of Slovenia and the Joint Yugoslav-U.S. Board for Scientific Research (project number 479). Part of this work was presented at the VIIth International Conference on Computers in Chemical Research and Education, Garmisch-Partenkirchen, June 1985.

REFERENCES

- 1 J. Zupan, M. Penca, D. Hadži and J. Marsel, *Anal. Chem.*, 49 (1977) 2141.
- 2 D. L. Dalrymple, C. L. Wilkins, G. W. A. Milne and S. R. Heller, *Org. Magn. Reson.*, 11 (1978) 535.
- 3 C. L. Fisk, G. W. A. Milne and S. R. Heller, *J. Chromatogr. Sci.*, 17 (1979) 441.
- 4 G. W. A. Milne, J. Zupan, S. R. Heller and J. A. Miller, *Org. Magn. Reson.*, 12 (1979) 289.
- 5 R. E. Carhart and C. Djerassi, *J. Chem. Soc. Perkin Trans. 2*: (1973) 1753.
- 6 N. A. B. Gray, J. G. Nourse, C. W. Crandell, D. H. Smith and C. Djerassi, *Org. Magn. Reson.*, 15 (1981) 375.
- 7 C. Djerassi, D. H. Smith, C. W. Crandell, N. A. B. Gray, J. G. Nourse and M. R. Lindley, *Pure Appl. Chem.*, 54 (1982) 2425.
- 8 H. N. Cheng and S. J. Ellingsen, *J. Chem. Inf. Comput. Sci.*, 23 (1983) 197.
- 9 M. Novič and J. Zupan, *Anal. Chim. Acta*, 151 (1983) 419.
- 10 J. Zupan, *Clustering of Large Data Sets*, Research Studies Press, Wiley, Chichester, 1982.
- 11 J. Zupan, *Anal. Chim. Acta*, 139 (1982) 143.
- 12 J. Zupan, *Proceedings, Systems Applications*, Vol. 2, Intersystems, Seaside, CA, 1984, p. 633.

- 13 J. Zupan and M. E. Munk, *Anal. Chem.*, 57 (1985) 1609.
- 14 See, e.g., H. B. Woodruff, C. R. Snelling, Jr., C. A. Shelley and M. E. Munk, *Anal. Chem.*, 49 (1977) 2075.
- 15 J. Zupan and M. E. Munk, *Vestn. Slov. Kem. Drus.*, 30 (1983) 61.
- 16 D. E. Long, *Anal. Chim. Acta*, 46 (1969) 193.
- 17 T. R. Brunner, C. L. Wilkins, T. F. Lam, L. J. Soltzberg and S. L. Kaberline, *Anal. Chem.*, 48 (1976) 1146.
- 18 S. N. Deming and L. R. Parker, Jr., *CRC Crit. Rev. Anal. Chem.*, (1978) 187.
- 19 S. N. Deming and S. L. Morgan, *Anal. Chem.*, 45 (1973) 278A.
- 20 M. W. Routh, P. A. Swartz and M. B. Denton, *Anal. Chem.*, 49 (1977) 1422.
- 21 S. L. Kaberline and C. L. Wilkins, *Anal. Chim. Acta*, 103 (1978) 417.
- 22 H. Abe, S. Kumazawa, T. Taji and S.-I. Sasaki, *Biomed. Mass Spectrom.*, 3 (1976) 151.
- 23 H. Margenau and G. M. Murphy, *The Mathematics of Physics and Chemistry*, Van Nostrand, Princeton, New Jersey, 1956.
- 24 J. Zupan and M. E. Munk, Presented at VIIIth International Conference on Computers in Chemical Research and Education, Garmisch-Partenkirchen, June 1985.

CLASSIFICATION OF THE QUALITY OF SURFACE WATERS BY MEANS OF PATTERN RECOGNITION

J. H. M. BARTELS, T. A. H. M. JANSE and F. W. PIJPERS*

Department of Analytical Chemistry, Catholic University, Toernooiveld, 6525 ED Nijmegen (The Netherlands)

(Received 21st August 1984)

SUMMARY

Pattern recognition is shown to provide a means of classifying various types of surface waters on the basis of physicochemical data. Based on eleven relevant features, five different clusters were found in an evaluation of about 150 000 observations made over a period of 8 years. Discrimination between these clusters pertaining to water quality required seven chemical and two physical features only. Combination of a selection of these features into one eigenvector, dominated by total ionic nitrogen and *ortho*-phosphate, and a second eigenvector dominated by nitrate and ammonia with different signs, defines a projection plane in a five-dimensional feature space that accounts for 91% of the information content of the data matrix; 65% is attributed to total ionogenic nitrogen and phosphate and 26% is associated with the nitrogen redox balance.

Some years ago, the quality of surface waters in the Netherlands deteriorated so much that government action became necessary. A program was started, and extended over several years, to study the quality of not only surface waters but also of air and soil. The quality of surface waters was judged by several chemical and physical parameters, some of which were combined mathematically to provide a quality number. Because many different laboratories collect data on surface water quality, the resulting data collections are not easy to handle or to interpret. Moreover, there is no relationship between the physicochemical data matrix and the implications for biological systems. The main difference between the physicochemical assessment and the biological assessment is the time scale on which effects are observed. A biological system may react slowly to environmental changes, so that months may pass before curative action is taken. For an ideal surveillance system, the relationship between physical, chemical and biological features should be known; pattern recognition methods offer a possible solution to this problem. Clustering of sampling locations is sought in relation to quality criteria, with the intention of identifying the most important feature(s) involved in the clustering. A firm relationship between these features and water quality in an ecological sense is not provided by pattern recognition but may be sought in a wider investigation. In this paper, a plan is described for handling the huge amount of data, collected over

eight years at 110 locations in the province of Utrecht in The Netherlands, in order to produce results in a form that can be assessed.

DATA SET

The data set used was measured and collected by the laboratory for water surveillance in Utrecht [1]. The features listed in Table 1 were measured from 1975 onwards at 110 locations in the Utrecht province; the general area is shown in Fig. 1. Heavy metals (copper, zinc, nickel, chromium, cadmium, mercury and iron) were also determined, but on a less regular basis, and are therefore omitted from this investigation. Physical descriptors such as flow rate of the water, detritus, plant growth, smell, colour, weather conditions and wind speed, are also not considered here. The geographical distribution of the surface waters of the Utrecht province includes: (1) the river Eem and its tributaries (route F, AM, G) to the east; (2) the combined rivers Kromme Rijn and Vecht at the centre in open communication with the Rhine at the Amsterdam-Rhine canal; (3) the waters of the meadows to the west; (4) waters in and around the city of Amersfoort; and (5) waters in and around the city of Utrecht.

The data set comprises about 150 000 measurements, collected during

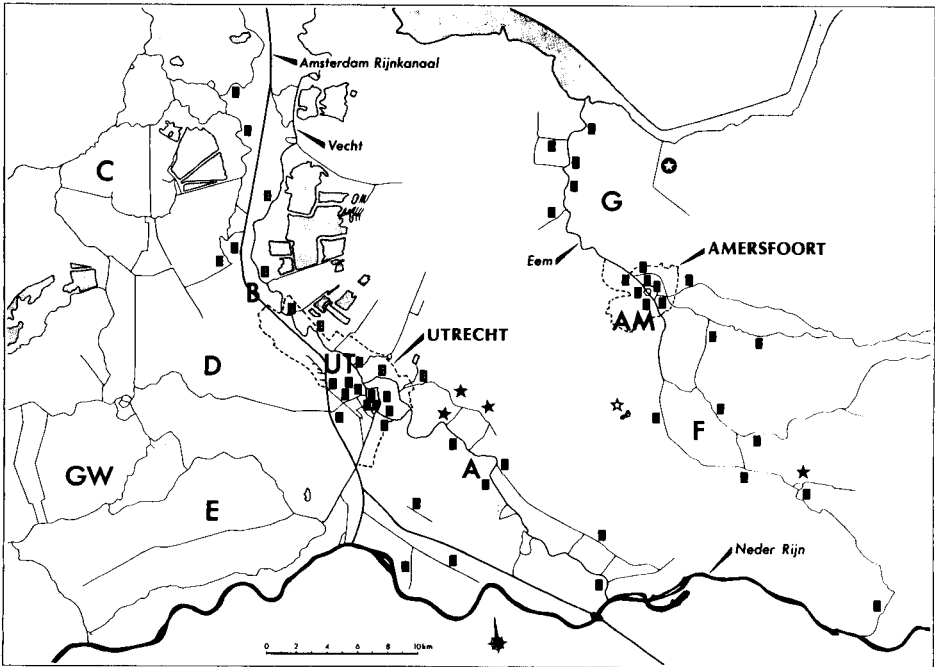


Fig. 1. Map of the province of Utrecht, with water sampling areas indicated. For further detail, see text.

1975–1982 at 110 sampling locations with a frequency of 2–48 samplings per year.

APPLICATION OF PATTERN RECOGNITION

In pattern recognition, a search is made for attributes with similar behaviour, here, water locations with about the same water quality. A pattern is defined here as a list of chemical measurements pertaining to a particular location, ordered in a vector. Each vector element denotes a particular chemical feature (e.g., ammonium or nitrate content). The order of the chemical features in a pattern vector is the same for all patterns (i.e., locations and/or sampling times). The end points of all vectors or patterns are positioned in a multidimensional feature space with the same dimensionality as the number of members in the vector. In pattern recognition, a search is made for vector and points (patterns) that cluster together in the feature space and denote water locations with similar chemical composition and thus, hopefully, similar quality.

Before the search for clusters was started, some preprocessing was needed. First, patterns where one or more features were missing were removed from the data matrix; patterns from locations that were examined less than six times a year were also removed. Of the sixteen features listed in Table 1, eleven were selected for description of the patterns (Table 2); features measured less frequently and/or with poor accuracy were removed. Then, because of the periodic behaviour of some features during the year, all features were corrected with a cosine function for seasonal fluctuations. This correction diminished the variance of the measurements per location and permitted a search for measurements that were obviously wrong (see Table 3) because of analytical or typing errors (6 patterns out of 110). After this seasonal correction, measurements during 1979–1982 were averaged per location.

From the original data matrix, 51 patterns were selected described by

TABLE 1

List of observed features^a

Feature	Symbol	Feature	Symbol
Temperature (°C)	T	Nitrate-nitrogen content ^b	NO ₃ -N
Oxygen content ^b	O ₂	Orthophosphate content ^b	o-PO ₄
Saturation with oxygen (%)	O ₂ %	Total phosphate content ^b	t-PO ₄
Biochemical oxygen demand ^b	BOD	Chloride content ^b	Cl
Chemical oxygen demand ^b	COD	Acidity	pH
Ammonium-nitrogen content ^b	NH ₄ -N	Conductivity (μS)	cond
Total nitrogen content ^b	Kj-N	Coliforms (ml ⁻¹)	MPNE
Nitrite-nitrogen content ^b	NO ₂ -N	Opacity (cm)	Op

^a 2–48 observations/year. ^b In mg l⁻¹.

TABLE 2

Features used in the initial pattern-recognition procedure, with variance weights

Feature	Variance weight	Feature	Variance weight	Feature	Variance weight
T	1.60	NO ₃ -N	3.36	pH	1.94
O ₂	1.68	o-PO ₄	2.41	cond	2.84
BOD	1.95	t-PO ₄	2.83	Op	1.83
NH ₄ -N	2.91	Cl	5.00		

TABLE 3

Correction for periodicity of the features and their variance weights

Feature	Amplitude ^a (mg l ⁻¹)	S.d. ^b	Phase ^a (radials)	S.d. ^b	Variance weight
NH ₄ -N	0.86	0.24	-0.45	0.42	6.55
NO ₃ -N	1.13	0.49	-0.77	0.70	6.27
o-PO ₄	0.37	0.12	2.24	0.64	5.24
O ₂	1.86	0.52	-1.16	0.44	2.12
BOD	1.15	0.74	-1.70	0.65	2.05

^a Averaged over 8 years. ^b Standard deviation based on the results from 8 years.

eleven features, from sampling points located along defined routes (A, UT, B; F, AM, G; Fig. 1). These patterns were used for the development of the first learning machine and are named the training set (see Table 5).

Standard pattern-recognition techniques [2-7] were used. All feature axes were autoscaled, to provide the same scale expressed in σ_i units, where σ_i is the standard deviation for feature i . The inter-feature Euclidean distances were calculated in order to construct a similarity matrix S where $S_{i,j} = 1 - D_{i,j}/D_{\max}$ denotes the similarity between two patterns i and j which are a Euclidean distance $D_{i,j}$ apart; D_{\max} is the maximum distance found in the inter-pattern distance matrix. Clustering was sought by means of the hierarchal technique and the minimal spanning tree.

This procedure resulted in four more or less distinct clusters of patterns, which after comparison with the map of the province could be named 'Vecht', 'Eem', 'Amersfoort city' and 'Rhine water inflow'. Hereafter, the supervised pattern recognition was started and improved clustering was obtained by weighting the features according to their ability to distinguish between these clusters (see Table 2). From this table it is seen that temperature, T , has the lowest weight (1.60), which is not surprising because in Utrecht there are no plants that produce excessive amounts of heat and thus spoil the ecological quality of water. It can also be seen that features such as O₂, Op, BOD and pH have relatively low variance weights and thus contribute little to the discrimination between clusters. The most important

features listed are Cl (5.00), $\text{NH}_4\text{-N}$ (2.91) and $\text{NO}_3\text{-N}$ (3.36). Because Cl results from the influx of Rhine water, and the aim is to describe water quality, where the chloride content is immaterial, the features Cl and cond that were highly correlated (correlation coefficient 0.77) were omitted from the data set. From the features t- PO_4 and o- PO_4 , which were almost ideally correlated with a correlation coefficient of 0.98, o- PO_4 was selected because its measurement is much less time-consuming than that of the total phosphate content, t- PO_4 . The features pH and Op were also removed because of their low discriminating ability.

This resulted in a new set of features, listed in Table 3, a new learning machine, and a somewhat revised clustering. In order to visualize the clustering, the features were linearly combined by means of a Karhunen-Loève transformation and ranked in decreasing amount of accounted variance. The two linear combinations (eigenvectors) with the highest variance (eigenvalues) define a plane on which the five-dimensional feature space may be projected with the least loss of information.

The importance of the various features in these two eigenvectors is seen in Table 4, in which the information content of the projected patterns is also listed. It must be noted that the algebraic signs of the features in the first eigenvector is the same (positive) but the signs of $\text{NH}_4\text{-N}$ and $\text{NO}_3\text{-N}$ in the second eigenvector are different. This is not apparent from their respective contributions, which follows from the squares of the coefficients. Figure 2 shows how the patterns are located in five different clusters; the notation of the various sampling locations in these clusters is listed in Table 5. The geographical implications of the clustering can be seen from Fig. 1. Although the clusters are named Eem, Vecht, etc., sometimes a surface water composition is found in, e.g., the Amersfoort cluster at a location

TABLE 4

Karhunen-Loève transformation: contribution of all five autoscaled and weighted features to the first two eigenvectors

Feature	Eigenvector	
	First ^a	Second ^b
$\text{NH}_4\text{-N}$	0.46	0.19
$\text{NO}_3\text{-N}$	0.23	0.68
o- PO_4	0.30	0.02
O_2	0.00	0.09
BOD	0.01	0.02
	1.00	1.00

Eigenvalue (i.e., information) $65 + 26 = 91\%$ ^c

^aAll signs the same. ^b $\text{NH}_4\text{-N}$ and $\text{NO}_3\text{-N}$ have different signs. ^cThe third, fourth and fifth eigenvectors contribute 6%, 2% and 1%, respectively.

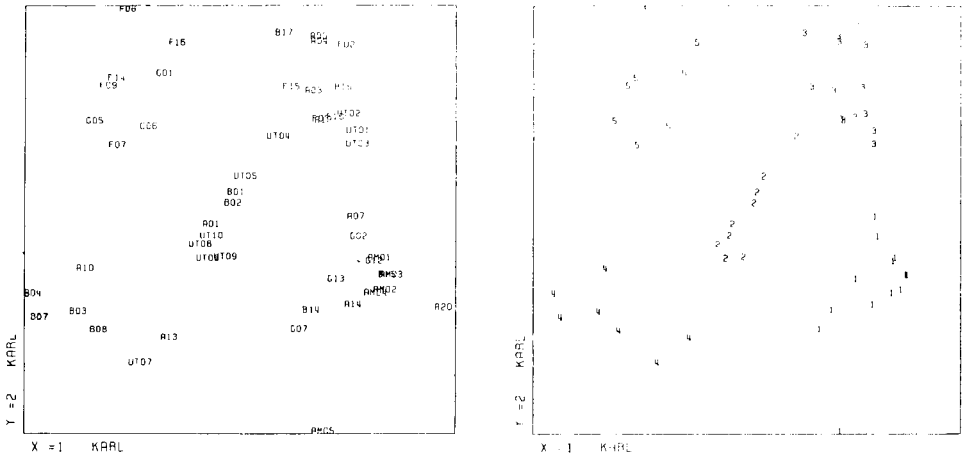


Fig. 2. Karhunen-Loève transformation based on five features of the training set after auto-scaling and weighting.

TABLE 5

Composition of clusters (see Fig. 1) in the training set

Cluster	Cluster no. ^a	Sample collecting location
Amersfoort	1	AM01, AM02, AM03, AM04, AM05; G02, G07, G12, G13; A07, A14, A20, B14, B15.
Utrecht	2	UT04, UT05, UT06, UT08, UT09, UT10; A01, B01, B02.
Rhine	3	UT01, UT02, UT03; F02, F06, F10, F15; A03, A04, A06, A19, B16, B17.
Vecht	4	B03, B04, B07, B08; A10, A13, UT07.
Eem	5	F07, F08, F09, F14, F16; G01, G05, G06.

^aCorresponding to the numbered squares in Fig. 1.

near the Vecht. This implies that the composition and thus the water quality is not always correlated with the geographical location suggested by the name of the cluster.

In order to relate the Karhunen-Loève transformation to the water quality, a global classification of the clusters is given in Table 6; only the most important features are presented to simplify the pattern. Of all the 3^3 possible quality classes, only five were actually encountered in practice.

The data set of 51 patterns used so far defines a so-called training set which is used to construct a learning machine. In order to visualize the time dependence of the location of the various sample points in the feature space, the patterns of each individual year 1979 up to 1983 were projected in the feature space defined by the learning machine and classified according to the nearest-neighbour method (Table 7). In order to simplify the table only

TABLE 6

Global classification of clusters based on the most important features

Cluster	Feature		
	NH ₄ -N	NO ₃ -N	t-PO ₄ ^a
Amersfoort (city)	low	low	low
Rhine (river)	low	medium	low
Utrecht (city)	medium	medium	medium
Vecht (river)	high	medium	high
Eem (river)	medium	high	high

^aBecause of the high correlation between o-PO₄ and t-PO₄ (0.98) only one of these was selected for this classification.

TABLE 7

Classification of sample locations that show a time-dependent quality^a

Sample location	Cluster no.	Classification in various years			
		1979	1980	1981	1982
AM05	1	1	1	1/2	1
A07	1	3	1	3	2
A14	1	4	1	1	1
A20	1	4	1	1	1
B14	1	1/2	1	1	1
B15	1	1	1/3	1	1
G02	1	3	1	1	1
G13	1	1	1	1	2
UT04	2	3	2	2	3
UT08	2	2	2/4	2	2
UT09	2	2	2/4	2	2
A19	3	4	3	3	1
B16	3	1	3	3	3
B17	3	1	3	3	3
A10	4	4	5	5	4
A13	4	4	2/4	2/4	2
UT07	4	4	4	2	2
F08	5	5	5	5	5/2
G06	5	2	5	5	5

^aThe nearest-neighbour method was used.

those sampling points are listed that move from one cluster towards another. Table 7 provides justification of the variance reduction obtained by averaging the analytical results over four consecutive years. The moving of one sampling point (A19) can readily be explained because a water purifica-

tion plant was started in that year (1980). The change over of the other sampling points results from their position near the 'boundary' of two clusters which strongly influences the nearest-neighbour voting system.

The classification of the entire collection of sampling locations was completed by positioning the four-yearly average patterns in the feature space of the training set (see Table 8). The patterns were again classified according to the nearest-neighbour method. In situations where the nearest neighbours were found in different clusters, the patterns are attributed to both clusters. The process is visualized in Fig. 3, where a Karhunen-Loève projection is given for the training set and the test set comprising 53 of the other sampling locations of Utrecht. It can be seen that the different clusters

TABLE 8

Classification of sample locations collected in a test based on the mean composition over four years

Cluster	Cluster no.	Sampling location
Amersfoort	1	C03, C04, C06, C11, C15, C16, C18, C20, D01, D03, E07, E08, E09, E10, E11, E17, E18, E19, F10a, G08, GW01, GW02, GW03, GW06, GW09, GW14, GW15, GW17, GW18, P01, P02, P03, P04, P06, P07, A07, A14, A20, B14, B15.
Utrecht Rhine	2	C10, D01, E01, GW04, GW06, GW11, GW12.
	3	C10, C21, D11, D11a, D12, D14, E01, E03, E04, E05, E12, E16, GW10, GW12, GW13.
Vecht	4	A11, A12, A13a, D02, F05, GW16.
Eem	5	—

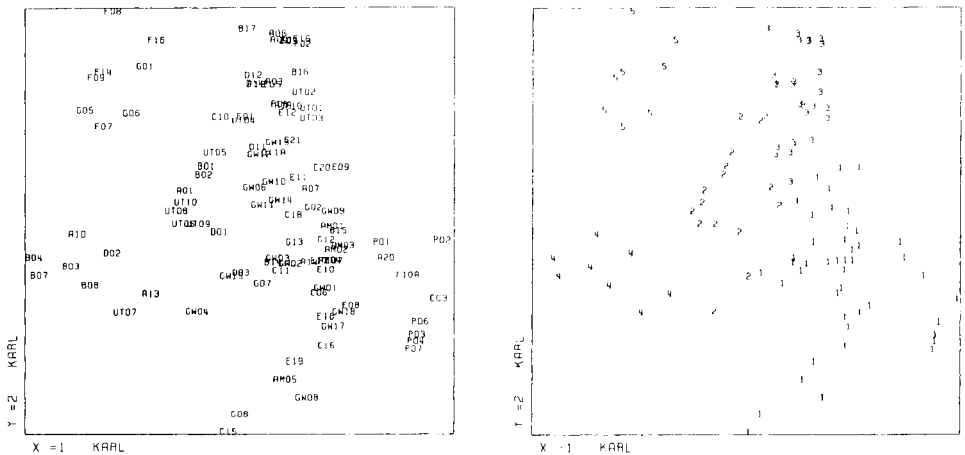


Fig. 3. Training set and test set patterns, composed from four-year average values of 53 other sampling locations.

cannot be linearly separated (separated by a flat plane in the multidimensional space) but the separation is clearly seen.

In order to interpret the clustering, the eigenvectors must be inspected more closely. Thus, the main contribution towards the first eigenvector is given by $\text{NH}_4\text{-N}$, o-PO_4 and $\text{NO}_3\text{-N}$ (see Table 4). The data listed are the squares of the coefficients of the scaled and weighted features. As the coefficients have equal signs, the combined nutrients, phosphate and nitrate/ammonia, provide a first descriptor of quality. The second eigenvector shows an important contribution of nitrate-nitrogen and to a less extent $\text{NH}_4\text{-N}$, but here the signs of these coefficients are different. It is tempting to interpret this eigenvector as the effect of aeration on the oxidation of $\text{NH}_4\text{-N}$ towards $\text{NO}_3\text{-N}$, which should have a beneficial effect on the quality of the water. From a biochemical point of view, one could say that the first eigenvector represents eutrophication and the second one aeration. A less speculative physicochemical interpretation of the water quality based on the results of the eigenvector projection is to regard the first eigenvector as the total ionogenic nitrogen and phosphate (TINP) and the second one as the nitrogen redox balance (NRB). A projection of the patterns of the training set on a plane defined by these parameters shows that the clustering is not inferior to that of the eigenvectors from the Karhunen-Loève transformation (Fig. 4).

From Fig. 4, it is obvious that on the horizontal axis (TINP) the points on the right-hand side indicate poor water quality. On the vertical axis, the higher points contain more $\text{NO}_3\text{-N}$ than $\text{NH}_4\text{-N}$, which can be interpreted as corresponding to better water quality according to the oxygen content of the water. However, this new feature is correlated to the nutrient content of the water; the difference between $\text{NO}_3\text{-N}$ and $\text{NH}_4\text{-N}$ can be high although the nutrient content may be low. According to this point of view, the

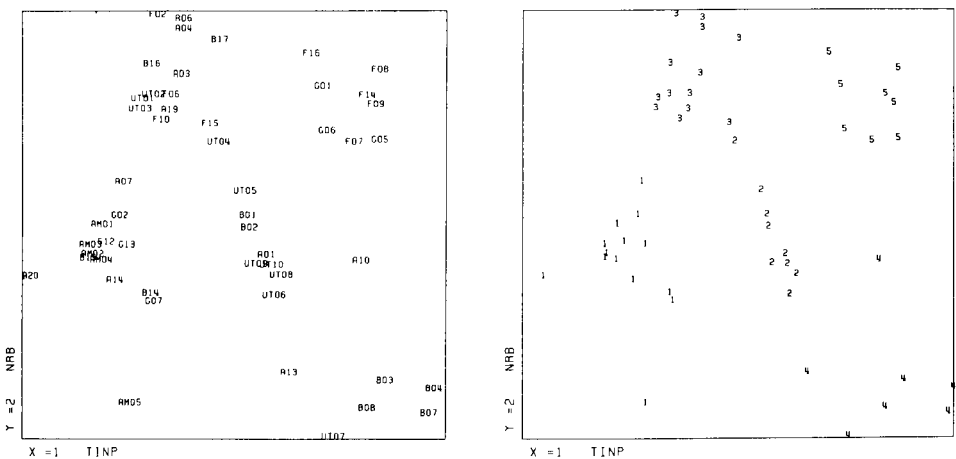


Fig. 4. Training set pattern projected on a plane defined by TINP and NRB.

patterns in the left upper corner show good water quality, while those in the right upper corner show bad quality because of nutrient content; in the left lower corner the quality is poor because of low oxygen content and in the right lower corner the quality is bad for both reasons. The patterns in the centre square are not of high quality, but the reason for this is obscure. From this point of view, there are very few points with good water quality in the province of Utrecht.

Another important observation pertaining to water quality is that other parameters such as oxygen content and BOD, which have been considered as important in the past, seem to play an insignificant role in the clustering procedure. This means that these parameters have almost the same numerical value in each cluster and in this respect the quality of the clusters is about equal. The effect of heavy metals and bacteriological concentrations on the quality of the water is not taken into account in this study. This is not because their influence on water quality is rated as unimportant, but because the low frequency of these measurements made their assessment meaningless.

Conclusions

In a pattern recognition procedure applied to about 150 000 observations of chemical and physical conditions of surface water in the province of Utrecht, collected at 110 locations during 1975–1982, a training set of 51 locations described initially by eleven features averaged over four years was selected. This training set provided a learning machine that showed five, mainly geographically distinguishable, clusters with different water qualities. The features could be subdivided into two groups of features, one comprising chloride and conductivity that here has little connection with water quality, and another comprising $\text{NH}_4\text{-N}$, $\text{NO}_3\text{-N}$, o-PO_4 , O_2 and BOD that does relate to water quality.

Contrary to expectation, oxygen content and BOD, normally regarded as important from an ecological point of view, are not important for distinguishing different clusters. A good description of the clustering was found with two (composed) parameters only: total ionogenic nitrogen and phosphate (TINP) which is a simple addition of autoscaled values for $\text{NH}_4\text{-N}$, $\text{NO}_3\text{-N}$ and o-PO_4 , and the nitrogen-redox balance (NRB) which is the absolute value of the difference between autoscaled $\text{NH}_4\text{-N}$ and $\text{NO}_3\text{-N}$ data. Based on these two parameters, the patterns of the training set were well separated. Addition of the other sampling locations, collected in a test set comprising 53 locations averaged over the same period of four years, showed the same clearly distinguishable clustering. Projection of patterns from sampling locations of individual years enhanced the intra-cluster variance but did not spoil the clustering. Interpretation of the descriptors as the total amount of fertilizer, producing eutrophication, and aeration of water needing purification, seems attractive but has no biological justification at present.

We thank the Provinciale Waterstaat Utrecht for generously supplying us with the data on water quality, Mr P. van Iersel of the Provinciale Waterstraat Utrecht for his interest in this work, Professor B. R. Kowalski for making the ARTHUR computer program (1975 version) available to us, and Mr F. van Pelt for his contribution to this work.

REFERENCES

- 1 Kwaliteit oppervlakte water provincie Utrecht 1975—1980, Provinciale Waterstaat Utrecht, Utrecht, 1982.
- 2 G. Kateman and F. W. Pijpers, *Quality Control in Analytical Chemistry*, Wiley, New York, 1981.
- 3 D. L. Massart, A. Dijkstra and L. Kaufmann, *Evaluation and Optimization of Laboratory Methods and Analytical Procedures*, Elsevier, Amsterdam, 1978.
- 4 B. R. Kowalski, *Chemometrics: Theory and Applications*, Am. Chem. Soc., Washington, D.C., 1977.
- 5 J. T. Tan and R. C. Gonzales, *Pattern Recognition Principles*, Addison-Wesley, Reading, MA, 1979.
- 6 R. C. Jurs and T. R. Isenhour, *Chemical Applications of Pattern Recognition*, Wiley, New York, 1975.
- 7 T. R. Isenhour, B. R. Kowalski and R. C. Jurs, *CRC Crit. Rev. Anal. Chem.*, 4 (1974) 1.

IMPROVEMENT OF THE REPRESENTATION OF WATER QUALITY BY APPLICATION OF INFORMATION THEORY

J. H. M. BARTELS, T. A. H. M. JANSE, F. W. PIJPERS* and P. C. THIJSSEN

Department of Analytical Chemistry, Catholic University, Toernooiveld, 6525 ED Nijmegen (The Netherlands)

(Received 9th October 1984)

SUMMARY

The quality of surface waters depends on chemical, physical and biological properties. An official definition of normal values of various chemical constituents for the construction of a classification scale of water quality has been in use for some years; water quality of each sampling location is presented on geographical maps by colour codes. The information content of these maps has decreased considerably in recent years, because of improving water quality. In the method described here, a different selection of class boundaries is used, so that all classes are well populated, and data are weighted to emphasize extreme situations. This improves the information content of the maps, simplifying choices of locations for remedial action.

In connection with a general study of the deteriorating quality of surface waters in the Netherlands, a quality index number was constructed, based on the measured values of oxygen content, biological oxygen demand (BOD), and ammonium ion content ($\text{NH}_4\text{-N}$); values for phosphates (t-PO_4) were also obtained. The selection of these variables from a set of many others, including heavy metal content and bacteriological concentrations, was not based on theoretical considerations, but was intended merely to serve as a practical means of reducing the enormous amount of physical and chemical data that were collected over a year to manageable proportions. The measurements on O_2 , BOD, $\text{NH}_4\text{-N}$ and t-PO_4 were collected, averaged per year and grouped in five classes with fixed class boundary values [1]. The classes were mutually distinguished with these class values for each of the water constituents mentioned and the final ranking of the quality, according to this system, followed from a summation of this yearly average of the class values for the individual constituents O_2 , BOD and $\text{NH}_4\text{-N}$. The classes were represented by a colour code, ranking from red for ecologically bad water, via orange, yellow and green, to blue for water with high ecological quality. On geographical maps, this colour code was used to paint the various streams and lakes in order to provide a broad indication of quality even to unskilled observers. However, because of various governmental actions taken some years ago, the quality of the surface waters improved considerably and thus some of the colours (e.g., red and orange)

no longer occurred on the quality maps. This had two implications: (1) the information yield per map diminished and the original code became obsolete; and (2) the quality of the water was no longer monitored in the best possible way, because other adverse effects, such as those of heavy metals or nutrients, which became more important as the primary effects were improved, were not visualized.

These observations were an incentive to investigate whether the information transfer could be enhanced with a modified quality index, and if it would be advisable to monitor other physicochemical features. The latter question was investigated by means of pattern recognition [2]; the problem of information yield is discussed in this paper.

INFORMATION THEORY

In order to compare different analytical procedures and methods, information theory can be useful [3–6]. According to this theory, each sample (e.g., sample of surface water) contains undeveloped or latent information that can be developed, at least partially, by application of analytical procedures. Thus an amount of latent information is converted to actual information; phrased in another way, the entropy of the sample, in the sense of information theory, is decreased. This statement can be quantified by comparing the number of possibilities relevant to the composition of the sample before and after the chemical analysis. The information gain thus depends on the analytical method chosen. In order to count the number of possibilities before the chemical analysis, a distribution function of all possible analytical results should be defined. Such a function may become a discrete one, by defining a finite resolution for each analytical method chosen.

A single measurement is thus represented by one number. A series of measurements results in a series of numbers that can be represented by a distribution function. Such a distribution function may be compared with a reference distribution function that represents the maximal information obtainable from a system, or with only that particular piece of information that is sought.

The representation of such a comparison generally suffers from a loss of information. If the reference distribution is found in the experimental results, this loss is minimal. However, if only one class is populated in the series of measurements, the loss is maximal. The entropy of representation produced by the measurements depends on the known reference distribution of the variable under investigation. This may be defined as decrease in relevant entropy and follows from Shannon's equation

$$H = - \sum_{i=1}^N P_i^* \text{ld } P_i^*$$

where H describes the relevant entropy developed by the representation of the results. Information is found from a change in the relevant entropy before and after the chemical analysis, and P_i^* is found from

$$P_i^* = W_i n_i / \sum_{i=1}^N W_i n_i$$

Here P_i^* is based on the discrete population n_i of class i , which is known from the chemical measurements, N is the number of classes and W_i is the weight of class i , based on the previously estimated probability of occurrence. The maximal value for H is found when all P_i^* values are equal, and is $H_{\max} = \text{ld } N$. Here a discrete rectangular reference distribution for N classes is described with the weights $W_i = 1$ for $i = 1, 2, 3 \dots N$. This provides the orthodox Shannon formulation.

However, it is likely in practice that situations where all classes show an equal population will be of little interest. Situations where only a few sampling points are found to show poor water quality, will prompt a more adequate, faster reaction of the responsible authorities than situations in which 1/5 of the sampling locations are bad and any incentive for action must be based on a (random) selection. Such situations, pertaining to clinical chemical analyses, have been described [7]; an attention function was formulated in order to focus the attention of the physician on extremely abnormal situations. The attention score was constructed by means of well chosen W_i values.

For example, if it is assumed that the original distribution function is Gaussian, and that the class boundaries lie in the ranges $|\infty, -3\sigma|$, $|-3\sigma, -\sigma|$, $|\sigma, +\sigma|$, $|+\sigma, +3\sigma|$ and $|+3\sigma, +\infty|$, then the surfaces below the distribution function will be 0.0013, 0.1574, 0.6826, 0.1574 and 0.0013, respectively. In order to describe these possible classes with equal intensity, the weight factor W_i would be 796.13, 6.67, 1.47, 6.67 and 769.13, respectively. According to this mathematical concept, the frequency distribution for different measurements (e.g., the $\text{NH}_4\text{-N}$ and o-PO_4 contents) may yield new classes, each formed by combination of one $\text{NH}_4\text{-N}$ class and one o-PO_4 class, producing a histogram with more detail. Here each combination gets its own P_i^* value. If the classes are unequally populated (i.e., different values for n_i are found for different combinations), the entropy may be optimized by choosing W_i values, such that $W_i n_i = 1/N$ for each class. In order to do this, the class boundaries for the individual measurements may be chosen such that classes with equal values for $W_i n_i$ are formed. This can be done sequentially for all measured variables until the decrease in entropy becomes insignificant. Thus the number of relevant variables to be taken into account can be found.

The total information gain arising from measurement of the second variable is less than the sum of the information gains of the individual variables because of the correlation between variables 1 and 2. For discrete classes, constructed by combination of the classes for the individual variables,

this is accounted for by counting the population of the classes. This correlation may be exemplified by considering the determination of $\text{NH}_4\text{-N}$ and o-PO_4 for ammonium dihydrogenphosphate; the determination of o-PO_4 produces no additional information on the content of this compound in the sample, if $\text{NH}_4\text{-N}$ has already been determined, if the precisions of the $\text{NH}_4\text{-N}$ and o-PO_4 measurements are the same, and if the sample does not contain either component from a different source.

WATER QUALITY

The description of water quality in the Netherlands is based on a set of chemical compositions listed in the IMP (Indicative Multiyear Planning), which are all positioned in one of five classes with fixed class boundaries. This provides the basis for a reference distribution which is used for comparison with the frequency distribution encountered in one particular year. The investigations described here are based on a data set measured and collected by the laboratory of Provincial Waterstaat Utrecht [1]. This data set was described in the preceding paper (see Fig. 1 and Table 1) [2]. From the set of 16 frequently measured physicochemical variables, only three are used to describe water quality by means of the IMP quality index number and its associated colour code. These variables are grouped in five classes, each of which theoretically allows a representation of entropy of $\text{ld } 5 = 2.32$ bit per variable per sampling point, provided that all classes are of equal population. The code-coloured map thus presents information corresponding to 2.32 times the number of sampling locations, assuming that there is no correlation between sampling points. However, if only two of the five classes are populated, the entropy drops from $M \times \text{ld } 5$ to $M \times \text{ld } 2$ (i.e., M bit) where M represents the number of sampling locations.

The representation of entropy for three variables, O_2 , BOD and $\text{NH}_4\text{-N}$, could theoretically amount to 3×2.32 bit per sampling point, provided that the three variables are completely uncorrelated. This implies that all 5^3 possible combinations of individual variable classes actually are found in practice. During recent years, the reference distribution has differed to such an extent from the situation actually found, that the entropy cannot be described optimally [1].

RESULTS AND DISCUSSION

The selection of $\text{O}_2\%$, BOD and $\text{NH}_4\text{-N}$ as variables for the description of the quality of surface waters by means of a single quality index requires some comment. The choice of oxygen content is obvious because the growth of micro-organisms, vegetation and fish depends on it. Chemically, however, this is not a good descriptor because the results for oxygen depend strongly on the time of day, illumination and temperature of the water. This makes any comparison of results obtained at different sampling locations and times

very dubious, and leads to high variance [2]. The measurement of BOD is not easily reproducible and is time-consuming. Because of the improved quality of the water in very recent years, the descriptive value of these variables has become low. However, they may serve to illustrate the improved quality description based on information theory.

For a start, all sampling locations along the river Eem were selected, route F, AM and G (see Fig. 1 in [2]) and the measurements during 1975 up to 1982 were collected. For each of the variables ($O_2\%$, BOD and NH_4-N), histograms were constructed (Fig. 1). In these histograms, new class boundary levels were constructed in such a way that $W_i = 1$ and all five P_i^* values for each class equal 0.2, for each individual year and for each constituent. This ensures a maximum amount of entropy per constituent. Later, this was done for all data. In practice, a class boundary is sometimes found that would separate some of the measured results of a given value in one class from the same values found in an adjacent class. In such situations, all measurements of the same value are collected in one class; this is at the expense of the maximal obtainable entropy.

The $O_2\%$ class boundary levels were chosen such that $O_2\% < 100\%$ were classified in five equivalent classes, as were values $> 100\%$. The population of the classes higher than 100% was added to that of the classes below 100%, i.e., the data of class 2 in the range 105–109% were added to the data of class 2 in the range 65–79% (see Table 1). This procedure was used to calculate the boundary levels for each year. Figure 2 shows how the class boundaries for class 3 varied during 1975–1982 for $O_2\%$; the classes fluctuate around a given value. The same procedure was used to construct the time dependence of the class boundaries for BOD and for NH_4-N . It can be seen from Fig. 2 that all the class boundaries for class 3 of the BOD gradually decrease with time. This reflects the improvement of the water quality.

In order to describe the water quality in the sense of information theory, a reference base is needed. Here BOD would cause problems, because of its time dependence in recent years. However, the earlier investigation by means of pattern recognition [2] showed that the weight of this variable was so low that the BOD value did not contribute to the discrimination of various types of water. Because of this, and because comparison between the quality index for successive years was sought, a constant reference base was selected, based on class boundary values obtained by averaging the values for 1975–1982. For the features $O_2\%$ and NH_4-N , this caused little difficulty because here the boundary levels fluctuate around a fixed value (see Fig. 2).

For this reference base, the entropy was calculated. Table 2 shows a comparison between the entropies calculated in this way and according to the traditional class boundaries. Although the theoretical amount of 2.32 bit (i.e., $\log_2 5$) is never reached, because of the averaging of the class boundaries and the collecting of data with the same value in one class, the new system loses much less information than the traditional one. Table 2 also

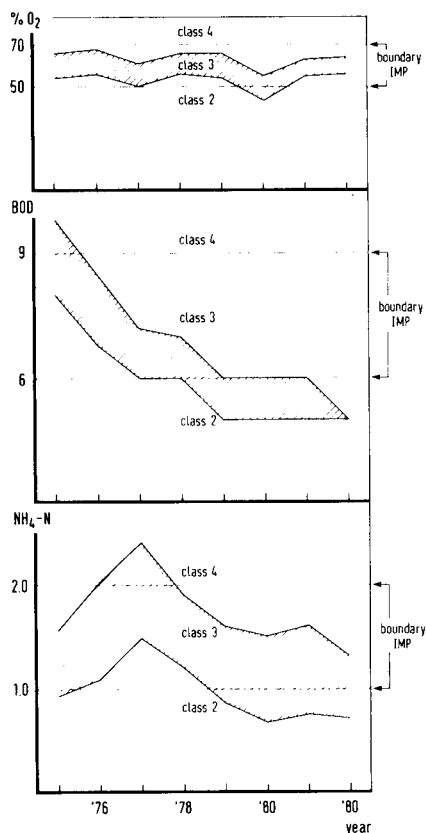
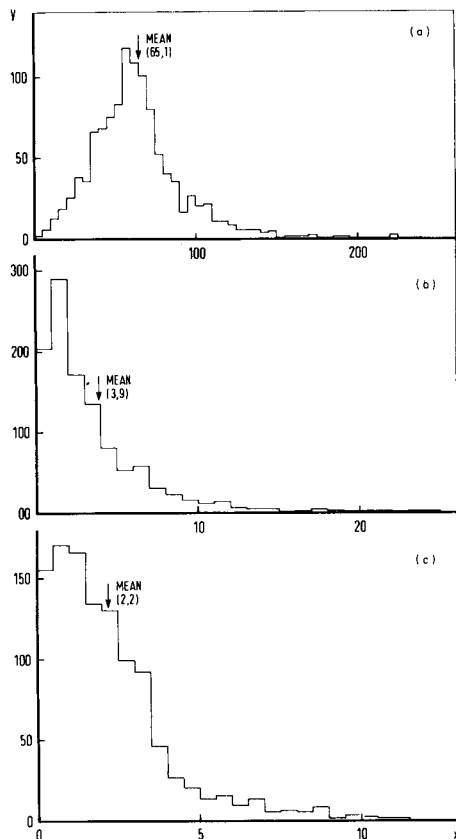


Fig. 1. Frequency distribution function of the three constituents: (a) $O_2\%$; (b) BOD; (c) NH_4-N .

Fig. 2. Class boundary values for $O_2\%$, BOD and NH_4-N during eight years. The boundary values between class 2 and 3, with equally populated classes, and those of 3 and 4 are defined on the base of maximal information gain. The conventional class boundary values are also indicated.

shows a comparison between the IMP classification calculated in the traditional way from the variables $O_2\%$, BOD and NH_4-N with fixed class boundary values, and that based upon optimally chosen class boundary values, obtained from averaging over the eight years (Table 1). The relative entropy calculated in the latter way is higher than that with traditional class boundaries for all the years considered. However, the entropy with new class boundaries is again below the maximum of 2.32 bit because of the algorithm used to calculate the IMP quality classes. In this algorithm, the class numbers of each variable of each sample are added. The number of combinations resulting in quality class 1 or 5 is only 4, that of combinations for

TABLE 1

Comparison between old class boundary values (IMP) and newly defined boundaries pertaining to maximized information transfer. The new class boundaries are the values averaged over eight years

Variable	Class boundaries	Class boundaries				
		1	2	3	4	5
O ₂ %	IMP	91-100	71-90	51-70	31-50	≤30
	New	101-110	111-120	121-130	—	>130
BOD	IMP	80-100	65-79	55-64	40-54	<40
	New	100-104	105-109	110-119	120-134	≥135
NH ₄ -N	IMP	≤3	≤6	≤9	≤15	>15
	New	≤1	≤2	≤3	≤5	>5
NH ₄ -N	IMP	≤0.5	≤1.0	≤2.0	≤5.0	>5.0
	New	≤0.5	≤1.0	≤1.75	≤3.0	>3.0

TABLE 2

Entropy of representation according to IMP class boundaries, compared with that according to the new boundaries (The maximum for five equally populated classes is $\text{ld } 5 = 2.32 \text{ bit.}$)

Year	O ₂ %		BOD		NH ₄ -N		Entropy	
	IMP	New	IMP	New	IMP	New	IMP	New
1975	1.99	2.23	1.40	1.03	1.95	2.19	1.59	1.75
1976	1.91	2.12	1.42	1.41	2.06	2.24	1.70	1.81
1977	1.96	2.20	1.44	1.61	1.66	1.91	1.36	1.56
1978	1.88	2.20	1.48	1.94	1.86	2.10	1.39	1.71
1979	1.81	2.15	1.27	1.99	2.09	2.28	1.50	1.89
1980	1.87	2.06	1.59	2.06	2.17	2.30	1.66	1.90
1981	1.87	2.21	1.21	2.03	2.07	2.24	1.41	1.76
1982	1.67	2.02	1.09	2.05	2.06	2.24	1.45	1.73

class 2 or 4 is 31 and that for class 3 is 55. If each of these 125 combinations has an equal probability of occurrence (which will not be the case), the distribution over the quality classes will be exactly normal. In other words, the reference distribution is normal and even when the distribution actually found is congruent with the reference distribution, the maximum information gain of 2.32 bit will not be obtained.

Because the orthodox Shannon formula counts every class with equal weight and is therefore used when a rectangular reference distribution is

needed, relevant information theory should be used for IMP representations. If one aims for a normal distribution, the information gain should be calculated with weighted classes. Table 3 lists the population of the various traditional classes by year; H_{abs} represents the entropy from the traditional IMP procedure with fixed class boundary values for the variables. This entropy is low (see Table 1). To calculate the relative entropy, H_{rel} , weighting values of 14.97, 4.14, 2.22, 4.14 and 14.97 were used, as obtained from the reciprocal of the surface below the Gaussian curve with class boundaries $|\infty, -1.8\sigma|, |-1.8\sigma, -0.6\sigma|, |-0.6\sigma, +0.6\sigma|, |+0.6\sigma, +1.8\sigma|$ and $|+1.8\sigma, +\infty|$. This H_{rel} is somewhat higher than the orthodox entropy, H_{abs} , but is still poor, because the distributions are extremely skew, especially in the later years. Most years there were no locations with water quality in class 5.

In Table 4, the class boundary values calculated as recommended above (Table 1) are used to calculate, with the IMP algorithm, the quality class of

TABLE 3

Distribution of sampling locations over the IMP quality classes^a

Year	Class ^b					H_{abs}	H_{rel}
	1	2	3	4	5		
1975	8	42	79	17	0	1.59	1.90
1976	9	58	52	13	1	1.70	1.97
1977	3	27	68	9	0	1.36	1.86
1978	4	65	65	7	0	1.39	1.70
1979	11	63	61	5	0	1.50	1.66
1980	9	54	68	9	3	1.66	2.09
1981	11	74	40	3	0	1.41	1.52
1982	14	59	43	1	0	1.45	1.44

^a H_{abs} and H_{rel} are, respectively, the orthodox and the weighted entropy in bits. Weighting is done as described in the text. ^bClass 1 is good and 5 is bad.

TABLE 4

Distribution of sampling locations over the new quality classes

Year	Class					H_{abs}	H_{rel}
	1	2	3	4	5		
1975	0	15	67	46	18	1.75	1.64
1976	3	14	65	38	13	1.81	2.04
1977	0	6	48	45	8	1.56	1.72
1978	3	14	73	42	9	1.71	2.16
1979	7	34	48	48	3	1.89	2.24
1980	4	19	59	48	13	1.90	2.11
1981	4	39	57	26	2	1.76	2.25
1982	4	38	54	19	2	1.73	2.24

every location. Again, the population of each class is followed by year. The column H_{abs} indicates that the entropy calculated from the traditional Shannon equation is somewhat better than that of the normal calculation of IMP classes (see Table 1). However, here the relative entropy H_{rel} is far better and closer to the ideal 2.32, especially in the later years. The weighting values were the same as those used for Table 4 to calculate H_{rel} . The distribution over the quality classes approaches the normal distribution which the IMP aims to achieve. An observer can readily select the locations with very bad and very good water quality without paying attention to the locations with intermediate water quality. The number of these very bad and very good locations is now sufficiently low for attention to be attracted quickly to these locations on a colour-coded map (cf. [7]).

Conclusions

The information content of geographical maps, coloured according to the IMP standard method for description of the quality of surface waters, is below the optimal possible information transfer. This is due to the relatively low proportion of the red and orange classes, representing water with inferior quality, in recent years. Another selection of class boundaries, such that all classes become about equally populated, enhances the entropy of the colour-coded maps considerably. A disadvantage of this change is the time-dependence of the judgement, which makes it difficult to compare the situations encountered in successive years.

Another approach to the information-transfer problem involves weighting of classes so that "extreme" situations get a relative high weight in comparison with "normal" situations. Such information may be useful when action on water purification is wanted and a location for action has to be chosen from various possible locations.

The authors thank Drs. P. van Iersel, Provinciale Waterstaat Utrecht, for making the measurements available, and for his interest in this work.

REFERENCES

- 1 Kwaliteit oppervlaktewater provincie Utrecht 1975-1980. Provinciale Waterstaat Utrecht, 1982 (in Dutch).
- 2 J. H. M. Bartels, T. A. H. M. Janse and F. W. Pijpers, *Anal. Chim. Acta*, 177 (1985) 35.
- 3 G. Kateman and F. W. Pijpers, *Quality Control in Analytical Chemistry*, Wiley, New York, 1981.
- 4 K. Eckschlager and V. Štěpánek, *Anal. Chem.*, 54 (1982) 1115A.
- 5 C. E. Shannon and W. Weaver, *The Mathematical Theory of Communication*, University of Illinois Press, Urbana, 1949.
- 6 D. L. Massart, A. Dijkstra and L. Kaufman, *Evaluation and Optimization of Laboratory Methods and Analytical Procedures*, Elsevier, Amsterdam, 1978.
- 7 H. M. J. Goldschmidt, J. F. Leyten and M. N. M. Scholten, *Anal. Chim. Acta*, 150 (1983) 207.

KALMAN FILTER APPLIED TO SETPOINT CONTROL IN CONTINUOUS TITRATIONS

P. C. THIJSSSEN*, N. J. M. L. JANSSEN and G. KATEMAN

Department of Analytical Chemistry, Faculty of Sciences, University of Nijmegen, Toernooiveld, 6525 ED Nijmegen (The Netherlands)

H. C. SMIT

Laboratory for Analytical Chemistry, University of Amsterdam, Amsterdam (The Netherlands)

(Received 25th May 1985)

SUMMARY

A state-space model is described for continuous titrations based on first-order dynamics. The Kalman filter allows on-line monitoring of an empirically established setpoint in the titration curve. The algorithm advocated is examined for potentiometric titrations of ca. 10^{-3} M solutions of acids, silver(I) and copper(II). Only gross indications of the essential parameters such as the time constant and noise covariances are required. The computer-controlled titration system is compared with a conventional setpoint titrator. Especially in cases of slow response times and steep inflections, there are advantages in both accuracy and speed when the Kalman filter is applied.

Titrimetric methods are widely used in chemical analysis because of their precision, accuracy and easy operation. Unknown samples are usually evaluated by adding known amounts of titrant until the equivalence point corresponding to stoichiometric reaction has been reached. If large numbers of samples have to be processed, manual operation becomes tedious and costly, thus automated titrators are now in widespread use, ranging from simple hardware devices to computer-controlled assemblies which handle the entire process from sample changing to output of the evaluated results [1–5]. In general, automated titrations can be of two types, one in which the complete titration curve is monitored and the other in which the addition of titrant is stopped as soon as a preset signal is reached. In potentiometry, the setpoint titration with feedback control is based on the assumption that the overall response time of the reaction, the mixing and the detector is fast. Obviously, the electrode must be reproducible and stable in the region of the setpoint. These conditions are fulfilled in many titrations, but if a slow response time is combined with a steep inflection, setpoint control may become time-consuming and the results inaccurate because of overshoot. Correctly, these titrations should be done by the equilibrium method: after each addition of titrant, the signal is allowed to equilibrate before measurement. The

titration can be done with equal volume increments or with proportional control to obtain equidistant potentials. In combination with cheap personal computers, these well established titration techniques have increased in popularity for routine purposes.

The present paper features the application of state-estimation techniques in automated titration systems. A state-space model was presented previously to estimate the potentiometric equilibrium curve with its first and second derivatives [8]. However, the Kalman filter causes a systematic deviation in the estimated state and in the location of the evaluated inflection points or end-points in the titration curve. This effect can be eliminated by an off-line modification of the Kalman filter called fixed-interval smoothing. Implementation of the Kalman filter allows on-line control of the volume addition in order to obtain equidistant measurements. This paper describes the extension of the state-space model for continuous titrations. The titrant is added continuously and the variation of the measured signal is recorded simultaneously. To achieve the final results, the dynamics of the titration system have to be investigated. A possibility of this approach is on-line control to a preset setpoint in the equilibrium curve by the Kalman filter. Therefore, the optimal settings of the tuning parameters, which determine the precision, accuracy and speed of the titrimetric analysis, were studied. The proposed algorithms are demonstrated in practice with a computer-controlled titrator and the results are compared with those obtained from a conventional setpoint titrator.

THEORY

Continuous titration model

A first-order linear dynamic system can be described by the following differential equation:

$$dx/dt + 1/T_x x = x_\infty \quad (1)$$

where x denotes the response at time t , T_x is the time constant and x_∞ is the steady state reached at $t = \infty$. Over a sampling period Δt , introducing $\phi = \exp(-\Delta t/T_x)$, the system can be represented in discrete time terms by

$$x(t + \Delta t) = \phi x(t) + (1 - \phi)x_\infty \quad (2)$$

Approximating the non-linear titration curve in the volume domain V with a second-order Taylor expansion readily provides the equations [8]

$$\begin{aligned} x(V + \Delta V) &= x(V) + \dot{x}(V)\Delta V + \frac{1}{2}\ddot{x}(V)\Delta V^2 \\ \dot{x}(V + \Delta V) &= \dot{x}(V) + \ddot{x}(V)\Delta V; \ddot{x}(V + \Delta V) = \ddot{x}(V) \end{aligned} \quad (3)$$

where x denotes the function value, \dot{x} the first derivative and \ddot{x} the second derivative at a given point of the titration curve. Replacing x_∞ in Eqn. 2 by $x(V)$ and employing the definition of $x_1(k) \equiv x(t + \Delta t)$, $x_2(k) \equiv x(V + \Delta V)$, $\dot{x}_3(k) \equiv \dot{x}(V + \Delta V)\Delta V$ and $x_4(k) \equiv \ddot{x}(V + \Delta V)\Delta V^2$ results in the required

state-space model:

$$\begin{pmatrix} x_1(k) \\ x_2(k) \\ x_3(k) \\ x_4(k) \end{pmatrix} = \begin{pmatrix} \phi & 1-\phi & 0 & 0 \\ 0 & 1 & 1 & \frac{1}{2} \\ 0 & 0 & 1 & 1 \\ 0 & 0 & 0 & 1 \end{pmatrix} \begin{pmatrix} x_1(k-1) \\ x_2(k-1) \\ x_3(k-1) \\ x_4(k-1) \end{pmatrix} + \mathbf{w}(k-1)$$

$$z(k) = (1 \ 0 \ 0 \ 0) \begin{pmatrix} x_1(k) \\ x_2(k) \\ x_3(k) \\ x_4(k) \end{pmatrix} + v(k) \quad (4)$$

Volume and time units are related to each other by the equation $\Delta V = \rho \Delta t$, where ρ is the rate of titrant addition. The given set of difference equations is an inferior approximation of the non-linear titration curve. In order to correct for modelling errors, the system noise $\mathbf{w}(k-1)$ is introduced. Additional noise $v(k)$ is encountered on the measurements $z(k)$. If the continuous titration is monitored potentiometrically, $z(k)$ denotes the measured potentials or pH. The state $\mathbf{x}(k)$ is described by the dynamic response x_1 , the equilibrium curve x_2 , its first derivative x_3 and its second derivative x_4 , respectively. The integration of the difference equations in time and volume introduces a systematic error of ΔV units in the equilibrium part $x_2 - x_4$ of the state. By means of a linear similarity transformation, an alternative state-space model can be derived, suffering only from the truncation error by the Taylor expansion $\frac{1}{2}\Delta V$ in the last state x_4 . Additional dead-time delays can be incorporated by extension of the state vector with one or more terms. In potentiometry, the relevant dynamics involve the concentration and not the measured potential. The given exponential relation allows a non-linear similarity transformation of the state. As a result, the noise covariances will be described in relative terms of the alternative state. Practically, however, there may be no need for these theoretical requirements.

State estimation

The state-space model can be summarized in the matrix-vector notation:

$$\begin{aligned} \mathbf{x}(k) &= F(k, k-1)\mathbf{x}(k-1) + \mathbf{w}(k-1) \\ z(k) &= \mathbf{h}^t(k)\mathbf{x}(k) + v(k) \end{aligned} \quad (5)$$

where k is the sequence number, $\mathbf{x}(k)$ the state vector, $F(k, k-1)$ the dynamic transition matrix, $z(k)$ the measurement and $\mathbf{h}^t(k)$ the transposed measurement vector. The system noise $\mathbf{w}(k-1)$ and the measurement noise $v(k)$ are assumed to be gaussian white with zero means and covariances $Q(k-1)$ and $R(k)$, respectively. The state-space model so described is directly applicable to state estimation. Table 1 lists the algorithms for prediction, filtering, smoothing, verification and selection. Detailed descriptions of the various equations are available [6-8]. The Kalman filter combines both prediction and filtering for the on-line estimation of the state based on the current measurement. Afterwards, the estimates of the Kalman

TABLE 1

State estimation^a

Model	$\mathbf{x}_k = F(k, k-1) \mathbf{x}_{k-1} + \mathbf{w}_{k-1}$ $z_k = \mathbf{h}^t k \mathbf{x}_k + u_k$
Prediction	$\hat{\mathbf{x}}_{k/k-1} = F(k, k-1) \hat{\mathbf{x}}_{k-1/k-1}$ $P_{k/k-1} = F(k, k-1) P_{k-1/k-1} F^t(k, k-1) + Q_{k-1}$
Filtering	$\hat{\mathbf{x}}_{k/k} = \hat{\mathbf{x}}_{k/k-1} + \mathbf{k}_k [z_k - \mathbf{h}_k^t \hat{\mathbf{x}}_{k/k-1}]$ $P_{k/k} = P_{k/k-1} - \mathbf{k}_k \mathbf{h}_k^t P_{k/k-1}$ $\mathbf{k}_k = P_{k/k-1} \mathbf{h}_k [\mathbf{h}_k^t P_{k/k-1} \mathbf{h}_k + R_k]^{-1}$ <p>where for $k = 0$, $\hat{\mathbf{x}}_{k/k} = 0$ and $P_{k/k} = I_n s_0^2$</p>
Smoothing	$\hat{\mathbf{x}}_{k/N} = \hat{\mathbf{x}}_{k/k} + A_k [\hat{\mathbf{x}}_{k+1/N} - \hat{\mathbf{x}}_{k+1/k}]$ $P_{k/N} = P_{k/k} + A_k [P_{k+1/N} - P_{k+1/k}] A_k^t$ $A_k = P_{k/k} F^t(k+1, k) P_{k+1/k}^{-1}$ <p>where for $k = N$, $\hat{\mathbf{x}}_{k/N} = \hat{\mathbf{x}}_{k/k}$ and $P_{k/N} = P_{k/k}$</p>
Verification	$\chi^2(k-n) = \sum_{i=1}^n [z_i - \mathbf{h}_i^t \hat{\mathbf{x}}_{i/l}]^2 / [\mathbf{h}_i^t P_{i/l} \mathbf{h}_i + R_i]$
Selection	$F(k1, k2) = [\chi^2(k1)/k1] [k2/\chi^2(k2)]$

^aA smoother gain matrix, F Fisher value, $F()$ transition matrix, \mathbf{h} measurement vector, I identity matrix, i, k, l indices, \mathbf{k} filter gain vector, n model dimension, N number of measurements, P covariance matrix, Q system noise covariance, R measurement noise covariance, v measurement noise, s_0^2 start covariance, \mathbf{x} state vector, z measurement, χ^2 chi-squared value; for other definitions, see text.

filter can be improved by performing off-line fixed-interval smoothing. Verification and selection of the state-space model and the numerical values of the noise covariances implemented are possible. In practice, the measurement noise variance $R(k)$ is known reasonably well. The system noise covariance $Q(k-1)$, especially the element q_{44} , is used as a tuning parameter to describe the titration curve in a statistically correct way; q_{44} describes the macroscopic effects of the physical and chemical relations and quantities covering the steepness of the equilibrium titration curve. A new feature in the continuous description is the incorporation of first-order dynamics in the state-space model. The term $\phi = \exp(-\Delta t/T_x)$ in the transition matrix $F(k, k-1)$ has to be known in advance and can be found by experimentation. The time constant T_x depends strongly on the mixing of the sample, the chemical reaction and the electrode response involved in the titration system.

For state estimation the optimal performance depends on the various

terms in the state-space model [5]. In general, the numerical values of $Q(k-1)$ and $R(k)$ have to be minimized. More complicated are the effects of the elements in $F(k, k-1)$ and $h^t(k)$, which depend greatly on the problem investigated [7]. Here, the dynamic term ϕ in $F(k, k-1)$ is one of the variables that can be manipulated experimentally. With $h^t(k)$ constant and $R(k)$ fixed experimentally, the contribution of the filtering part in Table 1 remains constant. For optimal selection only the prediction part of the Kalman filter is of interest. The choice of sampling time Δt affects both $\phi = \exp(-\Delta t/T_x)$ and $Q(k-1)$ by the relation $\Delta V = \rho \Delta t$. With a fixed experimental value for T_x , the sampling time Δt has to be minimized within the given instrumental constraints. Simultaneously, the highest rate of titrant addition (ρ) possible should be selected. The observability criterion $M = |h, F^t h, \dots, (F^t)^{n-1} h| \ll 0$ is satisfied when $\phi < 1$ in the transition matrix. The state-space model becomes unobservable in the equilibrium part $x_2 - x_4$ for ϕ approaching 1. Theoretically, this means that a zero sampling time Δt or an infinite volume addition speed ρ are impossible as a result of the particular model structure employed. For Δt to infinity (i.e., ϕ to zero), the state-space model becomes equal to the discrete equilibrium model delayed by one single volume unit ΔV .

Setpoint control

In automated titrations, continuous addition of titrant may lead to systematic errors if the time constant is not known correctly. Accuracy may be achieved when the titrant is added stepwise and the measured potentials are allowed to equilibrate. The application of state estimation for this approach has been described [8]. Here, the implementation of the Kalman filter allows control of the discrete volume addition to obtain equidistant measurements on-line. Alternatively, on-line control may be used to an empirically established setpoint in the equilibrium curve, in which the dynamics of the titration system are taken into account. The only way to manipulate experimentally the performance of the titration is by setting the burette on or off in a given time transition. The Kalman filter is based on the given state-space model [5] and the algorithm for setpoint control described by

$$\begin{aligned}
 x_{\max} &= \hat{x}_2(k/k-1) + 3 p^{1/2} 22(k/k-1) \\
 x_{\max} \geq x_{\text{set}} &\rightarrow \delta = 0 \text{ (burette off)} \\
 x_{\max} < x_{\text{set}} &\rightarrow \delta = 1 \text{ (burette on)} \\
 z(k) \geq x_{\text{set}} &\rightarrow \text{endpoint reached}
 \end{aligned} \tag{6}$$

where \hat{x}_2 denotes the second element of $\hat{\mathbf{x}}(k/k-1)$ and $p22$ denotes the second diagonal element of $P(k/k-1)$. The expected value of x_{\max} , based on the estimated equilibrium state and its associated covariance is compared with the prefixed setpoint x_{set} . In the time sequence $k-1$ to k , $\delta = 1$ if the burette is on and $\delta = 0$ if the burette is off. To account for a variable volume addition in time, the extra term δ is introduced in the transition matrix $F(k, k-1)$:

$$F(k, k-1) = \begin{pmatrix} \phi & 1-\phi & 0 & 0 \\ 0 & 1 & \delta & \frac{1}{2}\delta^2 \\ 0 & 0 & 1 & \delta \\ 0 & 0 & 0 & 1 \end{pmatrix} \quad (7)$$

The observability criterion $M \ll 0$ is satisfied when $\delta = 1$ but when $\delta = 0$ the state-space model (Eqn. 4) is not observable in the states x_3 and x_4 which should remain constant. The Kalman filter cannot separate numerically the observable part from the unobservable part in the state. Therefore, some additional modifications are needed. In practice, this is done most easily by using a system noise covariance $q_{44} \delta$ for prediction and the gains $k_3 \delta$ and $k_4 \delta$ for filtering. As a result, the Kalman filter can only affect numerically the estimates and covariances of x_1 and x_2 in the case of no addition.

The setpoint control algorithm operates similarly to a conventional hardware titrator, which is controlled by feedback of the detector signal. For a proper start, reagent is dispensed at a relatively fast rate. When the signal reaches a preset anticipation level, the speed of addition is decreased until the established setpoint is obtained. For a conventional titrator, the most important instrumental controls are the volume addition speed, the setpoint level, the proportional band and delay time of shut off. Here, the well-defined tuning parameters for setpoint control are the system noise covariance, measurement noise covariance, time constant, the sampling period and the setpoint level. It is appropriate to study the effects of the variation in the various essential parameters. Some of these tuning parameters are fixed experimentally in advance and others have to be chosen properly to obtain the highest precision possible. In practice, the only degree of freedom is the volume addition speed. A low addition rate will result in a precise setpoint but gives a long analysis time. A high rate of addition will give fast results lacking in precision or accuracy.

EXPERIMENTAL

Apparatus

The Radiometer ABU13 autoburette used has a volume counter in units of 0.01 ml. Volume delivery is controlled by an external input relay and the electronic counter is output as 4 BCD digits. The burette is filled or emptied under manual control. The titrant speed (ρ) is selected in %/min of the total burette volume (25 ml). The Radiometer TTT2b autotitrator for automated potentiometric setpoint titrations used has a hardware controller for the autoburette and a pH/mV meter with an analogue input and output. Select options are upscale/downscale, setpoint level, proportional band and delay time of shut off. The electrodes were Orion pH, chloride and copper ion-selective electrodes with a single-junction reference electrode. The pH meter was calibrated with standard buffers at pH 4 and pH 7.

A HP9845B desk-top computer and a HP6940B multiprogrammer mounted with a 12-bit ADC, 12-bit parallel input and relay card were used. The digitizing rate is controlled by a real-time clock. The hardware of this computer-controlled titrator employed has been described [9].

Software

Software programs were written in HP-BASIC with use of double-precision floating point arithmetics and matrix operations. The entire program for the setpoint control algorithm requires less than 50 lines and allows for a sampling period of 0.36 s. Successively, the measurement of the potential, burette control, Kalman filtering and setpoint computations are performed by the program. When the established setpoint is reached, the volume counter of the burette is read and the final result is output.

Procedures

The following titrations were tested; (a) 50 ml of citric acid (0.00060–0.00120 M) with sodium hydroxide (0.020–0.030 M); (b) 50 ml of phosphoric acid (0.00160 M) with sodium hydroxide; (c) 50 ml of silver nitrate (0.0010 M) with potassium chloride (0.0991 M); (d) 50 ml of copper(II) chloride (0.0031 M) with EDTA (0.0499 M).

All solutions were prepared from reagent-grade chemicals with a constant ionic strength of 0.1 M potassium nitrate. If necessary, the solutions were standardized by conventional procedures [10].

RESULTS

If the measured potentials are used directly for evaluation of the endpoint, the entire titration curve is shifted over a time interval proportional to the overall time constant. When the same type of titration is done at different rates of titrant addition, the plot of addition rate versus uncorrected endpoints should be a straight line; the intersection with the endpoint axis is the correct endpoint and the slope is the overall time constant. When the concentration of the sample is varied and a constant rate of addition is used, the relationship should also be linear; the intercept at zero concentration gives the time constant after correction for the rate of titrant addition [4]. In Fig. 1 these two experiments are shown for the titration of citric acid with sodium hydroxide monitored with a pH electrode. The uncorrected endpoints are evaluated by means of fixed-interval smoothing and the procedure described previously for discrete titration curves [8]. All titrations were done in triplicate to estimate the variation in the results. The evaluated endpoints of Fig. 1(a) bend towards the addition speed axis. The slope according to the least-squares fit yields a time constant of 15 s. The reproducibility of the results decreases significantly as the rate of addition increases. Varying the sample concentration (Fig. 1b) gives the linear behaviour it should. The intercept of the least-squares fit gives a time constant of

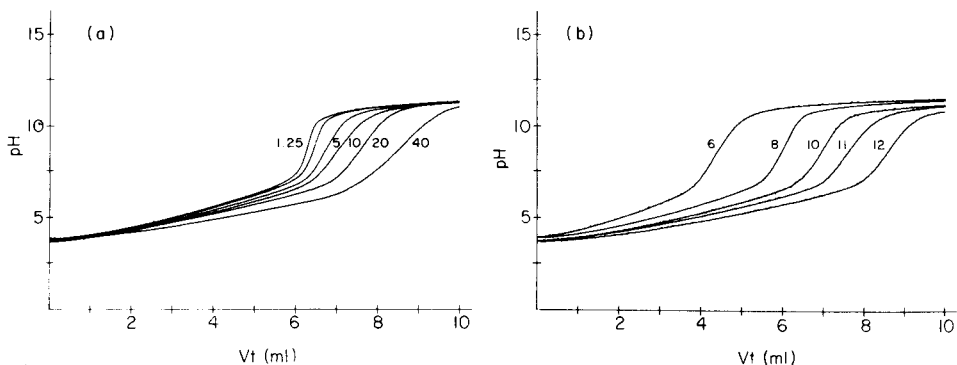


Fig. 1. Continuous measurements for 50 ml of citric acid titrated with sodium hydroxide (each curve represents 1000 sampling points). (a) 0.00105 M Citric acid titrated with 0.0252 M NaOH and a varying speed ρ in % of the total burette volume/min; the slope of the uncorrected endpoints V at pH 9 as a function of the volume addition speed gives a time constant $T_x = 15$ s. (b) A constant speed $\rho = 10\%$ (i.e., 0.0416 ml s^{-1}) and a varying concentration in units of 10^{-4} M citric acid titrated with 0.0229 M NaOH; the intercept of the uncorrected endpoints V at pH 9 as a function of the concentration of citric acid gives a time constant $T_x = 16$ s.

16 s. The time constant $T_x = 15$ s and a sampling time $\Delta t = 0.21$ s give $\phi = 0.986$ in the transition matrix $F(k, k-1)$ of the state-space model (Eqn. 4). Figure 2(a) depicts the performance of the Kalman filter for a chosen system noise covariance $q_{44} = 10^{-3}$ and a measurement noise covariance $R = 10^{-3}$. The standard deviation of the measurement noise of about 0.03 pH units is found experimentally from the fluctuations in the signal. In Fig. 2(a) the shift in the estimated dynamic curve \hat{x}_1 and its associated equilibrium curve \hat{x}_2 is demonstrated clearly. The noise in the state estimates is reduced by the fixed-interval smoother as shown in Fig. 2(b). It also shows that the expected behaviour of the derivatives \hat{x}_3 and \hat{x}_4 is diminished. The experimental χ^2 values indicate good statistical performance of the proposed state-space model, explaining the measurements of the continuous titration quite well. The evaluated endpoints at pH 9 of the Kalman filter, $V = 6.55$ ml, and of the fixed-interval smoother, $V = 6.56$ ml, are close to the theoretical value 6.59 ml. When the time constant is not known correctly in advance, the final results are inaccurate. State estimation introduces a systematic error proportional to the difference between the implemented and real time constants. In principle, the uncorrected endpoints may be corrected afterwards by the overall time constant. However, in this way the titrimetric analysis becomes similar to a normal calibration procedure.

When a first-order response is used for the potentials, on-line control to a prefixed setpoint in the equilibrium curve is possible by applying Eqn. 6. The same titration of citric acid was tested with burette control to a setpoint of pH 9. The Kalman filter used a system noise variance $q_{44} = 10^{-3}$, measurement noise variance $R = 10^{-3}$, time constant $T_x = 15$ s and

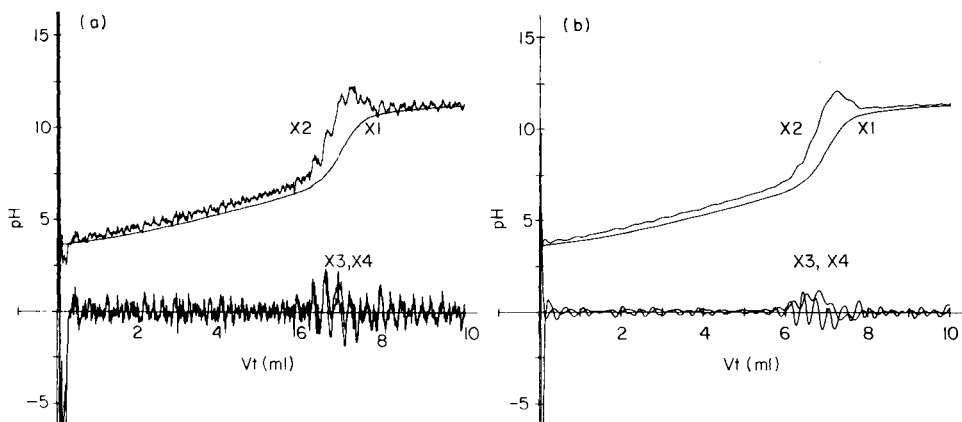


Fig. 2. Continuous titration of 50 ml of 0.00100 M citric acid with 0.0229 M NaOH (cf. Fig. 1b); system noise variance $q_{44} = 10^{-3}$, measurement noise variance $R = 10^{-3}$, time constant $T_x = 15$ s and sampling time $\Delta t = 0.21$ s; the critical chi-squared values are $\chi_{0.025}^2(996) = 910.4$ and $\chi_{0.975}^2(996) = 1085.3$. (a) Estimated state $x_1 - x_4$ by the Kalman filter ($V_{\text{pH } 9} = 6.55$ ml and $\chi^2 = 279.1$). (b) Estimated state $x_1 - x_4$ by the fixed-interval smoother ($V_{\text{pH } 9} = 6.56$ ml and $\chi^2 = 241.9$).

sampling time $\Delta t = 0.36$ s (i.e., $\phi = 0.976$). Figure 3(a) shows the performance of the measured pH with the burette settings on or off. After the titration has started, the burette is kept on because the measurements are still far from the established setpoint; the burette is then closed more and more frequently until the setpoint is finally reached. Figure 2(b) shows the corresponding state estimates. When the burette is off the states \hat{x}_3 and \hat{x}_4 remain constant. Near the setpoint, the dynamic state \hat{x}_1 gets close to the equilibrium state \hat{x}_2 , as provided by the control algorithm. A second practical example involves the titration of phosphoric acid with successive setpoints at pH 5 and pH 9. Figure 4(a) shows the pH measurements and the burette on/off settings, and Fig. 4(b) the corresponding estimated states.

The various tuning parameters used for setpoint control affect both the speed and accuracy of the titrations. Some titrations of citric acid were done around the best settings $q_{44} = 10^{-3}$, $R = 10^{-3}$, $T_x = 15$ s and $\Delta t = 0.36$ s. Figure 5(a–d) shows how the analysis times vary and indicates the mean value and standard deviation of five replicates for the setpoint volume. The observed analysis times are reproducible (within seconds). Figure 5(a) shows that a decreasing system noise covariance q_{44} ensures accurate results with a slightly increasing standard deviation; simultaneously the analysis time decreases moderately. For values of the measurement noise covariance R below 10^{-3} , results are inaccurate (Fig. 5b); the analysis time increases considerably with increasing R . For the time constant T_x (Fig. 5c), results are inaccurate if the constant is too small (the correct value is 16 s); if T_x is not known accurately, a higher value should be implemented at the expense of some analysis time. To summarize, in practice, only gross indi-

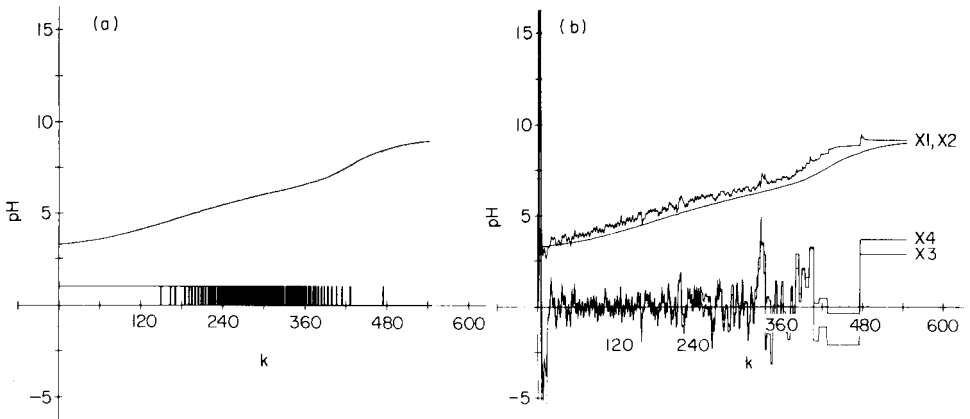


Fig. 3. The titration of 50 ml of 0.00073 M citric acid with 0.0260 M NaOH with on-line control to a preset pH 9 ($\rho = 10\%$, $\Delta t = 0.36$ s, $T_x = 15$ s, $q_{44} = 10^{-3}$ and $R = 10^{-3}$). The analysis time is 3.3 min and the volume $V_{\text{set}} = 4.24$ ml. (a) pH measurements with burette control on/off as shown; (b) estimated state $x_1 - x_4$ by Kalman filter.

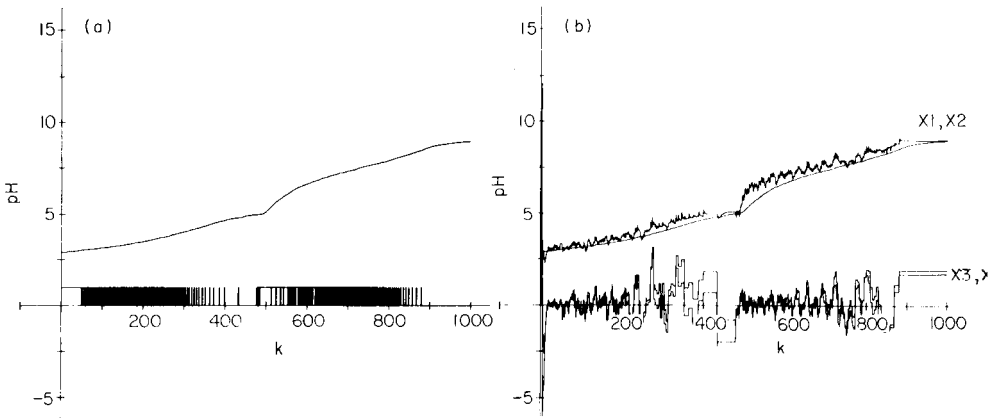


Fig. 4. The titration of 0.0016 M phosphoric acid with 0.0260 M NaOH under on-line control to setpoints at pH 5 and pH 9 ($\rho = 10\%$, $\Delta t = 0.36$ s, $T_x = 15$ s, $q_{44} = 10^{-3}$ and $R = 10^{-3}$). The total analysis time is 6.0 min for the two setpoints, the respective volumes being $V = 2.97$ ml and $V = 5.98$ ml. (a) pH measurements and burette control on/off; (b) estimated state $x_1 - x_4$ by Kalman filter.

cations of the various tuning parameters have to be known for setpoint control with the Kalman filter. Only at extremely incorrect values will inaccurate results and poor analysis times be obtained.

Finally, the advocated control algorithm is compared with the performance of a hardware titrator. Table 2 lists the settings and results for the titration of citric acid with sodium hydroxide, for silver nitrate with potassium chloride, and for copper chloride with EDTA. For the autotitrator, the titrant addition rate, the proportional band and the shut-off delay time

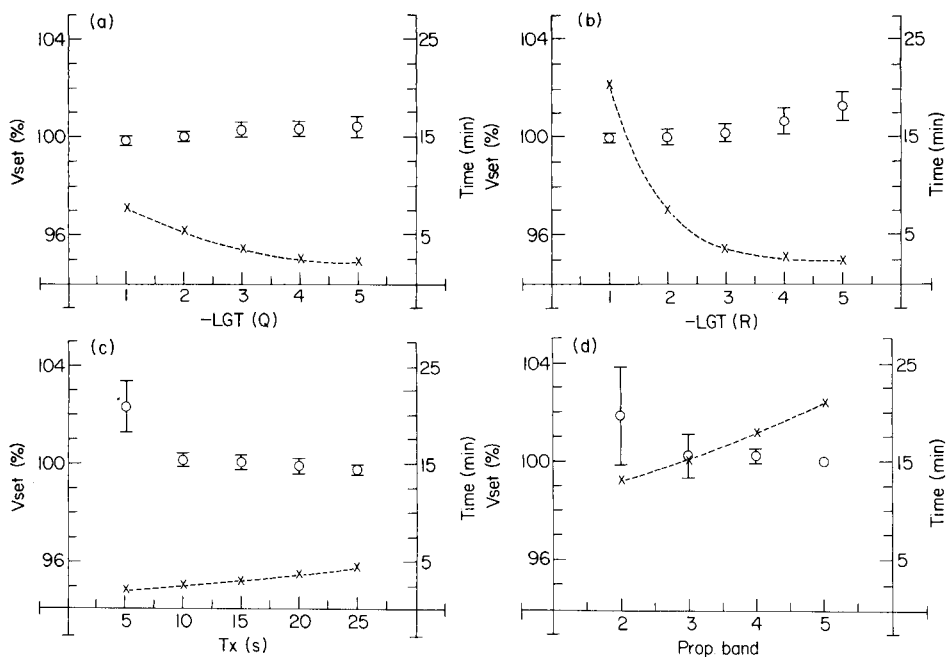


Fig. 5. The effect of tuning parameters on the analysis time (---) for the titration of citric acid with sodium hydroxide under on-line control to pH 9 (initial settings as in Fig. 3). For the setpoint volume, the mean and relative standard deviation of five replicates are indicated by bars. (a) Kalman filter, varying system noise variance $q44$; (b) Kalman filter, varying measurement noise variance R ; (c) Kalman filter, varying time constant T_x ; (d) autotitrator, varying proportional band (delay = 10 s and $\rho = 1.25\%$).

were manipulated until the standard deviation of the results was close to the best value obtainable; Fig. 5(d) shows the effect of variation of the proportional band with a fixed addition speed ($\rho = 1.25\%$) for citric acid. An increasing proportional band increased the analysis time but inferior results were obtained for a proportional band below 5 pH units or an addition speed above 1.25% (not shown). For citric acid with the highest time constant and steepest inflection, the analysis time is decreased by a factor of three when the Kalman filter is used. For the less steep inflections and smaller time constants of the silver and copper titrations, the improvements are only by a factor of two. Of course, further improvements may result in a better performance for the proposed procedure of setpoint control with the Kalman filter. The sampling time, Δt , is constrained here by the hardware and software of the computer-controlled titrator. Increasing the addition speed to 20% gives faster analysis but less accurate results for the Kalman filter; the rate of titrant addition is then so high that about 0.03 ml is added in a sampling period of 0.36 s. Reduction of the model to a state description of exclusively $x_1 - x_3$ allows a sampling period of 0.28 s but introduces

TABLE 2

Settings and results for Kalman filter and autotitrator (V_{set} and RSD are for $N = 5$)

<i>Kalman filter</i>									
Titration	T_x (s)	Q	R	ρ (%)	x_{set}	V_{set} (ml)	RSD (%)	T_a (min)	$x >$
Citric/NaOH ^a	15	10^{-3}	10^{-3}	10	pH 9	4.90	0.5	4.8	0.1
Citric/NaOH ^a	15	10^{-3}	10^{-3}	20	pH 9	4.91	0.6	4.2	0.2
AgNO ₃ /KCl ^b	5	10^{-7}	10^{-6}	10	-220 mV	5.09	0.6	2.4	3.0
CuCl ₂ /EDTA ^c	2	10^{-6}	10^{-6}	10	-66 mV	3.16	0.4	2.2	3.0
CuCl ₂ /EDTA ^c	2	10^{-5}	10^{-6}	20	-66 mV	3.22	1.1	1.8	5.0
<i>Autotitrator</i>									
Titration	Prop. band	Delay (s)	ρ (%)	x_{set}	V_{set} (ml)	RSD (%)	T_a (min)	$x >$	
Citric/NaOH ^a	5	10	1.25	pH 9	4.90	0.4	15.0	0.1	
AgNO ₃ /KCl ^b	100	10	10	-220 mV	5.09	0.3	4.0	1.0	
CuCl ₂ /EDTA ^c	200	10	10	-66 mV	3.16	0.4	3.0	3.0	

^a50 ml of 0.00075 M citric acid with 0.0230 M NaOH. ^b50 ml of 0.0010 M AgNO₃ with 0.0991 M KCl. ^c50 ml of 0.0031 M CuCl₂ with 0.0499 M EDTA.

higher inaccuracy in the results. At this point, instrumental improvements are possible by using a faster computer and a faster interfacing. Dedicated computers can allow speed improvements by a factor of 10–100; one sampling period would then need less than 0.1 s.

CONCLUSION

The application of state estimation in continuous titrations has been presented. The state-space designed is based on the dynamic behaviour of the titration system. From the measurements, the Kalman filter estimates on-line the dynamic curve and the equilibrium curve with its derivatives. Thereafter, improvements can be obtained by fixed-interval smoothing. For potentiometric titrations, the overall time constant is usually not known accurately in advance and this introduces a systematic error in the results. In practice, therefore, on-line control by the Kalman filter to an empirically established setpoint is of interest. Only gross indications of the overall time constant, the system noise covariance and the measurement noise covariance have to be fed into the computer-controlled titration system. In comparison with a conventional autotitrator, analysis time can be improved three-fold without sacrifice of accuracy. This is mainly due to better modelling of the titration system when a slow response or a steep inflection are encountered. For optimal performance, a minimal sampling period and a

maximal rate of titrant addition are dictated by instrumental constraints. Further improvements are possible by employing a faster computer and faster interfacing. Another possibility is improvement of the burette resolution. The design of an automatic setpoint titrator based on the state estimation presented here still requires much investigation.

This work was supported by The Netherlands Research Organization Z.W.O. Special thanks are expressed to Dr. F. W. Pijpers for evaluating the manuscript.

REFERENCES

- 1 T. W. Hunter, J. T. Sinnamon and G. M. Hieftje, *Anal. Chem.*, 47 (1975) 497.
- 2 T. F. Christiansen, J. E. Bush and S. C. Krogh, *Anal. Chem.*, 48 (1976) 1051.
- 3 A. H. B. Wu and H. V. Malmstadt, *Anal. Chem.*, 50 (1978) 2090.
- 4 J. C. Smit and H. C. Smit, *Anal. Chim. Acta*, 143 (1982) 45.
- 5 E. Pungor, Z. Feher, G. Nagy and T. Toth, *CRC Crit. Rev. Anal. Chem.*, 14 (1983) 175.
- 6 P. C. Thijssen, S. M. Wolfrum, G. Kateman and H. C. Smit, *Anal. Chim. Acta*, 156 (1984) 87.
- 7 P. C. Thijssen, *Anal. Chim. Acta*, 162 (1984) 253.
- 8 P. C. Thijssen, N. H. M. de Jong, G. Kateman and H. C. Smit, *Anal. Chim. Acta*, 170 (1985) 265.
- 9 A. M. van de Wijdeven, P. C. Thijssen and L. G. G. van Dongen, *Lab. Microcomput.*, 3 (1984) 37.
- 10 Netherlands Normalization Institute, *Chemical Analysis*, NEN 3103 UDC 543.024 (1973) and NEN 3104 UDC 543.062 (1984).

SCALING OF ANALYTICAL DATA

OLAV MARTIN KVALHEIM

Department of Chemistry, University of Bergen, 5000-Bergen (Norway)

(Received 6th June 1985)

SUMMARY

The effects of normalization and weighting on principal component analysis (p.c.a.) of gas chromatographic data are investigated. The weighting procedure called autoscaling masks the patterns inherent in the data if it is not applied separately to the different groups (classes) of samples (objects) in the data set. When p.c.a. is used unsupervised on objects characterized by variables differing greatly in relative size, logarithmic transformation of raw data seems preferable. This transformation has the ability both to unmask systematic variation in "small" variables, and to retain the data structure, avoiding the problem of closure. The logarithmic transformation also makes the distribution of each variable more normal.

Principal component analysis (p.c.a.) is now a well established tool in the interpretation of analytical data. The great potential of the method has been proved through its applications in various spectrometric and chromatographic techniques [1, 2]. When p.c.a. is used to analyse gas chromatographic (g.c.) data, the raw data (peak areas or peak heights) are usually preprocessed in two steps: normalization of each chromatogram (object) to compensate for differences in the amount injected (or, more precisely, amount measured) is followed by weighting of each peak (variable) to reduce differences in absolute variance between peaks caused by the varying amount of each constituent.

Normalization of g.c. data is usually done by expressing the area under each peak as a percentage of the total area of each chromatogram [3]. As has recently been pointed out, this closure or constant sum procedure, can seriously influence the structure of the data [4]. When some peaks increase, others have to decrease. This can lead to false negative correlations between major peaks and false positive correlations between minor peaks [5–8]. Fortunately, by picking out peaks with approximately the same mean and variance for use in the normalization step, it seems possible to reduce the risk of spurious correlations [4].

Because of the great differences in absolute size between the various peaks in a chromatogram, systematic variation in small peaks is masked by the much larger absolute variation of the major peaks. The same problem arises with spectroscopic data, e.g., n.m.r. shift data [9]. The data used in p.c.a.

are therefore transformed prior to their evaluation to reduce the relative importance (weight) of the largest variables. Several methods have been proposed for this weighting [10–16]. The most drastic is to equalize the variance of each variable, e.g., autoscaling [10, 11]. This scaling gives each variable a variance of one. Autoscaling has classically been applied to the whole data set. As pointed out by Albano et al. [12], autoscaling of each class separately gives much better resolution in p.c. modelling of classes. This approach has given good results with g.c. data [13, 14]. Another common transformation of g.c. data is to use the logarithm of either the raw [15] or normalized data [16].

The aim of the present study was to examine the consequences of different procedures used in the preprocessing stage of raw data. This step can be crucial because the results of p.c.a. depend on the scaling used.

THEORY

Principal components analysis has two different applications in analytical chemistry; it can be used unsupervised to uncover groups of similar objects or supervised, as in SIMCA multivariate data analysis, to model known classes [1, 12, 17–19]. Usually, the first step, even in supervised p.c.a., is a display of the whole multivariate data set onto a few-dimensional factor space [20]. Similar objects group together in clusters (classes) in this factor space.

The data analysed with p.c.a. are collected in a $n \times m$ data matrix \mathbf{X} organized so that each row of the matrix contains the m measured variables of one of the n objects. Correlations between variables are expressed through the variance-covariance matrix: $\mathbf{V} = \mathbf{X}'\mathbf{X}$. The diagonal of this matrix contains the variance $v(i)$ of each variable. The principal components (PC's) are the solution of the equation $\mathbf{X}'\mathbf{X}\mathbf{B} = \Lambda\mathbf{B}$. These components are orthogonal linear combinations of all the variables. Each row of the $m \times m$ matrix \mathbf{B} contains the coefficients (loadings) of one PC. The diagonal $m \times m$ matrix Λ contains the variances $\lambda(i)$ explained by each PC. The total variance of the original variables is of course the same as the total variance of the PC's, i.e., the total variance is conserved:

$$v_{\text{total}} = \sum_{i=1}^m v(i) = \sum_{i=1}^m \lambda(i)$$

If the variables are highly correlated, the first few PC's explain most of the total variance so that the data can be approximated with a PC model with F product terms [1, 12]:

$$\mathbf{X} = \mathbf{1}\bar{\mathbf{X}} + \mathbf{T}\mathbf{B}' + \mathbf{E}; \quad v_{\text{model}} = \sum_{i=1}^F \lambda(i)$$

Here, $\bar{\mathbf{X}}$ is the $1 \times m$ matrix of the mean values of each variable, $\mathbf{1}$ is a $n \times 1$ matrix of 1's, \mathbf{B}' is the $F \times m$ matrix of the loadings of the F first PC's in \mathbf{B} .

T is the $n \times F$ matrix of projections (scores) of the objects along the F principal components, while E is the $n \times m$ matrix of the residuals.

Usually, the initial step in p.c.a. is some preprocessing of raw data. With g.c. data or spectral intensity data, normalization is often done prior to logarithmic conversion or weighting: $x_{ki} \rightarrow w_i x_{ki}$. This weighting of variable i of each object k with the factor w_i has a profound effect on the distribution of the total variance among the variables: $v(i) \rightarrow w_i^2 v(i)$.

When the variables used in the analysis differ very much in absolute size, weighting is utilized to reduce the masking effect of the largest variables. Two gas chromatographic peaks with the same relative variance, but differing in absolute size by a factor of two, differ in absolute variance by a factor of four, giving the larger peak four times the weight of the smaller in p.c.a. A weighting which treats these peaks more equally seems justified. Autoscaling uses the inverted standard deviation of each variable as weight factors, giving an equal distribution of the total variance among all the variables. As will be shown below, this scaling has drawbacks and must be applied with caution.

RESULTS AND DISCUSSION

In this investigation, the g.c. patterns of female blue mussels from polluted (class 1) and unpolluted (class 2) locations were examined. The raw data were taken from an earlier study on the g.c. patterns shown by naturally occurring constituents in the gonad tissue of blue mussel [14, 21]. Dropping the smallest and most varying peaks left 29 peaks to be used in this investigation. To simplify the discussion, only female samples were treated. One of the samples was considered to be an outlier because of the small amount injected compared with the rest, leaving 9 samples in each class. These were labelled 1–4 and 6–10 for class 1 and 11–19 for class 2. Calculations were done with both raw data and normalized data followed by logarithmic conversion or autoscaling. The SIMCA program [22], implemented on a Univac 1100/82 [23], was used for all calculations.

Figure 1 shows the score plots (the eigenvector projection or the Karhunen-Loewe transformation [1, 20]) of the samples in the plane spanned by the two first PC's. Several conclusions can be drawn from these plots. First, comparison of Fig. 1(a), (b) and (c), which display the score plots calculated from raw data, autoscaled raw data and logarithmic raw data, respectively, shows that the logarithmic transformation reveals most clearly a grouping into two classes, with a possible subgrouping of class 2 into 2 clusters. In the score plot (Fig. 1c) calculated from logarithmic data, the two classes are clearly separated along the first PC. Also, when the scores of the samples along the second PC in Fig. 1(c) are compared, they are found to correlate with the amounts injected. In class 1, sample 3 is the gas chromatogram corresponding to the least amount injected while sample 8 corresponds to the largest injection. The amounts injected also explain the subgrouping of class 2 into 2 clusters. It can be concluded from Fig. 1(a–c) that the

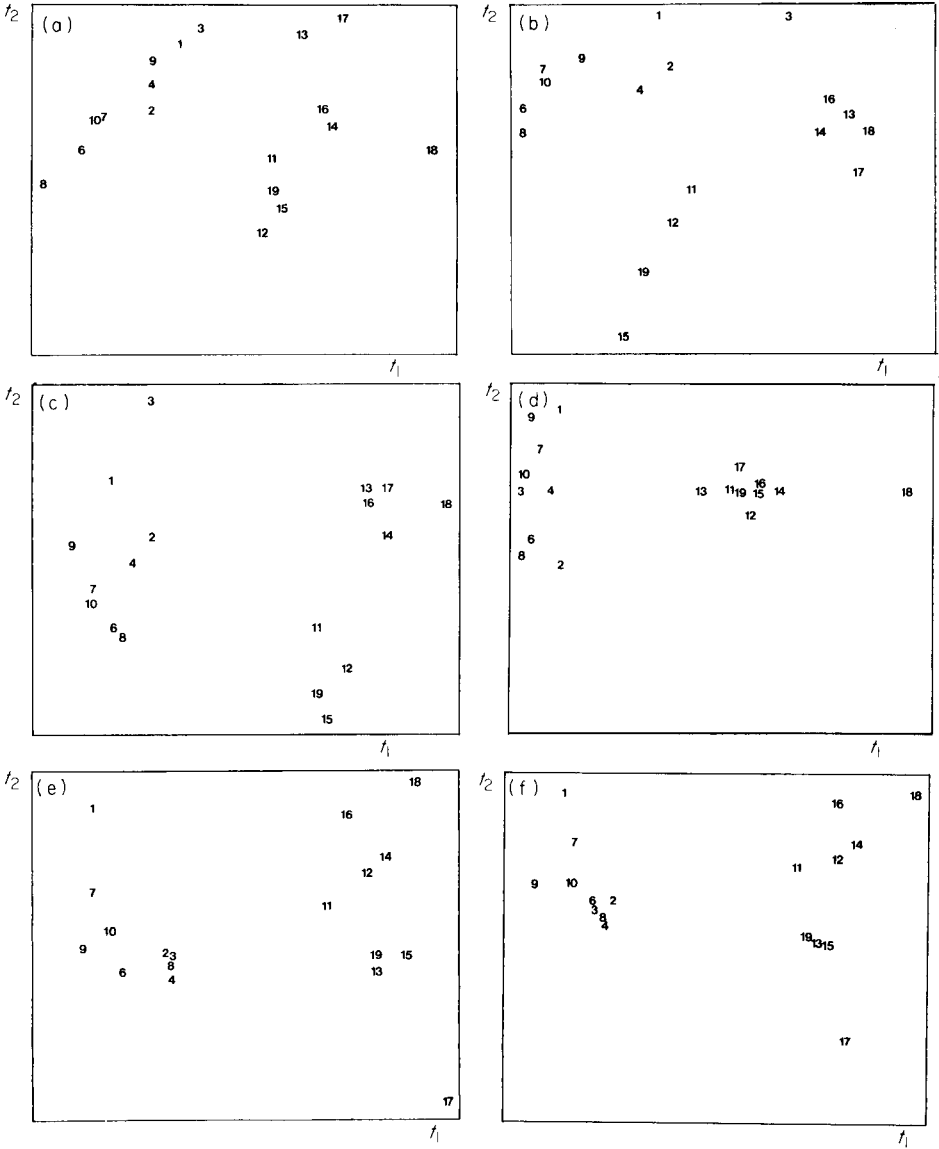


Fig. 1. Projections (t_1 and t_2) of the samples along the first and second PC with six different pretreatments of data: (a) raw data; (b) autoscaled raw data; (c) logarithmic raw data; (d) normalized data; (e) autoscaled normalized data; (f) logarithmic normalized data.

logarithmic transformation is superior to the others when unsupervised p.c.a. is applied to samples from different classes. In situations where closure is a serious problem, the logarithmic transformation of raw data therefore seems favourable. If used for class modelling, the first PC within each class explains the different amounts injected [15].

Secondly, when Fig. 1(d), (e) and (f) which display the score plots calculated from normalized data, autoscaled normalized data and logarithmic normalized data, are examined, it is clear that the samples group into two classes along the first PC in all these plots. The logarithmic data give tighter classes than the autoscaled data. The normalized data in Fig. 1(d) group sample 18 outside the normal range of class 2, probably because some variables for sample 18 have values outside the normal range of the class. Both the logarithmic transformation and autoscaling reduce the weights of such variables in the data analysis, the logarithmic transformation by narrowing the range of the variables and making them less skew, and autoscaling by reducing the weights of the variables with the largest absolute variances. The use of the logarithmic transformation as a tool to make skewed distributions more normal has been discussed by Christie and Wold [24].

By utilizing the knowledge of the class membership of the samples, the interclass (between-class) to intraclass (within-class) variation for the scores on a PC can be calculated to produce F ratios for the different preprocessing procedures used in unsupervised PCA. Table 1 shows the calculated ratios based on scores on the first PC. Clearly, the logarithmic transformations provide the best grouping into classes, thus confirming the conclusions found by inspection of the score plots (Fig. 1).

Table 2 shows the class mean and percentage variance of each variable in the first PC together with the total percentage variance explained by this PC when the two classes are treated jointly (unsupervised p.c.a.). Four effects are evident from these numbers. First, regardless of the transformation used, more variance is explained by the first PC with normalized data compared to raw data. This is not surprising because normalization removes that part of the intraclass variance which corresponds to the different amounts injected, thereby reducing the total variance of the data. Secondly, raw or normalized data give a PC dominated by the largest variables, masking the variation in the smallest variables. This effect is further displayed in Fig. 2 which compares the distribution of the total variance among the variables when normalized and logarithmic normalized data are used. Thirdly, the logarithmic transformation provides nearly the same results with raw and normalized data. This was further confirmed by plotting the loadings of the first PC

TABLE 1

Interclass to intraclass F ratios calculated from scores on the first PC (unsupervised p.c.a.)

	F ratios	
	Raw data	Normalized data
Not weighted	57.0	129.6
Autoscaled	11.2	196.7
Logarithmically transformed	223.8	467.6

(d.f.: $f_1 = 16, f_2 = 1$)

TABLE 2

Distribution of variance in the first PC with different preprocessing of data

Peak no.	Peak heights Class mean (mm)		% _{oo} of total variance in PC 1					
			raw	norm	log		autoscaling	
	1	2			raw	norm	raw	norm
1	104	76	4	3	21	17	51	43
2	29	22	1	0	20	16	70	50
3	57	63	0	0	0	0	11	0
4	752	662	97	49	4	3	73	54
5	40	57	0	1	5	10	0	38
6	23	32	0	0	5	10	0	38
7	33	24	0	0	21	18	82	47
8	32	21	0	0	27	24	20	21
9	142	121	6	2	9	6	43	24
10	59	266	166	232	324	339	21	67
11	159	404	218	335	125	136	10	60
12	118	117	0	0	0	0	6	0
13	104	113	0	0	0	0	18	1
14	18	15	0	0	13	10	49	8
15	43	52	0	0	0	0	0	10
16	574	422	172	142	22	19	74	59
17	68	126	6	12	45	53	0	72
18	101	190	15	30	47	56	0	66
19	61	40	3	2	44	37	66	55
20	22	15	0	0	37	33	47	50
21	544	366	304	183	28	23	57	32
22	46	37	1	1	16	13	81	52
23	27	22	0	0	7	5	43	0
24	84	47	8	8	78	71	63	45
25	11	10	0	0	0	0	21	2
26	17	29	0	0	26	29	0	34
27	15	9	0	0	43	36	61	26
28	18	11	0	0	36	32	56	23
29	23	31	0	0	7	9	0	26
% of total variance			53.1	75.7	41.9	57.1	34.9	41.2
Class distance ^a			4.4 ^b	5.8	4.1	4.3	3.2	3.4
							6.3 ^c	9.8 ^c

^aPC model described by 3 components. ^bPC model described by 2 components. ^cPC model of separate autoscaling within each class, 3 components.

from logarithmic normalized data versus the loadings from logarithmic raw data. All the variables fitted close to a straight line, confirming that the variables are correlated in the same way in the two cases. Fourthly, autoscaling gives completely different correlations with normalized data compared to raw data. Also, by comparing the class mean of the variables, the PC's calculated from autoscaled data seem dominated by variables with limited ability

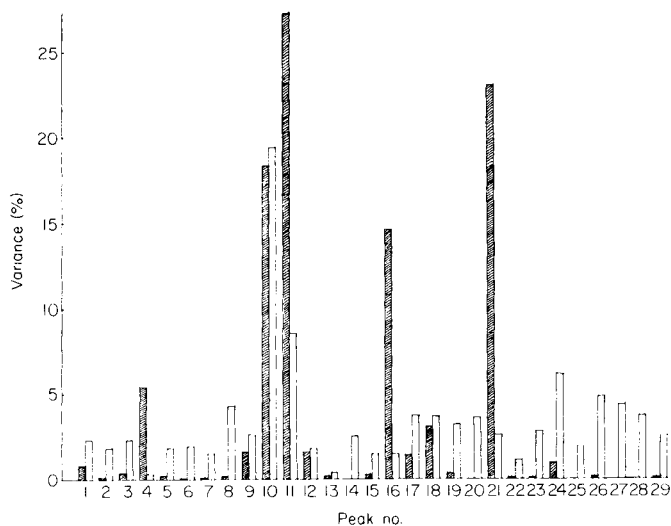


Fig. 2. Distribution of total variance with normalized (shaded) and logarithmic normalized data.

to group the samples into classes, especially for the autoscaled raw data. This effect can be understood if the variation of each variable is split into two parts: intraclass and interclass variation, i.e.,

$$v(i) = v_1(i) + v_2(i) + v_{12}(i)$$

(The same symbol is used to denote variation as was used earlier for variance.) If a variable discriminates clearly between the two classes, then v_{12} is also large compared with v_1 and v_2 (see appendix). Conversely, if a variable has a low discrimination ability, then v_{12} approaches zero. Because the relative standard deviations for the peaks are approximately constant within a class, classical autoscaling reduces the importance of the variables with high discrimination ability ($v_{12} \gg v_1 + v_2$) and increases the weights of variables with low ability to discriminate. In Table 2, this effect is demonstrated for variables 10 and 11 where the intraclass variations are very small compared with the interclass variations, giving these peaks much smaller weight with autoscaled data than with logarithmic data. This effect can also be expected in supervised p.c.a. of the two classes, when autoscaled data calculated from both classes jointly are used. A variable with high interclass variation is compressed and has little weight in p.c.a. of each class separately. Separate autoscaling eliminates this problem, as was reported by Albano et al. [12] and confirmed by Derde et al. [13].

In SIMCA modelling, the separation between two classes is usually quantified by calculating the class distance [12]. According to Albano et al. [12], class distances greater than 3–4 correspond to good separation. Table 2 shows the distances between the two classes. Separate autoscaling of each

class gives the best class distance, while classical autoscaling shows the poorest separation.

Although demonstrated on g.c. data, the conclusions obtained in this work are expected to be valid also for similar analytical data.

The author thanks O. Grahl-Nielsen for stimulating discussions during this work.

APPENDIX

To show the partition of the total variation of a variable into intra- and inter-class variation, two classes of samples labelled $\{p, q\}$ are first defined. Class means and numbers of samples are defined as $\{\bar{x}_p, \bar{x}_q\}$ and $\{n_p, n_q\}$, respectively. These numbers obey the following relations:

$$N = n_p + n_q, N\bar{x} = n_p\bar{x}_p + n_q\bar{x}_q$$

Johnston [25] used the identity

$$x_k - \bar{x} = (x_k - \bar{x}_g) + (\bar{x}_g - \bar{x})$$

where k labels a particular sample from $\{p, q\}$ and \bar{x}_g denotes the class mean of sample k , i.e., either \bar{x}_p or \bar{x}_q . Squaring both sides of the identity and summing over all samples gives the relation:

$$\sum_{k=1}^N (x_k - \bar{x})^2 = \sum_{k=1}^N (x_k - \bar{x}_g)^2 + \sum_{k=1}^N 2(x_k - \bar{x}_g)(\bar{x}_g - \bar{x}) + \sum_{k=1}^N (\bar{x}_g - \bar{x})^2$$

The cross term is easily seen to give zero contribution, reducing the expression to

$$\sum_{k=1}^N (x_k - \bar{x})^2 = \sum_{k=1}^{n_p} (x_k - \bar{x}_p)^2 + \sum_{l=1}^{n_q} (x_l - \bar{x}_q)^2 + \sum_{k=1}^{n_p} (\bar{x}_p - \bar{x})^2 + \sum_{l=1}^{n_q} (\bar{x}_q - \bar{x})^2$$

This expression contains the total variation on the left side and the intraclass variation of the classes as the two first terms on the right side, the last two terms being the interclass variation, i.e.,

$$v(i) = v_1(i) + v_2(i) + v_{12}(i)$$

The expression for the intraclass variation can be simplified:

$$v_1(i) = \sum_{k=1}^{n_p} x_k^2 - n_p\bar{x}_p^2; v_2(i) = \sum_{l=1}^{n_q} x_l^2 - n_q\bar{x}_q^2$$

Also the expression for the interclass variation can be simplified:

$$v_{12}(i) = n_p(\bar{x}_p - \bar{x})^2 + n_q(\bar{x}_q - \bar{x})^2 = n_p\bar{x}_p^2 + n_q\bar{x}_q^2 - N\bar{x}^2$$

If $n_p = n_q$ this expression simplifies further to

$$v_{12}(i) = (N/4)(\bar{x}_p - \bar{x}_q)^2$$

i.e., the interclass variation is proportional to the squared difference between class means.

REFERENCES

- 1 S. Wold, C. Albano, W. J. Dunn III, U. Edlund, K. Esbensen, P. Geladi, S. Hellberg, E. Johansson, W. Lindberg and M. Sjöström, in B. R. Kowalski (Ed.), *Chemometrics — Mathematics and Statistics in Chemistry*, Reidel, Dordrecht, 1984.
- 2 E. R. Malinowski and D. G. Howery, *Factor Analysis in Chemistry*, Wiley, New York, 1980.
- 3 G. Blomqvist, E. Johansson, B. Söderström and S. Wold, *J. Chromatogr.*, 173 (1979) 7.
- 4 E. Johansson, S. Wold and K. Sjödin, *Anal. Chem.*, 56 (1984) 1685.
- 5 W. Skala, *Chem. Geol.*, 27 (1979) 1.
- 6 E. Spjøtvoll, H. Martens and H. Volden, *Technometrics*, 24 (1982) 173.
- 7 H. L. C. Meuzelaar, J. Haverkamp and F. D. Hileman, in *Pyrolysis Mass Spectrometry of Recent and Fossil Biomaterials*, Elsevier, Amsterdam, 1982.
- 8 L. M. Karrer, H. L. Gordon, S. M. Rothstein, J. M. Miller and T. R. Jones, *Anal. Chem.*, 24 (1983) 1723.
- 9 M. Sjöström and U. Edlund, *J. Magn. Reson.*, 25 (1977) 285.
- 10 B. R. Kowalski and C. F. Bender, *J. Am. Chem. Soc.*, 94 (1972) 5632.
- 11 B. R. Kowalski and C. F. Bender, *J. Am. Chem. Soc.*, 95 (1973) 686.
- 12 C. Albano, G. Blomqvist, D. Coomans, W. J. Dunn III, U. Edlund, B. Eliasson, S. Hellberg, E. Johansson, B. Norden, D. Johnels, M. Sjöström, B. Söderström, H. Wold and S. Wold, *Proc. Symposium on Applied Statistics*, Copenhagen, 1981.
- 13 M. P. Derde, D. Coomans and D. L. Massart, *Anal. Chim. Acta*, 141 (1982) 187.
- 14 O. M. Kvalheim, K. Øygard and O. Grahl-Nielsen, *Anal. Chim. Acta*, 150 (1983) 145.
- 15 B. Söderström, S. Wold and G. Blomqvist, *J. Gen. Microbiol.*, 128 (1982) 1783.
- 16 S. Wold, E. Johansson, E. Jellum, I. Bjørnson and R. Nesbakken, *Anal. Chim. Acta*, 133 (1981) 251.
- 17 S. Wold, *Pattern Recognition*, 8 (1976) 127.
- 18 S. Wold and M. Sjöström, in B. Kowalski (Ed.), *Chemometrics, Theory and Application*, Am. Chem. Soc. Symp. Ser., 52 (1977).
- 19 C. Albano, W. Dunn III, U. Edlund, E. Johansson, B. Nordén, M. Sjöström and S. Wold, *Anal. Chim. Acta*, 103 (1978) 429.
- 20 D. L. Massart and L. Kaufman, in *The Interpretation of Analytical Chemical Data by the Use of Cluster Analysis*, Wiley, New York, 1983.
- 21 K. Øygard, *Cand. real. Thesis*, University of Bergen (1981).
- 22 S. Wold, *SIMCA 3B Manual*, 2nd edition, Umeå University (1983).
- 23 O. M. Kvalheim, *SIMCA Users Guide*, University of Bergen (1985).
- 24 O. H. J. Christie and S. Wold, *Anal. Lett.*, 12 (1979) 979.
- 25 R. J. Johnston, *Multivariate statistical analysis in geography*, Longman, New York, 1978, p. 54.

EXTENDING THE USE OF CERTIFIED REFERENCE SEDIMENTS FOR ASSESSMENT OF ACCURACY IN DETERMINATIONS OF TRACE METALS

ROBIE W. MACDONALD* and MARY C. O'BRIEN

Institute of Ocean Sciences, P.O. Box 6000, Sidney, B.C. V8L 4B2 (Canada)

(Received 12th June 1985)

SUMMARY

Straightforward analysis for components in a single certified reference sediment is of limited use for assessing the accuracy of environmental determinations. A systematic approach requires mixing of certified sediments, one with another and with environmental samples, and the preparation of secondary reference material by the laboratory. Use of Youden pairs, reference material embedded in samples and linear models should enable valid accuracy statements to be made based on well known statistical concepts. For assessing accuracy, reference sediments which are matched in particle size, and are end-members for components or sediment types are most useful.

The value of certified reference materials (CRM) for environmental chemistry is indisputable and recent guidelines [1, 2] correctly recommend their incorporation into any environmental sampling program. Specific directions on how such material is to be used are scant, and this is reflected by the lack of systematic approaches evident in the literature. Therefore there is a need to clarify how CRM's should be used and the aim of this paper is to outline a few techniques which go beyond the direct analysis of a single CRM. The discussion is restricted to the problem of trace metals in marine sediments; however, it is clear that the techniques have direct application for any trace components contained in a particulate matrix.

Reference materials suffer from two major limitations; each is in finite supply, and only a few exist. The latter problem is compounded by variety not only between but within classes of environmental substrates which CRM's are supposed to represent. For many substances, there simply is no appropriate CRM. Examples of indiscriminate application of CRM (e.g., use of orchard leaves for oyster tissue analysis) are not uncommon, but easy to disregard. More subtle and much commoner is use of a CRM which is sufficiently different from samples being analyzed to make it of questionable value in an assessment of analytical performance. This matter is rarely discussed. For materials of widespread interest, marine sediment in the present case, and popular analytical targets such as metallic elements, there is wider choice of CRM's. However, a recent survey [3] lists only three pertinent marine CRM's

currently available, National Bureau of Standards (NBS) estuarine sediment SRM 1646, and National Research Council of Canada (NRCC) marine sediments MESS-1 and BCSS-1. It is unreasonable to expect that these CRM's, which are compositionally very similar, can be stretched to represent all marine sediments.

Determination of precision for any method is relatively straightforward, will always involve replicates and does not require recourse to reference material. Here precision is defined as tightness of grouping of replicates, bias as the difference between the average of a large number of determinations and the "true" value, and accuracy comprises both. This follows Water Research Centre usage as outlined by Kirchmer [4]. Reference materials, therefore, are used to assess bias and accuracy of an analytical procedure when applied to specific material. In principle, accuracy of a procedure is assessed for the CRM and then extrapolated to environmental samples; thus the requirement of similarity. This should enable analysts to set their data in the context of measurements performed by others, using the same or different methods, but without benefit of direct inter-laboratory comparison. This is important because the option of interlaboratory comparisons is not always practical; use of CRM's is. The value of CRM's, therefore, is to provide comparability.

A review of published data for determination of metals in sediments leaves the impression that reference material is often not used, or if it is and performance on it reported, one is left to pass judgement on what this may imply about accuracy. The reader is seldom in the best position to judge because he may not know how appropriate the CRM was, nor the model (i.e., blind, random, number of replicates, etc.) under which the CRM was determined. Extrapolating beyond the range of calibration for an instrument entails unknown risks and is not recommended [1]. However, this caution seems not to have been carried into the use of reference material, and one often has only a single reference point with which to evaluate accuracy for a broad range of sediments. This is tantamount to using a single calibrant, assuming linearity through origin, and assuming that matrix or interference effects are identical in all samples. These are extremely risky assumptions.

How reference materials should be used depends on analytical objectives and problems specific to determination of an analyte in the substrate [5]. Contamination has been a centre of focus in marine analytical chemistry, particularly for trace elements and compounds in sea water. However, for metals in sediments, contamination has proved, for the most part, to be relatively unimportant; interferences, matrix effects and incomplete recovery of the species determined are more serious concerns. It is here, therefore, that sediment CRM's can be most usefully applied. Reference materials can be used to validate a method [5, 6] and estimate its performance characteristics. Clearly, knowing the correct answer helps to determine causes of problems and to revise procedures to produce data with minimum bias. However, it is important that the analyst demonstrates statistical control of the procedure

before turning to the problem of bias estimation using certified audit samples. Reference materials are probably best not applied to this control task in view of their limited supply and expense. A good control needs only to be representative and uniform within subsampling, and laboratory personnel can prepare suitable inexpensive controls. Reference materials are also generally unsuitable for external or internal audits and laboratory performance checks because their compositions are widely known and easily recognized by astute analysts.

From the above, it is clear that an expanded set of CRM's would be desirable if confidence in comparing and evaluating data sets is to be achieved. Few organizations are capable of certifying large amounts of material, and other more pressing needs for CRM's suggest that these will not soon be forthcoming. The intent of this paper is to illustrate how presently available CRM's can be augmented and tailored to provide better estimates of accuracy for determinations of trace elements in marine sediments.

MANIPULATION OF REFERENCE SEDIMENTS

Effort in preparing certified marine sediments of carefully controlled composition and careful determination does not make them sacrosanct. Direct determinations on them will remain an important exercise, but their value lies in helping analysts to evaluate performance on their own samples. Mixing, if done properly, can create a range of certified "authentic" sediments [7] with composition, known only to the mixer, controlled by two or more certified end points.

To extend the use of certified material, the laboratory should prepare its own reference material (here termed secondary reference) from sediments sampled from the region of interest. These materials will not be certified but this disadvantage is more than offset by the representative nature of sediment and it certainly can be applied for control purposes. Saving some material for later use by other laboratories interested in related problems, or determination by other methods will strengthen its usefulness.

Another way of altering sediments is to spike them [1, 7] with a soluble form of the species to be determined to produce a "synthetic" sample. While some results can be achieved, for metals the information is usually of a negative sort, i.e., recovery of spike does not guarantee that the species is being removed from the matrix. Therefore, this idea, admittedly useful in certain circumstances [8], will not be pursued here.

Certified reference sediments are usually distributed as a sterilized dried powder which has been screened, usually after grinding. According to their specifications, BCSS-1 and MESS-1 pass a 125- μ m sieve, and NBS SRM 1645 pass a 180- μ m sieve. By definition, sediments (certified or otherwise) are heterogeneous and may be subject to fractionation by magnetic, electrostatic and mechanical forces. They should always be remixed by tumbling or rolling for a minute or two in their container just before sub-sampling. Secondary

references can be prepared by following similar procedures [9], sieving freeze-dried sediments and even irradiating the product to eliminate biological activity. Small quantities (<1 kg) can be effectively mixed in a blender or by tumbling for a day or two to achieve acceptable uniformity [9], but this must be evaluated from subsequent analyses. Mixing and blending sediments is optimal if particle sizes are closely matched, and once prepared, secondary reference should be treated with the same respect as is given to certified material.

To prepare and blend sediments, one must be aware of well known sampling problems unique to heterogeneous particles. Kratochvil et al. [10] have recently reviewed the relevant literature and their paper should be consulted for more detail. When small numbers of particles are sampled, and the analyte is unevenly distributed among them, a considerable sampling variance will arise. To reduce this variance to an acceptable level, samples must be made sufficiently large, and theory has been applied to the problem of choosing appropriate sample size. For a well-mixed, 2-component particulate assemblage, each component containing a different percentage of the analyte in question, Kratochvil et al. [10] give Benedetti-Pichler's formula as

$$n = [d_1 d_2 / \bar{d}^2]^2 [100(P_1 - P_2) / Q\bar{P}]^2 p(1 - p) \quad (1)$$

where d_1 and d_2 are the respective particle densities, \bar{d} is the average density, P_1 and P_2 are the concentrations of analyte in the two components, \bar{P} is the average concentration in the mixture (P_1 , P_2 and \bar{P} must have identical units) and p is the fraction of one component in the mixture. The number of particles, n , which should be included in the sample to achieve acceptable sampling relative standard deviation, $Q\%$, can be translated into weight if particle density and size are known. For example, suppose that a blend with about $1.3 \mu\text{g g}^{-1}$ cadmium content is required. It would be possible to mix 9 parts of NBS SRM 1646 ($0.36 \mu\text{g g}^{-1}$ Cd) with 1 part of NBS SRM 1645 ($10.2 \mu\text{g g}^{-1}$ Cd). (This reference material is river sediment and so could be used as an estuarine end-member. Its high Cd, Pb and Zn contents make it an obvious choice for pollution studies, but this is partially offset by its abnormally high chromium content of about 3%.) The reasonable assumption that particle densities are equal (2.5 g cm^{-3}) and a target sampling error, $Q = 1\%$, yields, according to Eqn. 1,

$$n = [1.0][100(10.2 - 0.36)/1.0 \times 1.34]^2 (0.10)(0.90) = 4.9 \times 10^4 \quad (2)$$

If it is assumed, as an extreme case, that all particles are $180 \mu\text{m}$, spherical in shape, and contain either 10.2 or $0.36 \mu\text{g g}^{-1}$ Cd, Eqn. 2 translates to about 370 mg . For a smaller grain size, say $125 \mu\text{m}$, a 125-mg sample should achieve the same sampling error. The certification process for BCSS-1 and MESS-1 relied on subsamples 500 mg or larger, although they are well mixed for trace metals even at 100-mg sample sizes (private communication, S. Berman, NRCC, 1984). The NBS SRM 1646 certification is also based on 500-mg samples but smaller amounts were used (100 mg) for NBS-SRM 1645

certification. The above considerations show that blending reference sediments in gram quantities and removing 500 mg or greater sub-samples should adequately control sampling error. Considerably smaller portions could probably be used, but this would have to be tested by analysis of replicated sub-samples and comparison of results with certified values or with results based on larger sub-samples [11].

If for any reason the mixing cannot be done satisfactorily the entire mix should be used [7]. In this case, suitable weights of the component sediment should not exceed the total mass of sample known to be within the ruggedness bounds of the method.

TECHNIQUES FOR USING REFERENCE MATERIALS

Control charts are basic to the principle of obtaining quality data [1, 5], and their design and interpretation have been well reviewed elsewhere [12]. Here three plans are outlined for using CRM's which should supplement normal control practices. Blending, as previously described, allows the preparation of samples of known but varied composition. Furthermore, there is the option of running the samples as knowns to assist the analyst in self-evaluation, or unknowns as part of a performance check.

Youden pairs

Paired reference materials of similar but not identical composition offer advantages in quality control and assessment, and in differentiating between systematic and random errors. In spite of very adequate descriptions of their use [13, 14], they seem almost never to be applied for sediment determinations. This may stem from reluctance to mix reference materials as is recommended here to produce control pairs, or general unfamiliarity with the method. Statisticians tend to favor genuine replicates but there is no reason why both approaches cannot be satisfied using an analysis of variance design. The main advantages of Youden pairs are their visual impact, and their use in separating and estimating systematic vs. random components of error. They thus show where effort should be applied to improve performance of a method.

An example of a Youden plot for the determination of copper (4 replicates) in BCSS-1/MESS-1 is shown in Fig. 1. These data come from an interlaboratory study [9], but the principles have useful intralaboratory application. If median lines are drawn, then random errors would result in an even distribution among the four quadrants. This is almost never observed and data will form an ellipse like that shown in Fig. 1. Systematic errors tend to cause data distribution in the upper-right lower-left quadrants. Good precision but systematic errors (between days, batches, laboratories, etc.) will tend to form a line with slope 45° . The copper determinations shown are dominated by systematic errors between laboratories. Most laboratories have obtained good precision but only 2 or 3 have been precise and accurate. With the

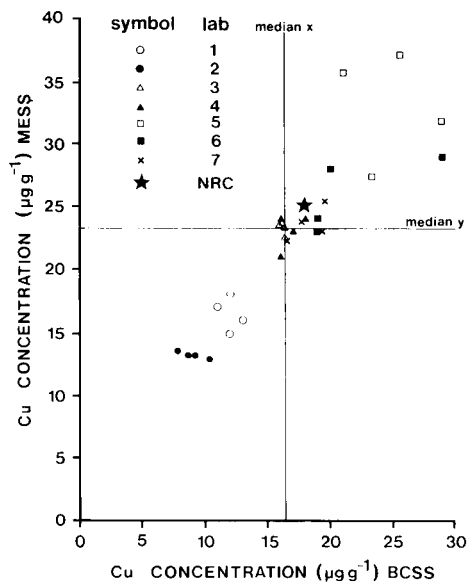


Fig. 1. Youden plot for the determination of copper in the pair BCSS–MESS. Systematic errors are evident as data spread along a 45° line, while random errors cause spread about the line. The small symbols represent 7 different laboratories each of which ran 4 replicates. The certified value is plotted as a star.

reasonable assumption that variance is approximately the same for both pairs, it can be shown that $s_R^2 = s_D^2/2$ and $s_S^2 = (s_T^2 - s_D^2)/2$, where s_R^2 is the random variance, s_S^2 the systematic variance, s_T^2 the variance associated with totals (pairs added) and s_D^2 with differences (pairs subtracted). For the data plotted on Fig. 1, $s_R = 2.0 \mu\text{g g}^{-1}$ and $s_S = 7.9 \mu\text{g g}^{-1}$. Attempts to increase precision would be wasted until systematic errors have been reduced.

Embedding

This can be considered as a type of standard addition. Instead of adding known spikes of analyte to a digest, one adds known amounts of a CRM to portions of a sample with the precautions outlined earlier. Most important is to arrange or choose samples and CRM's which match in particle size. The advantage of this procedure over simple spiking of an extract or sediment (synthetic sample) is that it will evaluate the effectiveness of digestion of CRM in the presence of real sample material. The confidence with which one can then evaluate digestion of the real sample will depend on how closely the two materials match in their bulk properties. (For example, a carbonate CRM would be a poor choice to evaluate digestion of a silicate sample.)

Suppose that a mixture is prepared from x g of a sample with composition X and r g of a CRM with composition R. Composition of the blend, Y, will be related to original compositions as

$$Y = (1/(x + r))[xX + rR] \quad (3)$$

If both mixture and sample are analyzed, the “embedded” reference can be retrieved because

$$[(x + r)/r]Y - (x/r)X = R \quad (4)$$

If variances associated with measuring Y and X are s_Y^2 and s_X^2 , respectively, propagation of error theory predicts that the variance associated with R calculated by Eqn. 4 is

$$s_R^2 = [(x + r)/r]^2 s_Y^2 + (x^2/r^2)s_X^2 \quad (5)$$

$$\text{if } s_Y^2 \approx s_X^2, s_R^2 = \{[(x + r)^2 + x^2]/r^2\} s_Y^2 \quad (6)$$

Equations 5 and 6 show that the power of resolving R is weak for single paired samples especially if the mixture contains only a small fraction of CRM, or if s_X or s_Y is large compared to R. The latter might arise if a CRM with very low analyte concentration were mixed with a contaminated sediment, and the relative standard deviation (%) was approximately constant. With prior knowledge or estimates of X, R, s_X and s_R , Eqns. 4 and 5 can be used to assess the practicality of the technique. Embedding is to be recommended primarily as an adjunct to extract more information from control charts or Youden pairs which are already being used on a regular basis.

The linear model

If analytical results on CRM's are plotted against their respective certified values, there are several linear possibilities [15, 16]. These comprise four cases: (1) the ideal data set having slope = 1, intercept = 0; (2) the data set having constant bias with slope = 1, intercept \neq 0; (3) the data set having bias as a function of concentration with slope \neq 1, intercept = 0; and the general situation (4) the data set having additive and multiplicative components of bias with slope \neq 1, intercept \neq 0. It is, of course, possible to find curvature and resort to non-linear equations to fit data [17]. However, in this case, error analysis becomes more complex, and severe curvature almost certainly indicates problems in conducting the method.

With a reasonable selection of CRM's (i.e., a wide concentration range for components of interest), it is possible to prepare references suitable for evaluating which of the above listed models is appropriate to the data. These CRM “calibrants” should be distributed among real samples, preferably replicated. For the linear model, five points are recommended [2, 15] (with experience, this may be dropped to three points), and replication should be used to evaluate linearity [18]. These requirements may be too stringent for small data sets but could certainly be implemented by laboratories routinely handling large numbers of samples and devoting 10–15% of their effort to quality practices. The advantage of constructing and testing a linear model is that it enables the analyst to evaluate accuracy systematically. With a single reference material, one is not sure which, if any, of the above linear cases apply to data. Case 1, however, will almost always be eliminated. The problem,

as with single-point calibrations, is that one is very uncertain what a single reference point implies for most if not all data [16].

Figure 2 shows two examples for which the linear model might be considered. For both, CRMs were analyzed for aluminum and zinc by two digestion methods (aqua regia and aqua regia/hydrofluoric acid); for purposes of illustration the actual method is not important. The CRM's analyzed included BCSS-1, MESS-1, OCSS-1 (a material prepared and evaluated in a round robin [9]) and three blind references made from mixtures of NBS SRM-1645 and NBS SRM-1646. For clarity, Fig. 2 shows average determinations of analyte in the CRM's; however, replicates were used and the least-squares line was constructed from original data.

For zinc (Fig. 2a), the linear model is appropriate to both methods as done here, although the results produced are apparently consistently low compared to certification. The aqua regia/hydrofluoric acid digest does not extract zinc more efficiently, and this method provides less precision. In Fig. 2(b), it is clear that aqua regia is insufficient to solubilize aluminum from the matrix. The aqua regia/hydrofluoric acid digest does considerably better, and error statements could be made in the concentration range 5–6% Al [16]. However, a linear model should not be applied to aluminum data outside the 5–6% range in view of the tight grouping of data. Assuming a line through the origin would entail risks of error which could be considerable at high or low concentrations. The solution to this problem is to obtain a wider range of CRM's.

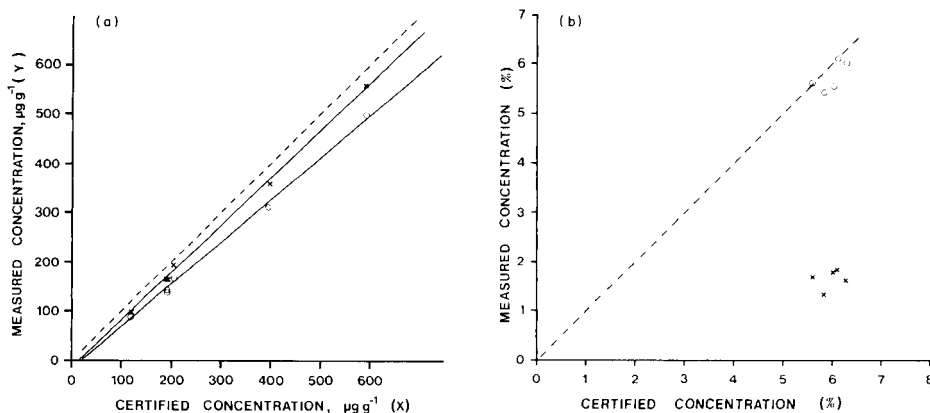


Fig. 2. (a) The measured concentration of zinc in reference sediments and mixtures thereof as a function of certified value for two different analytical methods: (x) an aqua-regia digest for which $m = 0.966$, $a = -16.8$, $s^2_{YX} = 48.7$, $n = 27$; (o) hydrofluoric acid/aqua-regia digest for which $m = 0.863$, $a = -18.0$, $s^2_{YX} = 185$, $n = 24$. Linear regression can be used for either method to convert data to "certified" and therefore put the two methods on a common reporting basis. (b) The measured concentration of aluminum in reference sediments: (x) aqua-regia digest; (o) hydrofluoric acid/aqua-regia digest. In this case, the linear model would be of limited use.

In principle, data which are traceable to certified references should be intercomparable. For large-scale, long-term monitoring programs which involve more than one laboratory, or for the analysis of trends, traceability is essential. The problem, as Taylor [16] states, is that a definitive protocol for traceability has not been established. He suggests that a measurement on an environmental sample can be corrected to "true" by multiplying by the certified/measured ratio for a simultaneously measured certified material. He cautions that the certified material must be of similar composition to the environmental sample and that both must provide similar instrumental responses. The underlying assumption that the measurement system is linear through zero (Case 1 or 3 above) cannot be tested with measurements on a single CRM; however, violation of this assumption (i.e., additive errors) would not be too serious provided that the certified and environmental samples match closely. With information on the standard deviation of the measurements and the degree of replication, Taylor gives appropriate equations to estimate error. In contrast, the measurement of several CRM's as suggested here allows one to evaluate linearity and choose the appropriate model for correcting data. Rather than depending on CRM's which closely match environmental samples, the method proposed depends on CRM's which span the range of environmental samples. Linear regression offers a simple and direct method of correcting measured values to certified, for which there are well established formulae for demonstrating linearity and calculating interval estimates [18]. Furthermore, this model provides more security in that it allows one to trace a measurement to two or more certified references simultaneously. If k replicate measurements are made on a sample, and a CRM "calibration" line based on n determinations is used, the confidence interval estimate is

$$X' = \bar{X} + [m(\bar{Y}' - \bar{Y})/K] \pm (t s_{YX}/K) \{ [(\bar{Y}' - \bar{Y})/SS_X] + [(1/n) + (1/k)]K \}^{1/2} \quad (7)$$

where $K = m^2 - t s_m^2$, $SS_X = \Sigma X^2 - (\Sigma X)^2/n$. The symbols have the following meanings: $t = t_{\alpha(2), n-2}$, m is the slope, s_m^2 the slope variance, s_{XY} the standard error of estimate, X' the predicted independent variable, \bar{X} the average of calibration X_i , \bar{Y} the average of calibration Y_i , and \bar{Y}' the average of k replicate sample determinations. For example, suppose duplicate zinc results (aqua-regia digest) for a sample were 333 and 347 $\mu\text{g g}^{-1}$. For the linear calibration (Fig. 2a), $\bar{Y}' = 340 \mu\text{g g}^{-1}$ is converted by means of Eqn. 7 to yield $\bar{X}' \pm 95\% \text{ CI} = 369 \pm 11 \mu\text{g g}^{-1}$. Confidence intervals (CI) would be larger for data further from the centre point of the line, and for lines based on fewer reference data. This method of assessing error depends on the assumption that precision is similar for samples and CRM's and that it is relatively homogeneous over the measurement range [19]. These assumptions should be evaluated from control charts and the use of replicate samples which span the range of interest. Therefore, the linear model augments but does not replace the use of sample replicates.

CONCLUSIONS

Environmental analysts now generally recognize the need to include results on CRM's and the number of reports without such support data is decreasing. However, if the objective of analyzing CRM's is to estimate accuracy, the analysis of a single CRM will not be very useful particularly if it differs from samples. In this paper, three general plans are outlined for applying CRM's to accuracy assessment and details are given on how to manipulate the CRM's properly. Which of the three techniques one chooses to apply depends on the analytical objectives, the number of samples routinely analyzed, and whether they are handled in batch or continuous mode.

The most straightforward approach is the linear model. This enables one to distinguish additive or multiplicative components of bias and then to make appropriate corrections as outlined above. The cost of running five or more replicate CRM's additional to a large number of environmental samples is minimal and, provided that the system is under statistical control, can be used to evaluate the whole data set. With time, a large number of such data can be collected and an assessment made of the stability of the method.

If the laboratory already runs control samples, the use of Youden pairs should entail little extra expense, at most requiring a doubling of the control samples. Offsetting this, the analyst may be able to reduce the frequency of control samples depending on the system stability. The technique of embedding could be applied during method validation, but will not be very cost-effective by itself. However, if the use of Youden pairs is adopted for control, it will cost no extra to prepare the pair sample by embedding. A control chart could be maintained for R (Eqn. 4) and the mean after a number of determinations compared with the certified value, yielding extra information.

If one is to apply the general plans suggested above, it would help if CRM's of similar particle-size distribution but widely varying composition were prepared. Given three CRM's, for example, it would be possible, by mixing, to construct a ternary system representing a wide range of sediments. Reference materials close in composition (MESS-1, BCSS-1, NBS SRM-1646) form a very restricted ternary system inappropriate to pollution studies.

The statements made here can be extended to include other particulate reference materials and other analytical targets. It is up to the analyst to use judgement in attempting to prepare mixtures which bracket the range in samples. If this can be done successfully, confidence in how the method is performing on real samples will be considerably strengthened.

We thank W. J. Cretney and J. A. J. Thompson for providing critical comment, V. Forsland for preparing the diagrams and J. Poulin for typing the manuscript. We are especially indebted to J. K. Taylor for suggesting several improvements and his support and encouragement during the preparation of this paper.

REFERENCES

- 1 L. H. Keith, W. Crummett, J. Deegan, Jr., R. A. Libby, J. K. Taylor and G. Wentler, *Anal. Chem.*, 55 (1983) 2210.
- 2 D. MacDougall, F. J. Amore, G. V. Cox, D. G. Crosby, F. L. Estes, D. H. Freeman, W. E. Gibbs, G. E. Gordon, L. M. Keith, J. Lal, R. R. Langner, N. I. McClelland, W. F. Phillips, R. B. Pojasek and R. E. Sievers (ACS Committee on Environmental Improvement), *Anal. Chem.*, 52 (1980) 2242.
- 3 D. S. Russel, Report No. 8 NRCC No. 23025, Marine Analytical Chemistry Standards, NRC of Canada, Ottawa, 1984, pp. 35.
- 4 C. J. Kirchmer, *J. Environ. Sci. Technol.*, 17 (1983) 174A.
- 5 J. K. Taylor, *ASTM J. Test. Eval.*, 11 (1983) 385.
- 6 J. K. Taylor, *Anal. Chem.*, 55 (1983) 600A.
- 7 Anonymous, ASTM Publication D 3975-80, (1980) 1191.
- 8 A. V. Holden, G. Topping and J. F. Uthe, *Can. J. Fish. Aquat. Sci.*, 40(2) (1983) 100.
- 9 R. W. Macdonald and H. Nelson, *Can. Technol. Rep. Hydrogr. Oc. Sci.* 33, Institute of Ocean Sciences, 1984, pp. 57.
- 10 B. Kratochvil, D. Wallace and J. K. Taylor, *Anal. Chem.*, 56 (1984) 113R.
- 11 C. O. Ingamells and P. Switzer, *Talanta*, 20 (1973) 547.
- 12 Anonymous, ASTM Special Publication 15D, 1976, American Society for Testing and Materials, Philadelphia, 161 pp.
- 13 W. J. Youden, *Precision Measurements and Calibration. Statistical Concepts and Procedures*, 1969 NBS Special Publication 300, Vol. 1, pp. 133-137.
- 14 W. J. Youden, *Statistical Manual of the Association of Official Analytical Chemists*, 1975, Assoc. Off. Anal. Chem. Arlington, 88 pp.
- 15 J. Mandel and T. W. Lashof, *Precision Measurements and Calibration Statistical Concepts and Procedures*, 1969, NBS Spec. Publ. 300, Vol. 1, p. 170.
- 16 J. K. Taylor, *Thalassia, Jugosl.*, 16 (1980) 111.
- 17 L. M. Schwartz, *Anal. Chem.*, 49 (1977) 2062.
- 18 M. G. Natrella, *Experimental Statistics, NBS Handbook 91*, U.S. Dept. of Commerce, Washington, D.C., 1966, Chap. 5.
- 19 L. M. Schwartz, *Anal. Chem.*, 51 (1979) 723.

ASSAY FOR AROMATIC L-AMINO ACID DECARBOXYLASE BASED ON FLUORESCENCE DERIVATIZATION WITH 1,2-DIPHENYLETHYLENEDIAMINE

MYUNGKOO LEE, HITOSHI NOHTA and YOSUKE OHKURA*

Faculty of Pharmaceutical Sciences, Kyushu University 62, Maidashi Higashi-ku, Fukuoka 812 (Japan)

BEONGTAE YOO

College of Pharmacy, Chungnam National University, Gung-dong, Chung-ku, Daejeon, Chungnam 300-31 (Korea)

(Received 15th April 1985)

SUMMARY

Methods based on fluorimetry and high-performance liquid chromatography (h.p.l.c.) for highly sensitive assay of aromatic L-amino acid decarboxylase are described. Dopamine formed enzymatically from a substrate, L-dihydroxyphenylalanine (L-DOPA), after chromatography on a small column of a cation-exchanger, Toyopak SP, is converted to a fluorescent compound by reaction with 1,2-diphenylethylenediamine. The derivative is measured by direct spectrofluorimetry or by reversed-phase h.p.l.c. with fluorimetric detection. The limits of detection for dopamine formed enzymatically in the direct and h.p.l.c. methods are 15 and 1 pmol per assay tube, respectively. The enzyme in rat liver, kidney, brain, heart, adrenal medulla and serum can be precisely assayed.

Aromatic L-amino acid decarboxylase (AADC; aromatic L-amino acid carboxy-lyase, EC 4.1.1.28) occurs in many tissues, and catalyzes the decarboxylation of aromatic L-amino acids to the corresponding amines. The enzyme has a high affinity especially for L-DOPA (L-dihydroxyphenylalanine) and 5-hydroxytryptophan (5-HTP) [1], and so it plays an important role in the biosyntheses of catecholamines (dopamine, norepinephrine and epinephrine) and serotonin.

Many assays for AADC in biological materials have been reported, including manometric [2], spectrophotometric [3, 4], fluorimetric [5, 6], high-performance liquid chromatographic (h.p.l.c.) [6–9] and radio-isotopic [1, 10] procedures. Only the h.p.l.c. method with electrochemical detection [6, 7, 9] and the radio-isotopic methods permit the assay of AADC in serum of experimental animals such as the rat, mouse, guinea pig and monkey, in which the AADC activity is extremely low. However, the former technique requires careful manipulation to attain high sensitivity and reproducibility, and the latter are rather complicated and require an expensive substrate.

Highly sensitive h.p.l.c. methods with pre-column derivatization for the determination of catecholamines in human urine [11] based on 1,2-diphenylethylenediamine (DPE), a selective fluorescence derivatization reagent for catechol compounds [12], have been developed in this laboratory. This paper describes direct and h.p.l.c. methods for sensitive assay of AADC in rat serum and tissue homogenates. The methods are based on the determination of dopamine formed from the substrate L-DOPA, under the optimum reaction conditions for the enzyme. Dopamine, after separation from L-DOPA, was unchanged after chromatography on a small column of cation exchanger, and was converted to a fluorescent compound by reaction with DPE. The compound was measured by conventional fluorimetry or reversed-phase h.p.l.c. with fluorescence detection using isoproterenol as an internal standard.

EXPERIMENTAL

Reagents and solutions

The reagents used were L-DOPA and D-DOPA (Sigma), dopamine hydrochloride and pyridoxal phosphate (Wako, Osaka), isoproterenol hydrochloride, 5-hydroxytryptophan and 3-hydroxybenzylhydrazine dihydrochloride (Nakarai Chemicals, Kyoto) and DPE (Dojindo Laboratories, Kumamoto). The DPE solution (0.1 M, apparent pH 6.7) was prepared by dissolving 212 mg of DPE in 10 ml of 0.1 M hydrochloric acid. A Toyopak SP (cation-exchanger, sulfopropyl resin, Na⁺ form; Toyo Soda, Tokyo) column was prepared by packing 1.0 ml of the cation-exchanger into a plastic tube (35 × 10 mm i.d.). The column was washed successively with 2 ml of 2 M sodium hydroxide, 5 ml of water, 2 ml of 2 M hydrochloric acid and 10 ml of water. The used column can be regenerated by washing in the same way and could be used more than five times.

Enzyme preparations

Male Donryu rats (4 weeks old) were decapitated, and the livers, kidneys, brains, hearts and adrenal medullas were immediately removed and chilled on ice. All further procedures were conducted at 0–5°C. Adrenal medulla (5 mg) was homogenized with 1.25 ml of 0.25 M sucrose, and the others (500 mg each) with 4.5 ml of the sucrose solution. Serum was obtained by centrifuging the blood at 1000g for 10 min at 5°C. The homogenates and serum were stored at –70°C until used and diluted with 0.25 M sucrose when required for use: liver and kidney, 500 times; brain, 30 times; heart, 20 times; serum, 5 times.

Apparatus

Uncorrected fluorescence excitation and emission spectra and intensities were measured with a Hitachi MPF-4 spectrofluorimeter using quartz cells (ca. 1.2 ml cell volume; 0.3 × 1.0 cm optical pathlengths). The excitation

and emission bandwidths were both set at 10 nm. The column was an Ultrasphere ODS (150 × 4.6 mm i.d.; Beckman). The column temperature was ambient (20–25°C). An Eyela PLC-10 liquid chromatograph (Tokyo Rika, Tokyo) was used, equipped with a sample injector valve (100- μ l loop) and a Shimadzu FLD-1 fluorescence detector fitted with a 14- μ l flow cell and an EM-4 emission filter. Uncorrected fluorescence excitation and emission spectra of the eluate were measured with a Hitachi 850 fluorescence spectrophotometer fitted with a 20- μ l flow cell, and emission and excitation bandwidths of 5 nm.

Procedures

Procedure for direct fluorimetry. To 100 μ l of the enzyme preparation were added 200 μ l of 0.2 M sodium phosphate buffer (pH 6.8) and 100 μ l of 50 μ M pyridoxal phosphate. The mixture was preincubated at 37°C for 10 min, and again incubated for 10 min after addition of 100 μ l of 8 mM L-DOPA. At the end of the incubation, 200 μ l of 1.5 M trichloroacetic acid was added to stop the reaction. The mixture was centrifuged at 1000g for 10 min at 4°C, and the supernatant liquid was poured onto a Toyopak SP column. The column was washed successively with 10 ml of water, 2 ml of 0.2 M phosphate buffer (pH 5.5) and 5 ml of water. The adsorbed amine was eluted with 2.0 ml of a mixture of ethanol and 1.0 M sodium chloride (7:3, v/v). To the eluate, 100 μ l each of DPE solution and 15 mM potassium hexacyanoferrate(III) were added and the mixture was allowed to stand at 37°C for 40 min to develop the fluorescence. For the blank, the enzyme preparation was taken through the procedure except that the order of addition of L-DOPA and trichloroacetic acid was reversed and incubation was omitted. The fluorescence intensities of the test solution and the blank were measured at an emission wavelength of 480 nm and an excitation wavelength of 350 nm.

Procedure for h.p.l.c. method. The same procedure as for the manual method was used except that 100 μ l each of 3.0 M trichloroacetic acid and 1.0 nmol ml⁻¹ isoprotenerol as an internal standard were used in place of 200 μ l of 1.5 M trichloroacetic acid. The preparation of a blank was unnecessary unless the chromatogram for the blank was to be investigated. The final mixture (100 μ l) was injected into the chromatograph. The mobile phase was a mixture (11:9, v/v) of acetonitrile and 50 mM Tris/hydrochloric acid buffer (pH 7.0) and the flow rate was 1.0 ml min⁻¹.

For the examination of the effect of 5-hydroxytryptophan on the formation of dopamine, 100 μ l of 8 mM L-DOPA in the procedure was replaced with 100 μ l of the L-DOPA solution containing 5-hydroxytryptophan (0.25 or 2.5 mM). To find the effect of 3-hydroxybenzylhydrazine, 0.2 M phosphate buffer (pH 6.8) containing this compound (0–1 mM) was used in place of the buffer.

RESULTS AND DISCUSSION

Conditions of the enzymatic reaction

The conditions were investigated mostly by using the h.p.l.c. method. The optimum pH for the AADC reaction in sodium phosphate buffer was 6.8 (Fig. 1), and that buffer gave maximum and constant activity at concentrations of 0.05–0.5 M for all the enzyme preparations. Although 0.1 M HEPES and 0.1 M TES buffers, and 0.1 M Tris/hydrochloric acid buffer gave maximum activity at pH 7.0–7.5, activity was only ca. $\leq 60\%$ that obtained in the pH 6.8 phosphate buffer. Thus 0.2 M sodium phosphate buffer, pH 6.8, was used in the procedure.

Maximum and constant activity of AADC was attained in the presence of 0.4–1.8 mM L-DOPA in the reaction mixture for the enzyme in liver, and identical results were also given for the enzyme in the other tissues. The value of the Michaelis constant for L-DOPA was ca. 0.1 mM, i.e., 0.09 mM for liver and kidney, 0.08 mM for adrenal medulla, 0.10 mM for heart and serum, and 0.11 mM for brain tissue. Thus 1.6 mM L-DOPA was used as a saturating concentration. Pyridoxal phosphate gave maximum and constant activity at concentrations of 1.0 μ M to 1.0 mM in the enzyme reaction mixture (Fig. 2); 10 μ M was selected in the procedure. Because dopamine

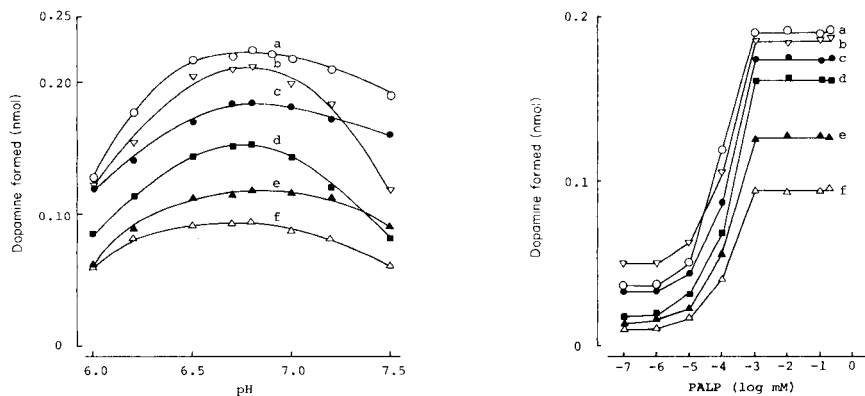


Fig. 1. Effect of pH of 0.2 M sodium phosphate buffer on amount of dopamine formed. Portions (100 μ l) of the AADC preparations were treated according to the procedure for the h.p.l.c. method at various pH values. AADC preparations (activities, nmol dopamine min^{-1} mg^{-1} protein in parentheses): (a) liver (6.91); (b) kidney (7.21); (c) brain (0.62); (d) heart (0.20); (e) adrenal medulla (1.45); (f) serum (0.46 nmol min^{-1} ml^{-1}).

Fig. 2. Effect of pyridoxal phosphate (PALP) concentration on the amount of dopamine formed. Portions (100 μ l) of the AADC preparations were treated according to the procedure for the h.p.l.c. method at various PALP concentrations. AADC preparations (activities, nmol dopamine min^{-1} mg^{-1} protein in parentheses): (a) liver (5.80); (b) kidney (6.40); (c) brain (0.62); (d) heart (0.22); (e) adrenal medulla (1.58); (f) serum (0.46 nmol min^{-1} ml^{-1}).

can be a substrate for monoamine oxidase (MAO) [13] and also is susceptible to oxidation with oxygen as well as other oxidizing agents, there is a possibility of oxidative degradation of dopamine formed enzymatically during the incubation period. The amounts of dopamine formed enzymatically, were unaffected, for all the enzyme preparations, by the addition of pargyline (0–0.3 mM) as a MAO inhibitor, or ascorbic acid, dithiothreitol or reduced glutathione (0–0.6 mM) as antioxidant to the enzyme reaction mixtures. Dopamine added to the enzyme reaction mixture of the blank was stable when incubated at 37°C for 10 min (prescribed incubation time). Thus neither pargyline nor antioxidant was used in the procedure.

L-DOPA is decarboxylated non-enzymatically as well as by the AADC-catalyzed reaction [14–18]. It has been reported that non-enzymatic decarboxylation occurs in the presence of some metal ions such as iron(II), iron(III) and copper(II) [14] and oxidizing substances such as sodium hexacyanoferrate(III) and oxyhaemoglobin [15, 16], and that such decarboxylation was inhibited by the addition of EDTA or reducing agents such as 2-mercaptoethanol and reduced glutathione, or both [17, 18]. In the present procedure, however, EDTA and 2-mercaptoethanol (1–500 μ M each in the enzyme reaction mixture) did not influence the amounts of dopamine formed. The formation of dopamine was not observed when D-DOPA was used in place of L-DOPA or when the enzyme preparations were denatured by heating at 95°C for 5 min. 3-Hydroxybenzylhydrazine, an AADC inhibitor [19], at concentrations of 0.1 and 5 μ M in the enzyme reaction mixture inhibited the activity by ca. 85 and 100%, respectively, for all the enzyme preparations. AADC works on 5-hydroxytryptophan as well as L-DOPA, and these amines can be competitive inhibitors for each other [3]. 5-Hydroxytryptophan competitively inhibited AADC in liver against L-DOPA (Fig. 3), with an observed inhibitory constant (K_i) value of 0.06 mM, which was obtained as described by Dixon [20]. 5-Hydroxytryptophan similarly acted as a competitive inhibitor towards AADC in brain with the same observed K_i value as in liver AADC. All the above observations suggest that dopamine formed in the present procedure results from the enzymatic decarboxylation of L-DOPA.

The amounts of dopamine formed enzymatically were proportional to the amounts (μ g/tube) of protein in the AADC preparations up to at least 33 (liver), 77 (kidney), 20 (adrenal medulla), 450 (brain) and 750 (heart), and to the volume of serum up to 100 μ l. The amounts (μ g/tube) used in the procedure were 3 (liver and kidney), 4 (adrenal medulla), 25 (brain), 80 (heart) and 20 μ l (serum); these amounts were selected for convenience. The AADC activities in all the enzyme preparations were linear with time up to at least 20 min (Fig. 4).

Clean-up of dopamine formed enzymatically

Because the substrate L-DOPA which had not reacted in the enzyme reaction mixture also reacted with DPE under the conditions of the

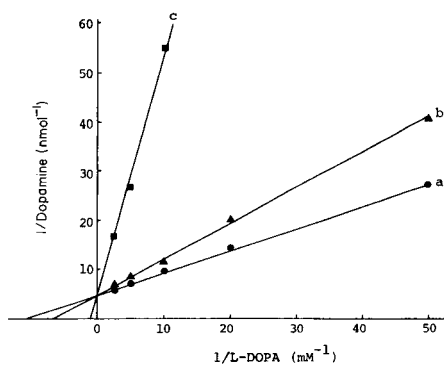


Fig. 3. Inhibition of liver AADC by 5-hydroxytryptophan. Portions (100 μ l) of the liver AADC preparation were treated according to the procedure for the h.p.l.c. method. Solid lines obtained by linear regression. Concentrations (mM) of 5-hydroxytryptophan in the reaction mixtures: (a) 0; (b) 0.25; (c) 2.5.

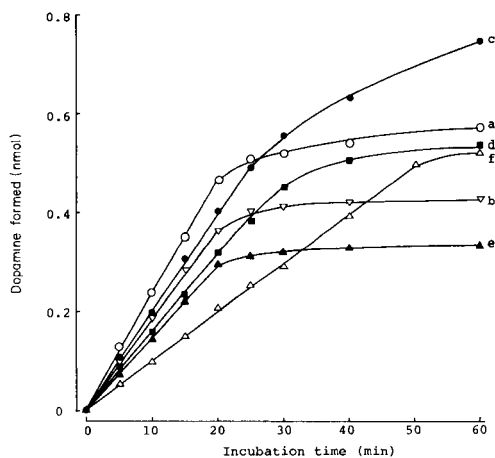


Fig. 4. Effect of incubation time on the amount of dopamine formed. Portions (100 μ l) of the AADC preparations were treated according to the procedure for the h.p.l.c. method for various incubation times. AADC preparations: (a) liver; (b) kidney; (c) brain; (d) heart; (e) adrenal medulla; (f) serum.

derivatization reaction to afford a fluorescent compound with excitation and emission spectra similar to those for dopamine [12], the L-DOPA had to be removed from the derivatization reaction mixture. This was successfully achieved by passage through a small column of the strongly acidic cation-exchanger Toyopak SP. This cation-exchanger allowed the application of the acidified enzyme reaction mixture (ca. 0.4 M trichloroacetic acid) without pH adjustment. The cation (hydrogen, lithium, sodium ion) form of the exchanger did not affect the recoveries of dopamine and isoproterenol. After the application of the reaction mixture, the column was washed with water and 0.2 M sodium phosphate buffer (pH 5.5) and dopamine and isoproterenol were eluted with a mixture of ethanol and 1.0 M sodium chloride (7:3, v/v). When the buffer was replaced by water, the eluate resulted in a strongly acidic solution (pH 1–2) and no fluorescent derivatization reaction occurred. The concentrations of phosphate buffer (0.1–0.25 M) and pH values (5.3–7.0) had no effect on the recoveries of dopamine and isoproterenol. The recoveries of these two compounds (0.1 nmol each) added to the incubated enzyme reaction mixture of the blank were 86% and 79% (liver), 88% and 87% (kidney, adrenal medulla and heart), 87% and 86% (brain) and 80% and 77% (serum) (mean of triplicate measurements in each case), respectively.

Direct fluorimetry

The conditions of the fluorescence derivatization reaction were the same as described previously [11]. The fluorescence excitation (maximum, 350 nm) and emission (maximum 480 nm) spectra for the final reaction mixtures of the enzyme preparations except for the adrenal medulla were identical with those of the reaction mixtures of dopamine. The preparation of adrenal medulla has relatively large amounts of endogenous norepinephrine and epinephrine as described later and they also react with DPE to afford corresponding fluorescent compounds which have fairly similar fluorescence excitation and emission spectra to those for dopamine. Though the endogenous norepinephrine and epinephrine could be removed from the preparation by dialysis against 0.25 M sucrose, AADC was unstable even at 4°C: the activity was reduced to one half after dialysis for 6 h. Thus the direct method does not permit a highly sensitive and reproducible assay for AADC in adrenal medulla.

The calibration graph for dopamine was linear up to at least 1 nmol/tube. The determinable limit for dopamine formed enzymatically was 15 pmol for all the enzyme preparations. The limit was defined as the concentration giving a fluorescence intensity twice the blank. The precision of the method was established by repeated assay ($n = 8$) by using an enzyme preparation from liver. The relative standard deviation (r.s.d.) was 2.9% for a mean AADC activity of $7.21 \text{ nmol min}^{-1} \text{ mg}^{-1}$ protein.

H.p.l.c. method

Figure 5 shows typical chromatograms obtained with the enzyme preparations from liver and adrenal medulla and those of the blank. Peak 1 in Fig. 5(a) and (c) had a retention time of 5.2 min and the eluate of the peak had fluorescence excitation (maximum, 350 nm) and emission (maximum, 480 nm) spectra identical with those for dopamine. Peaks 3 and 4 in Fig. 5(c) and (d) had retention times of 2.1 and 3.6 min, respectively, and fluorescence excitation (maxima 350 and 360 nm) and emission (maxima 470 and 480 nm) spectra identical with those for norepinephrine (NE) and epinephrine (E), respectively. The heights of peaks 3 and 4 in Fig. 5(c) were the same as those in Fig. 5(d). Therefore, those peaks can be ascribed to endogenous NE and E, respectively.

A linear relationship was observed between the ratios of the peak height of dopamine to that of isoproterenol and the amount of dopamine added in the range 0.01–0.4 nmol to the incubated enzyme reaction mixture of the blank. The limit of detection for dopamine formed enzymatically was 1 pmol/tube (45 fmol/100 μl injected) at a signal-to-noise ratio of 2, 15 times less than the direct method. The precision of the method was established with respect to repeatability by using the enzyme preparations from liver and adrenal medulla. The r.s.d. were 1.4 and 2.6% ($n = 10$) for mean activities of 8.2 and 2.3 $\text{nmol min}^{-1} \text{ mg}^{-1}$ protein, respectively.

The AADC activities in liver, kidney, adrenal medulla, brain, heart and

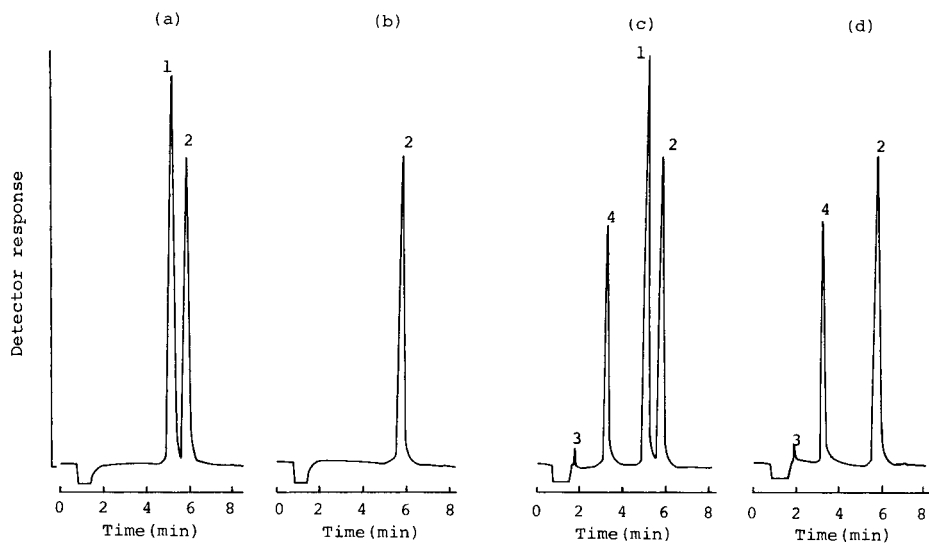


Fig. 5. Chromatograms obtained with the AADC preparations from (a) rat liver, and (c) rat adrenal medulla; (b) and (d) are the respective blanks. Portions ($100 \mu\text{l}$) of the AADC preparations were treated according to the procedure for the h.p.l.c. method. Peaks: (1) dopamine; (2) isoproterenol; (3) norepinephrine (endogenous, $0.14 \text{ nmol mg}^{-1}$ tissue); (4) epinephrine (endogenous, $2.85 \text{ nmol mg}^{-1}$ tissue). AADC activity ($\text{nmol min}^{-1} \text{ mg}^{-1}$ protein): liver, 5.25; adrenal medulla, 2.31.

TABLE 1

AADC activities in rat tissues obtained by h.p.l.c.

Tissue	AADC activity ^a ($\text{nmol dopamine min}^{-1} \text{ mg}^{-1}$ protein)
Liver	7.64 ± 1.58
Kidney	7.23 ± 0.78
Brain	0.64 ± 0.03
Heart	0.25 ± 0.07
Adrenal medulla	3.16 ± 1.76
Serum	0.41 ± 0.08^b

^aMean \pm s.d., obtained from 5 rats (Donryu, male, 4 weeks old). ^b $\text{nmol min}^{-1} \text{ ml}^{-1}$.

serum preparations from rats (Donryu, male, 4 weeks old) assayed by this method (Table 1) were in reasonable agreement with reported data [6].

The direct method is simple and rapid enough to assay 10 samples within 3 h. The h.p.l.c. method also permits assay for AADC in adrenal medulla, and is highly sensitive. Therefore, both the methods should be useful for biological and biomedical investigations of catecholamines and their metabolism.

REFERENCES

- 1 J. G. Christenson, W. Dairman and S. Udenfriend, *Arch. Biochem. Biophys.*, 141 (1970) 356.
- 2 H. Blaschko, *J. Physiol.*, 101 (1942) 337.
- 3 C. Streffer, *Biochim. Biophys. Acta*, 139 (1967) 193.
- 4 A. Charteris and R. John, *Anal. Biochem.*, 66 (1975) 365.
- 5 R. Kuntzman, P. A. Shore, D. Bogdanski and B. B. Brodie, *J. Neurochem.*, 6 (1961) 226.
- 6 M. K. Rahman, T. Nagatsu and T. Kato, *Biochem. Pharmacol.*, 30 (1981) 645.
- 7 T. Nagatsu, T. Yamamoto and T. Kato, *Anal. Biochem.*, 100 (1979) 160.
- 8 M. D'Erme, M. A. Rosei, A. Fiori and G. D. Stozio, *Anal. Biochem.*, 104 (1980) 59.
- 9 M. K. Rahman, T. Nagatsu and T. Kato, *Life Sci.*, 28 (1981) 485.
- 10 S. H. Snyder and J. Axelrod, *Biochem. Pharmacol.*, 13 (1964) 805.
- 11 H. Nohta, A. Mitsui and Y. Ohkura, *Bunseki Kagaku*, 33 (1984) E263.
- 12 H. Nohta, A. Mitsui and Y. Ohkura, *Anal. Chim. Acta*, 165 (1984) 171.
- 13 N. H. Neff and H. Y. T. Yang, *Life Sci.*, 14 (1974) 2061.
- 14 W. H. Vogel, *Naturwissenschaften*, 56 (1969) 462.
- 15 S. Okuno and H. Fujisawa, *Anal. Biochem.*, 129 (1983) 405.
- 16 H. Yanabe and W. Lovenberg, *Biochem. Biophys. Res. Commun.*, 47 (1972) 733.
- 17 E. D. Mackowiak, T. A. Hare and W. H. Vogel, *Biochem. Med.*, 12 (1975) 137.
- 18 S. Okuno and H. Fujisawa, *Anal. Biochem.*, 129 (1983) 412.
- 19 K. Modigh, *Psychopharmacologia*, 30 (1973) 123.
- 20 M. Dixon, *Biochem. J.*, 55 (1953) 170.

EVALUATION OF ARYL OXALATES FOR CHEMILUMINESCENCE DETECTION IN HIGH-PERFORMANCE LIQUID CHROMATOGRAPHY

KAZUMASA HONDA, KIMITOSHI MIYAGUCHI and KAZUHIRO IMAI*

Faculty of Pharmaceutical Sciences, University of Tokyo, 7-3-1 Hongo, Bunkyo-ku, Tokyo 113 (Japan)

(Received 4th April 1985)

SUMMARY

The chemiluminescence reaction between an aryl oxalate, hydrogen peroxide and a fluorescent compound is well known for use in h.p.l.c. post-column reactors. Here, several aryl oxalates are evaluated for this purpose in terms of intensity, rate of chemiluminescence decay, solubility in different solvents, and stability in the presence of hydrogen peroxide. Five oxalates are selected for different pH ranges of column eluates: bis(pentafluorophenyl) oxalate for pH < 2, bis(2,4-dinitrophenyl) oxalate for pH 2–4, bis(2-nitrophenyl) oxalate for pH 4–6, bis(2,4,6-trichlorophenyl) oxalate for pH 6–8, and bis(2,4,5-trichlorophenyl-6-pentyloxy-carbonyl) oxalate for pH > 8.

Recently, reactions of aryl oxalates such as bis(2,4,6-trichlorophenyl) oxalate (TCPO) with hydrogen peroxide have been used as the basis of chemiluminescence detectors in high-performance liquid chromatography (h.p.l.c.) for fluorescent compounds. Dansylated amino acids [1–4] and drugs [5], fluorescamine-labelled catecholamines [6], polynuclear hydrocarbons [7, 8], and *o*-phthalaldehyde-derivatized and 7-nitro-2,1,3-benzoxadiazole-labelled alkylamines [9] have been separated on reversed-phase columns and sensitively detected by a chemiluminescence detector. The mechanism is shown in Fig. 1. TCPO has been exclusively used on account of its stability [10]. However, in the course of studies on the determination of fluorescent compounds by h.p.l.c., the present authors encountered difficulties with TCPO because it can be used only at pH ca. 7.

In this paper, therefore, the chemiluminescent reactions of the aryl oxalates shown in Table 1 at various pH values are described; a stopped-flow technique was used. The oxalates are evaluated in terms of chemiluminescence intensity, decay constant of the chemiluminescent reaction, solubility, and stability in the presence of hydrogen peroxide.

EXPERIMENTAL

Chemicals

Distilled water for fluorescence analysis, methanol for fluorescence analysis, and acetonitrile for pesticide residue analysis (all from Kanto Chemicals Co., Tokyo) were used as received.

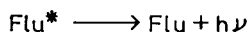
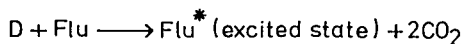
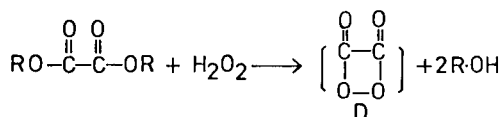
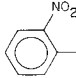
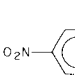
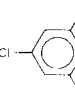
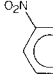
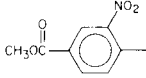
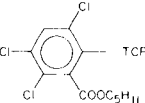
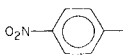
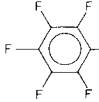
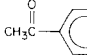


Fig. 1. Proposed mechanism for peroxyoxalate chemiluminescence. The fluorescer is indicated by Flu.

TABLE 1

Oxalate esters $\text{Ar}-\text{O}-\overset{\text{O}}{\parallel}{\text{C}}-\overset{\text{O}}{\parallel}{\text{C}}-\text{O}-\text{Ar}$ studied		
Ar	Ar	Ar
 2-NPO	 DNPO	 TCPO
 3-NPO	 MCNO	 TCPCO
 4-NPO	 PFPO	 4-APO

Bis(2,4,6-trichlorophenyl) oxalate (TCPO) was prepared as reported by Mohan and Turro [10]. Bis(2-nitrophenyl) oxalate (2-NPO), bis(4-nitrophenyl) oxalate (4-NPO), bis(2,4-dinitrophenyl) oxalate (DNPO) and bis(pentafluorophenyl) oxalate (PFPO) were prepared by the method of Rauhut et al. [11]. All oxalates were recrystallized from acetonitrile except PFPO which was recrystallized from dichloromethane.

Bis(3-nitrophenyl) oxalate (3-NPO) was synthesized as follows. A solution of 3-nitrophenol (21.3 g, 0.153 mol) in 400 ml of benzene was dried by azeotropic distillation. The solution was cooled to 10°C under nitrogen and 21.0 g (0.151 mol) of triethylamine was added. Oxalyl chloride (6.4 ml, 0.075 mol) was added with mechanical stirring; the temperature was kept below 20°C on an ice bath. After 2 h stirring, the precipitate was collected with suction and dried under vacuum. The product was washed well with two 100-ml portions of chloroform to dissolve triethylammonium chloride and dried under vacuum. Recrystallization from acetonitrile afforded 1.42 g

(6%) of pale yellow platelets. [M.p. 226°C. Mass spectrometry $m/z = 332$ (M^+). Calc. for $C_{14}H_8O_8N_2$: 50.6% C, 2.4% H, 8.4% N; found, 50.7% C, 2.3% H, 8.4% N.]

Bis(4-acetylphenyl) oxalate (4-APO) was prepared by the procedure described above with 4-hydroxyacetophenone as the starting material and recrystallization from dioxane. [M.p. 280°C (dec.). $m/z = 326$ (M^+). Calc. for $C_{18}H_{14}O_6 \cdot 0.3H_2O$: 65.2% C, 4.4% H; found, 65.3% C, 4.4% H. 1H-n.m.r. (TMS/DMSO- d_6), δ (ppm): 2.60(3H, s), 7.48(2H, d, $J = 9.2$ Hz), 8.12 (2H, d, $J = 9.2$ Hz).] Bis(4-methoxycarbonyl-2-nitrophenyl) oxalate (MCNO) and bis(2,4,5-trichlorophenyl-6-pentyloxycarbonyl) oxalate (TCPCO) were kindly provided by Wako Pure Chemicals Co. (Tokyo) and American Cyanamid Co. (Bound Brook, NJ), respectively. The structures of the oxalates are summarized in Table 1. All the other chemicals were of reagent grade.

Procedures

Fluorescence measurement of phenols. A 10-mM solution of phenol in methanol was diluted 100 times with distilled water and the fluorescence was measured with a Hitachi 650-10S fluorescence spectrophotometer (Tokyo) with 5.0-nm slit-width for both monochromators. All wavelengths were uncorrected.

Stopped-flow apparatus. A stopped-flow spectrophotometer RA-401 (Union Giken Co. Osaka) with a photomultiplier type R268 (Hamamatsu Photonics Co., Tokyo) was used. The system consisted of a rapid-mixing device (jet mixer) with a dead time of 500 μ s and a quartz cell (2 mm i.d.). It was connected with a SORD microcomputer M-200, mark II (SORD Tokyo), a monitor scope, and an x - y plotter.

Procedure for chemiluminescence measurements. A mixture (2:1 v/v) of 0.7 M hydrogen peroxide in acetonitrile and 10 mM citrate/10 mM phosphate/10 mM borate buffer (sodium salts) was placed in one reservoir, and 0.5 mM oxalate and 0.5 μ M 9,10-diphenylanthracene (DPA) in acetonitrile in the other reservoir. These solutions were pumped in equal volumes by nitrogen pressure into the line through the jet mixer to start the reaction. The generated light was measured by the photomultiplier and the signal was sent to the microcomputer. The intensity/time curves obtained by the accumulation of data from three repeat experiments were displayed on the oscilloscope and recorder.

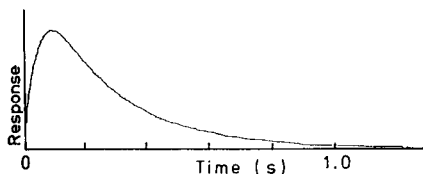


Fig. 2. Intensity/time response for the chemiluminescence reaction of 2-NPO at pH 6.9, measured by the stopped-flow method.

The intensity first increased to reach maximum intensity (I_{\max}) and decreased according to a pseudo-first-order equation with rate constant k (Fig. 2). I_{\max} and k were calculated from this curve.

Solubility of oxalates in acetonitrile. Excess of each oxalate was added to acetonitrile and mixed vigorously for 30 s seven times at 5-min intervals [12]. The mixture was filtered through glass wool and the solubility was evaluated by the following two methods. In method A, 4.0 ml of 0.1 M sodium hydroxide was added to 200 μ l of the saturated solution and, after standing overnight, the phenolic hydrolysis product was determined spectrophotometrically; this method was applied to DNPO, 2-NPO, 3-NPO, 4-NPO and 4-APO. In method B, 2.0-ml of the saturated solution was evaporated and dried under vacuum to constant weight; this method was applied to DNPO, MCNO, PFPO, TCPO and TCPCO. The results for DNPO by both methods were not significantly different.

Stability of oxalates in the presence of hydrogen peroxide in acetonitrile. Equal volumes of 1.0 mM oxalate in acetonitrile and 0.1 M hydrogen peroxide in acetonitrile were premixed ($T = 0$ h). A portion of the mixture was collected at certain time intervals with a microsyringe, added immediately to a borosilicate glass tube (6×50 mm), containing 8-anilino-1-naphthalenesulphonic acid (ANS) as fluorescer in aqueous buffer, and mixed vigorously with a vortex mixer. The tube was immediately inserted into a Chem-Glow photometer (Aminco, Baltimore, MD) and the chemiluminescence intensity was measured. The emission at 5 s after the addition of the pre-mixed solution was taken as the parameter for the stability of the oxalate. Precise experimental conditions (the kind of buffers, buffer pH, and volume of solutions) are summarized in Table 2.

The intensity obtained 5 s after mixing the fluorescer, hydrogen peroxide and the oxalate solution in equal volumes (2-NPO, MCNO, TCPCO) or in volume ratios of 2.5:2.5 = 1 (DNPO, PFPO, TCPO), in this order, was arbitrarily taken as 100% intensity ($t = 0$ h).

TABLE 2

Experimental conditions for evaluating the stability of the oxalates

Oxalate	Vol. of oxalate/ H ₂ O ₂ mixture (μ l)	ANS (μ M)	Buffer	Volume (μ l)
2-NPO	400	2	30 mM citrate/30 mM phosphate (pH 5.5, Na ⁺)	200
DNPO	500	1	30 mM potassium hydrogen- phthalate	100
MCNO	400	1	30 mM citrate/30 mM phosphate (pH 5.5, Na ⁺)	200
PFPO	500	1	30 mM potassium hydrogen- phthalate	100
TCPO	500	1	100 mM imidazole (pH 7.0, NO ₃ ⁻)	100
TCPCO	400	10	10 mM citrate/10 mM phosphate/ 10 mM borate (pH 8.0, Na ⁺)	200

RESULTS AND DISCUSSION

Selection of phenols for oxalates

Rauhut et al. [11] reported that strong chemiluminescence was observed from aryl oxalates substituted by electronegative groups whereas little emission was detected from oxalates substituted by electron-donating groups or weak electron-withdrawing groups. Therefore it was proposed to synthesize oxalates substituted by electronegative groups such as $-\text{NO}_2$, $-\text{CN}$, $-\text{COCH}_3$, $-\text{COOCH}_3$, $-\text{Cl}$ or $-\text{F}$ from the appropriate phenols and oxalyl chloride, with triethylamine as catalyst. However, several such phenols are fluorescent, e.g., 2-cyanophenol (λ_{ex} 298 nm, λ_{em} 378 nm), 4-cyanophenol (254, 304 nm), methyl salicylate (299, 368 nm), methyl 4-hydroxybenzoate (273, 325 nm) and 2-hydroxyacetophenone (270, 298 nm), and would cause high background luminescence. So only non-fluorescent phenols were selected, and the nine oxalates shown in Table 1 were prepared and studied.

Effect of pH

The maximum intensity and rate constant, k , were measured at various pH values. The values obtained are plotted in Figs. 3 and 4; DNPO (at pH 6) gave the largest intensity, followed by MCNO (also at pH 6) and 4-NPO

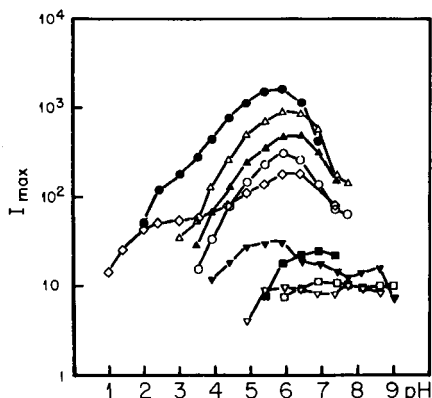


Fig. 3. Effect of pH on maximum intensity for: (●) DNPO; (▲) MCNO; (○) 2-NPO; (▼) 3-NPO; (▲) 4-NPO; (◇) PFPO; (■) TCPO; (□) TCPCO; (▽) 4-APO.

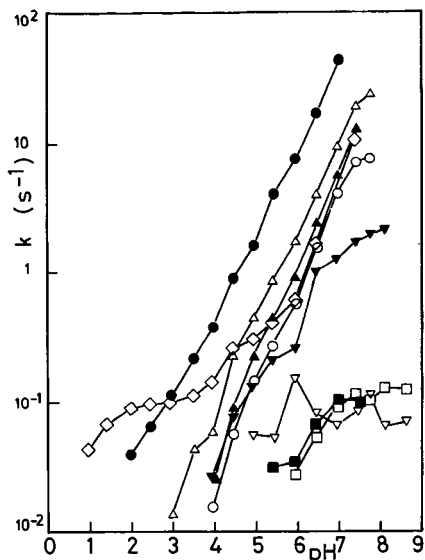


Fig. 4. Effect of pH on the decay rate constants k for oxalate chemiluminescence; symbols are the same as in Fig. 3.

(pH 6.0–6.5). The values for k at pH 6 were in the order DNPO > MCNO > 4-NPO > PFPO > 2-NPO > 3-NPO > 4-APO > TCPO > TCPCO, an order almost the same as that for the intensity values.

The k values at pH 6 for the oxalates having a nitrophenyl moiety increased as the pK_a of the corresponding phenols decreased, but this trend was not followed by oxalates having a halophenyl moiety, for which the reaction seems to be complex.

De Jong et al. [5] mentioned that a larger k value is desirable for a large flow cell (several ml) on account of a 'chemical band-narrowing effect' but the 100- μ l flow cell used in the present system would not produce the band-narrowing effect caused by larger k values. On the contrary, a smaller k value would give good reproducibility because of the smaller variation in intensity caused by variation of the flow rate of the delivery pumps. A high maximum intensity is also desirable for improved sensitivity. In this respect, oxalates or reaction conditions which give the highest I_{\max}/k values may be valuable for h.p.l.c. detection systems.

The factors I_{\max}/k (the data obtained when the half-life of the decay was >1 s, i.e., $k > 0.693 \text{ s}^{-1}$, were omitted for practical use) were plotted against buffer pH (Fig. 5). The oxalate giving the highest I_{\max}/k value depended on the pH.

Solubility of oxalates and their stability in the presence of hydrogen peroxide

Solubility was considered important because the intensity increases with increasing oxalate concentration. Thus, 2-NPO, DNPO, MCNO, PFPO and TCPCO are relatively soluble in acetonitrile, but 3-NPO, 4-NPO and 4-APO are less soluble and are not useful for this system (Table 3).

Good stability of the oxalate in the presence of the oxidant is useful because this would allow premixing of the oxalate and hydrogen peroxide,

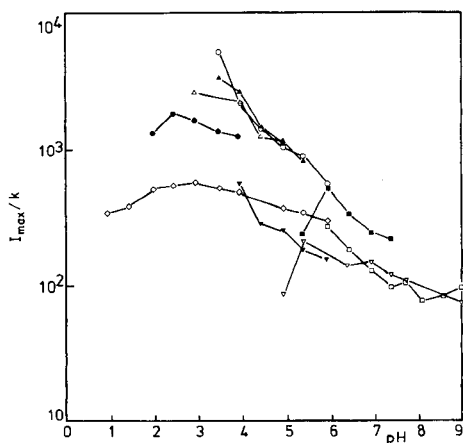


Fig. 5. Effect of pH on I_{\max}/k for various oxalate esters. (Symbols as in Figs. 3 and 4.)

TABLE 3

Solubility of oxalates in acetonitrile at $26 \pm 2^\circ\text{C}$

Oxalate	Solubility (mM)	Oxalate	Solubility (mM)
2-NPO	30	PFPO	34
3-NPO	2.2	TCPO	5
4-NPO	1.4	TCPCO	67
DNPO	22	4-APO	0.082
MCNO	23		

TABLE 4

Stability of oxalates in hydrogen peroxide

Oxalate	Relative intensity after 8 h ^a	Oxalate	Relative intensity after 8 h ^a
2-NPO	88.6 ± 2.7	PFPO	27.0 ± 0.8
DNPO	6.0 ± 0.3	TCPO	104.4 ± 1.6
MCNO	48.0 ± 2.2	TCPCO	82.5 ± 1.0

^aIntensity at start, arbitrarily taken as 100; average of 5 results.

and only one pump would be required for the delivery of the oxalate/peroxide solution to the detector. Table 4 shows the residual intensities after 8-h storage of the oxalates with hydrogen peroxide, and indicates that 90%, 100% and 80% remained of the original intensities for 2-NPO, TCPO and TCPCO, respectively. It has been reported that a catalyst (organic base [10] or hydroxide [1]) is needed for the oxalate/peroxide reaction, so it seems likely that without such a catalyst the reaction is slow. The above three oxalates are relatively stable even in the presence of hydrogen peroxide. MCNO and 2-NPO have similar I_{max}/k values, but MCNO is relatively unstable in the presence of hydrogen peroxide and is therefore unsuitable for this chemiluminescence detection system.

Evaluation of oxalates as detection reagents for h.p.l.c.

From the above studies of I_{max}/k , solubility and stability, it is proposed that five oxalates, PFPO, 2-NPO, DNPO, TCPO and TCPCO, are applicable for h.p.l.c. detection, and that the oxalates could be selected on the basis of the pH of the column eluents. For effluents of pH < 2, 2–4, 4–6, 6–8 and > 8, the recommended oxalates are PFPO, DNPO, 2-NPO, TCPO and TCPCO, respectively, although minor corrections to the reaction conditions may sometimes be necessary.

In peroxyoxalate chemiluminescence detection systems for h.p.l.c. so far reported, only TCPO has been used and the pH range available has been restricted. The present studies show that the use of other oxalates makes it possible to expand the practical pH range of such detection systems.

The authors thank Professor T. Nakajima, University of Tokyo, for his valuable suggestions and discussion. They are also grateful to Dr. M. Nakanishi, University of Tokyo, for his kind advice and for operating the stopped-flow apparatus. Thanks are also due to the American Cyanamid Co. and Wako Pure Chemicals Co. for providing TCPCO and MCNO, respectively.

REFERENCES

- 1 S. Kobayashi and K. Imai, *Anal. Chem.*, 52 (1980) 424.
- 2 G. Mellbin, *J. Liq. Chromatogr.*, 6 (1983) 1603.
- 3 K. Miyaguchi, K. Honda and K. Imai, *J. Chromatogr.*, 303 (1984) 173.
- 4 K. Miyaguchi, K. Honda and K. Imai, *J. Chromatogr.*, 316 (1984) 501.
- 5 G. J. de Jong, N. Lammers, F. J. Spruit, U. A. Th. Brinkman and R. W. Frei, *Chromatographia*, 18 (1984) 129.
- 6 S. Kobayashi, J. Sekino, K. Honda and K. Imai, *Anal. Biochem.*, 112 (1981) 99.
- 7 K. W. Sigvardson and J. W. Birks, *Anal. Chem.*, 55 (1983) 432.
- 8 K. W. Sigvardson, J. M. Kennish and J. W. Birks, *Anal. Chem.*, 56 (1984) 1096.
- 9 G. Mellbin and B. E. F. Smith, *J. Chromatogr.*, 312 (1984) 203.
- 10 A. G. Mohan and N. J. Turro, *J. Chem. Educ.*, 51 (1974) 528.
- 11 M. M. Rauhut, L. J. Bollyky, B. G. Roberts, M. Loy, R. H. Whitman, A. V. Iannotta, A. M. Semsel and R. A. Clarke, *J. Am. Chem. Soc.*, 89 (1967) 6515.
- 12 *Pharmacopoeia of Japan*, X (1981), general notice 22.

EVALUATION OF FLUORESCENT COMPOUNDS FOR PEROXYOXALATE CHEMILUMINESCENCE DETECTION

KAZUMASA HONDA, KIMITOSHI MIYAGUCHI and KAZUHIRO IMAI*

*Faculty of Pharmaceutical Sciences, University of Tokyo, 7-3-1 Hongo, Bunkyo-ku,
Tokyo 113 (Japan)*

(Received 11th April 1985)

SUMMARY

The behaviour of 19 fluorescent compounds of various types in peroxyoxalate chemiluminescence reactions was studied in terms of the relation of their excitation efficiency to their singlet excitation energy and oxidation potential. Compounds having low singlet excitation energy and low oxidation potential were excited effectively. As a result of the study, 3-aminoperylene was selected as a fluorophore for derivatization of simple carboxylic acids. The derivatives were separated by reversed-phase microbore h.p.l.c. and were detected by a peroxyoxalate chemiluminescence reaction detector. The detection limit was 0.1 fmol.

Peroxyoxalate chemiluminescence has been recognized as potentially useful for the detection of fluorescent compounds (fluorescers) after separation by high-performance liquid chromatography (h.p.l.c.) and has been applied to the detection of the fluorescers separated on reversed-phase columns, as summarized earlier [1]. In order to predict further applications, however, the desirable characteristics of a fluorescer in a chemiluminescence reaction must be clarified. In this paper, these characteristics are evaluated by measuring the chemiluminescence intensities and excitation yields of the fluorescers. A detection system for newly-designed fluorescent-labelled carboxylic acids separated by microbore h.p.l.c. is reported.

EXPERIMENTAL

Chemicals

Distilled water and acetonitrile (for fluorescence analysis; Kanto Chemicals Co., Tokyo) were used as received. Bis(2,4-dinitrophenyl) oxalate (DNPO) [2], bis(2,4,6-trichlorophenyl) oxalate (TCPO) [3] and bis(2-nitrophenyl) oxalate (2-NPO) [2] were prepared as described in the literature and recrystallized from acetonitrile. *N*-(7-Nitro-2,1,3-benzoxadiazol-4-yl)-L-proline (NBD-proline) [4] and ammonium 7-(2-hydroxyethylthio)-2,1,3-benzoxadiazole-4-sulfonate (SBD-mercaptoethanol) [5] were also prepared as described previously. 9,10-Diphenylanthracene (DPA; liquid scintillation

grade; Nakarai Kagaku Co., Tokyo), perylene (gold label; Aldrich), dansyl(DNS)-glycine and -alanine (Sigma Chemical Co.) and rhodamine B and fluorescein (laser grade; Eastman Kodak Co.) were used. Benzo[a]-pyrene, 3-methylcholanthrene, and aflatoxin B were kindly donated by Dr. E. Hara of the Saitama Cancer Research Institute and α -tocopherol by Dr. K. Abe of the Eisai Co. (Tokyo). All the other chemicals were of reagent grade.

Screening of fluorescers via DNPO chemiluminescence [6]

A 200- μ l portion of 0.50 M hydrogen peroxide in citrate buffer (0.010 M, pH 3.5, Na⁺) and 200 μ l of a fluorescer in acetonitrile were premixed in a borosilicate glass tube (6 \times 50 mm) for 10 s, and 200 μ l of 1.0 mM DNPO in acetonitrile was added with a microsyringe and mixed in vigorously with a vortex mixer. The tube was immediately placed inside a Chem-Glow photometer (Aminco, Baltimore, MD) and the chemiluminescence intensity was measured. The time course of the intensity was recorded after adding DNPO solution and the relative intensity at 5 s after addition was compared with the intensity for 100 nM DNS-alanine, which was arbitrarily taken as 100.

For fluorescers insoluble in acetonitrile, e.g., water-soluble vitamins, 100 μ l of 1.0 M hydrogen peroxide in the citrate buffer, 100 μ l of fluorescer in the citrate buffer, and 400 μ l of 0.50 mM DNPO in acetonitrile were treated as described above. In both methods, the ratio of acetonitrile to citrate buffer and the concentrations of the reagents in the reaction solution were the same and there were no significant differences in the intensity and the reaction rate under the two sets of reaction conditions with DNS-alanine as fluorescer.

Calculation of the relative excitation yield of the fluorescer, Y'_{df}

Two sets of experiments were done; the DNPO and TCPO systems were applied and the value of Y'_{df} was calculated for each. All the wavelengths measured were uncorrected.

The theoretical basis of the calculations was as follows [7]. At low concentrations of fluorescer, the chemiluminescence intensity, I_{cl} , is linearly dependent on the concentration of the fluorescer, so $I_{cl} = k_1 D Y_{df} Y_f F$ [8], where k_1 , D , Y_{df} , Y_f and F are a constant, the concentration of the intermediate (1,2-dioxetanedione), the excitation yield of the fluorescer, the fluorescence quantum yield, and the concentration of the fluorescer, respectively. The fluorescence intensity I_f is given by $I_f = k_2 \epsilon I_0 Y_f F$, where k_2 , ϵ and I_0 are a constant, the molar absorptivity, and the intensity of the light source, respectively. From these equations

$$Y_{df} = k_2 \epsilon I_0 I_{cl} / k_1 I_f D \quad (1)$$

which suggests that Y_{df} can be calculated by measuring ϵ , I_0 , I_{cl} , I_f and D . However, it is difficult to measure the absolute values of I_0 , I_{cl} , I_f and D .

Therefore the relative molar absorptivity (ϵ'), the relative intensity of the light source (I'_0), the relative fluorescence intensity (I'_f), and the relative chemiluminescence intensity (I'_{cl}) were calculated with respect to 9,10-diphenylanthracene (DPA). This gave the relative value of Y'_{df} as

$$Y'_{df} = \epsilon' I'_0 I'_{cl}/I'_f \quad (2)$$

General procedures

Fluorescence and absorbance measurements. A 2.0-ml portion of the fluorescer in acetonitrile and 0.40 ml of citrate buffer (0.010 M, pH 3.5; Na^+) for DNPO or 1.0 ml of phosphate buffer (0.010 M, pH 6.0, Na^+) for TCPO were mixed. The fluorescence excitation maxima (λ_{ex}) and emission maxima (λ_{em}) were measured, with a 5-nm slit-width for both the monochromators of a Hitachi 650-10S spectrophotometer. Next, the fluorescence intensity was measured at λ_{ex} (± 5.0 nm) and λ_{em} (± 10.0 nm), and the relative fluorescence intensity (I'_f) was calculated for DPA ($\lambda_{ex} = 392$ nm, $\lambda_{em} = 408$ nm). The relative intensity of the light source (I'_0) at λ_{ex} was obtained by using 7.9 g l^{-1} rhodamine B in ethylene glycol in a triangular cell ($\lambda_{em} = 620 \pm 10$ nm).

The relative molar absorptivity ϵ' at λ_{ex} (± 5.0 nm) was calculated in a similar way, by using a Uvidec-505 spectrophotometer (Japan Spectroscopic Co., Tokyo).

Chemiluminescence measurements. The fluorescer in acetonitrile (1.0 ml) and 0.40 ml of 0.50 M hydrogen peroxide in pH 3.5 0.010 M sodium citrate buffer (for DNPO) or 1.0 ml of 0.50 M peroxide in pH 6.0 0.010 M phosphate buffer (for TCPO) were premixed in a glass tube for 10 s. Then 1.0 ml of 1.0 mM DNPO or TCPO in acetonitrile was added instantly and mixed vigorously in a vortex mixer for a few seconds. The reaction mixture was immediately transferred to a quartz cell (1×1 cm), and set inside the 650-10S fluorescence spectrometer with the light source off. The intensity measured at λ_{em} (± 10.0 nm) 10 s after the addition of the DNPO or TCPO solution was taken as a measure of the total chemiluminescence intensity. The variations of the values of the half-life of the chemiluminescence decay were within 10%. The relative intensity (I'_{cl}) was calculated with respect to the chemiluminescence intensity of DPA. All the experiments were done at $25 \pm 1^\circ\text{C}$.

Calculation of Y'_{df} . The Y'_{df} values were calculated from Eqn. 2 from the values of I'_{cl} , I'_f , I'_0 and ϵ' ; λ^{-1} is defined as $(\lambda_{abs}^{-1} + \lambda_{em}^{-1})/2$.

Oxidation potential measurement. A 1 mM solution of fluorescer in acetonitrile containing 0.1 M lithium perchlorate as the supporting electrolyte was bubbled with argon to remove oxygen, and the oxidation potential was measured with a Yanagimoto type P-1000 voltammetric analyzer (Yanagimoto Co., Tokyo) with platinum working and counter electrodes and a calomel reference electrode. The analyzer was operated in the differential pulse mode (modulation amplitude 5 mV, scan rate 2 mV s^{-1}).

Synthesis of 3-aminoperylene and acetylamino aromatic compounds

All melting points are uncorrected.

3-Nitroperylene. Perylene (3.01 g, 0.0119 mol) was dissolved in chloroform and filtered to remove insoluble impurities. The solvent was evaporated and 330 ml of anhydrous acetic acid was added. Nitric acid (1.0 ml, $d = 1.50$) in 50 ml of anhydrous acetic acid was slowly added to the stirred solution under nitrogen. About 4 h was required for this stage. After all the nitric acid had been added, 400 ml of aqueous 0.1 M sodium acetate was added. The solution was filtered through a sintered glass filter and the red precipitate was washed with water on the filter until the washings were neutral. The product was dried under vacuum and purified by silica gel column chromatography (1:1 chloroform/hexane) and recrystallized from benzene. A brown powder (2.3 g) was obtained. [Yield 64%. M.p. 211–212°C (lit. 210–211°C [9]). Mass spectrometry: $m/z = 297$ (M^+). Calc. for $C_{20}H_{11}NO_2$, 80.8% C, 3.7% H, 4.7% N; found, 81.1% C, 3.3% H, 4.7% N.]

3-Aminoperylene. A solution of 15.0 g of sodium hydrosulfide (0.187 mol) in 70 ml of water was added to a mixture of 2.05 g (6.88×10^{-3} mol) of 3-nitroperylene, 280 ml of ethanol and 20 ml of water and refluxed for 8 h. The solution was filtered and the precipitate washed with water until the smell of hydrogen sulfide had disappeared. The red solid was dried under vacuum and purified by silica-gel column chromatography (1:1 ethyl acetate/n-hexane) and recrystallized from ethyl acetate/ethanol. Pale yellow crystals were obtained. [Yield 10%. M.p. 230–233°C (dec.) (lit. 220–230°C [9]). $m/z = 267$ (M^+). Calc. for $C_{20}H_{13}N$, 89.9% C, 4.9% H, 5.2% N; found, 89.2% C, 4.9% H, 5.4% N.] The amine was converted to the hydrochloride by bubbling dry hydrogen chloride gas through an ethyl acetate solution.

3-(Acetylamino)perylene. To a solution of 3-aminoperylene hydrochloride (59.8 mg, 1.97×10^{-4} mol) in 10 ml of pyridine was added 10 ml of acetic anhydride. After standing overnight, 400 ml of ethyl acetate was added and shaken three times with 1 M hydrochloric acid. The organic layer was dried over anhydrous sodium sulfate and evaporated under vacuum. The yellow-brown residue was purified on a silica-gel column (ethyl acetate eluent) and recrystallized from ethyl acetate to yield 7.9 mg of yellow needles [Yield 13%. M.p. $>300^\circ\text{C}$; m/z , 309 (M^+). Calc. for $C_{22}H_{15}NO$, 85.4% C, 4.9% H, 4.5% N; found, 84.4% C, 4.8% H, 4.6% N.]

1-(Acetylamino)anthracene and 1-(acetylamino)pyrene. These compounds were prepared by literature methods [10, 11], and were recrystallized from methanol and ethanol, respectively. The m.p. of the former was 218–219°C (lit. 212°C) and the latter, 271–272°C (lit. 260–261°C).

Labelling of a carboxylic acid with 3-aminoperylene

Equal volumes of the carboxylic acid in benzene, 10 mM 3-aminoperylene hydrochloride in pyridine and 100 mM 1,3-dicyclohexylcarbodiimide (DCC) in benzene were mixed in a well-sealed glass container; quantitative reaction

was obtained at 60°C after 2 h or at 40°C after 8 h. The solution was then diluted with the eluent and subjected to h.p.l.c. The use of DCC was superior to EDC (1-ethyl-3-(3-(dimethylamino)propyl)carbodiimide hydrochloride), as EDC reduced the labelling yield. Dichloromethane instead of pyridine or tetrachloromethane instead of benzene did not give any reaction. The labelled compound was stable for >11 h at 60°C and >27 h at 40°C in the reaction medium.

Microbore h.p.l.c. apparatus and chemiluminescence detection system based on 2-NPO and hydrogen peroxide

A schematic diagram for the system is shown in Fig. 1. The pumps used were a Gilson Model 302 (Villiers-Bel, France) for the eluent and Shimadzu LC-3A (Shimadzu Seisakusho Co., Tokyo) for the reagent. The injection valve (Rheodyne 7140, Cotati, CA) with a 0.5- μ l loop and microbore column (MBC-ODS-2, 1.0 i.d. \times 250 mm; 10 μ m) were from Shimadzu Seisakusho. The chemiluminescence monitor having a sensitive photomultiplier tube (Type 6199; Hamamatsu Photonics Co., Tokyo) set close to a spiral flow cell (100 μ l), was obtained from Atto Co. (Tokyo).

RESULTS AND DISCUSSION

Screening of fluorescers for chemiluminescence intensity

Various fluorescers such as polynuclear aromatic hydrocarbons (PAHs), fluorescent-labelled compounds, fluorescent dyes and fluorescent vitamins were applied to the DNPO chemiluminescent reaction. The intensities are summarized in Table 1, which indicates that strong emission was observed from PAHs such as perylene and rubrene, and fluorescent dyes having red fluorescence such as rhodamine B and rose Bengal. Only weak chemiluminescence was observed from heterocyclic fluorescers.

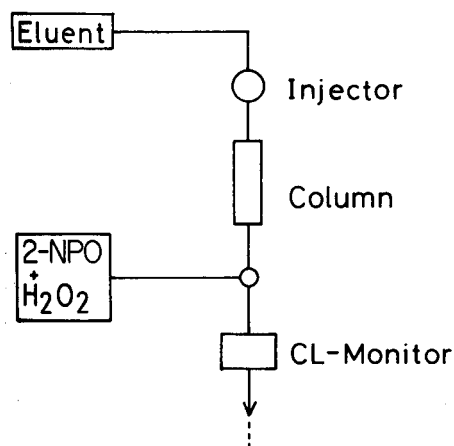


Fig. 1. Flow diagram for the microbore h.p.l.c. chemiluminescence detection system.

TABLE 1

Relative chemiluminescence intensities of various fluorescent compounds in the DNPO reaction

	Rel. intensity		Rel. intensity
Perylene	850	9,10-Dibromoanthracene	2.1
Rubrene	290	Riboflavin	0.3
Rhodamine B	170	Fluorescein	0.2
DNS-alanine	100	SBD-mercaptoethanol	0.1
3-Methylcholanthrene	94	Umbelliferone	0.1
Rose Bengal	57	α -Tocopherol	<0.1
Benzo[a]pyrene	25	NADH	<0.1
NBD-proline	5.5	Pyridoxine · HCl	<0.1

Relative excitation yield of the fluorescer

It has been reported that various PAHs having emissions spanning the visible-infrared spectrum may be excited by peroxyoxalate [8, 12–14], and that fluorescers having fluorescence characteristics in the u.v. region are less excited by the reaction [12, 14]. Lechtken and Turro [14] reported that the proposed intermediate, 1,2-dioxetanedione, can transfer as much as 105 kcal mol⁻¹ (\approx 272 nm) of energy to the fluorescers and the chemiluminescence intensity corrected for the fluorescence quantum yield decreases as the singlet excitation energy of the fluorescers increases.

A plot of Y'_{df} vs. the singlet excitation energy as suggested by Lechtken and Turro is shown in Fig. 2. It gives a similar curve for PAHs, as reported previously [7]. However, some heterocyclic fluorescers do not lie on the curve, which suggests that the singlet excitation energy alone is insufficient to predict the chemiluminescence intensity.

McCapra [15] and Rauhut [16] speculated that the energy-transfer steps include a charge-transfer step where one electron transfers from the fluorescer to the intermediate and they form a "charge-transfer complex" as the transition state. In other chemiluminescence reactions, there are several examples which have the charge-transfer transition state [17–21]. Diphenoyl peroxide, for example, with a suitable fluorescer, forms a charge-transfer transition state with the fluorescer and transfers its energy to the partner [17]. Schuster [22] named this type of chemiluminescence a CIEEL (chemically induced electron exchange luminescence) reaction. In such a reaction there are linear relationships between the rate of exciting a fluorescer by the "activator" and the oxidation potential of the fluorescer. Conversely, this linear relationship proves that a chemiluminescence reaction is a CIEEL reaction.

Figure 3 shows the linear relationships between Y'_{df} and the oxidation potentials of the fluorescers in the DNPO and TCPO systems. The correlation coefficients (r) for 13 samples (excluding α -tocopherol,

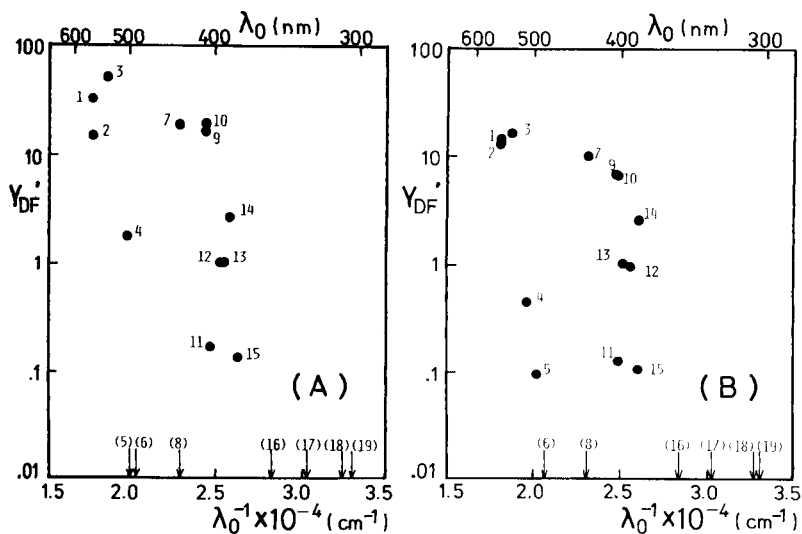


Fig. 2. Plot of the relative excitation yield (Y'_{df}) vs. singlet excitation energy (λ_0^{-1}) for the fluorescer: (A) DNPO system; (B) TCPO system. Compounds: (1) rhodamine B; (2) rose Bengal; (3) rubrene; (4) NBD-proline; (5) fluorescein; (6) riboflavin; (7) perylene; (8) SBD-mercaptoethanol; (9) DNS-glycine; (10) DNS-alanine; (11) 9,10-dibromoanthracene; (12) benzo[a]pyrene; (13) 9,10-diphenylanthracene; (14) 3-methylcholanthrene; (15) NADH; (16) umbelliferone; (17) 2-pyridone; (18) α -tocopherol; (19) pyridoxine hydrochloride.

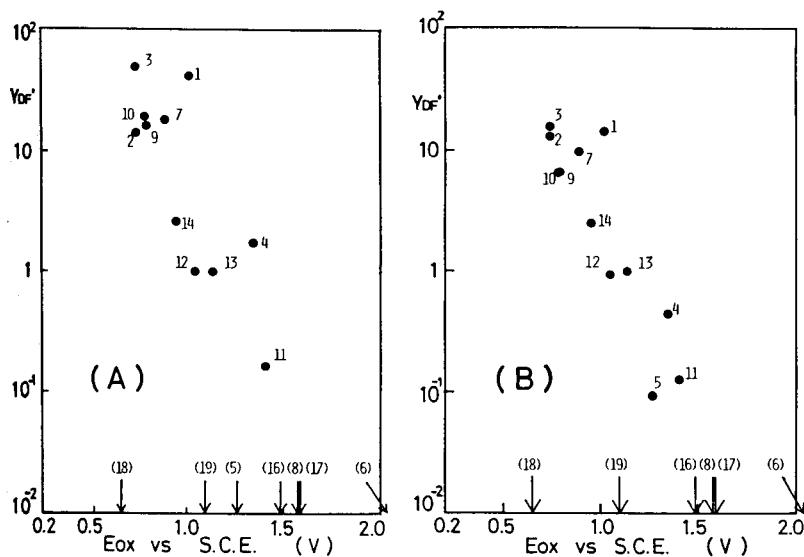


Fig. 3. Plot of the relative excitation yield (Y'_{df}) vs. oxidation potential (E_{ox}) of the fluorescer: (A) DNPO system; (B) TCPO system. Compounds as in Fig. 2. NADH was not measured because of insolubility.

riboflavin, pyridoxine hydrochloride, umbelliferone and 2-pyridone) were 0.819 ($p < 0.01$) in the DNPO system and 0.919 ($p < 0.01$) in the TCPO system. Those results indicate that peroxyoxalate chemiluminescence is a CIEEL reaction. Fluorescein in the DNPO system seems to have a smaller Y'_{df} than expected, which might be ascribed to its lactone form at pH 3.5, which is not fluorescent [23] and would not have chemiluminescence. Rubrene and rhodamine B have reversible second oxidation potentials at 1.18 V and 1.11 V, respectively. They can be oxidized by two dioxetanedione molecules at the same time and therefore they are possibly more efficiently excited. The intermediate is unlikely to be able to excite α -tocopherol, pyridoxine hydrochloride, umbelliferone and 2-pyridone because the singlet excitation energies of these fluorescers are more than 70 kcal mol⁻¹ ($\lambda_0^{-1} = 2.5 \times 10^4$ cm⁻¹). Although Sigvardson et al. [24] reported similar results for the detectability of PAHs by h.p.l.c., this is the first report of a systematic proof of such results, using various heterocyclic fluorescers commonly found in biological systems.

Consequently, fluorescers having a low oxidation potential and low singlet excitation energy can be sensitively detected by the peroxyoxalate detection system (e.g. perylene, rubrene, rhodamine B, rose Bengal and dansyl derivatives, as listed in Table 1).

Synthesis of 3-aminoperylene and evaluation of the chemiluminescence characteristics of acetylamino aromatic compounds

Based on the results obtained above, a new derivative having a perylene basis was designed, in which the amino group of 3-aminoperylene was condensed with a carboxyl group using a carbodiimide. 3-(Acetylamino)perylene was taken as a typical example, and, for comparison, 1-(acetylamino)anthracene and 1-(acetylamino)pyrene, which have commonly used fluorophores [25] were synthesized and evaluated.

The relative chemiluminescence intensities of the acetylamino aromatic compounds were measured under the same conditions as in Table 1. The relative intensity of 3-(acetylamino)perylene was 720 relative to dansyl-alanine (=100), whereas those for 1-(acetylamino)pyrene and 1-(acetylamino)anthracene were 1.3 and 7.7, respectively. The value for 3-(acetylamino)perylene was only slightly less than that for perylene (Table 1). 3-(Acetylamino)perylene was also found to have a high Y'_{df} value (Fig. 4) which indicates that it is a preferable labelling reagent for chemiluminescent labelling of carboxylic acids.

Microbore h.p.l.c. with chemiluminescence detection

The labelled carboxylic acids were separated by microbore h.p.l.c. and detected by the peroxyoxalate detector. 2-NPO was used as the peroxyoxalate because of its high intensity, slow intensity decay, stability, and solubility [1]. Figure 5 shows the chromatogram of 100 fmol levels of acetic, butyric and valeric acids labelled by 3-aminoperylene. Propionic

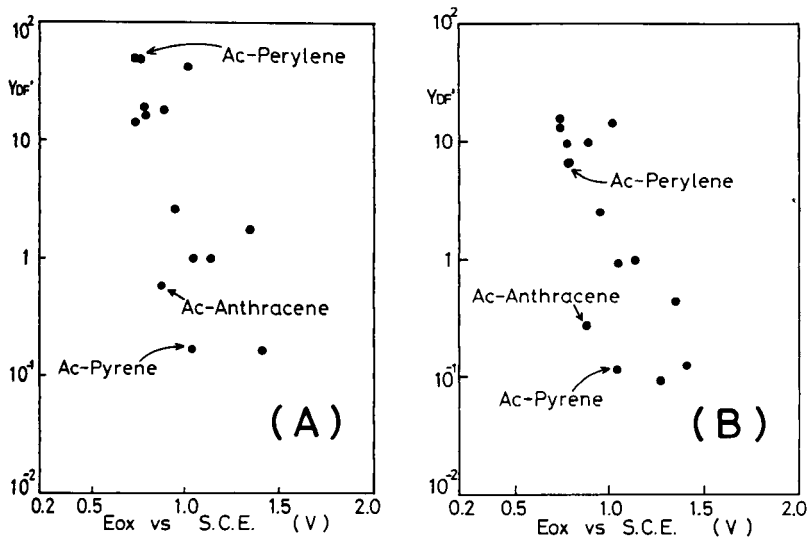


Fig. 4. Plot of the relative excitation yield (Y'_{df}) vs. oxidation potential (E_{ox}) for some acetylamino aromatic compounds: Ac-Perylene, 3-(acetylamino)perylene; Ac-Anthracene, 1-(acetylamino)anthracene; Ac-Pyrene, 1-(acetylamino)pyrene. (A) DNPO system; (B) TCPO system.

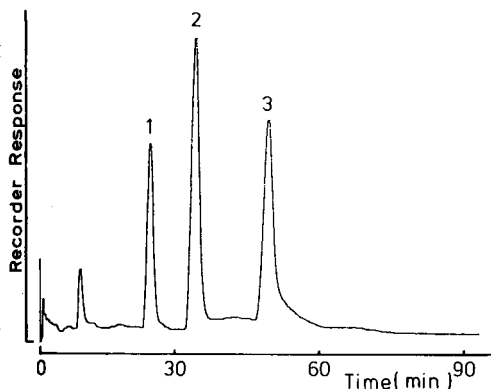


Fig. 5. Chromatogram of carboxylic acids derivatized with 3-aminoperylene: (1) acetic acid (70 fmol); (2) butyric acid (130 fmol); (3) valeric acid (100 fmol). Eluent: 0.1 M imidazole (pH 5.6, nitrate/acetonitrile (55/45)), 0.2 ml min⁻¹. Reagent: 0.25 mM 2-NPO; 38 mM H₂O₂ in acetonitrile, 0.2 ml min⁻¹.

acid labelled in this way was not separated from the labelled acetic acid, but it might be separated with use of a lower capacity column than ODS (C₁₈). The detection limit ($s: n = 3$) and the relative standard deviations for the peak heights of 0.5-fmol injections were 0.1 fmol and 5.7% ($n = 5$), respectively, which indicates that this method has a detection power better by

about two orders of magnitude than the conventional fluorescence labelling and detection system in h.p.l.c. [26].

However, there remains the problem that it is the less practical, because the labelling needs >2 h at 60°C in a non-aqueous medium. An improvement of this process is the next stage in the investigation.

The authors thank Professor T. Nakajima of the University of Tokyo for his valuable suggestions and discussion. They are also grateful to Drs. T. Nagano, S. Ohta and M. Mashino of the University of Tokyo for their kind advice and cooperation in measuring the oxidation potentials of the fluorescers. Thanks are also due to Dr. Y. Hashimoto, University of Tokyo, for his kind advice and cooperation in the synthesis of 3-aminoperylene.

REFERENCES

- 1 K. Honda, K. Miyaguchi and K. Imai, *Anal. Chim. Acta*, 177 (1985) 103.
- 2 M. M. Rauhut, L. J. Bollyky, B. G. Roberts, M. Loy, R. H. Whitman, A. V. Iannotta, A. M. Semsel and R. A. Clarke, *J. Am. Chem. Soc.*, 89 (1967) 6515.
- 3 A. G. Mohan and N. J. Turro, *J. Chem. Educ.*, 51 (1974) 528.
- 4 T. Toyooka, Y. Watanabe and K. Imai, *Anal. Chim. Acta*, 149 (1983) 305.
- 5 J. L. Andrews, P. Ghosh, B. Ternai and M. W. Whitehouse, *Arch. Biochem. Biophys.*, 214 (1982) 386.
- 6 K. Imai, *Bunseki*, (1984) 888.
- 7 K. Imai, K. Miyaguchi and K. Honda, in K. van Dyke (Ed.), *Luminescence Detection. Applications and Instrumentation*, CRC Press, Cleveland, OH, 1985, in press.
- 8 M. M. Rauhut, B. G. Roberts, D. R. Maulding, W. Bergmark and R. Coleman, *J. Org. Chem.*, 40 (1975) 330.
- 9 M. J. S. Dewar and T. Mole, *J. Chem. Soc.*, (1956) 1441.
- 10 S. M. Verma and M. D. Singh, *J. Org. Chem.*, 42 (1977) 3736.
- 11 D. P. Smith, M. R. Kilbourn, J. H. McDowell and P. A. Hargrave, *Biochemistry*, 20 (1981) 2417.
- 12 P. A. Sherman, J. Holtzbecher and D. E. Ryan, *Anal. Chim. Acta*, 97 (1978) 21.
- 13 P. J. Hanhela and D. B. Paul, *Aust. J. Chem.*, 34 (1981) 1669, 1687, 1701.
- 14 P. Lechtken and N. J. Turro, *Mol. Photochem.*, 6 (1974) 95.
- 15 F. McCapra, *Prog. Org. Chem.*, 8 (1973) 258.
- 16 M. M. Rauhut, *Acc. Chem. Res.*, 2 (1969) 80.
- 17 G. B. Schuster, B. D. J. Koo, S. P. Schmidt and J. P. Smith, *Photochem. Photobiol.*, 30 (1979) 17.
- 18 J. P. Smith and G. B. Schuster, *J. Am. Chem. Soc.*, 100 (1978) 2564.
- 19 W. Adam and I. Erden, *J. Am. Chem. Soc.*, 103 (1981) 3068.
- 20 B. G. Dixon and G. B. Schuster, *J. Am. Chem. Soc.*, 103 (1981) 3068.
- 21 S. P. Schmidt and G. B. Schuster, *J. Am. Chem. Soc.*, 102 (1980) 306.
- 22 G. B. Schuster, *Acc. Chem. Res.*, 12 (1979) 366.
- 23 S.-C. Chen, H. Nakamura and Z. Tamura, *Chem. Pharm. Bull.*, 27 (1979) 475.
- 24 K. W. Sigvardson, J. M. Kennish and J. W. Birks, *Anal. Chem.*, 56 (1984) 1096.
- 25 R. W. Frei and J. F. Lawrence, *Chemical Derivatization in Analytical Chemistry*, Vol. 2, Plenum Press, New York, 1982.
- 26 N. Nimura and T. Kinoshita, *Bunseki*, (1982) 305.

A FIBER-OPTIC ABSORPTION CELL FOR REMOTE DETERMINATION OF COPPER IN INDUSTRIAL ELECTROPLATING BATHS

J. E. FREEMAN, A. G. CHILDERS, A. W. STEELE and G. M. HIEFTJE*

Department of Chemistry, Indiana University, Bloomington, IN 47405 (U.S.A.)

(Received 5th August 1985)

SUMMARY

A device for remote optical sensing is developed and evaluated for monitoring the concentration of copper(II) ions in an industrial plating bath. The sensor consists of an absorption cell which resides in the plating bath, and utilizes fiber optics to direct light into and out of the cell. The sensor is capable of being located in harsh environments for extended periods of time (on the order of weeks to years) and thus is ideal for long-term monitoring applications. The light source and detection electronics can be maintained in a controlled environment and can be multiplexed to several sensors of similar design, if desired. The sensor constructed operates by measuring the copper(II) absorbance with a near-infrared light-emitting diode (820 nm) as the light source. The device is capable of measuring copper(II) ion concentrations from 50 mM to 500 mM with relative standard deviations less than 1%. The construction and operation of the sensor are described and the effects of various interferences found in plating baths are evaluated, including those from temperature variations and variations in the concentrations of concomitant species in the plating bath. Also, drift compensation and noise sources are considered, with an evaluation of the long-term stability of the sensor and the feasibility of its use in an industrial environment.

Real-time determinations of species in industrial processes are important applications for many analytical techniques. Unfortunately, many methods cannot easily be applied to problems of this type. Commonly, the instrumentation required by a particular method cannot be located in the process environment. In addition, many techniques require extensive sample preparation or a significant amount of time for data reduction. Finally, many techniques are simply not suited for continuous sample throughput, a valuable qualification for a continuous process monitor.

Electroplating is a good example of a process which could benefit from real-time chemical analysis. Determinations of major components, such as the metal being plated, are usually done by instrumental or wet-chemical techniques that require lengthy, labor-intensive procedures. For example, the techniques used for the determination of copper in plating-bath solutions include titration, polarography, spectrophotometry, atomic absorption, and x-ray fluorescence. In each case, procedures will usually involve sample

collection and some further treatment such as dilution or the addition of appropriate reagents. Besides being expensive, these procedures can be significant sources of imprecision and inaccuracy.

This paper describes a sensor for copper(II) ion in a sulfuric-acid electroplating bath. The sensor is based on a simple optical absorption measurement of aquated Cu^{2+} in the near-infrared spectral region. The absorption cell has a flow-through design and utilizes optical fibers to transmit light into and out of the sample solution. The simplicity and ruggedness of the cell allow its placement directly in the plating bath and the use of optical fibers makes it possible to locate the measuring instrumentation remotely from the process environment. Source, detector, and data-acquisition equipment can be kept in a central laboratory from which separate optical fibers provide light pathways to each of several sensor locations. The fact that communication to and from the sensors is accomplished optically rather than electronically enhances the noise immunity, ruggedness, and corrosion resistance of this measurement system. Other chemical sensors incorporating optical fibers, or "optrodes", are being developed for a number of applications [1-4].

This remote-sensing approach is ideal for on-line monitoring, because it requires no sample handling or work-up. Nevertheless, there are several potential problems which need to be considered. Changes in solution temperature or changes in the concentration of solution components other than Cu^{2+} might interfere with the absorbance measurement. The effects of dirt and bubbles in the plating baths must also be evaluated. Finally, the need for a blank reading for the absorbance measurements must be considered. If the system is to function continuously as an on-line sensor it is clearly undesirable to require that actual blank measurements be recorded. Each of these concerns, and their effects on the precision of the Cu^{2+} concentration determination are addressed in the following discussion.

EXPERIMENTAL

Instrumentation

The absorption cell developed here for remote monitoring of copper in an industrial electroplating bath is shown in Fig. 1. The optical absorption sensor consists of two jacket-protected silica optical fibers (200- μm core; Model QSF-200, Math Associates, Westbury, NY) that directly face each other across a 2-mm absorption path. Standard SMA connectors (Series 905, Amphenol, Oak Brook, IL) were placed on one end of each fiber with the other end being left bare. The bare ends of the optical fibers were aligned and held in place by epoxy resin in a machined Vespel housing shown in Fig. 2. The Vespel housing was constructed from a 5/8-in. (15.9-mm) o.d. solid rod 7/8-in. (22.2-mm) long. A slot (2-mm wide) was cut 3/8 in. (9.5 mm) into the side of the Vespel rod. Two 0.89-mm (No. 74 drill) holes were drilled through the length of the Vespel rod 3/8 in. (9.5 mm)

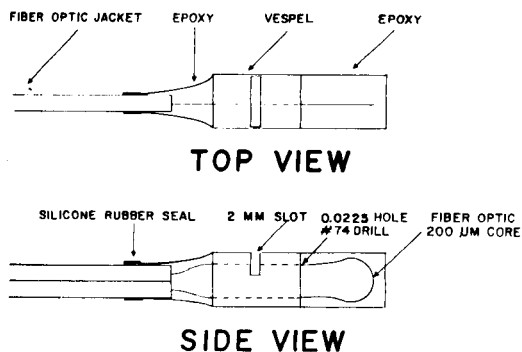


Fig. 1. Fiber-optic-based Cu^{2+} absorption cell. One fiber passes through a hole in the bottom of the Vespel housing, emerges at the other end, and is bent around to fit through a second hole in the top of the Vespel housing. The second optical fiber is inserted into the hole in the top of the Vespel housing. The optical fibers are fixed in place with epoxy resin.

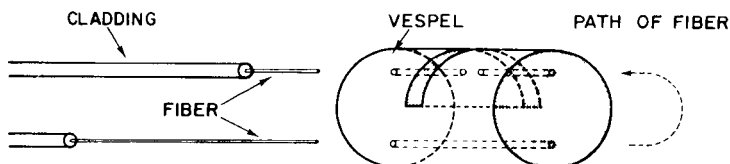


Fig. 2. Cross-sectional view of the fiber-optic absorption cell. Light is transmitted from the light source to the cell by an optical fiber and collected across a gap machined into the Vespel housing by a second optical fiber. The collected light is sent to a detector and the absorbance of the solution in the gap is determined.

apart and aligned so that the top hole was centered in the slot. The bare ends of the optical fibers were prepared for mounting into the Vespel housing by removing 10 cm of the protection jacket from one fiber and 2 cm from the other. The cladded fibers were then inserted into the Vespel housing as shown in Fig. 2 and held in place with epoxy resin. The exposed fiber on the ends of the housing was potted in epoxy (Type 302, Epoxy Technology, Billerica, MA) for protection. Silicone rubber was used to form a water-tight seal at the point of entrance of each fiber into the cell. After the cell had been constructed, the exposed ends of the optical fibers were polished.

A gallium arsenide light-emitting diode (LED) optimized for emission at 820 nm (Model IRE-161, M/A-COM Inc., New Brunswick, NJ) was used as the absorption light source and was powered by a constant-current source (Model 225, Keithley, Cleveland, OH) for stability. The light returning from the absorption cell was detected by a red-sensitive photomultiplier tube (Model R928, Hamamatsu, Middlesex, NJ) biased at -600 V by a high-voltage supply (Model 244, Keithley, Cleveland, OH). The photomultiplier current was amplified by a picoammeter (Model 414S, Keithley) and

monitored with a digital multimeter (Model 179, Keithley) and strip-chart recorder (Model SR-204, Heath, Benton Harbor, MI). The time constant for all measurements was established by the electronics; no additional filtering was used. When data were obtained for the calibration curves, approximately 10 s was required between successive measurements to allow equilibration of the sample solution; the system electronics responded within 1 s.

Procedures

Sample test solutions were prepared according to a conventional recipe for copper plating baths (R. Lamoureux, Hughes Aircraft Co.; personal communication). The nominal concentrations of each component were as follows: 0.300 M copper(II) sulfate pentahydrate, 10% (v/v) sulfuric acid, 60 mg kg⁻¹ chloride (from HCl), and 0.4% (v/v) Gleam-PC; Gleam-PC consists of 0.4 g l⁻¹ Carbowax-5000, 0.001 g l⁻¹ 2-thiazolidienethione, and 0.015 g l⁻¹ methyl violet. The copper sulfate (reagent grade, MCB) was weighed and transferred to a beaker, where it was dissolved in 500 ml of deionized water. Then sulfuric acid was added gradually and the solution was cooled to room temperature before being transferred to a 1-l volumetric flask. Hydrochloric acid and most of the remaining water were added and the solution was again cooled. Finally the Gleam-PC (Lea Ronal, Freeport, NY) was added and the solution was diluted to the 1-l mark. Solutions with varying concentrations of each of the components were also prepared in order to study interference effects.

Absorbance measurements were made by immersing the cell in a stirred solution and comparing the transmitted signal with that from a blank solution (no copper, all other components at their nominal concentrations). Calibration curves were obtained by immersing the cell in a solution of known copper concentration and diluting it with blank solution from a buret.

RESULTS AND DISCUSSION

Linearity and stability

The sensor constructed here was designed to monitor the Cu²⁺ concentration in a printed-circuit plating bath. In such applications, the Cu²⁺ concentration must be maintained within $\pm 10\%$ of the nominal value, which usually lies in the range 0.20–0.40 M. Figure 3 shows three successive calibration plots obtained with the optrode over this range. Correlation coefficients greater than 0.999 were obtained for each calibration plot. The excellent linearity of these plots was somewhat unexpected; Beer's law is often thought to apply rigorously only at concentrations below 10⁻² M [5]. The linearity of the calibration graphs probably arises from the broad absorption band of aqueous Cu²⁺, which extends from near 600 to over 1100 nm [6] and from the relatively short absorption path length used here.

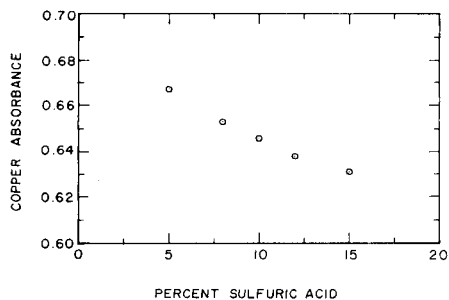
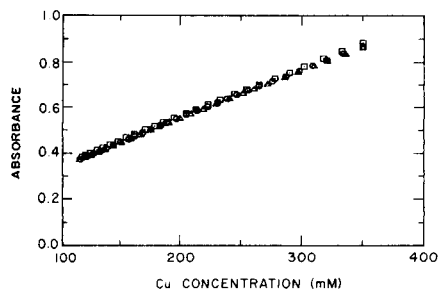


Fig. 3. Three successive calibration graphs for the copper optrode. Graphs were recorded on three separate days by diluting 0.400 M solutions with blank from a 50-ml buret.

Fig. 4. Effect of sulfuric acid concentration on Cu^{2+} absorbance at 820 nm. Measurements were made at the nominal concentrations of Cu^{2+} , chloride, and Gleam-PC.

Figure 3 also demonstrates the excellent reproducibility of the optrode. The three plots were obtained several days apart and agreement between them is very good, with the relative standard deviations of the slope and intercept being 0.006 and 0.12, respectively. Two curves are indistinguishable from each other, and the third curve shows a variation that would lead to a maximum error of only 1.7% in the concentration of Cu^{2+} . This error probably arises from variations in the ambient temperature of the laboratory; the temperature was 32°C and varied by several degrees during the time the data were obtained.

Interference effects

An important requirement for the optrode designed for this study was freedom from the influence of concomitants in the plating bath or variations of the environment of the optrode. The amount of chloride used for the plating bath was quite small, and therefore chloride was not investigated as an interferent. Changes in the Gleam-PC concentration of $\pm 25\%$ produced no measurable effect on the absorbance at 820 nm of the plating solution. In contrast, sulfuric acid did produce a change in the absorbance of the plating bath as shown in Fig. 4. Fortunately, the concentration of sulfuric acid in the printed-circuit bath is not expected to vary by more than $\pm 10\%$ between 9 and 11% (v/v); consequently, errors in determining the Cu^{2+} concentration would be less than 0.8%, according to Fig. 4. Figure 5 shows that the same kind and magnitude of effect are observed when a red LED (620 nm) is used as the light source; therefore, the measurement error could be decreased if measurements at the two wavelengths were ratioed. The interference from sulfuric acid is probably caused by changes in refractive index [5].

Environmental interferences expected to affect the measured absorbance are air bubbles that enter the absorption cell and changes in the temperature of the optrode assembly. Immunity from air bubbles is especially important

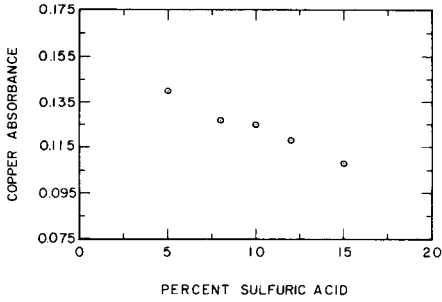


Fig. 5. Effect of sulfuric acid concentration on Cu^{2+} absorbance at red LED wavelength (620 nm). Measurements were made at the nominal concentrations of Cu^{2+} , Cl^- , and Gleam-PC.

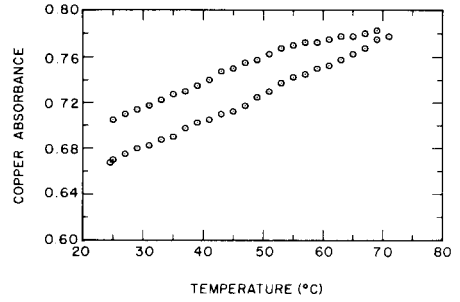


Fig. 6. Effect of solution temperature on measured absorbance. Heating cycle (lower curve) and cooling cycle (upper curve) differ because of solution evaporation.

here because plating baths are often agitated with compressed air. The design of the optrode was such that bubbles could not enter the absorption cell; in fact, all attempts to encourage air bubbles to enter the cell failed.

The effect of solution temperature is illustrated in Fig. 6. These measurements were made by successively heating and cooling a single solution; the higher absorbance measurements for the cooling cycle can be attributed to evaporation of the sample solution that occurred during the earlier heating period. The initial and final measurements were found to be equal after blank solution was added to the evaporated sample to restore it to its original volume. The plating baths are maintained at room temperature ($\pm 2^\circ\text{C}$); accordingly, temperature is not expected to contribute a serious interference.

Drift compensation

For acceptance in practical applications, the sensor must require little maintenance and must be able to remain in the plating bath for long periods of time. Because the sensor cannot practicably be removed from the bath, conventional blank measurements cannot be obtained. Therefore, a means to correct for drift in the optical sensor is required. As mentioned previously, corrections for interference of concomitants such as sulfuric acid could be made by a two-wavelength measurement. Errors caused by dirt accumulation or degradation of the end surfaces of the optical fibers could be corrected in the same way, because they produce an error which is wavelength-independent. The following analysis applies to such a wavelength-independent error.

The absorbance of the analyte (Cu^{2+}) at two wavelengths can be described by the Beer-Lambert law

$$A_1 = -\log(P_1/P_{01}); A_2 = -\log(P_2/P_{02})$$

where the analyte absorbance at wavelength i is denoted by A_i and the transmitted radiant power through an interferent-free sample and through a blank are P_i and P_{0i} respectively. In the presence of an interferent, the analyte absorbance is described by

$$A_1 = -\log[P'_1/(P_{01} - EP_{01})]; A_2 = -\log[P'_2/(P_{02} - EP_{02})]$$

where E is the fraction of incident radiation attenuated by a wavelength-independent error and P'_i is the transmitted power through the sample containing the interferent. Substitution using Beer's law and rearrangement gives

$$a_1bc = -\log[P'_1/P_{01}(1 - E)] \quad (1)$$

$$a_2bc = -\log[P'_2/P_{02}(1 - E)] \quad (2)$$

where a_i is the molar absorptivity of the analyte, b is the path length, and c is the analyte concentration. Subtracting Eqn. 2 from Eqn. 1 yields

$$c(a_1b - a_2b) = -\log(k_s P'_1/P'_2) \quad (3)$$

where P_{02}/P_{01} is a constant, k_s , for the given source intensities. Rearrangement of Eqn. 3 yields

$$c = [-\log(k_s P'_1/P'_2)]/(a_1b - a_2b) \quad (4)$$

which provides a straightforward means of determining analyte concentration in the presence of wavelength-independent errors through the easily measured variables P'_1 and P'_2 .

By measuring the radiant power at two different wavelengths, one can correct for drift in response caused by degradation of the optical surfaces, particulates in the plating bath, and that from any other wavelength-independent interferent.

Noise and precision

Traditionally, improvements in the precision of absorption spectrophotometry have been obtained by reducing readout noise. A readout-noise-limited measurement implies that maximum precision will be obtained at an absorbance value of 0.434 [7]. However, the present optrode system is limited in stability by fluctuations in the source intensity; therefore, source flicker noise will limit the measurement precision. As a result, precision can be improved by increasing the absorbance within practical limits [8]. A practical limit for this experiment would be the point where source flicker noise would be equal to or greater than the detector or readout noise. The readout device used in this experiment was a 4 1/2 digit digital voltmeter, and therefore the readout precision was ± 0.1 mV for the 1 V full scale setting. This corresponds to a relative standard deviation of 0.01%. The cell used in this study had a transmittance (light throughput efficiency) of 2%, and the relative standard deviation (RSD) of twelve successive absorbance measurements on a 0.300 M plating solution was 1.1%. Therefore it was assumed

that the measurement was source-flicker-noise limited. In addition, the cell provided adequate sensitivity, and therefore a longer pathlength cell was not required. Moreover, any further improvements in precision could be obtained only by reducing or correcting source-intensity fluctuations. A reduction of source drift might be realized by controlling the temperature of the LED. Additionally, the output intensity of the source could be monitored and the measured absorbance values could be corrected accordingly. Monitoring the source intensity would require either a separate amplification and detection system or the use of optical switches in the fiberoptic path. In either case, the noise introduced by the extra components might negate any gain in precision. However, as shown in Fig. 3, long-term source drift was not a problem with the present optrode design. As a result, these correction methods were not used.

Conclusions

The simple, rugged optrode for the continuous monitoring of Cu^{2+} in a plating bath is relatively free from serious interferences expected to be found in the plating bath, and provides adequate precision for the monitoring of Cu^{2+} . The optrode is capable of being operated over long distances, thus allowing the cell to be located far from the source and detection system. A prototype of the optrode is presently being evaluated in an industrial setting.

The authors greatly appreciate the helpful comments and support offered by T. Hirschfeld and S. Klainer during the course of this investigation. The work was supported in part by the Office of Naval Research, by the Upjohn Company, and by ST & E Technical Services.

REFERENCES

- 1 S. A. Borman, *Anal. Chem.*, 53 (1981) 1616A.
- 2 W. R. Seitz, *Anal. Chem.*, 56 (1984) 16A.
- 3 J. I. Peterson, R. V. Fitzgerald and D. K. Buckhold, *Anal. Chem.*, 56 (1984) 62.
- 4 B. J. Tromberg, J. F. Eastham and M. J. Sepaniak, *Appl. Spectrosc.*, 38 (1984) 38.
- 5 H. A. Strobel, *Chemical Instrumentation: A Systematic Approach*, 2nd Edn., Addison-Wesley, Reading, MA, 1973.
- 6 J. Bjerrum, C. J. Ballhausen and C. K. Jorgensen, *Acta. Chem. Scand.*, 8 (1954) 1275.
- 7 D. G. Peters, J. M. Hayes and G. M. Hieftje, *Chemical Separations and Measurements*, Saunders, Philadelphia, PA, 1974.
- 8 J. D. Ingle, Jr. and S. R. Crouch, *Anal. Chem.*, 44 (1972) 1375.

MINIMIZING THE EFFECT OF ORGANIC MATRICES IN THE ANALYSIS OF TIN-CONTAINING EXTRACTS BY ELECTROTHERMAL ATOMIC ABSORPTION SPECTROMETRY

Determination of Tin in Rocks

A. B. VOLYNSKY, E. M. SEDYKH, B. YA. SPIVAKOV and YU. A. ZOLOTOV*

V.I. Vernadsky Institute of Geochemistry and Analytical Chemistry, U.S.S.R. Academy of Sciences, Moscow (U.S.S.R.)

(Received 1st April 1985)

SUMMARY

The effect of the nature of the extracted complex and of the organic solvent on the sensitivity of the extraction/atomic absorption determination of tin in a graphite-furnace atomizer is investigated. It is recommended that extracts of tin as its chloride complex, or chelates with *N*-benzoyl-*N*-phenylhydroxylamine or 8-quinolinol, in organic solvents which do not contain chlorine should be used. The depressive effect of the organic matrix can be significantly decreased by using ascorbic acid as matrix modifier, by atomization from a graphite platform, and by using an atomizer coated with tungsten carbide. The procedure developed is applied to the determination of tin in rocks. For tin concentrations of 0.1–10 $\mu\text{g g}^{-1}$, the relative standard deviation does not exceed 10%.

At present much attention is given to hybrid methods of analysis [1] and there is significant interest in the use of atomic absorption spectrometry (a.a.s.) with electrothermal atomization in combination with liquid-liquid extraction. However, the analysis of organic extracts in electrothermal atomizers is sometimes less sensitive and precise than the analysis of aqueous solutions [2]. The development of procedures for suppressing the negative effect of an organic matrix on the final results enables this hybrid method to be used more effectively in determining trace elements in complex matrices.

Quite important and difficult is the problem of determining tin in rocks at the 0.1–10 $\mu\text{g g}^{-1}$ level [3]. It can be solved by the use of a.a.s., particularly in combination with the generation of volatile hydrides [4–6]. High accuracy and precision can also be attained with the use of electrothermal atomization of the sample after separation of tin from the matrix by liquid-liquid extraction [7]. This paper describes an investigation of the determination of tin in organic extracts of its chelates with *N*-benzoyl-*N*-phenylhydroxylamine (BPHA), cupferron, 8-quinolinol, diethyldithiocarbamate (DDTC) and thenoyltrifluoroacetone (TTA), as well as its chloride and iodide complexes by graphite-furnace a.a.s. It is mainly concerned with minimizing the negative

effect of the organic matrix on the measurements. The data obtained were used in developing a procedure for the determination of traces of tin in rocks.

EXPERIMENTAL

Apparatus and reagents

A Perkin-Elmer atomic absorption spectrometer Model 603 fitted with an HGA-76B graphite furnace, a deuterium arc background corrector and a standard tin hollow-cathode lamp were utilized. The tin 286.3-nm line was used in the analysis of rocks and 224.6-nm line was used in the analysis of other extracts. The spectral bandwidth was 0.2 nm in all cases. Perkin-Elmer graphite tubes, with and without pyrolytic coating, were used, as well as rectangular platforms of pyrolytic graphite produced by the same manufacturer (with and without protrusions at the corners). Rectangular platforms (without protrusions) of the same size cut from porous graphite SU-204 (Czechoslovakia) were also tested. The platforms and graphite tubes were coated with tungsten carbide [8]. Argon was used as shielding gas with an oxygen content of $\leq 7 \times 10^{-4}\%$.

All chemicals were of analytical reagent grade. Methyl isobutyl ketone (MIBK) was distilled in vacuum; cupferron and 8-quinolinol were recrystallized from water and *o*-xylene, respectively. The stock solution of tin was prepared by dissolving 100 mg of tin metal in 2.5 ml of (1 + 3) HCl/HNO₃; the volume was brought to 100 ml with 3 M HCl. Working solutions of tin in 0.5 M HCl were stable for at least two weeks.

Procedures

General procedure. Extractions were conducted under the optimal conditions for the chosen systems [9]. The concentration of tin in the aqueous phase at equilibrium was determined by the standard addition technique. The data obtained were used to calculate the tin concentration in the extract. The atomic absorption determination consisted of three stages; the atomizer heating rate was set by the push-button selector. A 20- μ l sample was dried for 20 s at a temperature 10°C above the boiling point of the solvent used (rate 1). When graphite platforms were used, the drying temperature was 30°C above the boiling point (rate 3), up to a maximum of 130°C (water, amyl acetate). The ashing temperature and time were optimized for all the investigated extracts and aqueous solutions. Atomization was done at 2600°C for 6 s (gas-stop mode, rate 0).

Procedure for tin in rocks. An accurately weighed sample (100–200 mg) was placed in a platinum crucible, wetted with water, and 10.5 ml of a (20 + 1) mixture of concentrated hydrofluoric and (1 + 1) sulphuric acid was added. The mixture was evaporated to dryness on a sand bath. Thereafter 0.5–1 g of lithium metaborate, preliminarily dried at 100°C, was added to the crucible, which was heated in a muffle furnace at 950°C for 45 min. After cooling, 5 ml of 3.2 M HCl was added to the crucible and the melt was

dissolved with slight stirring, fresh portions of 3.2 M HCl being added periodically. The final volume was made up to 50 ml with 3.2 M HCl. An aliquot (1–15 ml, depending on the tin content) of this solution was mixed with 0.2–3.0 ml of freshly prepared 15% (w/v) ascorbic acid solution.

Tin was extracted into 1 ml of 0.1 M trioctylamine (TOA) in a (2 + 1) mixture of heptane and amyl acetate, the equilibration time being 5 min. Standard tin solutions (0, 15, 30 and 60 ng ml⁻¹) were prepared by the same procedure from stock solutions of tin containing lithium metaborate at the same concentration as the sample solutions. Tin was determined in the graphite tube without a pyrolytic coating but with a platform made of pyrolytic graphite. A 20- μ l portion of solution was injected into the furnace, and the background corrector was turned on. The operating conditions of the atomizer were: drying, 130°C, 25 s, rate 1; ashing, 800°C, 20 s, rate 3; atomization, 2600°C, 6 s, rate 0, gas-stop mode.

RESULTS AND DISCUSSION

The effect of the nature of the extracted complex

As regards the effect of the nature of the extracted complex on the behaviour of organic extracts in the atomizer, the investigated compounds can be subdivided into three groups. The first group comprises the chloride complexes of tin (extracted with MIBK or 0.1 M TOA in MIBK), the non-volatile chelates of *N*-benzoyl-*N*-phenylhydroxylamine and cupferron [10, 11], and the 8-quinolinol chelate (*o*-xylene used as diluent). For extracts containing these complexes, the form of the absorbance/ashing temperature curve (ashing curve) and the sensitivity of the tin determination are little different from the corresponding characteristics for solutions of tin in 0.5 M HCl (Fig. 1). Signals attain a constant value at an ashing time of 5–10 s (for chloride complexes in 0.1 M TOA in MIBK, the ashing time was 40 s, Fig. 2).

The second group comprises extracts based on diethyldithiocarbamate in chloroform and thenoyltrifluoroacetone in MIBK. For these extracts the tin signals are 2–5 times smaller than those for aqueous hydrochloric acid solutions (Figs. 3, 4). The required duration of the ashing stage increases significantly. For instance, for the tin/TTA chelate, the signal fails to attain a constant level even after 200 s of ashing (Fig. 5). Losses of tin in the form of its diethyldithiocarbamate at lower temperatures (700°C) are apparently due to its sublimation [10, 12]. For determinations in the graphite furnace, chelate sublimation is likely to be promoted by very rapid atomizer heating at the ashing and atomization stages [12]. Slow heating of the atomizer up to the ashing temperature provides a significant increase of tin signal for such extracts (Table 1 and Fig. 3, curve 2). The magnitude of the signal is also significantly affected by the thermal properties of the compounds formed during the decomposition of the complexes. The low sensitivity for tin as its diethyldithiocarbamate is attributed to an incomplete dissociation of tin monosulphide formed by thermal decomposition of this complex [13].

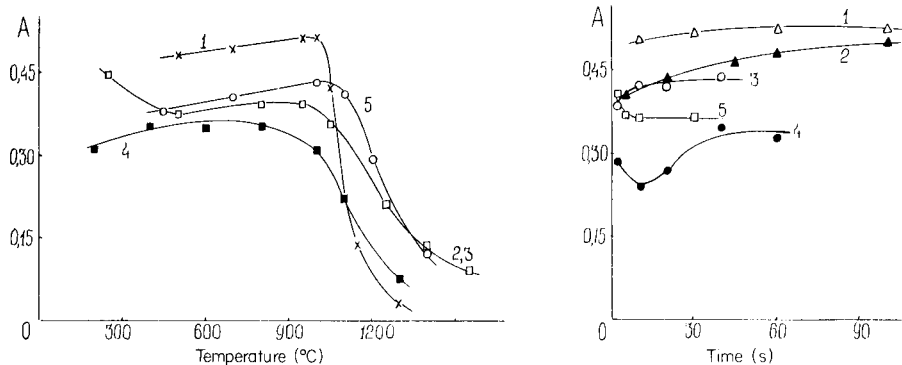


Fig. 1. Effect of ashing temperature on peak-height absorbance of tin (ashing for 10 s, rate 1; $0.15 \mu\text{g Sn ml}^{-1}$): (1) 0.5 M HCl, ashing for 20 s; (2) BPHA chelate in *o*-xylene; (3) cupferron chelate in *o*-xylene; (4) 8-quinolinol chelate in *o*-xylene; (5) chloride complex in MIBK.

Fig. 2. Effect of ashing time on the peak-height absorbance of tin (ashing at $800\text{--}900^\circ\text{C}$, rate 0–1, $0.15 \mu\text{g Sn ml}^{-1}$): (1) 3 M HNO_3 + 0.004 M HCl; (2) 2.94 M HCl; (3) chloride complexes in MIBK; (4) chloride complexes in 0.1 M TOA in MIBK; (5) BPHA chelate in benzene.

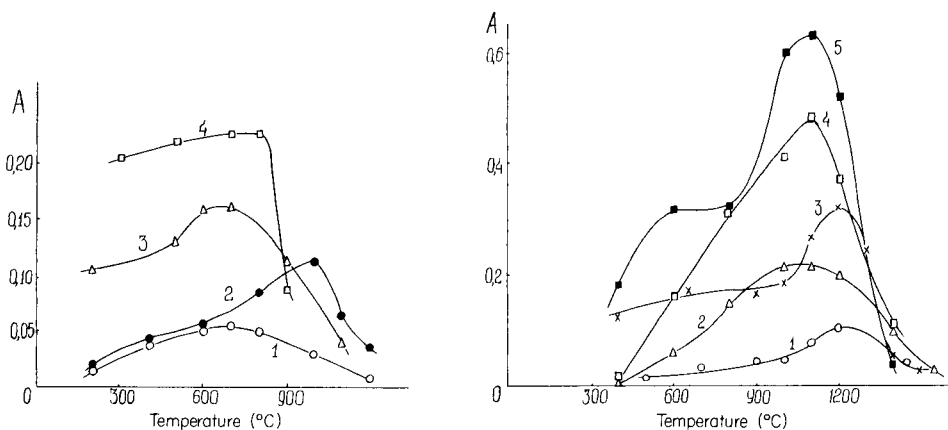


Fig. 3. Effect of ashing temperature on the peak-height absorbance of tin as its DDTC chelate in chloroform (ashing for 20 s, rate 0, $0.15 \mu\text{g Sn ml}^{-1}$): (1–3) porous graphite tube; (2) ashing rate 1×30 ; (3) with 5% ascorbic acid added; (4) tube with coating of pyrolytic graphite and tungsten carbide (ashing for 40 s).

Fig. 4. Effect of ashing temperature on the peak-height absorbance of tin as its TTA chelate in MIBK ($0.15 \mu\text{g Sn ml}^{-1}$, porous graphite furnace; tube coated with tungsten carbide for curves 4 and 5): (1) ashing for 20 s, rate 1×30 ; (2) with 5% ascorbic acid added, ashing for 20 s, rate 1; (3) atomization from a pyrolytic graphite platform, ashing for 20 s, rate 1×30 ; (4) ashing for 60 s, rate 1; (5) atomization from a pyrolytic graphite platform coated with tungsten carbide, ashing for 60 s, rate 1×30 .

TABLE 1

Effect of heating rate in the ashing step on the tin peak-height absorbance in porous graphite tubes (ashing time, 20 s)

Reagent	Solvent	Tin conc. ($\mu\text{g ml}^{-1}$)	Ashing temp. ($^{\circ}\text{C}$)	Heating rate ($^{\circ}\text{C s}^{-1}$)					
				600	400	180	70	20	8
BPHA	Benzene	0.15	1000	0.37	0.38	0.37	0.38	—	—
8-Quinolinol	<i>o</i> -Xylene	0.15	900	0.34	0.33	—	0.35	0.33	0.35
DDTC	CHCl_3	0.5	1000	0.17	—	0.19	0.33	0.37	0.42
TTA	MIBK	1.0	900	0.22	—	0.23	—	0.27	0.26
TTA ^a	MIBK	0.5	900	0.62	—	0.58	0.60	0.60	—
TTA ^b	MIBK	0.5	900	0.55	—	0.58	—	0.68	0.65

^aTube coated with tungsten carbide. ^bWith aqueous 5% (w/v) ascorbic acid added.

The third group comprises a MIBK extract containing uncharged tin iodide. Direct analysis of this extract in the graphite furnace is impossible because of the high volatility of SnI_4 [14].

The effect of the nature of the organic solvent

The influence of the organic solvent on the analysis of extracts was studied for the system with BPHA, as an example. The shape of the ashing curve does not alter when changing from *o*-xylene to benzene or *n*-heptane; the height of the signal diminishes slightly. No correlation between tin sensitivity and the density or viscosity of the solvents could be found.

Analysis of tin-containing extracts based on *o*-xylene in a furnace with pyrolytic graphite coating is practically impossible because of a strong non-specific absorption signal at 224.6 nm during the atomization stage which is not compensated by the background corrector (ashing at 800°C for 40 s). When other solvents, among them aromatic ones (benzene, toluene) were used, no such interferences were observed. Güger and Massmann [15] suggested that such non-specific absorption is due to volatilization of undecomposed aromatic molecules at the atomization stage. Complete removal of aromatic compounds from the graphite furnace at the ashing stage may not be achieved because of their very strong sorption by graphite.

Also significant is the nature of the atomizer surface. If the graphite tube or platform with a pyrolytic graphite surface are additionally coated with tungsten carbide, they can be used for the analysis of *o*-xylene extracts. The non-specific absorption can also be fully compensated by the background corrector when an atomizer of porous graphite without pyrolytic coating is used.

When chloroform is the extractant, the tin signal is significantly suppressed at relatively low ashing temperatures (Fig. 6, curve 1). Presumably, this is due to the formation of a stable (dissociation energy 404 kJ mol^{-1}) [16] and

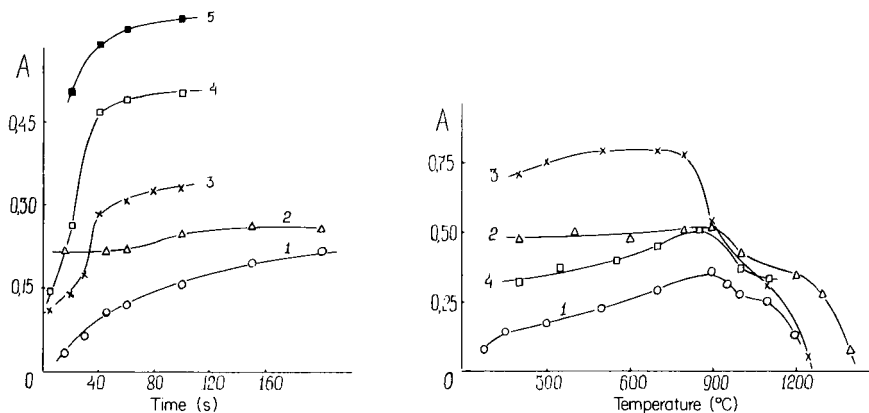


Fig. 5. Effect of ashing time on the peak-height absorbance of tin as its TTA chelate in MIBK: (1) ashing at 1100°C, rate 1, 0.15 $\mu\text{g Sn ml}^{-1}$, porous graphite tube; (2) as for (1) with 5% ascorbic acid added; (3) as for (1) but with atomization from a pyrolytic graphite platform (ashing at 1200°C); (4) as for (1) but with tube coated with tungsten carbide; (5) as for (3) but with platform and tube coated with tungsten carbide.

Fig. 6. Effect of ashing temperature on the absorbance of tin as its BPHA chelate in chloroform (0.15 $\mu\text{g Sn ml}^{-1}$): (1) ashing for 40 s, rate 0; (2) with 5% ascorbic acid added, ashing for 40 s, rate 2; (3) atomization from a pyrolytic graphite platform, ashing for 20 s, rate 3; (4) tube coated with tungsten carbide, ashing for 20 s, rate 0.

volatile tin monochloride. A high ashing temperature leads to an increase of tin signal because of more complete removal of chlorine from the atomizer. As the graphite tube ages, the ashing curve may be displaced with respect to the temperature axis [17], which should lead to a decline in tin sensitivity and to increased error. Therefore, a maximum in the ashing curve should be avoided.

The chlorine content of the analysed solution largely dictates the duration of ashing; the chemical form of tin is of secondary importance. This is true for the analysis of both aqueous (Fig. 2) and organic (Fig. 7) solutions. For instance, for chloride complexes of tin in MIBK, ashing for 10 s is sufficient (Fig. 2), while for the non-volatile BPHA chelate in chloroform, ashing requires 20–80 s (Fig. 7).

It is to be noted that the analysis of extracts is more sensitive to variations in instrumental parameters than the analysis of aqueous solutions. Thus, the ashing time may increase more than three-fold as the graphite cones wear down (Fig. 7); the sensitivity likewise declines. A similar effect is produced by wear of the graphite tube.

On the basis of the data obtained, most conventional organic solvents may be used for tin determination. Halogen-containing solvents that may suppress the tin signal are an exception.

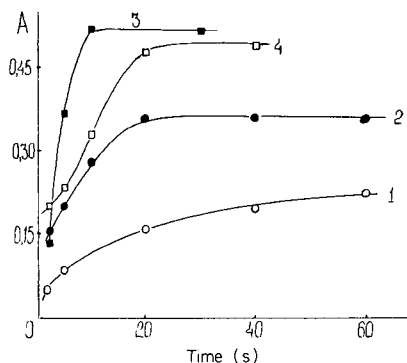


Fig. 7. Effect of ashing time on the absorbance of tin ($0.15 \mu\text{g ml}^{-1}$) as its BPHA chelate in chloroform. Conditions: (1, 4) old graphite cones; (2, 3) new graphite cones; (1) ashing at 800°C , rate 0; (2) ashing at 700°C , rate 1; (3) ashing at 650°C with 5% ascorbic acid added, rate 1; (4) ashing at 650°C , rate 3, atomization from a pyrolytic graphite platform.

Minimizing the effect of organic matrix

To minimize the effect of the nature of the extracted complex and the solvent, methods for suppressing the effect of the inorganic matrix and improving the sensitivity were used. These included atomization from a graphite platform [18], treatment of the atomizer surface with refractory compounds [19], and the use of a matrix modifier (ascorbic acid) [20]. Their use is quite promising as regards the analysis of extracts in graphite atomizers [2, 21].

Solutions of tin in 0.5 M HCl and of the tin/BPHA chelate in *o*-xylene were used to investigate the effect of the material of the platform and graphite tube on tin sensitivity (Table 2). As can be seen, aging of the graphite tube is accompanied by a decrease in tin sensitivity, particularly in extracts. This is possibly due to the destruction of the graphite structure and to increasing tin losses caused by soaking of the analyte solution into the graphite, the latter being more significant for extracts. As a result, extracts were afterwards always analyzed in tubes that had been used for not more than 70 determinations. Maximum sensitivity for tin is achieved with graphite tubes coated with tungsten carbide and atomization from a pyrolytic graphite platform. For the analysis of aqueous tin solutions, a pyrolytic graphite platform treated with sodium tungstate solution and with and without protrusions at the corners were tested, but no significant differences were observed. The use of graphite platforms along with ascorbic acid leads to insignificant further increase in signals. Improvements in the sensitivity in the presence of ascorbic acid in the furnace and with the use of a graphite tube coated with tungsten carbide are largely caused by the decrease in the concentration of free oxygen in the gas phase in the furnace [22, 23].

It must be emphasized that, even for the extracts of the first group, conditions could not be selected that would secure long-term coincidence between calibration graphs for aqueous and organic solutions.

TABLE 2

Effect of platform material and graphite tube surface on the calibration slope for tin^a

Tube surface	Platform material	Slope		Ratio of slopes (aq:org.)
		SnCl ₄ in 0.5 M HCl	Tin-BPHA in <i>o</i> -xylene	
Porous graphite	—	1.0 ^c	1.0 ^c	1.3
	Porous graphite	1.2	1.3	1.2
	Pyrographite	1.7	—	—
	Pyrographite/tungsten carbide	1.8	1.3	1.7
Porous graphite ^b	—	0.8	0.6	1.7
	Porous graphite	—	1.1	—
	Pyrographite	1.3	—	—
	Pyrographite/tungsten carbide	1.4	1.2	1.5
Porous graphite/tungsten carbide	—	1.2	1.1	1.4
	Porous graphite/tungsten carbide	1.3	1.6	1.1
	Pyrographite/tungsten carbide	1.8	1.7	1.4
	—	1.4	1.4	1.3

^aAshing at 800°C for 20 s, rate 1. ^bTube used for >100 determinations. ^cCalibration slopes, i.e., sensitivities, normalized to this result for each column.

Examples illustrating the elimination of the negative effect of chloroform are given in Figs. 6 and 7 (tin was quantified in extracts of its BPHA chelate). The presence of ascorbic acid and atomization from a platform makes it possible to decrease the ashing time 2–3 times, as well as to smooth out the maximum in the ashing curves. Possibly, the active carbon, formed as a result of the thermal decomposition of ascorbic acid, binds chlorine as CCl (dissociation energy 387 kJ mol⁻¹). Coating with tungsten carbide eliminates to a lesser extent interferences from large amounts of chlorine, although it leads to higher sensitivity.

The procedures used are also reasonably effective in eliminating the effect of the nature of the extracted complex. The presence of ascorbic acid and atomization from the graphite platform permits the duration of ashing to be decreased (Fig. 5). However, the best results for extracts of the second group were obtained by using graphite tubes and platforms coated with tungsten carbide (Figs. 3 and 4). Possibly, tungsten compounds catalyze the decomposition of volatile tin chelates [24].

Analysis of rocks

Fusion with lithium metaborate is apparently the most effective and acceptable procedure for dissolving samples [5]. Complete dissolution is achieved by fusion at 950°C for 45 min with a 5-fold excess of flux. Silicon is removed beforehand as silicon tetrafluoride by heating the sample with

TABLE 3

Results of tin determination in standard reference rocks

Rock	Type	No. of samples	No. of determinations on each sample	Tin content ($\mu\text{g g}^{-1}$)	
				Certificate	Found ^a
SGD-IA	Gabbro	4	2	3.7 ± 0.6	3.9 ± 0.4
MK-2	Granodiorite	3	2	4.6 ± 0.5	4.5 ± 0.3

^aMean with standard deviation.

concentrated hydrofluoric acid (in the presence of a small amount of sulphuric acid to prevent tin losses). It was found that such treatment does not lead to tin losses and permits the flux dissolution time to be significantly decreased.

Direct analysis of sample solutions containing high flux concentrations is impossible because of great matrix interferences. For separating tin from the matrix and for preconcentration, the tin chloride complexes were extracted with 0.1 M TOA solution in a (2 + 1) mixture of heptane and amyl acetate. This system is characterized by a wide range of aqueous acidity (0.5–3.5 M HCl) within which quantitative extraction of tin is achieved (equilibration time 5 min, 1:8 ratio of volumes of organic to aqueous phase). The concentration coefficient for this system may reach 20 without significant losses of tin. To prevent extraction of iron(III), it was reduced to iron(II) with freshly prepared ascorbic acid solution. Table 3 gives the results of tin determination in standard reference materials available in the U.S.S.R. It is seen that the certificate data and those obtained by using the present method are in good agreement.

The above method was used for tin determinations in a wide variety of rocks. The relative standard deviation did not exceed 10% for tin contents of 0.1–10 $\mu\text{g g}^{-1}$.

The technical assistance of Mrs. T. N. Shemarykina in the analysis of rocks is gratefully acknowledged.

REFERENCES

- 1 Yu. A. Zolotov, *Analyst* (London), 103 (1978) 56.
- 2 A. B. Volynsky, B. Ya. Spivakov and Yu. A. Zolotov, *Talanta*, 31 (1984) 449.
- 3 V. L. Barsukov, *The Main Features of Tin Geochemistry*, Nauka, Moscow, 1974 (in Russian).
- 4 K. S. Subramanian and V. S. Sastri, *Talanta*, 27 (1980) 469.
- 5 A. Hall, *Chem. Geol.*, 30 (1980) 135.
- 6 C. Y. Chan and M. W. A. Baig, *Anal. Chim. Acta*, 136 (1982) 413.
- 7 L. Zhou, T. T. Chao and A. L. Meier, *Talanta*, 31 (1984) 73.
- 8 H. Fritzsche, W. Wegscheider, G. Knapp and H. M. Ortner, *Talanta*, 26 (1979) 219.
- 9 V. B. Spivakovsky, *Analytical Chemistry of Tin*, Nauka, Moscow, 1975 (in Russian).
- 10 H. Takaharu, I. Hisanori, S. Shigeki and K. Toshiyasu, *Anal. Chem.*, 50 (1978) 1545.

- 11 R. A. Meyer, J. F. Hazel and W. McNabb, *Anal. Chim. Acta*, 31 (1964) 419.
- 12 D. C. Hilderbrand and E. E. Pickett, *Anal. Chem.*, 47 (1975) 424.
- 13 P. Hocquellet and N. Labeyrie, *At. Absorpt. Newsl.*, 16 (1977) 124.
- 14 Gmelin Handbuch der anorganischen Chemie, 8 Auflage, Zinn. Teil CI, Springer, Berlin and Heidelberg, 1972, S.469.
- 15 S. Güger and H. Massmann, *Spectrochim. Acta, Part B*: 38 (1983) 573.
- 16 K. S. Krasnov (Ed.), *Molecular Constants of Inorganic Substances*, Khimia, Leningrad, 1979 (in Russian).
- 17 A. B. Volynsky, E. M. Sedykh, B. Ya. Spivakov and Yu. A. Zolotov, *Zh. Anal. Khim.*, 38 (1983) 435.
- 18 B. V. L'vov, L. N. Pelieva and A. I. Sharnopolsky, *Zh. Prikl. Spectrosk.*, 27 (1977) 395.
- 19 I. A. Kuzovlev, Yu. N. Kuznetsov and O. A. Sverdlina, *Zavod. Lab.*, 39 (1973) 428.
- 20 J. G. T. Regan and J. Warren, *Analyst (London)*, 101 (1976) 220.
- 21 L. N. Sukhoveeva, G. G. Butrimenko and B. Ya. Spivakov, *Zh. Anal. Khim.*, 35 (1980) 649.
- 22 G. D. Rayson and J. A. Holcombe, *Anal. Chim. Acta*, 136 (1982) 249.
- 23 A. B. Volynsky and E. M. Sedykh, *Zh. Anal. Chim.*, 39 (1984) 1197.
- 24 T. M. Vickrey and M. S. Buren, *Anal. Lett.*, 13A (1980) 1465.

SIMULTANEOUS MULTI-ELEMENT DETERMINATION OF TRACE METALS IN SEA WATER BY INDUCTIVELY-COUPLED PLASMA ATOMIC EMISSION SPECTROMETRY AFTER COPRECIPITATION WITH GALLIUM

TASUKU AKAGI, KEIICHIRO FUWA and HIROKI HARAGUCHI*

Department of Chemistry, Faculty of Science, University of Tokyo, Bunkyo-ku, Tokyo 113 (Japan)

(Received 11th April 1985)

SUMMARY

Coprecipitation with gallium hydroxide is studied for the preconcentration of trace metals in sea water before multi-element analysis by inductively-coupled plasma/atomic emission spectrometry. Gallium precipitates at pH 9 only when magnesium is present. Optimum conditions are established for multi-element preconcentration and removal of matrix elements. The method is almost free from contamination because of the use of highly pure gallium metal and only a small amount of sodium hydroxide for pH adjustment. Spectral interferences from gallium are negligible and a concentration factor of more than 200 can be obtained. Detection limits range from a few ng l^{-1} to 150 ng l^{-1} for Al, Co, Cr, Fe, La, Mn, Ni, Ti, V, Zn, Y and Pb. Artificial and natural sea-water samples can be analyzed with adequate precision.

Inductively-coupled plasma atomic emission spectrometry (i.c.p./a.e.s.) is a very sensitive technique for multi-element determinations, which has often been applied to sea waters. Preconcentration of trace elements and decrease in matrix element concentrations have been studied [1–5]. The concentrations of most elements in sea water are close to or below the detection limits for i.c.p./a.e.s., as can be seen in Fig. 1, where the detection limits cited are the lowest values found in the literature [6–8]. Therefore, preconcentration of trace elements is required for sea waters. With 20-fold preconcentration, 13 elements (Al, As, Cr, Cu, Fe, Li, Mn, Mo, Ni, P, Ti, Y, and Zn) can be detected in coastal sea water and these elements except Ti can be detected in open sea water. A 200-fold preconcentration gives the possibility of detecting 18 elements including Cd, Co, Hg, Pb and Se in coastal waters and 16 elements (those mentioned except Co and Pb) in open sea water. However, such high preconcentration often leads to large blank and contamination problems as well as tedious purification of reagents.

Berman et al. [2] used a chelating resin column (Chelex-100) for Fe, Mn, Cu, Ni, Zn, Pb, Co, and Cd, with ultrasonic nebulization. They preconcentrated trace elements by a factor of 100 in a class 100 clean-air laboratory. McLeod et al. [3] concentrated analytes (Cd, Cu, Fe, Mo, Ni, V, and Zn)

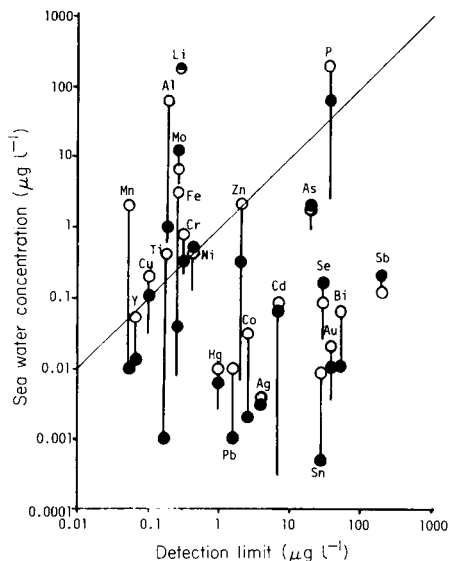


Fig. 1. Plot of concentration of trace elements in sea water vs. i.c.p. detection limits: (●) mean concentration in open sea water [9]; (○) concentration in coastal water; Al [10], P [11], Ti [12], Cr [13], Mn [14], Fe, Co, Ni and Zn [15], Cu, Ag, Cd and Pb [16], As [17, 18], Se [19], Y [20], Mo [21], Sn [22], Sb [23], Au [24], Hg [25], Li [26], Bi [27].

500 times using a liquid-liquid extraction method with two chelating reagents. Complicated, time-consuming purification of the reagents was needed to achieve low blank levels. Watanabe et al. [4] collected trace metals (Cd, Zn, Pb, Ni, Mn, Fe, and Cu) as their 8-quinolinol chelates on C_{18} -bonded silica gel. They reported that purification was needed to decrease the blank especially for zinc and iron.

Coprecipitation methods have been used in i.c.p./a.e.s. to preconcentrate many elements from artificial sea water [5, 28], waste water [29] and brines [30]. Coprecipitation has the advantages that most elements except the alkali and alkaline earth metals are efficiently concentrated and that the procedures are generally simple. However, it has the disadvantages that the coprecipitation reagents provide different matrices and that the impurities from the coprecipitation reagent and the alkali used for pH adjustment often produce errors. If a highly pure coprecipitation reagent which gives relatively few emission lines in i.c.p./a.e.s. can be used, coprecipitation would be more promising for preconcentration of trace elements in sea water. From such a point of view, Hirade et al. [28] indicated the possibility of using indium as a coprecipitation reagent, combined with the flotation technique prior to i.c.p./a.e.s.; their work was only preliminary for sea water analysis. In the present study, gallium coprecipitation is evaluated for simultaneous multi-elemental analysis of sea water using i.c.p./a.e.s. Gallium is chosen because of

its characteristic behavior in sea water, its small number of emission lines and the availability of pure gallium metal.

EXPERIMENTAL

Apparatus and chemicals

The instrumental components and operating conditions are summarized in Table 1. The emission lines used are shown in Table 2. A pH meter (Ionalyzer 407A) equipped with a glass electrode (91-01, Orion Research) was used for pH measurement.

All chemicals used were of analytical-reagent grade. The standard solutions (1000 mg l^{-1}) for Al, Cd, Co, Cr, Cu, Fe, Mg, Mn, Ni, Pb, Sb, Ti, and Zn were prepared from pure metals, and those for As, La, Mo, V, Y, Na, K and Ca from common salts or oxides. The nitric and hydrochloric acids were of extra-pure grade (Wako Chemicals Co.). Sodium hydroxide solution (9 M) used for pH adjustment was prepared by dissolving the solid (Suprapur; Merck) in 100 ml of pure water. Gallium solution was prepared by dissolving 1 g of gallium metal (99.99%; Nakarai Chemicals Ltd.) in 10 ml of (1 + 1) nitric acid and diluting to 200 ml with water. All the chemicals were used without further purification.

Sea-water samples

Samples were collected in clean polyethylene bottles at various sites near the Japan Islands. Some coastal sea water was collected in Tokyo Bay and Hiroshima Bay. Some open sea waters were collected far from the Sagami Bay. Most were filtered on ship through Nuclepore filters (pore size $0.4 \mu\text{m}$), immediately after collection. Some samples were acidified with sub-boiled nitric acid to pH 2 prior to filtration, for sample preservation. Artificial sea water, which was used for all the recovery tests, was prepared as reported previously

TABLE 1

Instrumental components and operating conditions

Spectrometer	Jarrell-Ash Plasma Atomcomp MK II
frequency	27.12 MHz
r.f. output power	1.1 kW
coolant gas	argon 15 l min^{-1}
auxiliary gas	argon 0.5 l min^{-1}
carrier gas	argon 1.0 l min^{-1}
observation height	17 mm above work coil
Nebulizer	Cross-flow type
Polychromator	Paschen-Rung type (75-cm focal length)
grating	2400 grooves mm^{-1}
reciprocal linear dispersion	0.54 nm mm^{-1} at 270 nm
entrance slit width	$25 \mu\text{m}$
exit slit width	$50 \mu\text{m}$
Monochromator	Ebert type (50-cm focal length)

TABLE 2

Comparison between interference equivalent concentrations of gallium and zirconium

Element	Wavelength (nm)	Interference equivalent concentration ^a		Element	Wavelength (nm)	Interference equivalent concentration ^a	
		Ga	Zr			Ga	Zr
Al	I 308.2	8.0	1220	Zn	I 213.8 ^b	0	69
Ti	II 334.9	1.2	81	As	I 193.6	1960	690
V	II 292.4	9.2	700	Y	II 371.0	0.5	92
Cr	II 205.5 ^b	17	25	Mo	I 202.0	110	150
Mn	II 257.6	0	140	Cd	I 228.8	2.0	23
Fe	II 259.9	4.8	260	Sb	I 217.5	73	1150
Co	II 228.6	0	170	La	II 398.8	3.2	660
Ni	II 231.6 ^b	8.2	140	Pb	II 220.3	20	700
Cu	I 324.7	0.3	140				

^aThe analyte concentration (ng l⁻¹) equivalent to the background emission intensity provided by 1 mg l⁻¹ matrix element at the wavelength shown. ^bSecond-order lines used.

[31] and acidified to pH 2 with concentrated nitric acid. All glassware was rinsed well with deionized/distilled water after soaking in (1 + 2) nitric acid for >5 days. Nuclepore filters were soaked in (1 + 1) hydrochloric acid for >10 days, and rinsed with deionized/distilled water just before use.

Coprecipitation procedure

A 1-ml portion of gallium solution (5 g l⁻¹) was slowly added to exactly 1 l of sea water, stirring with a magnetic stirrer. Then pH was adjusted to 9 by adding 9 M sodium hydroxide, and the precipitate was aged for 24 h. This was necessary for rapid filtration. The solution was filtered through a Nuclepore filter. The precipitate on the filter was washed with 20 ml of deionized/distilled water, in order to remove Na, Mg, K, and Ca retained on the precipitate. The precipitate was dissolved with 2.5 ml of 1 M hydrochloric acid, and the resulting solution was diluted to exactly 5 ml with water. Consequently, a 200-fold preconcentration was achieved.

RESULTS AND DISCUSSION

Recovery of trace metals by coprecipitation

The coprecipitation behavior of each element depends on the pH. Therefore, the pH dependences of recoveries for various elements including matrix salts by gallium coprecipitation were investigated by using 10 mg of gallium added to 1 l of artificial sea water. The results are shown in Figs. 2 and 3. The behavior of gallium in the pH range 2–10 is shown in Fig. 4. It should be stressed that gallium did not precipitate quantitatively below pH 5 nor in the pH range 6.0–8.6 in sea water, and also that gallium did not form a

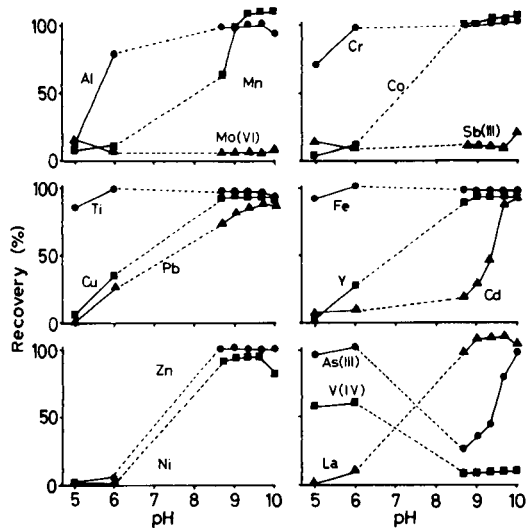


Fig. 2. pH dependences of recoveries for various trace elements in artificial sea water. Concentrations are as those shown in the last column in Table 4; the values indicated with dashed lines could not be obtained because no precipitate was formed.

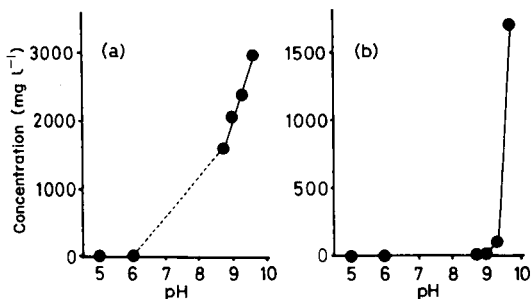


Fig. 3. The concentrations of magnesium (a) and calcium (b) in the preconcentrated solution at various pH values. Original concentrations of Mg and Ca were 1330 and 420 mg l⁻¹, respectively, which are the same as those in sea water; 10 mg Ga was added to 1 l of sea water.

precipitate at pH >8 without magnesium ions in the solution. Furthermore, when the pH was increased above 10, considerable precipitation of magnesium often occurred, so that filtration was difficult. Thus, the pH range examined was limited to 5.0–6.0 and 8.7–10.0.

As can be seen in Fig. 2, the recoveries of most elements increased at higher pH except for V(IV), Mo(VI) and Sb(III) which showed lower recoveries at the higher pH. In the lower pH region, Fe, As(III), Ti and Cr showed almost quantitative recoveries at pH 6. In the higher pH region, Al, Mn, Cr, Co, Ti, Cu, Fe, Y, Zn, Ni and La were recovered quantitatively at

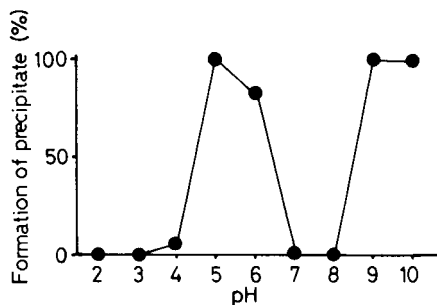


Fig. 4. Formation curve of gallium precipitate in sea water (10 mg l^{-1} gallium).

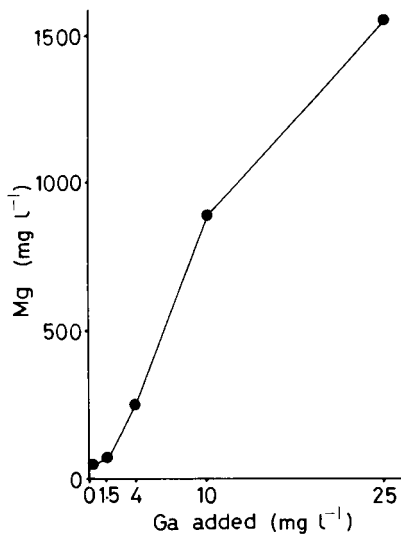


Fig. 5. Concentration of magnesium in the preconcentrated solution vs. concentration of gallium added to the sea-water sample. The original magnesium concentration was 1330 mg l^{-1} .

pH 9, while Cd, Pb and As(III) gave better recoveries at pH 10. Lead gave recoveries of $<90\%$ even at pH 10. Low recoveries of Mo(VI), Sb(III) and V(IV) at high pH may result from their oxoanion forms, which are not easily coprecipitated with or adsorbed onto gallium hydroxide. The recoveries for trace elements at pH 9 are summarized in Table 4 (see below). Figure 3 outlines the concentrations of magnesium and calcium in the preconcentrated sample solution after coprecipitation at various pH values. These concentrations increased with pH, and that of calcium increased markedly above pH 9. The concentrations of sodium and potassium did not show significant dependence on pH.

According to these results, three experimental problems have to be considered when gallium coprecipitation is applied to the preconcentration of metal ions in sea water near pH 10. First, spectral interferences from adjacent magnesium and calcium lines degrade accuracy and precision [32]. Secondly, contamination from the sodium hydroxide used for pH adjustment increases with the volume of sodium hydroxide consumed. Thirdly, there is difficulty in filtration when large amounts of magnesium are precipitated. At pH 9.0, the concentrations of Na, K, Mg, and Ca in the concentrated solution were 10, 1, 400 and 10 mg l^{-1} , respectively, when 5 mg of gallium was added to 1 l of water. At these concentrations, spectral interferences from Na, K, and Ca were negligible, but magnesium at 400 mg l^{-1} still gave spectral interference. This could be avoided by use of a standard solution which contained 400 mg l^{-1} magnesium.

Optimization of gallium concentration

The concentration of the carrier obviously influences the recoveries of the analytes. In the present investigation, all elements except for cadmium and lead showed recoveries independent of the amount of gallium added (1.5–25 mg l⁻¹) when the concentrations of spiked elements taken were those listed in the last column in Table 4 (see below). The recoveries of cadmium and lead were improved by 20% and 50%, respectively, when 25 mg of gallium was added instead of 1.5 mg. Magnesium, however, precipitated almost proportionally when the amount of gallium added was increased, as can be seen in Fig. 5, although the precipitation of other major elements (Na, Ca, and K) did not show any significant dependence on the amount of gallium. This may be due to the formation of insoluble polynuclear hydroxides between gallium and magnesium. Furthermore, when the concentration of gallium was 1.5 mg l⁻¹, the recovery of gallium was poor. Therefore, the optimum concentration of gallium in sea water was considered to be 5 mg l⁻¹. This is rather small compared to other coprecipitation methods; e.g., 10 mg l⁻¹ for zirconium coprecipitation [5] and 100 mg l⁻¹ for indium coprecipitation [28]. The small amount of coprecipitation reagent has, however, the merit that contamination and spectral interferences arising therefrom are decreased.

Spectral interference from gallium

Spectral interference by the coprecipitation reagent must be considered because the final concentration of the reagent is quite high in the concentrated sample. Some coprecipitation reagents can contribute severe spectral interferences, which result in large blank signals, and deterioration of accuracy and precision. The i.c.p. emission spectra obtained for zirconium and gallium solutions and pure water are compared in Fig. 6. Zirconium solution was chosen as a reference, because hydrated zirconium oxide is a popular carrier and has been previously applied to sea-water analysis by i.c.p./a.e.s. [5]. It can clearly be seen that gallium provides far fewer emission lines than zirconium. The spectrum of gallium is also much simpler than those of aluminum, iron and lanthanum, which are also popular coprecipitation reagents. This is a great advantage for the use of gallium as a coprecipitation reagent over others such as Zr, Al, Fe and La. In Table 2, interference equivalent concentrations of gallium and zirconium are summarized for comparison. As can be seen, the values for gallium are smaller than those for zirconium by two or three orders of magnitude except for As, Mo, Cr and Sb. Large interference equivalent concentrations of gallium may be due to recombination radiation for arsenic, and due to neighboring emission lines for Cr, Mo, and Sb. The analytical errors for chromium caused by gallium spectral interference could be decreased by using standard solutions which contained 1000 mg l⁻¹ gallium. For As, Mo and Sb, gallium spectral interference could not be corrected for, because of the poor recoveries of these elements. Because spectral interferences were generally small, the concentration of

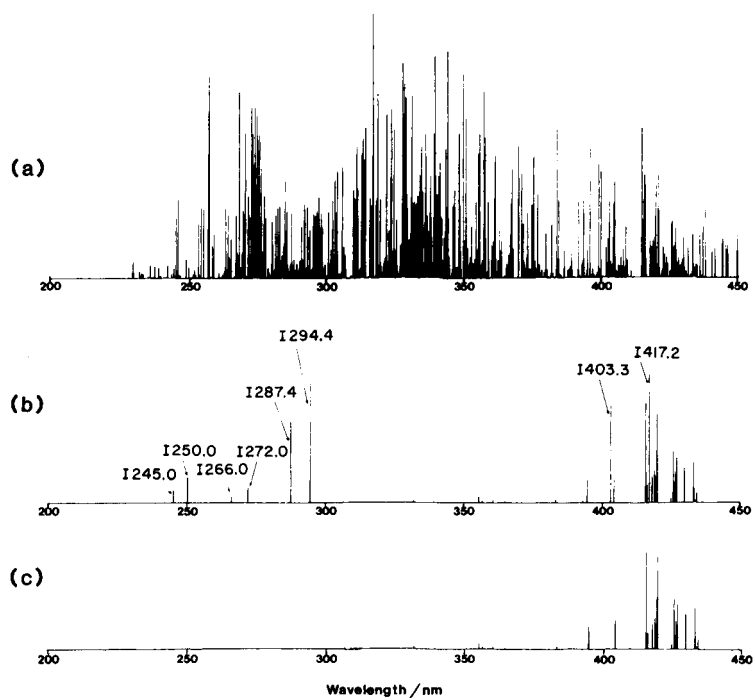


Fig. 6. I.c.p. emission spectra obtained with: (a) 500 mg l⁻¹ zirconium solution; (b) 500 mg l⁻¹ gallium solution; (c) pure water.

gallium in the final solution could be higher than those permissible for other coprecipitation reagents. Therefore, a larger preconcentration factor could be obtained for gallium coprecipitation (200-fold) than for zirconium coprecipitation (20-fold).

Impurities in reagents

Because gallium is widely used as a raw material for semiconductors, pure gallium metal is readily obtained. In the present experiments, 99.99% purity gallium was used. Table 3 shows the analytical errors which arose from the impurities in 1 ml of 5000 mg l⁻¹ gallium solution. The values shown are the concentrations of impurities measured, and were obtained by observing the peak profiles around the emission wavelengths of the analytes. As can be seen, the errors for most elements except chromium were negligible.

One of the common problems of hydroxide coprecipitation methods is contamination from the alkaline solution added to adjust the pH of the sample solutions. Well-known coprecipitation carriers such as hydrated iron, aluminum, lanthanum and zirconium oxides are completely soluble only at low pH (pH 2–3), and precipitate appreciably at pH 9–10. Therefore a large amount of an alkaline solution is consumed for pH adjustment, which often

TABLE 3

Contamination of trace metals from impurities in sodium hydroxide and gallium

Element	Contaminant conc. ^a (ng l ⁻¹)		Element	Contaminant conc. ^a (ng l ⁻¹)	
	NaOH ^b	Gallium ^c		NaOH ^b	Gallium ^c
Al	9	0	Zn	4	38
Ti	0.3	0	As	0.6	0
V	0.1	0	Y	0.0	0
Cr	8	250	Mo	0.2	0
Mn	3	0	Cd	0.03	0
Fe	110	31	Sb	0.9	0
Co	0.3	0	La	0.0	0
Ni	4	0	Pb	1	0
Cu	0.3	8			

^aConcentrations converted to those in original sea-water sample. ^bContamination from 0.1 ml of 9 M NaOH. ^cContamination from 1.0 ml of 0.5% gallium solution.

provides significant contamination. As shown in Fig. 4, gallium in sea water does not precipitate below pH 3 nor in the pH range 7–8. Natural sea water, which is usually at pH 7.0–8.2, was slightly acidified to pH 6.5–7.5 when 1 ml of 5 g l⁻¹ gallium solution was added. Because gallium was soluble in this pH range, a pH change only from 7 to 9 was required in the present gallium coprecipitation method. Consequently, only a very small amount (ca. 1.3×10^{-3} mol) of sodium hydroxide was used. In Table 3, possible contamination from the sodium hydroxide addition is shown for each element. The values were obtained by aspirating the solution concentrated from sodium hydroxide by zirconium coprecipitation [5]. Contamination from sodium hydroxide was negligible except for iron, and even here the error was <10% of the concentration of iron in sea water.

Analytical figures of merit

Some analytical figures of merit for various elements are summarized in Table 4. The detection limits for the standard solutions with and without gallium, and those with gallium and magnesium are shown. The detection limits for sea water were obtained by dividing the detection limits of the standard solution containing gallium and magnesium by the concentration factor for each element. All the detection limits in Table 4 were estimated as the analyte concentration corresponding to three times the standard deviation of the background emission intensity at each wavelength. As can be seen, the detection limits of arsenic and antimony were poor in the presence of gallium, and those of Al, Mn and Zn deteriorated when magnesium was present. Other elements showed no significant changes in the detection limits with and without gallium and magnesium. The sea water detection limits for As, Mo, Cd and Sb were not much improved, because of the low recoveries for these elements. From the comparison between the detection limits of the

TABLE 4

Analytical figures of merit for the gallium coprecipitation i.c.p./a.e.s. method

Element	Detection limit for standard solution ^a ($\mu\text{g l}^{-1}$)			Detection limit for sea water ^b (ng l^{-1})	Recovery at pH 9 ^c (%)	Concn. added ($\mu\text{g l}^{-1}$)
	Pure soln.	1 g l ⁻¹ Ga added	1 g l ⁻¹ Ga + 0.4 g l ⁻¹ Mg added			
Al	13	10	18	90	101	40
Ti	1	1	1	5	100	4
V	3	5	3	20	27	30
Cr	4	4	4	20	97	40
Mn	0.1	0.1	1	5	95	40
Fe	3	3	3	15	98	200
Co	6	7	6	30	91	4
Ni	12	15	13	60	96	40
Cu	2	2	2	10	96	40
Zn	3	3	6	30	101	40
As	22	60	60	1500	19	40
Y	1	1	1	6	88	4
Mo	6	8	8	4000	1	40
Cd	3	3	2	300	5	5
Sb	17	28	29	1500	5	40
La	4	3	3	20	82	50
Pb	30	30	30	150	94	40

^aObtained by direct nebulization without coprecipitation. ^bObtained for standard solution preconcentrated 200-fold by gallium coprecipitation at pH 9. ^cObtained by 200-fold concentration at pH 9.

present method and the concentrations in natural sea waters (see Fig. 1) eleven elements (Al, Ti, V, Cr, Mn, Fe, Co, Cu, Zn, Y and La) in coastal sea water and ten elements (Al, Ti, V, Cr, Mn, Fe, Ni, Cu, Zn and Y) in open sea water may be determined by the gallium coprecipitation i.c.p./a.e.s. method

The relative standard deviation (r.s.d.) for each of 13 elements is given in Table 5 for the concentration levels of trace metals in the artificial sea water. Comparison of the results in Tables 4 and 5 shows that the trace metal concentrations are >5 times the detection limits except for Co, Cd and La. The r.s.d. was $\leq 6\%$ for Al, Cr, Mn, Fe, Ni, Zn, Y and Pb. The poor precision for titanium and copper could be caused by their low detection limits.

Determination of trace metals in sea water

The results for some samples of coastal and open sea waters along with the sampling location and salinity data are summarized in Table 6. When the sample was not acidified, the concentrations of trace metals found were very low even in coastal sea water, and they were near or below the detection limits in open sea water. When acidified, the concentrations measured were

TABLE 5

Results for trace metals in artificial sea water

Element	Mean concn. ^a ($\mu\text{g l}^{-1}$)	Element	Mean concn. ^a ($\mu\text{g l}^{-1}$)	Element	Mean concn. ^a ($\mu\text{g l}^{-1}$)
Al	4.7 (4)	Co	0.077 (9)	Y	0.036 (6)
Ti	0.17 (20)	Ni	1.37 (6)	Cd	0.08 (14)
Cr	1.00 (1)	Cu	0.26 (11)	La	0.056 (8)
Mn	0.99 (4)	Zn	17.2 (5)	Pb	1.80 (3)
Fe	5.2 (4)				

^aMean of 5 determinations with relative standard deviation (%) in parentheses.

TABLE 6

Results for surface sea water

Element	Concentration ($\mu\text{g l}^{-1}$)				
	Coastal water			Open sea	
	Not acidified		Acidified ^a	Not acidified	
	Tokyo Bay ^b	Tokyo Bay ^b	Inland Sea ^c	Sagami Bay ^d	Sagami Bay ^d
Al	0.39	6.5	9.6	— ^e	0.95
Ti	0.025	0.20	0.05	0.010	0.051
Cr	—	0.07	0.09	—	0.07
Mn	0.046	36.1	1.06	0.090	1.05
Fe	0.23	14.4	1.27	—	0.66
Co	0.04	0.14	0.14	—	—
Ni	0.30	1.5	0.18	—	—
Cu	0.025	0.31	0.19	—	0.067
Zn	0.67	2.0	0.80	0.03	0.12
Y	0.006	0.005	0.021	—	—
La	—	0.05	0.04	—	—
Pb	—	1.7	—	—	—

^aThe samples were acidified at pH 2 with nitric acid prior to filtration. ^bCollected at 35° 31'N, 139° 51'E on May 14, 1982; salinity 30.2‰. ^cCollected at 33° 42' 64N, 132° 28' 42E on May 17, 1982; salinity 33.55‰. ^dCollected at 34° 59' 9N, 139° 20' 9E on March 4, 1983; salinity 34.62‰. ^eDashes mean that the element was not detected.

much higher than those for the unacidified samples. These results indicate that trace elements dissolved from particulate matter suspended in sea water during acidic sample storage. Results for V, As, Mo, Cd and Sb could not be obtained for all sea-water samples because of poor recoveries and/or detection limits for those elements. In the case of coastal sea water, the concentrations

of 9 and 12 elements were above the detection limits for the unacidified and acidified samples, respectively. For open sea water, concentrations of 4 and 7 elements were measured for the unacidified and acidified samples, respectively. The concentrations in acidified coastal sea water were similar to the values reported elsewhere [10, 12–16]. The concentration levels of Ti, Mn, Ni and Zn for the unacidified open sea-water sample agreed well with those reported recently by Hunt and Turekian [9]. The amount of sodium hydroxide consumed to adjust the pH of the unacidified sample was about twenty times less than that for the acidified sample. For the unacidified samples, therefore, the blank values were negligible for all elements except iron and chromium. Even for acidified sample, contamination from sodium hydroxide was not serious when trace metals at the concentration levels shown in Table 6 were determined.

Conclusions

Gallium is suitable as a coprecipitation reagent because of its very few spectral interferences and its availability in high purity. The proposed method is simple and uses small amounts of reagents, making the method almost contamination-free. The coprecipitation with gallium combined with i.c.p./a.e.s. has proved to be very effective for multi-element determinations in coastal and open sea waters. It should be noted that the method cannot be applied to fresh water because gallium does not coprecipitate without magnesium (more than 500 mg l⁻¹ is required for gallium to precipitate). The mechanism of gallium coprecipitation with magnesium requires further examination.

The authors thank Prof. S. Horibe and his staff at the Ocean Research Institute, University of Tokyo, Prof. H. Tsubota, University of Hiroshima, and Prof. T. Yoshida, Tokyo University of Fisheries, for their help with sea-water samples and for valuable discussions. This research was supported by a Grant-in-Aid in the Special Research Project for Environmental Science (Grant No. 59030023) from the Ministry of Education, Culture and Science.

REFERENCES

- 1 A. F. Ward, H. R. Sobel and R. L. Crawford, *ICP Inf. Newsl.*, 3 (1977) 90.
- 2 S. S. Berman, J. W. McLaren and S. N. Willie, *Anal. Chem.*, 52 (1980) 488.
- 3 C. W. McLeod, A. Otsuki, K. Okamoto, H. Haraguchi and K. Fuwa, *Analyst (London)*, 106 (1981) 419.
- 4 H. Watanabe, K. Goto, S. Taguchi, J. W. McLaren, S. S. Berman and D. S. Russell, *Anal. Chem.*, 53 (1981) 738.
- 5 T. Akagi, Y. Nojiri, M. Matsui and H. Haraguchi, *Appl. Spectrosc.*, 39 (1985) 662.
- 6 R. K. Winge, V. J. Peterson and V. A. Fassel, *Appl. Spectrosc.*, 33 (1979) 206.
- 7 P. W. J. M. Boumans, *Spectrochim. Acta, Part B*: 36 (1981) 169.
- 8 P. W. J. M. Boumans, *Line Coincidence Table for Inductively Coupled Plasma Atomic Emission Spectrometry*, Vol. 1, Pergamon, Oxford, 1980.
- 9 M. S. Q. Hunt and K. K. Turekian, *Trans. Am. Geophys. Union*, 64 (1983) 130.

- 10 T. Korenaga, S. Motomizu and K. Toei, *Analyst (London)*, 105 (1980) 328.
- 11 J. D. Smith and A. R. Longmore, *Nature (London)*, 287 (1980) 532.
- 12 T. Kiriya, M. Haraguchi and R. Kuroda, *Fresenius Z. Anal. Chem.*, 307 (1981) 352.
- 13 D. F. Marino and J. D. Ingle, Jr., *Anal. Chem.*, 53 (1981) 294.
- 14 R. R. Greenberg and H. H. Kingston, *J. Radioanal. Chem.*, 71 (1982) 147.
- 15 A. P. Mykytiuk, D. S. Russell and R. E. Sturgeon, *Anal. Chem.*, 52 (1980) 1281.
- 16 M. Murozumi, *Bunseki Kagaku*, 30 (1981) S19.
- 17 M. Yamamoto, K. Urata, K. Murashige and Y. Yamamoto, *Spectrochim. Acta, Part B*: 36 (1981) 671.
- 18 S. Tanaka, M. Kaneko, Y. Konno and H. Hashimoto, *Bunseki Kagaku*, 32 (1983) 535.
- 19 G. A. Cutter, *Science*, 217 (1982) 829.
- 20 T. Akagi, H. Haraguchi and K. Fuwa, unpublished data.
- 21 A. I. Kulathilake and A. Chatt, *Anal. Chem.*, 52 (1980) 828.
- 22 V. F. Hodge, S. L. Seidel and E. D. Goldberg, *Anal. Chem.*, 51 (1979) 1256.
- 23 M. O. Andreae, J.-F. Asmode, P. Foster and L. Van't Dack, *Anal. Chem.*, 53 (1981) 1766.
- 24 J. C. Yu, J. M. Lo and C. M. Wai, *Anal. Chim. Acta*, 154 (1983) 307.
- 25 C. W. Baker, *Nature (London)*, 270 (1977) 230.
- 26 T. Fujinaga, T. Kuwamoto, E. Nakayama and S. Tanaka, *J. Oceanogr. Soc. Jpn.*, 36 (1980) 196.
- 27 D. S. Lee, *Anal. Chem.*, 54 (1982) 1982.
- 28 M. Hirade, T. Ito, M. Baba, H. Kawaguchi and A. Mizuike, *Anal. Chem.*, 52 (1980) 804.
- 29 K. Himeno, K. Yanagisawa, T. Yuki and Y. Nakamura, *Bunseki Kagaku*, 33 (1984) T43.
- 30 A. S. Buchanan and P. Hannaker, *Anal. Chem.*, 56 (1984) 1379.
- 31 D. R. Kester, I. W. Duedall, D. N. Connors and R. M. Pytkowicz, *Limnol. Oceanogr.*, 12 (1967) 176.
- 32 R. K. Winge, V. A. Fassel, R. N. Kniseley, E. DeKalb and W. J. Haars, Jr., *Spectrochim. Acta, Part B*: 32 (1977) 327.

AN ENZYME ELECTRODE FOR L-LACTATE WITH A CHEMICALLY-AMPLIFIED RESPONSE

FUMIO MIZUTANI*, TADAE YAMANAKA, YOSHIKAZU TANABE and KEISHIRO TSUDA

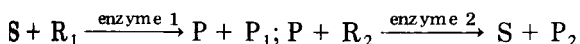
Research Institute for Polymers and Textiles, 1-1-4 Yatabe-Higashi, Tsukuba, Ibaraki 305 (Japan)

(Received 26th March 1985)

SUMMARY

An enzyme electrode with a chemically-amplified response for L-lactate is constructed from an oxygen electrode and a layer containing immobilized lactate oxidase, to oxidize L-lactate, and lactate dehydrogenase, to regenerate the L-lactate. Regeneration enables oxygen to be consumed beyond the stoichiometric limitation, which results in an electrode response amplified 2–250 times according to the variation in the layer properties such as the V_{\max} and K_m values of the immobilized enzymes and the thickness of the layer. The detection limit is as low as 5×10^{-9} M. An equation is derived to relate the rate of oxygen consumption in the layer to the experimental parameters; the equation successfully explains the experimental results.

Chemical amplification in enzymatic substrate determinations is an excellent way of increasing sensitivity [1, 2]. The basic principle is the use of enzymes which cycle the substrate and cause a relatively large concentration change of a measurable species:



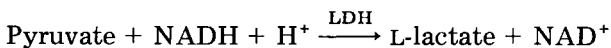
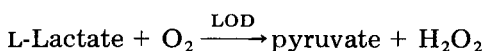
If only enzyme 1 is used for the determination of the substrate S, the concentration change of the reactant R_1 or the product P_1 is stoichiometrically limited by the concentration of S. In contrast, the additional use of the enzyme 2 permits a consumption/regeneration cycle for S, and this results in an increased concentration change of R_1 or P_1 beyond the stoichiometric limitation. The increased concentration change provides an inherent gain in sensitivity for measuring S. For example, Lowry et al. [3, 4] have developed highly-sensitive measurements of coenzymes at concentrations as low as 10^{-9} – 10^{-13} M by applying enzymatic cycling procedures.

These cycling methods [2–4], nevertheless, are not widely used for analytical purposes because they require considerable effort in manipulation and a long incubation time. Enzyme electrodes, however, have proved to be convenient tools for the determination of various substrates [5, 6]. Therefore, the combination of the cycling procedure with an enzyme electrode can be

advantageous for providing simple and rapid substrate assays with high sensitivity.

Davis and Mosbach [7] and also Blaedel and coworkers [8, 9] have reported enzyme electrodes in which enzymatic cycling reactions were used. However, they have applied the cycling reactions to a purpose different from amplifying the electrode response for the substrate [7-9]: the cycling system consisted of a re-oxidation of immobilized coenzyme after a coenzyme-reducing indicator reaction.

Recently, an enzyme electrode for L-lactate (or pyruvate) was developed in these laboratories which involved an immobilized enzyme layer containing lactate oxidase from *Pediococcus sp.* (LOD) and lactate dehydrogenase (EC 1.1.1.27; LDH), [10] as an amplification system. The reactions were:



The consumption of oxygen by the LOD reaction was monitored by using a Clark oxygen electrode. By combination of the L-lactate-regenerating LDH reaction with the indicating LOD reaction, a 60-fold increase in the electrode response for L-lactate was obtained [10] which resulted in a detection limit of 8×10^{-8} M L-lactate. This was much better than that of previously reported L-lactate electrodes each of which used only an immobilized indicator enzyme, such as LOD [11-14], decarboxylating LOD (EC 1.13.12.4) [15, 16], LDH [8, 9, 17, 18], or a cytochrome type of LDH (EC 1.1.2.3) [19].

For further development of such a cycling enzyme electrode as an analytical tool, the following studies are required: examination of the relationship between chemical gain and the properties of an immobilized enzyme layer, and estimation of the possible magnitude of the gain by the use of such an electrode system. In the present paper experimental and theoretical approaches to these problems are reported. The electrode response for the LOD/LDH system for L-lactate was examined in connection with several properties of the immobilized enzyme layer, such as V_{\max} and K_m for each enzyme, the diffusion coefficient in the layer and the thickness of the layer. An equation relating oxygen consumption in the layer to the above parameters was derived in order to interpret the results.

EXPERIMENTAL

Materials

The enzymes used were LOD (from *Pediococcus sp.*, 17 U mg^{-1} ; Toyo Jozo), LDH (EC 1.1.1.27, from rabbit muscle, 700 U mg^{-1} ; Sigma Chemical Co. L1245), and peroxidase (EC 1.11.1.7, from horseradish, 250 U mg^{-1} ; Boehringer Mannheim 108090); an LOD with a very low NADH-oxidase activity was selected. Lithium L-lactate, sodium pyruvate and bovine serum

albumin (BSA) were obtained from Sigma Chemical Co., and NADH from Boehringer Mannheim. A photo-crosslinkable poly(vinyl alcohol) bearing stilbazolium groups (PVA-Sa) [20, 21] was a gift from Dr. K. Ichimura of this Institute. Deionized, twice-distilled water was used for all experiments.

Enzyme immobilization

Two immobilizing methods were used for the preparation of the layers containing LOD and LDH. Type I layers, the photo-crosslinked PVA-Sa layers in which both enzymes were physically entrapped, were prepared as follows. A certain amount of a mixture of LOD/LDH/PVA-Sa (8 wt.% aqueous solution, pH 7.0), 1:1:30 by weight was spread on a teflon plate and dried for 12 h at 4°C. The dried film was removed from the plate and irradiated for cross-linking with a xenon arc lamp (30 mW cm⁻²) for 5 min on each side. The thickness of the enzyme layer was adjusted in the range 4.0×10^{-3} – 4.0×10^{-2} cm by changing the amount of mixture dropped onto the plate.

Type II layers, involving chemically-attached LOD and LDH, were prepared as described previously [22], with slight modification. A solution containing cellulose triacetate/glutaraldehyde/1,8-diamino-4-aminomethyloctane, 5:1:4 by weight, was spread on a glass plate and dried for 3 days. The dried film was removed from the plate and activated with glutaraldehyde (1% in 0.1 M phosphate buffer, pH 7.7). The enzymes were attached by immersing the activated layers into a phosphate buffer solution (0.1 M, pH 7.4) containing LOD (1 mg ml⁻¹) and LDH (1 mg ml⁻¹) for 12 h at 4°C. The thickness of the type II layers prepared was 3.3×10^{-3} cm, and the layers were stacked to be 6.6×10^{-3} – 6.0×10^{-2} cm thick, for use on the enzyme electrode.

In order to evaluate the diffusion coefficient of L-lactate in the layer, LOD-free layers were required as described below. Type I and II layers with immobilized BSA and LDH, therefore, were prepared by substituting BSA of the same weight for LOD in the above procedures.

All layers were stored in a phosphate buffer solution (0.1 M, pH 7.0) at 4°C. The values of thickness given were measured by the use of a microscope immediately after removing the sample from the solution; the values were measured in the wet state.

Assembly of enzyme electrode system

The LOD/LDH layer was placed on the teflon membrane of a Clark oxygen electrode (Ishikawa Manufacturing; battery type with a platinum cathode 6×10^{-2} cm² in area) and covered with a polyester mesh (2 cm in diameter). The mesh was held in place with rubber rings so that the enzyme layer was directly in contact with the teflon membrane. The enzyme electrode thus prepared was immersed in 10 ml of phosphate buffer (0.1 M, pH 7.4) containing 0 or 1 mM NADH, in a cylindrical cell. The pH of the buffer solution used was very close to the optimal pH for LOD [14] and LDH [23] for the production of L-lactate. The NADH concentration of 1 mM was suitable in order to achieve high chemical gain [10]. The solution was saturated with air

and stirred with a magnetic bar. The temperature of the solution was kept at $30.0 \pm 0.1^\circ\text{C}$. The current from the electrode was measured with an ammeter (Hokuto Denko, Model HM-101) and displayed on a chart recorder (Yokogawa Electric Works, Model 3066).

Determination of kinetic parameters and diffusion coefficient of enzyme layers

For both types of layers, parameters such as V_{\max} and K_m of immobilized LOD for lactate and of immobilized LDH for pyruvate, and the diffusion coefficient for L-lactate, were evaluated by the following procedures. All the measurements were made in the same buffer and at the same temperature as those used for measuring the enzyme electrode response.

The LOD activities in the LOD/LDH layers at various lactate concentrations were measured by using the 4-aminoantipyrine/phenol/peroxidase color-producing system [24]. The V_{\max} and K_m values of LOD for L-lactate and LDH for pyruvate were determined by Lineweaver/Burk plots [25]. The LDH activities in the layers at various pyruvate concentrations were measured by monitoring the rate of consumption of NADH [23]. A spectrophotometer (Hitachi, type 323) equipped with a temperature-controlled cell holder was used for the measurements.

The diffusion coefficient, D , for L-lactate in the layer was measured by using the apparatus shown in Fig. 1. The H-shaped cell was divided into two compartments by the BSA/LDH layer; each compartment contained 10 ml of buffer. An L-lactate-sensing enzyme electrode (4) was placed in compartment 1. First, a low concentration of L-lactate was added to compartment 1 in order to calibrate the electrode. Secondly, L-lactate of a certain concentration was added to compartment 2. The increase in L-lactate concentration in compartment 1 by diffusion of the substrate from compartment 2 was monitored by the electrode. In this case, the LOD/LDH layers could not be used because a portion of L-lactate coming from compartment 2 was consumed at the layer, resulting in a serious error in the measurement.

RESULTS

Enzyme layer parameters

Figure 2 shows a typical example of a current/time curve for the enzyme electrode. The current decrease, Δi_1 , which occurred after the addition of L-lactate into compartment 1 was measured in order to calibrate the electrode. The rate of current decrease in the linear region, $\Delta i_2/\Delta t$, was recorded after addition of L-lactate. The rate is proportional to the increase of L-lactate concentration in compartment 1 by diffusion from compartment 2 across the layer. The correlation between the calibration parameter, $\Delta i_1/C_1$ and the rate, $\Delta i_2/\Delta t$, gives the flux of L-lactate across the layer. The flux F is expressed as follows by taking into account the area of the layer, a , and the volume of the solution in compartment 1, v [26]:

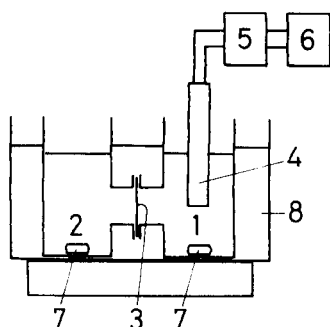


Fig. 1. Schematic diagram of the apparatus for measuring the diffusion coefficient of L-lactate in the layer: (1) compartment 1; (2) compartment 2; (3) sample layer; (4) enzyme electrode for L-lactate; (5) ammeter; (6) recorder; (7) magnetic stirring bar; (8) thermostat.

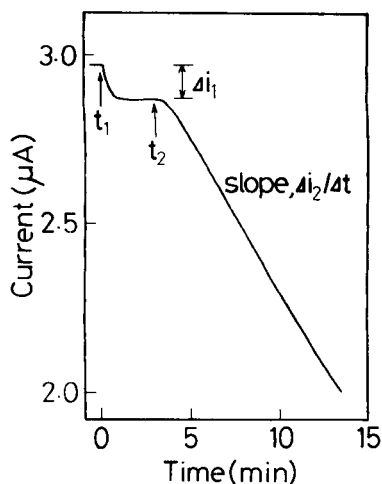


Fig. 2. Time/current plot for the determination of the diffusion coefficient. A type I layer with a thickness of 8.0×10^{-3} cm and an area of 1.0 cm² was used as the sample; t_1 and t_2 are the times when L-lactate ($C_1 = 20$ μ M) was added to compartment 1 and when L-lactate ($C_2 = 0.1$ M) was added to compartment 2, respectively.

$$F = (\Delta i_1 / C_1)^{-1} (\Delta i_2 / \Delta t) a^{-1} v$$

The value of D can be determined from the results obtained from Fig. 2 by applying Fick's first law:

$$D = FLC_2^{-1} = \Delta i_1^{-1} \Delta i_2 C_1 C_2^{-1} \Delta t^{-1} a^{-1} v L$$

where L is the thickness of the layer.

The parameters measured for type I and II layers are summarized in Table 1; each value is the average of five measurements with different samples. The type I layer gave larger V_{\max} values and rate constants for both enzymes and a smaller D value than the type II layer. The K_m values for each enzyme hardly differed for the two-kinds of layer. The K_m value of LDH in each layer was very close to that in solution, 1.6×10^{-7} mol cm⁻³ [27].

Response/time curves of the enzyme electrodes

Because NADH is indispensable in the regeneration of L-lactate by LDH, the present electrode based on enzymatic cycling shows its expected characteristics when NADH is added to the test solution. The electrode behaved as a simple LOD-based electrode in the absence of NADH. Therefore, the electrode responses in the presence and absence of NADH were compared, in order to investigate the characteristics of the cycling enzyme electrode.

TABLE 1

Parameters obtained for type I and II layers

Type of layer	Enzyme	V_{\max} (mol cm ⁻³ s ⁻¹)	K_m (mol cm ⁻³)	$K (= V_{\max}/K_m)$ (s ⁻¹)	D (cm ² s ⁻¹)
I	LOD	1.2×10^{-6}	4.4×10^{-7}	2.7	2.5×10^{-7}
	LDH	2.0×10^{-6}	1.7×10^{-7}	12	
II	LOD	2.6×10^{-7}	2.6×10^{-7}	1.0	9.0×10^{-7}
	LDH	1.8×10^{-7}	1.7×10^{-7}	1.1	

Figure 3 shows the response/time curves of the electrode for 10 μ M L-lactate in the presence and absence of NADH. The cycling electrode had an enhanced steady-state current decrease compared to the conventional electrode, but took longer to reach the steady state. The responses were almost superimposable for the first 30 s after addition of L-lactate. If the type I layer was thicker than 2×10^{-2} cm for the electrode in the presence of NADH, however, the time course of the electrode response changed to that shown in Fig. 4. On addition of L-lactate, the current decreased for 3 min and then increased to reach a steady state after ca. 15 min. Such a response may be a result of the decrease in the rate of the LDH reaction with time, as briefly discussed below.

Enhancement of current decrease at steady state

The ability of this cycling enzyme electrode to achieve a chemically-amplified response was examined in connection with the properties of the enzyme layer. The ability can be evaluated by the ratio of the steady-state current decrease in the presence of NADH to that in the absence of NADH for a certain concentration of L-lactate. In practice, the ratio (i.e., chemical gain) was evaluated as follows. The calibration curves of the enzyme electrode were obtained in the presence and absence of NADH by plotting the steady-state current decrease against L-lactate concentration. The slope of each calibration graph in its linear region was measured, and the ratio of the slope in the presence of NADH to that in the absence of NADH was calculated. This was used as the chemical gain. This procedure was introduced because direct comparison of the current decreases for a certain concentration of L-lactate in the presence and absence of NADH was sometimes difficult. A very low concentration of L-lactate did not give a discernible response in the absence of NADH. In contrast, a higher concentration of L-lactate, which was sufficient to give a discernible response in the absence of NADH, was often beyond the linear region of the calibration curve in the presence of NADH.

Figure 5 shows the relationship between the chemical gain and the thickness of the enzyme layer used for the electrode, for type I and II layers. As shown, the chemical gain increased with increasing thickness of the layers, over all the range examined with type II layers and up to 2.0×10^{-2} cm with

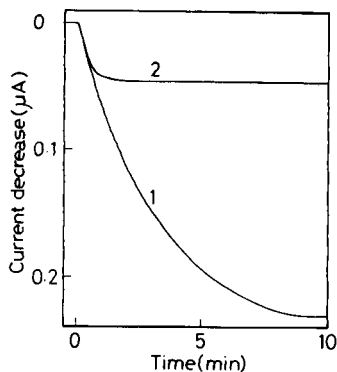


Fig. 3. Response/time curves of the enzyme electrode. L-Lactate ($10 \mu\text{M}$) was added to the buffer solution: (1) with NADH; (2) without NADH. Three sheets of type II layers (total thickness $1.0 \times 10^{-2} \text{ cm}$) were used.

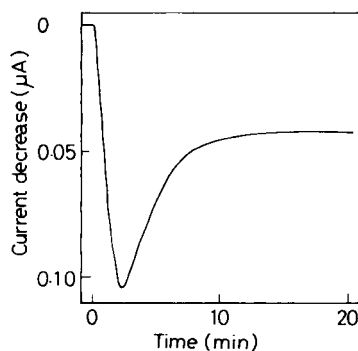


Fig. 4. Response/time curve of the enzyme electrode obtained when a type I layer ($4.0 \times 10^{-2} \text{ cm}$ thick) was used. L-Lactate ($0.2 \mu\text{M}$) was added to the buffer containing 1 mM NADH, 10 min after immersing the electrode in the solution.

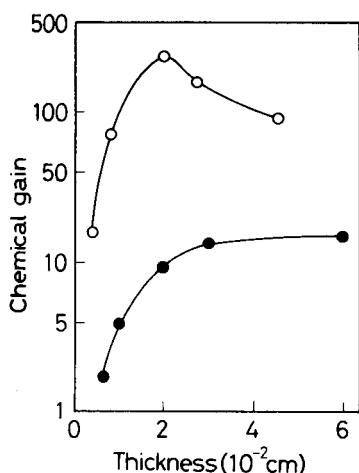


Fig. 5. Relationship between the chemical gain and the thickness of the enzyme layer: (○) type I layer; (●) type II layer.

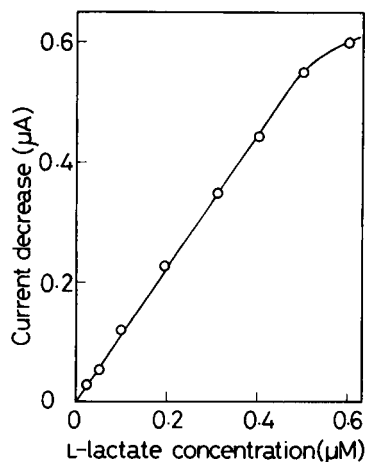


Fig. 6. Calibration graph for the buffer containing L-lactate (type I layer, $2.0 \times 10^{-2} \text{ cm}$ thick, 1 mM in NADH).

type I layers. Further increase in the thickness of type I layers decreased the chemical gain; the gain began to decrease in association with the appearance of the spike-shaped response (Fig. 4). The use of a type I layer resulted in a much larger chemical gain than the type II layer at a fixed thickness, approximately by an order of magnitude.

The highest value of the chemical gain obtained was ca. 250. This value was obtained by using a type I layer with a thickness of 2.0×10^{-2} cm (Fig. 5). The calibration graph for the electrode with this layer is given in Fig. 6. It is linear up to $0.5 \mu\text{M}$ L-lactate with a detection limit (signal/noise = 2) of 5 nM. The relative standard deviation was 3% for 10 successive measurements, carried out daily over two weeks, of the steady-state current decrease for $0.1 \mu\text{M}$ L-lactate. The average value of the measurements on each day did not decrease by more than 10% of the initial value during that period.

DISCUSSION

The present cycling enzyme electrode incorporating LOD and LDH exhibited the following characteristics, as compared with the conventional enzyme electrode based only on LOD. The electrode required a longer time to reach a steady-state response (Fig. 3), the steady-state response was increased significantly (Figs. 3 and 5), and the extent of the enhancement (chemical gain) depended on the type and the thickness of the layer used (Fig. 5). In order to understand such characteristics, an equation was derived for the rate of oxygen consumption in the enzyme layer, J , as a function of the properties of the layer. The equation can, of course, be applied to any oxidase/dehydrogenase couples. It is also useful for exploring the possibilities for further improvement of the cycling enzyme-electrode system. The magnitude of J is considered to be proportional to the change in the current from the oxygen electrode, except for possible delay which is mainly ascribed to the diffusion of oxygen through the teflon membrane of the oxygen electrode.

In the system shown in Fig. 7, it is assumed that the diffusional mass transport terms and the Michaelis-Menten kinetic terms concerning the substrates A (L-lactate) and B (pyruvate) within the layer ($0 \leq x \leq L$) determine the substrate concentrations in the layer at any time [28–30] and that the concentration of each substrate in the layer is significantly lower than the Michaelis constant of the corresponding enzyme. According to these assumptions,

$$\partial C_A / \partial t = (D \partial^2 C_A / \partial x^2) - k_1 C_A + k_2 C_B \quad (1)$$

$$\partial C_B / \partial t = (D \partial^2 C_B / \partial x^2) + k_1 C_A - k_2 C_B \quad (2)$$

where D , the substrate diffusion coefficient, is assumed to be the same for A and B, and k_1 and k_2 are the first-order rate constants of E_1 (LOD) for A and E_2 (LDH) for B, respectively. When substrate A is added to the solution to give a concentration C^0 at time $t = 0$, the following initial and boundary conditions are introduced:

$$C_A(x, 0) = C_B(x, 0) = 0 \quad (3)$$

$$C_A(L, t) = C^0, C_B(L, t) = 0 \quad (4)$$

$$\partial C_A(0, t) / \partial x = \partial C_B(0, t) / \partial x = 0 \quad (5)$$

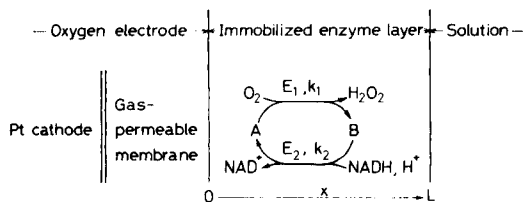


Fig. 7. Schematic diagram of the cycling enzyme-electrode system: (A) L-lactate; (B) pyruvate; (E_1) LOD; (E_2) LDH; (k_1) first-order rate constant of LOD for L-lactate; (k_2) first-order rate constant of LDH for pyruvate.

Equation 5 represents the facts that substrates A and B do not diffuse toward the gas-permeable membrane side ($x < 0$) and also that neither A nor B reacts at $x = 0$.

The function to be solved, J , is expressed as:

$$J = k_1 \int_0^L C_A dx$$

Two kinds of infinite series are given as the solution for J by applying Laplace transformations to Eqns. 1–5 [31]. The following infinite series is more useful for the present study because it converges far more rapidly for all t -values unless they are very close to zero:

$$J C_0^{-1} k_1^{-1} L^{-1} = (k_1 k^{-3/2} D^{1/2} L^{-1}) \tanh(k^{1/2} D^{-1/2} L) + k_2 k^{-1} - 2k^{-1} \sum_{n=1}^{\infty} \{k_1 \alpha_n^{-1} \exp(-\alpha_n D L^{-2} t) + k_2 \beta_n^{-1} \exp(-\beta_n D L^{-2} t)\} \quad (6)$$

where $k = k_1 + k_2$, $\alpha_n = \pi^2(n - 1/2)^2 + k D^{-1} L^2$, and $\beta_n = \pi^2(n - 1/2)^2$.

Two cases at the enzyme layer, the cycling enzyme electrode and the conventional enzyme electrode, are considered. In the former case, the rate constants for E_1 and E_2 are given as k_1 and $r k_1$ ($= k_2$; $r \neq 0$), and in the latter case, they are given as k_1 and 0 ($r = 0$), respectively.

The time dependence of the J values at $r \neq 0$ and $r = 0$ is numerically calculated by using Eqn. 6, in order to compare the response/time characteristics of the two cases. Figure 8 shows the relationships between two non-dimensional parameters ($-J C_0^{-1} k_1^{-1} L^{-1}$ and $D L^{-2} t$) at $k_1^{1/2} D^{-1/2} L = 10$, at r values of 1 and 0. As shown in Fig. 8, the J value at $r = 1$ require a much longer time to reach the steady state than that at $r = 0$, whereas J values were almost similar at values of $D L^{-2} t < 10^{-2}$. This agrees with the experimental results shown in Fig. 3. However, the transient response shown in Fig. 4, i.e., the gradual decrease in the electrode response, could not be explained by using Eqn. 6. This equation (and also Fig. 8) shows that the J value increases monotonously with time. The decrease in the electrode response may appear as a result of a decrease in the rate of the LDH reaction with

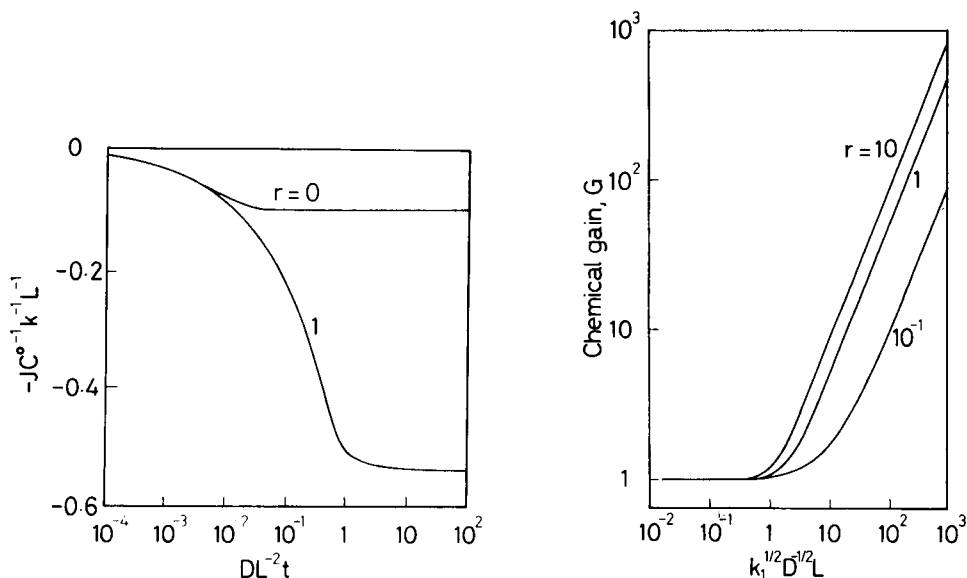


Fig. 8. Time dependence of the rate of oxygen consumption in the enzyme layer; $-JC^{0-1} k_1^{-1} L^{-1}$ values as a function of $DL^{-2} t$, obtained by using Eqn. 6 at $k_1^{1/2} D^{-1/2} L = 10$ and $r = 1$ or 0.

Fig. 9. Chemical gain, G , as a function of $k_1^{1/2} D^{-1/2} L$ for various r values. Results were obtained by using Eqn. 8.

time, as follows. If a thick layer having a small D value (see Table 1) is used, there would be some difficulty in the transport of coenzymes in the layer because they are larger molecules than L-lactate. Therefore, the concentrations of the coenzymes in the layer would change during the LDH reaction so as to decrease the reaction rate and, consequently, the electrode response. Further problems concerning the transient response are currently under investigation.

The effect of various parameters on the J value at the steady state, J_s , are discussed below in detail. At $t \rightarrow \infty$, Eqn. 6 simplifies to give J_s :

$$J_s C^{0-1} k_1^{-1} L^{-1} = (1+r)^{-3/2} k_1^{-1/2} D^{1/2} L^{-1} \tanh [(1+r)^{1/2} k_1^{1/2} D^{-1/2} L] + r(1+r)^{-1} \quad (7)$$

The ratio of the J_s value at $r \neq 0$ to that at $r = 0$ gives the chemical gain, G , which is expressed as follows by using Eqn. 7:

$$G = \{r(1+r)^{-1} k_1^{1/2} D^{-1/2} L + (1+r)^{-3/2} \tanh [(1+r)^{1/2} k_1^{1/2} D^{-1/2} L]\} \\ \times [\tanh (k_1^{1/2} D^{-1/2} L)]^{-1} \quad (8)$$

Variation of the G value with a non-dimensional parameter $k_1^{1/2} D^{-1/2} L$ was calculated numerically from Eqn. 8 for the different r values of 0.1, 1, and

10. The results are given in Fig. 9. As shown, the larger $k_1^{1/2}D^{-1/2}L$ value as well as the larger r value gave the larger G value. This means that an enzyme layer which has the following properties is suitable for giving a high chemical gain: a high k_1 value (or high E_1 activity); a high r value (or higher activity of E_2 than E_1); a low D value; and a large L value. Unless the low D value and large L value decreased the rate of the E_2 reaction, the enzyme layer having such properties actually gave a high chemical gain. The use of a type I layer, for which k values of both enzymes were higher and D values were lower than for a type II layer (Table 1), resulted in a higher chemical gain than that found for a type II layer (Fig. 5). Further, the chemical gain increased with increasing thickness of the layers of each type if the LDH reaction proceeded well (Fig. 5).

The above descriptions are quantitatively displayed in Fig. 10, where the G values for types I and II layers, calculated from Eqn. 8 by using the parameters given in Table 1, are shown as a function of layer thickness, and are compared with the chemical gains obtained experimentally (Fig. 5). The G values calculated agree well with the experimental results except for very thick type I layers.

The characteristics of the present cycling-enzyme electrode could therefore be explained quite well by applying Eqn. 6. In order to increase the sensitivity by increasing the chemical gain, therefore, it is necessary to achieve very high k values (or activities) for both immobilized enzymes (e.g., see Fig. 9). Enzyme activities in several kinds of immobilized layers [32–37] are summarized in Table 2. They show that the type I layer gives much higher enzyme activities than the other layers. This indicates that the application of an immobilization method other than the use of PVA-Sa (type I layer) would give a lower chemical gain. However, numerous methods for enzyme

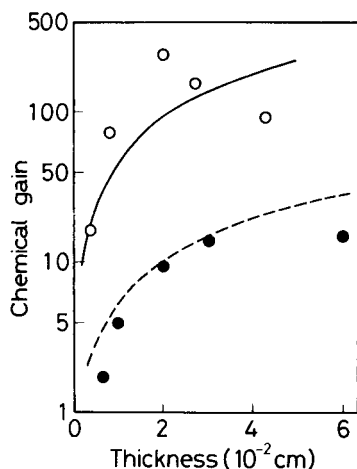


Fig. 10. Variation of the chemical gain with enzyme layer thickness: (\circ) type I layer; (\bullet) type II layer. The lines are the calculated chemical gains.

TABLE 2

Enzyme activities in the immobilized layers

Supporting layer	Enzyme	Enzyme activity (U cm ⁻³ of support)	Ref.
Poly(acrylamide)	Glucose oxidase (EC 1.1.3.4)	0.2	32
Collagen	Glucose oxidase	1–2	33
Aminated poly(acrylonitrile)	Choline oxidase (EC 1.1.3.17)	30	34
Chitosan	Uricase (EC 1.7.3.3)	0.03 ^a	35
Collagen	Glucose oxidase	8 ^a	36
	Cholesterol oxidase (EC 1.1.3.6)	0.3 ^a	
	Galactose oxidase (EC 1.1.3.9)	3 ^a	
PVA-Sa (type I support)	Glucose oxidase	70	37
	Choline oxidase	40	
	L- α -Glycerine-3- phosphate oxidase	80	
PVA-Sa (type I support)	LOD	70	This work
	LDH	120	
Type II support	LOD	16	This work
	LDH	11	

^aCalculated from the value of the activity per unit area of the layer assuming that the layer thickness is 0.1 mm.

immobilization are available [38], and immobilizing techniques may be found which provide higher activities than the type I layer. Nevertheless, it seems difficult to achieve a gain much larger than 10², as attained by the use of type I layer, at the present time.

The combination of some additional features with the present cycling system is required, therefore, in order greatly to increase the sensitivity. The introduction of an additional cycling stage, to give "double cycling" [3, 4], is one approach. Another, is to improve the electrode design; various modifications have been reported aiming at substrate assays with better sensitivity [6, 22, 33, 38–41]. The use of double cycling in combination with modification of the electrode system for decreasing background noise [6, 33] would provide an extremely sensitive device. Such an investigation is now in progress.

For the practical use of the present LOD/LDH electrode, e.g., for the assay of L-lactate in food or biological fluids, reactivity to pyruvate as well as L-lactate [10] may sometimes produce serious errors. However, as described previously [10], separate determinations of L-lactate and pyruvate are easily done by employing a pre-treatment system for the sample such as an enzyme column consisting of another to be of LOD (EC 1.1.3.12.4) or pyruvate oxidase (EC 1.2.3.3). Another problem is the relatively long time required

for the assay. Although this seems inevitable with the present system (Fig. 8), this is balanced by the high sensitivity and simplicity of the system.

The authors are grateful to Dr. Kunihiro Ichimura and Dr. Kunio Matsumoto for providing PVA-Sa and LOD, respectively.

REFERENCES

- 1 W. J. Blaedel and R. C. Bougslaski, *Anal. Chem.*, 50 (1978) 1026.
- 2 H. U. Bergmeyer, in H. U. Bergmeyer (Ed.), *Methods of Enzymatic Analysis*, Verlag Chemie/Academic Press, New York, 1974, Vol. 1, p. 131.
- 3 O. H. Lowry, J. P. Passonneau, D. W. Shulz and M. K. Rock, *J. Biol. Chem.*, 236 (1961) 2746.
- 4 O. H. Lowry, *Acc. Chem. Res.*, 6 (1973) 289.
- 5 G. G. Guilbault, *Handbook of Enzymatic Methods of Analysis*, Dekker, New York, 1976, p. 460.
- 6 P. W. Carr and L. D. Bowers, *Immobilized Enzymes in Analytical and Clinical Chemistry*, Wiley, New York, 1980, p. 197.
- 7 P. Davis and K. Mosbach, *Biochim. Biophys. Acta*, 370 (1974) 329.
- 8 W. J. Blaedel and R. A. Jenkins, *Anal. Chem.*, 48 (1976) 1240.
- 9 W. J. Blaedel and R. C. Engstrom, *Anal. Chem.*, 52 (1980) 1691.
- 10 F. Mizutani, Y. Shimura and K. Tsuda, *Chem. Lett.*, (1984) 199.
- 11 I. Karube, T. Matsunaga, T. Teraoka and S. Suzuki, *Anal. Chim. Acta*, 119 (1980) 271.
- 12 T. Matsunaga, I. Karube, T. Teraoka and S. Suzuki, *Anal. Chim. Acta*, 127 (1981) 245.
- 13 T. Matsunaga, I. Karube, T. Teraoka and S. Suzuki, *Eur. J. Appl. Microbiol. Biotechnol.*, 16 (1982) 157.
- 14 F. Mizutani, K. Sasaki and Y. Shimura, *Anal. Chem.*, 55 (1983) 35.
- 15 M. Mascini, G. Palleschi and D. Moscone, in T. Seiyama, K. Fueki, J. Shiokawa and S. Suzuki (Eds.), *Chemical Sensors*, Kodansha-Elsevier, Tokyo and Amsterdam, 1983, p. 683.
- 16 M. Mascini, D. Moscone and G. Palleschi, *Anal. Chim. Acta*, 157 (1984) 45.
- 17 A. K. Chen and C. C. Liu, *Biotechnol. Bioeng.*, 19 (1977) 1785.
- 18 T. Yao, Y. Kobayashi and S. Musha, *Anal. Chim. Acta*, 138 (1982) 81.
- 19 T. Shinbo, M. Sugiura and N. Kamo, *Anal. Chem.*, 51 (1979) 100.
- 20 K. Ichimura, *U. S. Pat.*, 4 269 941 (1982).
- 21 K. Ichimura, *J. Polym. Sci., Polym. Chem. Ed.*, 22 (1984) 2817.
- 22 M. Koyama, Y. Sato, M. Aizawa and S. Suzuki, *Anal. Chim. Acta*, 116 (1980) 307.
- 23 H. U. Bergmeyer and E. Bernt, in H. U. Bergmeyer (Ed.), *Methods of Enzymatic Analysis*, Verlag Chemie/Academic Press, New York, Vol. 1, p. 574.
- 24 G. A. Hamilton, *Adv. Enzymol.*, 32 (1969) 55.
- 25 H. Lineweaver and D. Burk, *J. Am. Chem. Soc.*, 56 (1934) 658.
- 26 A. Peterlin, in H. B. Hopfenberg (Ed.), *Permeability of Plastic Films and Coating*, Plenum Press, New York, 1974, p. 9.
- 27 V. Zewe and H. J. Fromm, *J. Biol. Chem.*, 237 (1962) 1668.
- 28 L. D. Mell and J. T. Maloy, *Anal. Chem.*, 47 (1975) 980.
- 29 J. E. Brady and P. W. Carr, *Anal. Chem.*, 52 (1980) 1170.
- 30 H. F. Hameka and G. A. Rechnitz, *Anal. Chem.*, 53 (1981) 1586.
- 31 J. Crank, *The Mathematics of Diffusion*, Clarendon Press, Oxford, 1975, p. 20.
- 32 L. D. Mell and J. T. Maloy, *Anal. Chem.*, 47 (1975) 299.
- 33 D. R. Thevenot, R. Sternberg, P. R. Coulet, J. Laurent and D. C. Gautheron, *Anal. Chem.*, 51 (1979) 96.
- 34 K. Matsumoto, H. Seijo, I. Karube and S. Suzuki, *Biotechnol. Bioeng.*, 22 (1980) 1071.

- 35 T. Tsuchida and K. Yoda, *Nippon Kagaku Kaishi*, (1982) 1347.
36 L. J. Blum, C. Bertrand and P. R. Coulet, *Anal. Lett.*, 16 (1983) 525.
37 K. Matsumoto, H. Mizuguchi and K. Ichimura, *Kobunshi Ronbunshu*, 41 (1984) 221.
38 K. Mosbach (Ed.), *Methods in Enzymology*, Academic Press, New York, 1976, Vol. 44.
39 D. L. Mell and D. T. Maloy, *Anal. Chem.*, 48 (1976) 1597.
40 J. M. Johnson, H. B. Halsall and W. R. Heineman, *Anal. Chem.*, 54 (1982) 1394.
41 T. Yao, *Anal. Chim. Acta*, 148 (1983) 27.

DETERMINATION OF ELEMENTAL SULFUR IN JET FUEL BY DIFFERENTIAL PULSE POLAROGRAPHY

BIRGITTA R. OLOFSSON^a

Chemistry Division, National Defence Research Institute (FOA 4), S-901 82 Umeå (Sweden)

(Received 25th June 1985).

SUMMARY

A sensitive method based on differential pulse polarography is described for the determination of elemental sulfur in jet fuels. Its sensitivity makes it suitable for following small changes in the sulfur content of jet fuel during storage. The supporting electrolyte is 0.19 M ammonium acetate/0.088 M acetic acid in 1:1 toluene/methanol. In this medium, the peak potential is -0.56 V vs. Ag/AgCl. Calibration is linear from 2 to 30 mg l⁻¹. The limit of detection is 0.1 mg l⁻¹; precision is better than 10% below 1 mg l⁻¹, and better than 5% above 2 mg l⁻¹. Accuracy is better than 5%. Interferences from oxygen, hydrogen sulfide, thiols, organic sulfides and disulfides, organic peroxides and fuel additives are shown to be of very minor significance.

During long-term storage of jet fuel on water beds in underground caverns, corrosive compounds can accumulate as a consequence of microbial activity in the water bed [1]. Incorporation of these compounds, especially hydrogen sulfide and elemental sulfur, into the fuel causes an impairment of product quality because of their corrosive activity. The determination of elemental sulfur in petroleum products is of great interest because it is known that sulfur not only causes corrosion but also decreases the efficiency of antioxidants. Corrosive fuels studied contained less than 5 mg l⁻¹ elemental sulfur. A sensitive analytical method was needed to follow small changes in the elemental sulfur content in stored jet fuel.

Several methods for the determination of elemental sulfur in petroleum products are available. These include reaction with mercury and visual measurements [2], reactions with cyanide or benzoin with spectrophotometric determination [3, 4], and polarography [5–9]. Detection limits, where reported, are at the mg l⁻¹ level. Chromatographic methods, including gas chromatography with electron-capture detection [10] and liquid chromatography with u.v. detection [11], for the determination of elemental sulfur have also been described. The sensitivity of the methods is reported to be sub- μ g l⁻¹ and 1–10 ng, respectively. The present work is concerned with

^aPresent address: Pharmacia AB, S-751 82 Uppsala, Sweden.

a method based on differential pulse polarography (d.p.p.). The sensitivity compared to earlier polarographic methods [5–9] has been improved by at least ten-fold.

EXPERIMENTAL

Apparatus and materials

The Model 303 static mercury drop electrode (s.m.d.e.) (PAR, E.G. and G., Princeton, NJ) used as the working electrode was connected to a PAR Model 174A Polarographic Analyzer and an Omnigraphic Model 100 x-y recorder (Houston Instruments, Austin, TX). Instrumental parameters were: operating mode, d.p.p.; detector mode, d.m.e.; drop size, small; drop time 1 s; current range, 0.05–5.0 μA ; scan rate, 2 mV s^{-1} ; potential range, -0.3 to -1.05 V; modulation amplitude, 25 mV.

All chemicals were of analytical grade. Crystalline sulfur, pretreated by heating above 100°C for several hours, was dissolved in toluene (0.5 mg/100 ml) and used as a standard. The heating procedure ensured transformation to the crystal form of any amorphous sulfur present [12]. No apparent difference in polarographic behavior was noticed, however, between standard solutions of analytical-grade and heat-treated sulfur. Argon, presaturated with methanol/toluene, was used for deoxygenation of electrolyte and samples prior to polarography.

The electrolyte consisted of 0.19 M ammonium acetate and 0.088 M acetic acid in 1:1 (v/v) methanol and toluene [6, 7]. Synthetic fuel was 85% n-hexane and 15% toluene. Non-corrosive jet fuel (JP4) was obtained directly from the refinery without being stored for longer periods.

Procedure

Samples (1 ml) of jet fuel were added to 9 ml of supporting electrolyte. After 4 min of purging with methanol/toluene-presaturated argon, the polarograms were obtained under the above conditions. Peak height (current) was measured at the peak potential -0.56 V (vs. Ag/AgCl). Results were compared to a calibration curve from standard additions of elemental sulfur in toluene to supporting electrolyte and a synthetic fuel. Additions made were 0.2, 1.0, 2.5 or 4.5 μg of sulfur per 10 μl . Purging was done for 30 s after each addition.

RESULTS AND DISCUSSION

Elemental sulfur is known to show great molecular complexity [13]. There is little information concerning sulfur configuration in non-polar liquids at ambient temperatures, however. The predominant form is probably the thermodynamically stable cyclo-octasulfur, S_8 . The crown-shaped structure of the molecule is presumably broken up during the polarography.

The electrode reaction showed a maximum when studied with normal

pulse polarography. The maximum increased with increased drop time, indicating the presence of a film-forming electrode reaction, in this case the oxidation of mercury with subsequent formation of mercury(II) sulfide. An alternative reaction would be the direct reduction of sulfur to hydrogen sulfide [14]; this was precluded by running a positive d.p.p. scan, which indicated that mercury sulfide was formed.

The response of the method was studied up to 150 mg l^{-1} sulfur. The calibration was linear between 2 and 30 mg l^{-1} . At concentrations above 30 mg l^{-1} ($1 \times 10^{-3} \text{ M}$), the polarographic current was no longer proportional to sulfur concentration, probably because of the film-forming electrode reaction similar to that found for sulfide [15]. Additional waves, as reported for sulfide, did not appear; instead, there was peak broadening and a potential shift towards more negative values, offering further evidence for the adsorptive nature of the reaction. At concentrations below 2 mg l^{-1} , the calibration curve deviated from linearity (Fig. 1); possible explanations could be adsorption on the walls of the electrolytic cell or complexation with trace impurities. Because of the non-linearity of the method at low concentrations of elemental sulfur, quantification was not done by the preferable standard addition method, but by comparison of peak current, i_p , to a calibration curve. Because it was necessary to use a sulfur-free fuel for this purpose, it was convenient to prepare a synthetic fuel, based on specifications for jet fuel, consisting of 15% aromatics and 85% n-alkanes. Samples analyzed and quantified from calibration curves for non-corrosive

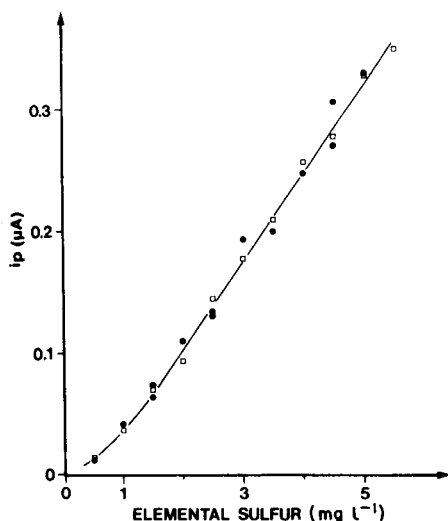


Fig. 1. Plot of peak currents (i_p) versus concentration of elemental sulfur added to synthetic fuel (\square) and non-corrosive jet fuel (\bullet). The line is the calibration curve for all data.

jet fuel and synthetic fuel showed no difference (Fig. 1). A typical d.p. polarogram is shown in Fig. 2.

Accuracy and precision were tested up to 10 mg l^{-1} and all field samples of stored jet fuel analyzed so far have been below this concentration. Precision, expressed as relative standard deviation, for samples analyzed several times during periods of 8 h, 5 days or 1 month was better than 10% (Table 1). For values of more than $2\text{--}3 \text{ mg l}^{-1}$, it was better than 5%. The accuracy of the method, estimated from the analysis of spiked synthetic or non-corrosive jet fuel, was better than 5%. The method was compared for a range of samples with the spectrophotometric method of Bartlett and Skoog [3] which has a detection limit of 2 mg l^{-1} . Over the concentration range $1\text{--}10 \text{ mg l}^{-1}$, there was good agreement between the two methods (Table 2).

The detection limit of the d.p.p. method was 0.1 mg l^{-1} with a precision of 15–20%, which corresponded to a peak current of $<2 \text{ nA}$. Increase of mercury drop size and modulation amplitude increased i_p (i.e. sensitivity). The effect of this on accuracy, precision and detection limit was not evaluated.

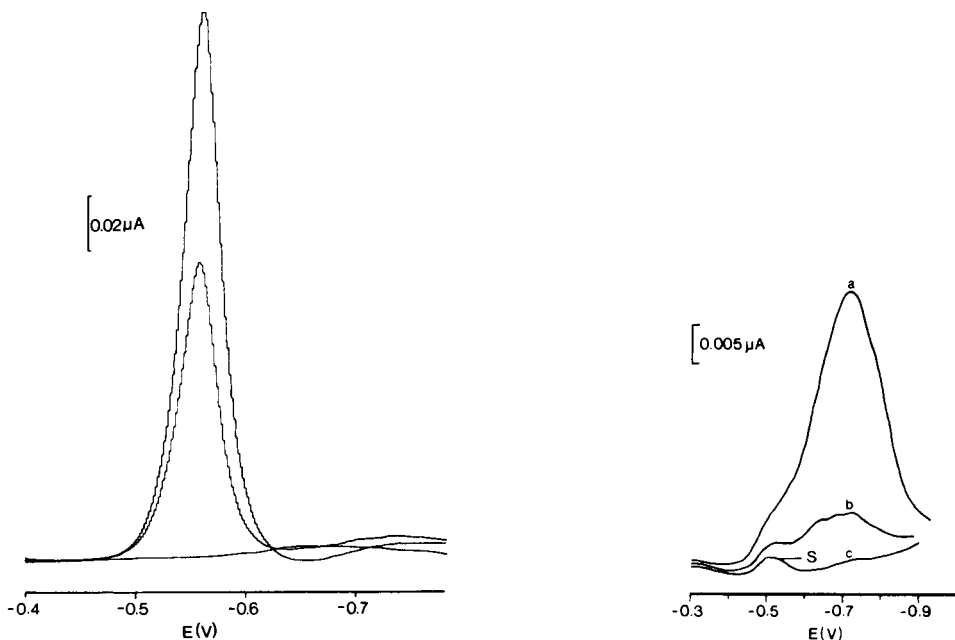


Fig. 2. Typical d.p. polarogram of a jet-fuel sample containing 3.6 mg l^{-1} elemental sulfur and a standard addition corresponding to 3 mg l^{-1} . Sample volume was 1.5 ml.

Fig. 3. D.p. polarogram of a jet-fuel sample containing 0.1 mg l^{-1} elemental sulfur (S) after: (a) 1 min, (b) 2 min, and (c) 4 min purging with methanol/toluene-presaturated nitrogen.

TABLE 1

D.p.p. of elemental sulfur (S) in jet fuel (samples 1–7) and spiked synthetic fuel (SF, samples 8–11). Determinations were evenly distributed over the time intervals stated (n is the number of determinations, and RSD the relative standard deviation)

Sample	S found (mg l ⁻¹)	RSD (%)	Period	n
F 3794 (3.3) ^a	0.33	8.4	5 days	5
F 3794	1.0	8.8	8 h	4
F 3794	1.2	4.7	5 days	5
F 3713A (2.5) ^a	1.4	8.9	5 days	5
F 3908	2.2	4.3	8 h	4
F 3713A	3.6	2.0	5 days	5
F 3713A	3.8	3.6	1 month	7
SF + 1.0 mg l ⁻¹	1.0	6.0	1 month	6
SF + 2.0 mg l ⁻¹	2.1	7.0	1 month	7
SF + 5.1 mg l ⁻¹	5.1	1.0	8 h	3
SF + 10.2 mg l ⁻¹	9.8	3.4	8 h	4

^aDilution factor.

TABLE 2

Determination of elemental sulfur in jet-fuel samples from storage sites, spiked synthetic fuel (SF) (85% n-hexane, 15% toluene), and spiked non-corrosive jet fuel (NF) by d.p.p. and a spectrophotometric method [3].

Sample	Spectrophotometry			Polarography		
	S found (mg l ⁻¹)	RSD (%)	n	S found (mg l ⁻¹)	RSD (%)	n
F 3794	1.6	8.0	4	1.0	8.8	4
F 3908	2.0	7.1	4	2.2	4.3	4
F 3713B	3.2	3.1	4	3.3	2.8	4
SF + 2.0 mg l ⁻¹	1.9	—	1	2.0	—	2
SF + 5.1 mg l ⁻¹	5.0	0.7	4	5.1	1.0	3
SF + 10.2 mg l ⁻¹	10.5	2.5	4	10.5	4.7	4
NF + 5.1 mg l ⁻¹	4.9	2.6	3	5.0	1.0	3
NF + 10.2 mg l ⁻¹	10.2	—	2	9.8	3.4	4

Interferences

The method was checked for interferences from other substances. One is molecular oxygen which has a peak potential vs. Ag/AgCl of -0.7 V. By purging with an inert gas, the oxygen concentration in the cell could be reduced to a non-interfering level (Fig. 3). Effective purging was especially important for low level detection (sub-mg l⁻¹).

Stored jet fuel may contain hydrogen sulfide which gives a polarographic

peak at approximately the same potential as elemental sulfur. For a sample spiked at the mg l^{-1} level with hydrogen sulfide, 95% of the sulfide was removed after purging for 4 min. Samples of stored jet fuel from rock caverns have, however, been found to contain only a few hundred $\mu\text{g l}^{-1}$ at most. Because of the sensitivity of hydrogen sulfide to oxidation in contact with air, careful sampling is important for correct sulfur determinations. If oxidation of hydrogen sulfide is likely to contribute to the original content of elemental sulfur in the sample, sampling should be done with no air contact, to avoid conversion of hydrogen sulfide to elemental sulfur during transport and storage before analysis, or hydrogen sulfide should be removed by purging directly after sampling.

Organic sulfur compounds in varying concentrations were added to samples in the presence and absence of elemental sulfur. Potentials were scanned from 0.0 V to -1.5 V. None of the tested compounds, i.e., butanethiol, phenylthiol, di-isohexyl sulfide and diphenyl disulfide, interfered at the peak potential for elemental sulfur, as shown in Table 3. The 5–10% decrease in the sulfur signal caused by thiol sulfur reported by Karchmer [5] was not found for the d.p.p. method nor was there any interference by the organic sulfide or disulfide tested.

Organic peroxides may be present in jet fuel. The reduction potential for *t*-butyl peroxide was more negative than that for sulfur. Only when the peroxide concentrations were above 1000 mg l^{-1} was it difficult to determine accurately the peak current of elemental sulfur. No interference problems were found for the jet fuel analyzed. Antioxidants and corrosion inhibitors are common jet-fuel additives. No effect on the peak currents for elemental sulfur was found for the antioxidant 2,4-dimethyl-6-*t*-butylphenol at $17\text{--}24 \text{ mg l}^{-1}$, or for the corrosion inhibitor Hitec E-515 at 12 mg l^{-1} , which are the concentrations specified for jet fuel.

The study on interferences in the present method indicated that if oxygen was successfully removed, sulfur concentrations lower than 0.1 mg l^{-1} could be detected. The method can also be used to detect the presence of thiol and

TABLE 3

Peak potentials, E_p , of sulfur compounds in d.p.p.

Sulfur compound	E_p (V)	S^a (mg l^{-1})
Elemental sulfur	-0.56	0-4
Butanethiol	-0.27	0.03-30
Phenylthiol	-0.35	0.03-30
Di-isohexyl sulfide	-	2-40
Diphenyl disulfide	-0.34, -0.95	0.5-30

^aThe concentrations are given in terms of sulfur for all compounds.

organic disulfide sulfur. Determinations based on these peaks have been studied briefly; they are strongly dependent on the volatility of the compounds. The method has so far been used only for jet fuels but it should also be useful in the analysis of other petroleum products.

I thank Robert Samuelsson, Department of Analytical Chemistry, University of Umeå, for his advice and valuable discussions, and Roger Roffey, Microbiology Division, FOA 4, for encouragement and advice. This work was supported financially by the National Board of Economic Defence, Sweden.

REFERENCES

- 1 R. Roffey, A. Norqvist and A. Edlund, in S. Barry (Ed.), *Biodeterioration 6, Commonwealth Agricultural Bureaux, Slough, U.K.*, 1985, in press.
- 2 K. Uhrig and H. Levin, *Anal. Chem.*, 23 (1951) 1334.
- 3 J. K. Bartlett and D. A. Skoog, *Anal. Chem.*, 26 (1954) 1008.
- 4 A. A. Stern and M. Babitz, *Bull. Res. Council. Isr.*, 8 (1960) 109.
- 5 J. H. Karchmer, *Anal. Chem.*, 30 (1958) 80.
- 6 M. E. Hall, *Anal. Chem.*, 25 (1953) 556.
- 7 B. H. Eccleston, M. Morrison and H. M. Smith, *Anal. Chem.*, 24 (1952) 1745.
- 8 H. V. Drushel, J. F. Miller, W. Hubis and R. O. Clark, *Anal. Chim. Acta*, 15 (1956) 394.
- 9 R. D. Obolontsev, B. T. Bulatova, A. Ya. Bajkova, *Khim. Seraorg. Soedin. Soderzh. Neftiyakh Nefteprod.*, 8 (1968) 306.
- 10 J. J. Richard and R. D. Vick, G. A. Junt, *Environ. Sci. Technol.*, 11 (1977) 1084.
- 11 R. H. Cassidy, *J. Chromatogr.*, 117 (1976) 71.
- 12 W. N. Tuller, in J. H. Karchmer (Ed.), *The Analytical Chemistry of Sulfur and its Compounds*, Wiley-Interscience, New York, 1970, Chap. 1.
- 13 B. Meyer, *Chem. Rev.*, 76 (1976) 367.
- 14 G. Proske, *Naturwissenschaften*, 33 (1946) 220.
- 15 D. R. Canterford, *Electroanal. Chem.*, 52 (1974) 144.

VOLTAMMETRIC DETERMINATION OF TRACE AMOUNTS OF GOLD WITH A CHEMICALLY MODIFIED CARBON PASTE ELECTRODE^a

KURT KALCHER

Institut für Analytische Chemie, Karl-Franzens-Universität Graz, Universitätsplatz 1, A-8010 Graz (Austria)

(Received 29th May 1985)

SUMMARY

A carbon paste electrode chemically modified with anion-exchangers is used for the voltammetric determination of gold(III). Tetrachloro- or tetrabromo-aurate(III) is pre-concentrated on the electrode surface, modified with Amberlite LA2, and the electrode is transferred to an electrochemical cell for voltammetric measurements by cathodic stripping. The response depends on the concentration of gold in the bulk solution, pre-concentration time, and other parameters. Detection limits are 100–300 $\mu\text{g l}^{-1}$ depending on the conditions. Many elements forming stable halo complex anions interfere.

Chemically modified electrodes (c.m.e.) have attracted much interest in recent years. Besides their importance in electrosynthesis, electrocatalysis, and energy conversion, these electrodes are being increasingly utilized in the sphere of electroanalysis [1]. Modifications of working electrodes with ion-exchangers promise a wide range of application in the determination of ionic species. Thus, cation-exchangers have been used to modify carbon paste electrodes in the determination of copper [2] and anion-exchangers for the determination of iodide [3]. The latter, in a membrane form, is suitable for the determination of chromate [4]. As many metals can be converted to anions by appropriate ligands, anion-exchangers seem promising for the determination of such species.

The aim of this work was to investigate the electrochemical behaviour of gold in its tetrahalo complexes, $[\text{AuCl}_4]^-$ and $[\text{AuBr}_4]^-$, on carbon paste electrodes modified with anion-exchangers. There are four main reasons for choosing this method of modifying the electrodes: (a) the high affinity of $[\text{AuX}_4]^-$ to anion-exchangers should influence the analytical properties favourably; (b) the background current of the electrode is relatively low in the region of gold reduction; (c) preparation and handling of the electrode is easy; and (d) gold can be accumulated on the electrode surface. To avoid interference between the ion-exchange process on the electrode surface and the electrochemical reaction during measurement, these steps are done

^aThis paper is dedicated to Professor Reinhold Pietsch on the occasion of his sixtieth birthday.

independently. Thus, gold is first accumulated at the electrode without application of a potential, and then, after exchange of the medium, a voltammetric method is applied to determine the preconcentrated gold.

EXPERIMENTAL

Apparatus and electrodes

Most measurements were made with a PAR model 384B polarograph (Princeton Applied Research). For cyclic voltammetry, a PAR 264B polarograph was connected via a laboratory-built interface (analog-to-digital conversion) to a Hewlett-Packard HP-1000 minicomputer which processed and evaluated the data; details will be reported elsewhere.

The electrode assembly consisted of a titration vessel (20–90 ml; 6.1415.220 from Metrohm) and a laboratory-built cell compartment made of plexiglas. The reference electrode was a saturated calomel electrode (SCE) which was in contact with the solution over a 1 M KCl salt bridge to avoid contamination of the electrode. The counter-electrode was a platinum wire.

The body of the working electrode was a teflon rod (10 mm o.d.) with a hole (7 mm diameter) bored at one end for the carbon paste filling. Contact was made with a platinum wire through the center of the rod. The carbon paste was packed in and smoothed off with a PTFE spatula. Four types of electrodes were investigated.

Type I. A carbon paste was prepared as described by Monien et al. [5]. A portion (5 g) of spectral carbon powder RWB (Ringsdorff Werke) was mixed thoroughly with 1.8 ml of paraffin (Uvasol, Merck); 350 μl of the weakly basic liquid anion-exchanger, Amberlite LA2 (Fluka) was added and mixed in to give a homogeneous paste. Commercially available carbon paste (EA-267c, Metrohm) mixed with LA2 (50 $\mu\text{l g}^{-1}$) gave the same results.

Type II. Spectral carbon powder RWB (5 g) was mixed with 2 ml of liquid ion-exchanger until the paste appeared homogeneous. To remove trapped air bubbles, which increased the background current, the mixture was exposed for some minutes to a vacuum (16 Torr) at a slightly raised temperature (45°C).

Type III. Carbon paste as prepared for type I, or the commercial carbon paste, was mixed with swollen and well-ground strongly basic anion-exchanger Dowex 1 (Fluka) in a 5:1 mass ratio.

Type IV. This was made like type III, but with the strongly basic gel-type anion-exchanger Amberlite R-IRA-400 (Aldrich).

Reagents and chemicals

Deionized water was distilled twice in a quartz still and then purified by a cartridge deionization system (Nanopure, Barnstead). The hydrochloric and hydrobromic acids, ammonia and sodium hydroxide were of Suprapur grade (Merck). All other chemicals were of analytical grade (p.a.; Merck).

A gold stock solution (1000 mg l^{-1}) was prepared in 0.01 M hydrochloric

acid from potassium tetrachloroaurate(III). Solutions of lower concentrations were prepared by dilution just before use. Stock solutions of other metals were 1000 mg l⁻¹ with respect to the metal.

Procedures

Preconcentration. For the determination of gold as tetrachloroaurate(III), the acidity of the sample solution was adjusted to 1.5 M. The electrode was dipped into 20 ml of this solution which was stirred constantly at a rate of 300 rpm. After the required period of time, the electrode was removed and rinsed with water for about 0.5 s. Then it was dipped into the voltammetric cell and connected to the polarograph. The solution in the cell was 0.1 M hydrochloric acid, which provided the greatest sensitivity.

For the determination of tetrabromoaurate(III) the concentration of hydrobromic acid in the test solution was 0.23 M and the cell solution was 0.05 M hydrobromic acid. The treatment of the electrode was the same as described above.

Voltammetry. All electrochemical measurements were preceded by an equilibration phase of 20 s to settle the solution and decrease the background current. The potential scan range was +0.6 to -0.2 V vs. SCE. For differential-pulse voltammetric measurements, scanning was done towards negative potentials at a rate of 8 mV s⁻¹; the pulse amplitude was 50 mV (repetition time 0.5 s).

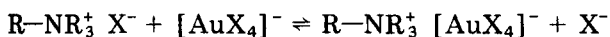
The parameters for cyclic voltammetry were 0.2-s repetition time and 20-mV s⁻¹ scan rate with a current range of 500 μA. The first cycle started at +0.6 V vs. SCE.

Regeneration of the working electrodes. After each electrochemical measurement, the working electrodes were regenerated and conditioned. For the chloride medium, the electrode was dipped into a 1 M ammonia solution for 2 min with constant stirring at 300 rpm. After a water rinse, 1 M hydrochloric acid was used under the same conditions to produce the chloride form of the anion-exchanger. For the bromide medium, the electrodes were regenerated by successive treatment with 2 M potassium cyanide for 1 min, 1 M sodium hydroxide for 2 min, and 1 M hydrobromic acid for 2 min. After each step, the electrode was rinsed with water.

These procedures were also applied to the virgin electrodes.

RESULTS AND DISCUSSION

Gold(III) in its tetrahalo complexes shows a high affinity to anion-exchangers [6]:



The gold accumulated on the electrode surface is reduced to the metal during the voltammetric measurement in a 3-electron reaction. This reduction is seen clearly in the cyclic voltammogram (Fig. 1). The elemental

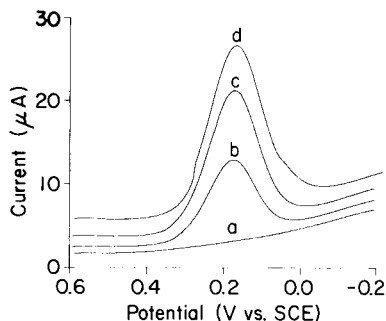
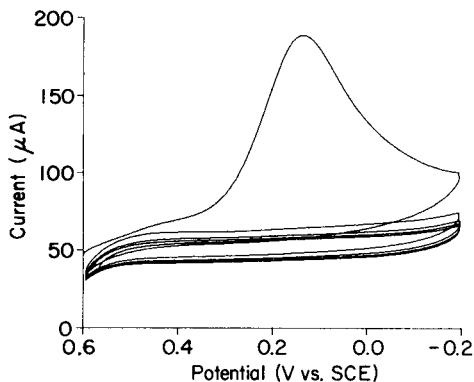


Fig. 1. Cyclic voltammogram of 5 mg l^{-1} Au(III) preconcentrated as $[\text{AuCl}_4]^-$ for 2 min on electrode type I.

Fig. 2. Differential pulse voltammograms with a type I electrode: (a) background; (b) 1 mg l^{-1} Au; (c) 2 mg l^{-1} Au; (d) 3 mg l^{-1} . Preconcentration time 3 min.

gold which is produced is adsorbed only slightly by the carbon paste; re-oxidation is not observed at this sensitivity.

The peak potential for reduction in differential pulse voltammetry lies at $+0.252 \text{ V vs. SCE}$ for the chloro complex and at $+0.170 \text{ V vs. SCE}$ for the bromo complex; it is not dependent on concentration. The resulting peak current is a function of the gold concentration in the test solution (Fig. 2). Not all the ion-exchangers produce the same effect. Figure 3 shows the fundamental difference between strongly (curves b and c) and weakly

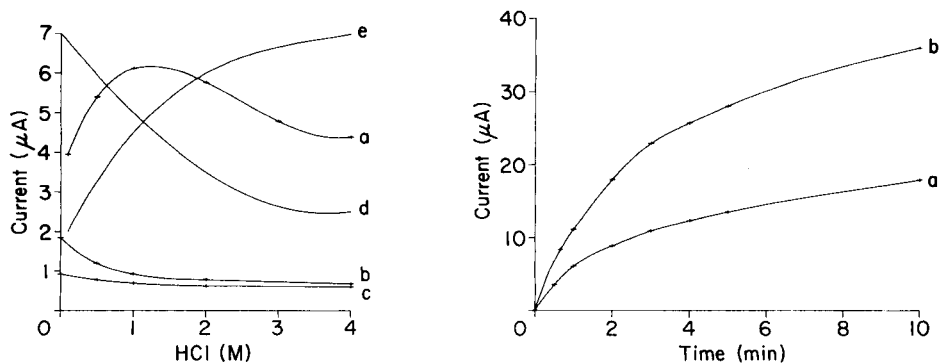


Fig. 3. Dependence of the peak current on the acidity of the test solution (5 mg l^{-1} Au, 3-min preconcentration time): (a) type I; (b) type III; (c) type IV electrode. (d) Ion-competition effect; (e) protonation contribution (synthetic curves).

Fig. 4. Relation between peak current and accumulation time for 5 mg l^{-1} Au; type I electrode; (b) type II electrode.

(curve a) basic anion-exchangers in the dependence of the peak current on the acidity of the test solution. The strongly basic exchangers are permanently dissociated so that the exchange process is dominated by a chloride competition reaction as the concentration of hydrochloric acid increases. For the secondary amine functional group of LA2, the peak current depends not only on the competitive effect, which diminishes the height with increasing amount of chloride (hypothetical curve d), but also on increasing protonation of the amine group at lower pH values (curve e). The intersection of these curves indicates the optimum acidity for the preconcentration (cf. curve a); with type II electrodes, the curve shape was the same but the peak currents were higher.

The small currents obtained and their lack of reproducibility excluded electrodes of type III and IV from further investigations. The low sensitivity is not due to smaller exchange capacity (Table 1) but rather be the extent of exposure of functional groups on the electrode surface to the solution. Clearly, a liquid phase will cover almost all the surface area whereas particles in a matrix will occupy much less of the surface area. Thus, the number of ion-exchange sites on the surface is much smaller in gel- and resin-type electrodes.

The physical and chemical changes of the surface during preconcentration and measurement must also be taken into account. To avoid having to refill the electrode after each determination, which leads to poor reproducibility of results, appropriate regeneration procedures must be applied. After the voltammetric step, the colloidal gold is adsorbed slightly by the carbon paste, probably as a result of electrostatic effects, and the residual peak currents will influence subsequent measurements if the electrodes are not regenerated. For the chloride medium, treatment with ammonia is sufficient to lower the interaction of the adsorbed gold and the functional groups can be regenerated with hydrochloric acid. For bromide-loaded electrodes, the equivalent procedure was not viable; small residual currents

TABLE 1

Ion-exchange capacities

	Capacity (meq g ⁻¹)		In carbon paste
	Dry	Wet ^a	
LA2	2.2–2.3	2.6–2.8	—
Dowex-1	3.5	1.3	(43%)
IRA-400	3.8	1.4	(42–48%)
Type I	—	—	0.11
Type II	—	—	0.90
Type III	—	—	0.40
Type IV	—	—	0.42

^aCapacity in meq ml⁻¹; moisture content in parentheses.

were always observed. The best regeneration method is described in the experimental part. Regenerations with rhodamine B in combination with cyanides, acids and bases produced no better results. Mercury extracted all the gold but adsorbed so strongly to the surface that the gold peak disappeared in the ensuing measurements. The three-step regeneration with potassium cyanide, sodium hydroxide and hydrobromic acid is preferable. Lengthy exposures to cyanides should be avoided, as the resulting $[\text{Au}(\text{CN})_2]^-$ is strongly adsorbed, leading to a second peak at about $+0.04$ V vs. SCE. Though the tetrabromoaurate determination is more sensitive than the analogous chloride method, the accompanying difficulties confined the analytical investigations mainly to the latter.

The dependence on the preconcentration time of the peak current for the chloride-loaded electrodes of type I and II is displayed in Figure 4. Because the ion-exchange reaction is not fast, the first part of the curves is quasi-linear. As the deposition time is increased, there is an asymptotic approach to a limiting value because the ion-exchange equilibrium is reached gradually. In addition to the chemical composition of the paste and of the bulk solution, the distribution coefficient, D_c , for $[\text{AuCl}_4]^-$ between the exchanger and the solution governs the limiting peak current. As expected, the electrode with the higher concentration of ion exchanger (type II) exhibits higher values than electrode type I. It must be noted that the handling of electrodes and the stirring of solutions must be done always in the same manner to yield comparable results.

The effect of the concentration of tetrachloroaurate(III) on the peak current in differential pulse voltammetry is shown in Fig. 5. The detection limit is not characterized by a particular signal-to-noise ratio but rather by

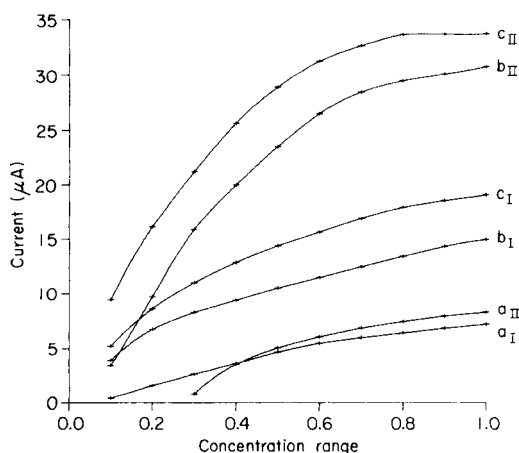


Fig. 5. Dependence of peak current on the gold concentration at different preconcentration times. I and II refer to electrode type. Deposition times and concentration ranges: (a) 5 min, 0–1 mg l^{-1} ; (b) 2 min, 0–10 mg l^{-1} ; (c) 20 s, 0–100 mg l^{-1} .

TABLE 2

Interferences with the determination of gold

Species	Added as	Conc. ($\times 10^{-4}$ M)	Possible anions	Type ^a	Peak change (%)
Cu(II)	CuCl ₂ /HCl	3.9	[CuCl ₃] ⁻ , [CuCl ₄] ²⁻	3	-13.6
Ag(I)	AgNO ₃ /H ₂ O	2.3	[AgCl ₂] ⁻ , [AgCl ₃] ²⁻ [AgCl ₄] ³⁻	3, 6	-15.3
Zn(II)	ZnCl ₂ /HCl	3.8	[ZnCl ₃] ⁻ , [ZnCl ₄] ²⁻	1	-1.8
Cd(II)	CdCl ₂ /HCl	2.2	[CdCl ₃] ⁻ , [CdCl ₄] ²⁻	2	-9.7
Hg(II)	Hg(NO ₃) ₂ /HCl	1.2	[HgCl ₃] ⁻ , [HgCl ₄] ²⁻	4, 5	-27.7
Ga(III)	Ga(NO ₃) ₃ /HCl	3.6	[GaCl ₄] ⁻	2	+8.3
In(III)	InCl ₃ /HCl	2.2	[InCl ₄] ⁻	1	-3.6
Tl(I)	TlNO ₃ /H ₂ O	1.2		2	-6.8
Tl(III)	Tl(NO ₃) ₃ /HCl	1.2	[TlCl ₄] ⁻	4	-45.7
Ge(IV)	GeCl ₄ /HCl	3.4	[GeCl ₅] ²⁻	1	-3.2
Pb(II)	Pb(NO ₃) ₂ /H ₂ O	1.2	[PbCl ₄] ²⁻	2	+7.3
NO ₃ ⁻	NaNO ₃ /H ₂ O	4.0	NO ₃ ⁻	1	+2.4
H ₂ PO ₄ ⁻	KH ₂ PO ₄ /H ₂ O	2.6	H ₂ PO ₄ ⁻	1	-1.7
As(III)	As ₂ O ₃ /NaOH	3.3	[AsCl ₄] ⁻ , [AsCl ₅] ^{2-b}	4, 5	-96.0
As(V)	As ₂ O ₅ /H ₂ O	3.3	H ₂ AsO ₄ ⁻	3	-18.3
Sb(III)	SbCl ₃ /HCl	2.1	[SbCl ₄] ⁻ , [SbCl ₅] ^{2-b}	4	-29.8
Sb(V)	SbCl ₅ /HCl	2.1	[SbCl ₅] ⁻ , [SbOCl ₄] ⁻ [SbO ₂ Cl ₂] ^{2-b}	4	+23.6
Bi(III)	BiCl ₃ /HCl	1.2	[BiCl ₄] ⁻ , [BiCl ₅] ²⁻ [BiCl ₆] ^{3-b}	4	-41.4
V(IV)	VO ₂ /H ₂ SO ₄	4.9	VO ₂ ⁺ , [VOCl ₄] ⁻	1	-4.4
V(V)	NH ₄ VO ₃ /HCl	4.9	[VOCl ₅] ²⁻ [NbOCl ₅] ^{2-b}	1	-3.3
Nb(V)	NbCl ₅ /HCl	2.7	[NbOCl ₅] ^{2-b}	1	+1.8
Ta(V)	TaCl ₅ /HCl	1.4	- ^b	2	-8.4
SO ₄ ²⁻	Na ₂ SO ₄ /H ₂ O	2.6	SO ₄ ²⁻ , HSO ₄ ⁻	1	-4.3
Se(IV)	SeO ₂ /HNO ₃	3.2	SeOCl ₃ ⁻ , SeOCl ₄ ²⁻ SeO ₂ Cl ⁻ , SeO ₂ Cl ₂ ²⁻	1	+1.0
Te(IV)	K ₂ TeO ₃ /HCl	2.0	[TeCl ₄] ^{2-b}	1	+0.3
Cr(III)	CrCl ₃ /HCl	4.8	[CrCl ₄] ⁻	2	-9.5
Cr(VI)	K ₂ Cr ₂ O ₇ /HCl	4.8	Cr ₂ O ₇ ²⁻ , CrO ₄ ²⁻	4, 5	-49.9
Mo(VI)	(NH ₄) ₂ MoO ₄ /NH ₃	2.6	(poly)molybdates	3	-14.1
W(VI)	Na ₂ WO ₄ /NaOH	1.4	[WO ₂ Cl ₃] ^{2-b}	1	-0.3
ClO ₄ ⁻	NaClO ₄ /H ₂ O	2.5	ClO ₄ ⁻	1	-0.9
Br ⁻	KBr/H ₂ O	3.1	Br ⁻	1	+3.0
I ⁻	KI/H ₂ O	2.0	I ⁻	5, 6	-100
Mn(II)	MnCl ₂ /H ₂ O	4.6	- ^b	3	-13.6
Fe(III)	FeCl ₃ /HCl	4.8	[FeCl ₄] ⁻	1	+0.3
Co(II)	CoCl ₂ /HCl	4.2	- ^b	2	-8.7
Ni(II)	NiCl ₂ /HCl	4.3	- ^b	2	-8.1
Ru(III)	RuCl ₃ /HCl	2.5	[Ru(H ₂ O) ₂ Cl ₄] ⁻	3, 5	-16.7
Rh(III)	RhCl ₃ /HCl	2.4	[RhCl ₆] ^{3-b}	4, 5	-21.6
Pd(II)	Na ₂ PdCl ₄ /HCl	2.4	[PdCl ₄] ²⁻	3	-13.5
Os(VI)	K ₂ OsO ₄ /H ₂ O	1.3	[Os ₂ O ₂ Cl ₄] ²⁻ , [OsCl ₆] ²⁻	3, 5	-13.1
Ir(III)	IrCl ₃ /HCl	1.3	[IrCl ₆] ^{3-b}	3, 5	-10.3
Ir(IV)	H ₂ IrCl ₆ /HCl	1.3	[IrCl ₆] ²⁻	2, 5	-8.9
Pt(II)	(NH ₄) ₂ PtCl ₄	1.3	[PtCl ₄] ²⁻	5, 6	-100
Pt(IV)	H ₂ PtCl ₆ /HCl	1.3	[PtCl ₆] ²⁻	3, 5	-17.8

^aSee text. ^bAnd partly hydrolyzed chloro complexes.

the minimal concentration which is necessary to produce a signal at all. It seems that the ion-exchange process takes place only if a certain amount of gold is present in the solution; otherwise, even increasing the deposition time has no effect. Thus, the detection limit was found to be 100 $\mu\text{g l}^{-1}$ gold for the type I electrode and 300 $\mu\text{g l}^{-1}$ for the type II electrode. It is

surprising and not self-evident that the carbon paste containing less ion-exchanger is more sensitive than the other. At higher concentrations, deviations from linearity owing to saturation effects on the electrode surface can be observed. The choice of electrode type and deposition time depends on the amount of gold present in the test solution. Quantitative evaluation can be done either from a calibration curve, or, when linearity exists, with standard addition methods.

Interferences

The influence of other ions was examined (Table 2). The interferences were classified roughly into the following categories (column 5 in the table): (1) no or weak interference (0–5% change in the peak current); (2) weak to medium interference (5–10%); (3) medium to strong interference (10–20%); (4) disastrous interference (>20%); (5) additional peak; and (6) probable redox reaction with gold(III). The degree of interference was measured with a type II electrode for 5 mg l⁻¹ gold(III) and 25 mg l⁻¹ element in 1.5 M hydrochloric acid. Basically, two kinds of interference can be distinguished: a simple competitive one which appears with almost all anionic species, decreasing the peak current, and an additional electrochemical effect which results in overlapping signals. The most serious effects are caused by anions with high affinity for ion-exchangers like dichromate and the chloro complexes of Tl(III), Sb(V) or Bi(III). Almost all the platinum metals affect the peak height severely because of the formation of stable chloro complexes. Most of them exhibit an additional peak at about 0 V vs. SCE. In the determination of gold, interferences of type 1 can be ignored up to concentrations of at least 25 mg l⁻¹, because the standard deviation for gold is 3% for 5 mg l⁻¹ gold with a 2-min deposition time. Strongly interfering anions must be separated by appropriate procedures before the determination.

Conclusions

The work presented is a further example of the increasing importance of chemically modified electrodes for voltammetric determinations especially with regard to high sensitivities. Modifications of carbon paste electrodes with ion exchangers seem also promising for other metal species in various kinds of complexing media.

The author thanks EG & G Munich, especially Dr. Nitsch, for lending a PAR model 384B polarograph for voltammetric measurements.

REFERENCES

- 1 A. R. Guadalupe and H. D. Abruna, *Anal. Chem.*, 57 (1985) 142.
- 2 J. Wang, B. Greene and C. Morgan, *Anal. Chim. Acta*, 158 (1984) 15.
- 3 K. Kalcher, *Fresenius Z. Anal. Chem.*, 321 (1985) 666.
- 4 J. A. Cox and P. J. Kulesza, *Anal. Chim. Acta*, 154 (1983) 71.
- 5 H. Monien, H. Specker and K. Zinke, *Fresenius Z. Anal. Chem.*, 225 (1967) 342.
- 6 A. Mizuike, Y. Iida, K. Yamada and S. Hirano, *Anal. Chim. Acta*, 32 (1965) 428.

RESPONSE CHARACTERISTICS OF A POTENTIOMETRIC DETECTOR WITH A COPPER METAL ELECTRODE FOR FLOW-INJECTION AND CHROMATOGRAPHIC DETERMINATIONS OF METAL IONS

PETER W. ALEXANDER* and PAUL R. HADDAD

Department of Analytical Chemistry, University of New South Wales, P.O. Box 1, Kensington, N.S.W. 2033 (Australia)

MAREK TROJANOWICZ

Department of Chemistry, University of Warsaw (Poland)

(Received 12th June 1985)

SUMMARY

The potentiometric response characteristics of a copper metal indicator electrode are reported in a flow-injection system when metal ions are injected into ligands of differing complexing strengths in buffered carrier streams. Theoretical Nernstian derivation of equations relating peak heights to both the injected metal ion concentration and the ligand concentration are shown to give good agreement with experimental peak height measurements for Ca^{2+} , Al^{3+} , Pb^{2+} , Cd^{2+} , Co^{2+} , Cu^{2+} , Ni^{2+} , Mn^{2+} , Zn^{2+} and UO_2^{2+} . A study of injections into buffered ligand streams containing EDTA, ethylenediamine, triethylenetetramine, iminodiacetate, citrate, or glutamate shows advantages for the use of the more weakly complexing ligands in the carrier stream. Linear responses are obtained at low (10^{-3} – 10^{-4} M) metal ion concentrations over narrow ranges. Some chromatographic applications are outlined.

Indirect determinations of metal ions by potentiometric compleximetric titrations can be done with various indicating electrodes. Many papers report applications of metal electrodes such as silver and mercury [1], membrane ion-selective electrodes [2, 3] and oxide electrodes [4] which are useful for such titrations within certain limitations. These titrations are usually done in the presence of low concentrations of indicating ions directly sensed by the indicator electrode, and detection is based on the shift of the complex equilibrium between the indicating ion and ligand in the presence of the titrated cation [1, 5]. A similar concept can be utilized for indirect flow-injection determinations of metal ions.

In several papers it has been shown that, in the absence of copper ions in solution, the potential of a copper (II)-selective membrane electrode [6, 7] or a metallic copper electrode [8–10] is a function of the concentration of copper complexing ligands. Comparative measurements for these types of electrodes for amino acids showed better dynamic behaviour of the metallic copper electrode [8]. The relationship between the electrode potential and ligand concentration can be utilized for indirect determination of metal

ions in a flow-injection system for faster determinations than by traditional titration methods.

The concept of such measurements has already been presented in a preliminary report [11], in which only a relatively strongly complexing ligand in the carrier stream (*viz.* EDTA) was investigated. The peak heights obtained when different metal ions were injected into EDTA were shown to depend on the EDTA concentration, pH and EDTA complex stability. In this present study, the ligand in the stream is varied; citric acid, ethylenediamine, triethylenetetramine, glutamic acid, and iminodiacetic acid are examined as well as EDTA. The effect of injecting metal ions into these ligand carrier streams is reported, and the measured peak heights are correlated with Nernstian theory for calculating expected peak-height data based on dispersion and stability of the complexes formed in the stream. It is concluded that the use of weakly complexing ligands in the carrier stream has advantages over the use of the EDTA ligand.

EXPERIMENTAL

Instrumentation

A flow cell with a copper wire electrode used in flow-injection measurements was described previously [10]. In steady-state measurements of the electrode response to copper-complexing ligands, a saturated calomel electrode was placed in the waste container down-stream from the flow cell. A manifold of the flow system is shown in Fig. 1. Flow rates used are given in the text. Steady-state measurements were made in the same manifold, using one pump line for the buffer solution and the other for the solutions of ligands. A peristaltic pump (Gilson type Minipuls 2) fitted with ElKay PVC tubing was used to control flow rates and was connected to a home-made rotary injection valve with a 75- μ l sample loop. The outlet of the injection valve was connected through a teflon T-connector to the flow cell via teflon tubing of 0.5-mm internal diameter. The wire electrodes and tubing in the flow cell and injection valve were mounted with Omnifit plastic connectors.

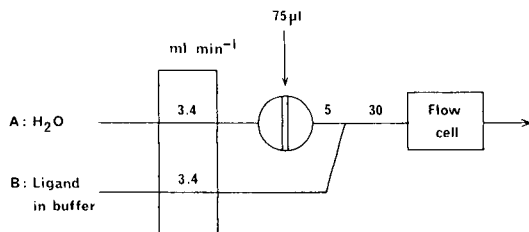


Fig. 1. Manifold of the flow system used in flow-injection determinations of metal ions.

The liquid chromatographic equipment consisted of a model M45 solvent pump and model U6K injector (Waters Associates, Milford, MA, U.S.A.). The column used was a Wescan (Santa Clara, CA) low-capacity, silica-based cation-exchange column (type 269-004; 250 × 4.6 mm i.d.).

Potentiometric data were recorded with a Radiometer PHM 62 pH/millivolt meter interfaced to a Houston Instruments Omniscrite strip-chart recorder, type EB 5117-5-S. Solution pH readings were measured with an Orion model 701A digital mV/pH meter fitted with a combination pH glass electrode.

Prior to use, the copper wire electrode was removed from the cell, briefly immersed in concentrated nitric acid and then rinsed with distilled water. The flow cell was then reassembled and carrier solution, or eluent in chromatographic measurements, was pumped through the cell until a stable baseline potential was attained.

Reagents

Metal nitrates were obtained from May and Baker, except for uranyl nitrate from Hopkin and Williams and manganese nitrate from Merck.

Buffer solutions were prepared from analytical-reagent grade potassium dihydrogenphosphate, sodium hydroxide, sodium acetate and anhydrous acetic acid (Ajax Chemicals, Sydney, Australia).

Ligands used in carrier solutions and eluents were obtained from various manufacturers: citric acid (Merck), EDTA disodium salt and ethylenediamine (May and Baker), triethylenetetramine (Trien; BDH Chemicals), L-glutamic acid (Koch-Light) and the disodium salt of iminodiacetic acid (IDA; Eastman Organic Chemicals).

All solutions were prepared in distilled deionised water. Carrier solutions and eluents for chromatographic measurements were filtered through a 0.45- μ m membrane filter. All solutions were degassed at a water suction pump.

RESULTS AND DISCUSSION

The principle of these indirect flow-injection determinations

The fundamental assumption concerning the copper electrode response characteristics is that a Nernstian relationship controls the potential dependence of the electrode potential on the concentration of ligand used in the carrier solution. The Nernstian range, however, is limited by two factors: (1) by the presence of oxygen in the solutions; and (2) by the strength of the copper/ligand complex which may decrease the electrode potential below the value at which solvent decomposition occurs, with formation of a mixed corrosion potential.

In the two-line manifold with excess of ligand in the stream approaching the detector, the relationship between peak height (H) and total concentration (C_M^0) of metal ions in the injected sample is given by the expression [11]

$$1 - 10^{H/S} = C_M^0 / (C_L^0 D) \quad (1)$$

where S is the slope of the electrode response, C_L^0 is the total concentration of ligand L in the carrier solution, and D is the dispersion coefficient expressing the dilution of the sample zone during transport to the detector and in the detector. In a single-line manifold, local dilution of the ligand occurs in the stream after injection, and from Eqn. 1 the following expression can be derived [10]

$$1 - 10^{H/S} = 1/D + C_M^0 / (D_L^0 D) \quad (2)$$

When a relatively weak complex ML is formed, however, the concentration of ligand C_L in the stream reaching the detector should be expressed by

$$C_L = C_L^0 - C_M^0 / D + [L]' \quad (3)$$

where $[L]'$ is the ligand concentration resulting from dissociation of complex ML . This concentration can be derived from the conditional stability constant as follows

$$K'_{ML} = (C_M^0 / D - [L]') / [L]' C_L \quad (4)$$

From Eqns. 3 and 4 the ligand concentration then becomes

$$C_L = C_L^0 - C_M^0 / D + C_M^0 / D (1 + K'_{ML} C_L) \quad (5)$$

When $[L]' \ll C_M^0 / D$, then $1 + K'_{ML} C_L \approx K'_{ML} C_L$. This approximation does not hold when $1/K'_{ML} > C_L$. The peak height (H) in flow-injection measurements can now be calculated from the difference between the initial ligand concentration (C_{DL}^0) and the value (C_L) calculated from Eqn. 5:

$$H = S \log C_L^0 - S \log C_L = S \log (C_L^0 / C_L) \quad (6)$$

Equation 5 shows that the value of the conditional stability constant, K'_{ML} , affects the observed peak height when the complex dissociates.

An illustration of this effect is provided by the results of model calculations presented in Fig. 2, where calculated peak heights (A) and the values of the expression $F = 1 - 10^{H/S}$ (B), are plotted versus metal ion concentrations in the injected samples, for different values of the conditional stability constant. The results obtained indicate that, for $K'_{ML} > 10^5$, peak heights do not depend on the conditional stability of the complex formed, but decrease when less stable complexes are formed. When very weak complexes are formed ($\log K'_{ML} < 3$), one can expect a linear relationship between peak height and metal concentration. Furthermore, at conditional stability constants lower than 10^5 , a linear calibration cannot be obtained for the dependence of function F on metal ion concentrations in the injected samples (Fig. 2B).

Steady-state electrode response towards ligands used

The choice of a ligand which exhibits reproducible Nernstian response in measurements with a copper electrode is required for indirect potentiometric

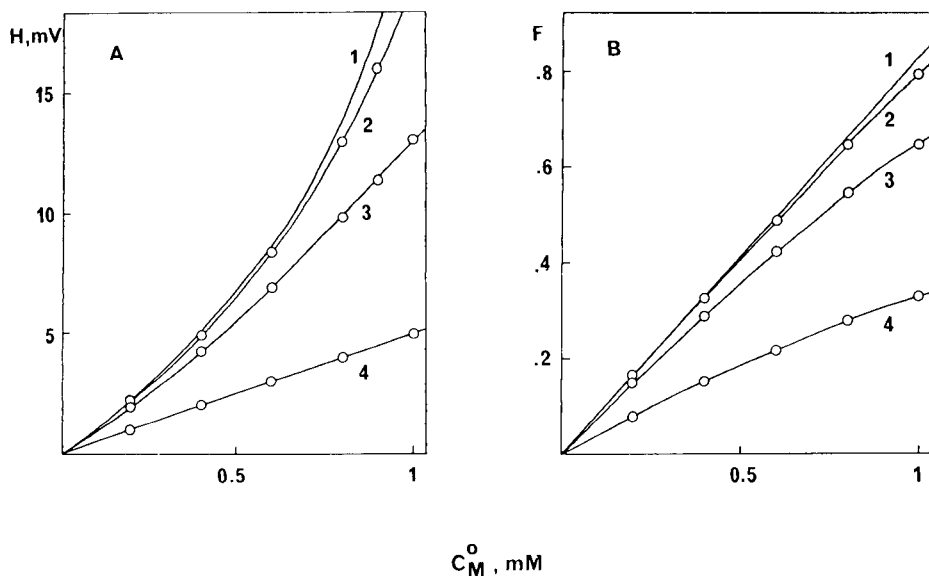


Fig. 2. Effect of the conditional stability constant of the metal complex on calculated peak height (A) and calibration function (B) in flow-injection determination of metal ions. Calculations were done for $C_L^0 = 1 \text{ mM}$, $D = 1.2$, $S = 29 \text{ mV}$, assuming negligible dissociation of formed complex (curve 1) and for $\log K_{ML}^0 = 5$ (curve 2), 4 (curve 3) and 3 (curve 4).

determination of metal ions. In recent papers [9, 10], such behaviour has been demonstrated for several inorganic and organic species such as halides, pseudohalides, amino acids and complexones. In the present study on the effect of conditional complex stability on indirect determinations of metal ions, several ligands that show differences between the complex stability with copper and other metal ions have been taken into consideration.

The electrode response towards these ligands was examined in steady-state continuous flow measurements for ligand concentrations ranging from 10^{-3} to 10^{-5} M . The flow system schematically shown in Fig. 1 was used, the ligand solutions were merged with buffer solution of appropriate concentration, and the pH and steady-state response for each ligand concentration were recorded. The result of these measurements are shown on Fig. 3. Relatively weakly complexing ligands such as IDA (curve 1 on Fig. 3A) or citrate [12] in diluted phosphate buffer show a Nernstian relationship between the electrode potential and ligand concentration. For EDTA, which was used in preliminary studies [11], the copper electrode potential depends significantly on the medium selected. In acetate and phosphate buffers, stable potential readings with slope close to Nernstian for divalent ions were obtained for concentrations of 10^{-3} to 10^{-4} M (Fig. 3B). However, in ammonia buffer, after change of EDTA concentration, stable potential readings were not obtained; not surprisingly, there are corrosion processes in

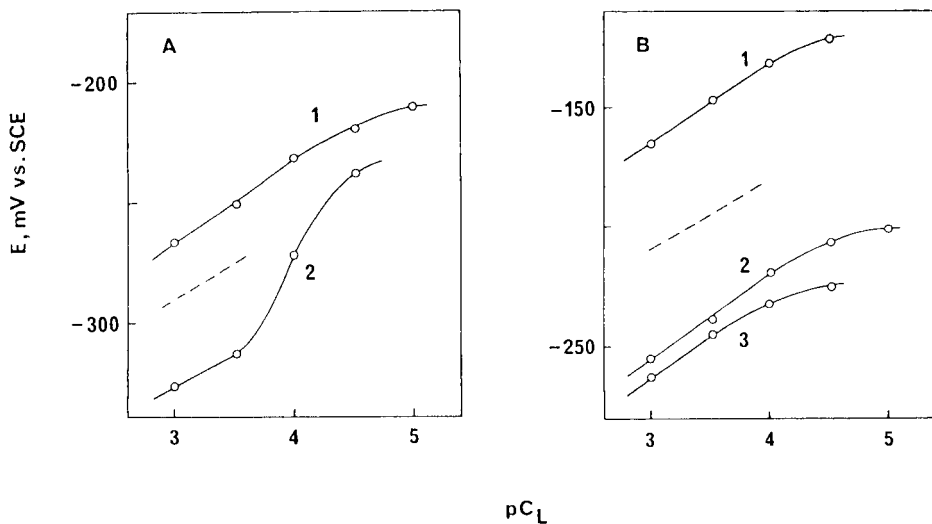


Fig. 3. Calibration curves obtained for various ligands in a continuous flow system. (A) IDA and Trien: (1) IDA in 0.01 M phosphate buffer, pH 8.0; (2) Trien in 0.1 M phosphate buffer, pH 8.0. (B) EDTA in (1) 0.1 M acetate buffer, pH 4.4; (2) in 0.1 M phosphate buffer, pH 6.8; (3) in 0.1 M phosphate buffer, pH 8.0. Dashed lines represent theoretical divalent Nernstian slope.

such a strongly complexing environment. In the case of another strongly complexing agent, Trien, stable potential readings in phosphate buffer were obtained, but Nernstian slope was found for ligand concentrations only below $pC_L = 3.5$ (Fig. 3A, curve 2).

Flow-injection determination of metal ions

The above conclusions on the dependence of peak height on complex stability are confirmed by the experimental results obtained, but several other conclusions can also be made. Peak heights obtained experimentally (Fig. 4) can be correlated with calculated values of conditional stability constants for EDTA complexes (Table 1) or calculated values of the side-reaction coefficient $\alpha_{M(L)}$ for other ligands studied for cations forming more than one complex with the given ligand (Table 2).

For EDTA, with both buffers used, peak heights for various cations differ very slightly when $K'_{ML} > 5$, except for aluminium, which is known to involve slow kinetics during complex formation. The same explanation can be applied to the low peaks observed for Ni^{2+} in phosphate buffer. Examples of typical peaks recorded for Cd^{2+} in acetate buffer containing EDTA are shown in Fig. 5. A linear relationship between function F and concentration was obtained up to 0.7 mM Cd^{2+} .

Citrate and iminodiacetate (IDA) form much weaker complexes than EDTA with many metal ions. Calculated values of $\log \alpha_{M(L)}$ for citrate (Table 2) show only moderate complexation of copper (II) and uranyl

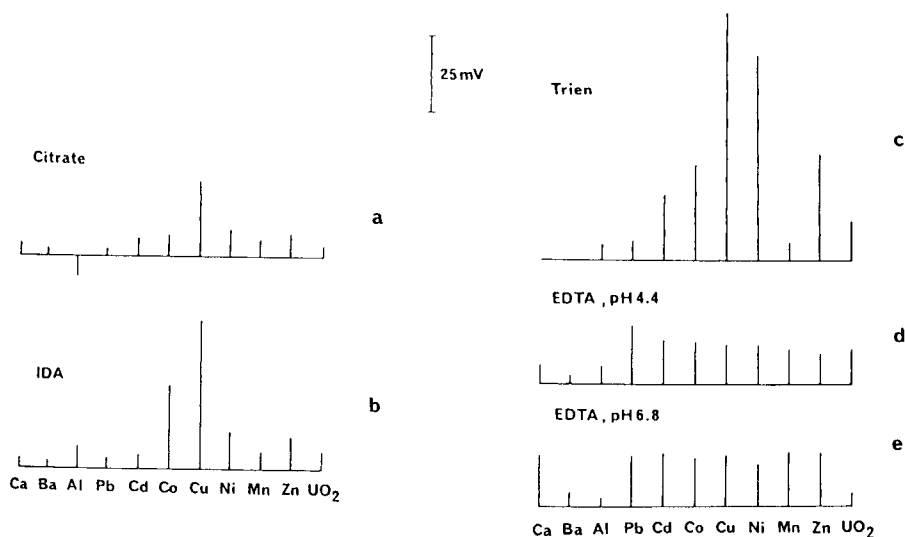


Fig. 4. Peak heights (mV) obtained from injections of 75 μ l of 1 mM metal ion solutions using various 1 mM ligand solutions in different buffers into line B of the manifold shown in Fig. 1: (a) citrate in 0.01 M phosphate buffer, pH 6.0; (b) IDA in 0.01 M phosphate buffer, pH 8.0; (c) Trien in 0.1 M phosphate buffer, pH 8.0; (d) EDTA in 0.1 M acetate buffer, pH 4.4; (e) EDTA in 0.1 M phosphate buffer, pH 6.8.

TABLE 1

Calculated values of logarithms of conditional stability constants for EDTA complexes. Stability constants taken from [13]

Metal ion	0.05 M Acetate pH 4.4	0.05 M Phosphate pH 6.8	Metal ion	0.05 M Acetate pH 4.4	0.05 M Phosphate pH 6.8
Ca ²⁺	3.0	6.9	Co ²⁺	8.6	12.0
Ba ²⁺	0.6	4.3	Cu ²⁺	10.9	13.5
Al ³⁺	8.8	8.9	Ni ²⁺	10.9	14.3
Pb ²⁺	9.7	8.1	Mn ²⁺	6.2	10.4
Cd ²⁺	8.6	12.8	Zn ²⁺	8.8	12.0

ions. Low peak heights, therefore, should be expected and were observed (Fig. 4a). Distinctly higher peaks for copper(II) ions can be attributed to direct electrode response to uncomplexed copper(II) ions rather than to the indirect response. An interesting and reproducible anomaly was found for aluminium. Injection of aluminium nitrate solutions into a citrate/phosphate buffer carrier solution initially produced a small positive peak and then a much larger negative peak (Fig. 6). With the copper metal electrode, a negative potential change can be caused by a local increase in ligand concentration in the carrier stream or by a local increase in hydroxide concentration when the buffer capacity is insufficient. Only the latter cause seems to be possible in the case of aluminium. This was confirmed by a decrease in

TABLE 2

Calculated values of logarithms of side-reaction coefficients $\alpha_{M(L)}$ for $C_L = 5 \times 10^{-4}$ M. Stability constants taken from [13]

Metal ion	Citrate pH 6.0	IDA pH 8.0	Trien pH 8.0	Metal ion	Citrate pH 6.0	IDA pH 8.0	Trien pH 8.0
Ca ²⁺	0.3	0	—	Cu ²⁺	2.4	7.3	19.3
Ba ²⁺	0.1	0	—	Ni ²⁺	1.9	4.8	8.1
Al ³⁺	—	5.7	—	Mn ²⁺	0.8	—	0.1
Pb ²⁺	0.7	2.7	4.6	Zn ²⁺	1.5	3.3	6.2
Cd ²⁺	0.5	1.3	4.8	UO ₂ ²⁺	3.9	4.3	—
Co ²⁺	1.5	3.0	5.2				

the negative peak height with increase in phosphate buffer concentration and the appearance of a small positive peak at pH 3.0. The negative peak increased at pH 5.0 (minimum of buffering capacity for phosphate buffer) but decreased at pH 6.8. Such response can be attributed to complex reactions of aluminium

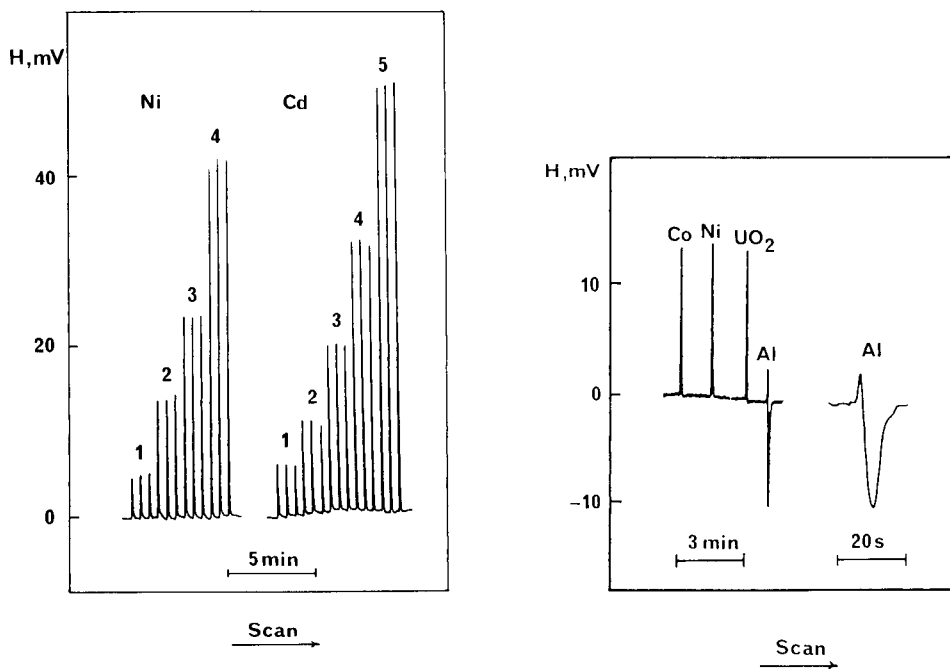


Fig. 5. Peaks obtained in flow-injection determination of Ni²⁺ with 1 mM Trien in 0.1 M phosphate buffer, pH 8.0, and Cd²⁺ with 0.5 mM EDTA in 0.2 M acetate buffer, pH 4.4. Concentration of injected metal ion solutions: (1) 0.2, (2) 0.4, (3) 0.6, (4) 0.8 and (5) 1.0 mM.

Fig. 6. Typical peaks observed for injection of metal ion solutions (Co²⁺, Ni²⁺, UO₂²⁺, Al³⁺) with 1 mM citrate in 0.01 M phosphate buffer, pH 5.0, as ligand/buffer stream.

forming hydroxy complexes, $\text{Al}(\text{OH})_n\text{L}$, with citrate [14]. The shape of the observed signal can be explained by fast addition of citrate to the hydroxide complex, $\text{Al}(\text{OH})^{2+}$ (positive peak), followed by slower release of hydroxide, responsible for the negative peak.

In many cases, small peak heights were also observed for metal ions injected into IDA in phosphate buffer at pH 8.0 (Fig. 4b), even though calculated values of side-reaction coefficients show strong complexation. However, cobalt(II) ions showed a larger potential change than Ni^{2+} , Al^{3+} or uranyl ions, despite the stronger complexation of these metal ions, because of the importance of kinetic factors in such fast flow-injection measurements. Although these lower signals can be utilized for analytical purposes, the sensitivity is very poor. The significantly larger peak potentials observed for Cu^{2+} and IDA in comparison with EDTA can be explained by the formation of both 1:1 and 1:2 complexes with IDA, causing larger ligand consumption and leading to mixed indirect and/or direct response of the electrode towards copper ions. Typical peaks recorded with IDA for Co^{2+} and Cu^{2+} are shown in Fig. 7. Calibration plots showed a linear relationship between

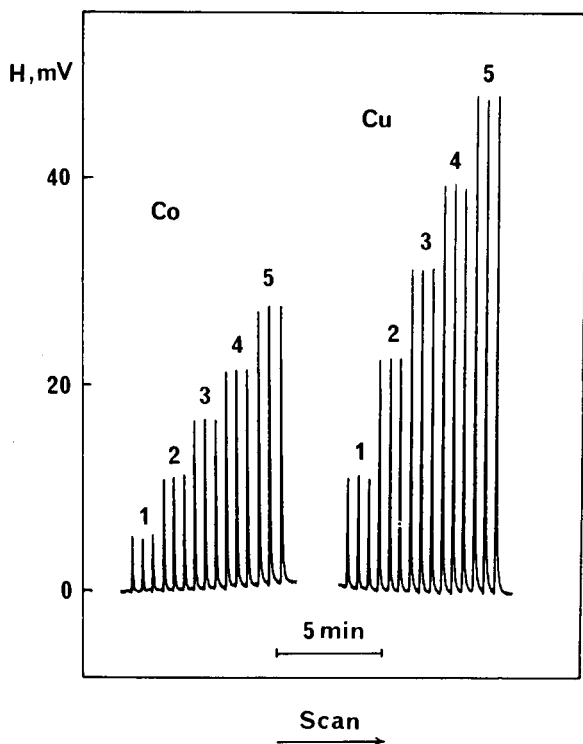


Fig. 7. Peaks obtained in flow-injection determinations of Co^{2+} and Cu^{2+} , with 1 mM IDA in 0.01 M phosphate buffer, pH 8.0. Concentration of injected metal ion solutions: (1) 0.2; (2) 0.4; (3) 0.6; (4) 0.8 and (5) 1.0 mM.

peak heights and concentration up to 0.6 mM for Co^{2+} and up to 0.5 mM for Cu^{2+} .

The dependence of peak height on the stability of the complexes formed can also be observed for carrier solutions containing Trien (Fig. 4c). The larger peak heights recorded in comparison to EDTA can be explained by an increase in the slope of the electrode response towards Trien when the Trien concentration is decreased (Fig. 3A). Examples of peaks recorded for determination of nickel(II) ions are shown in Fig. 5. The relationship between peak height and concentration was non-linear in the working concentration range, while the calibration plot of function F vs. concentration was linear up to 0.4 mM Ni^{2+} .

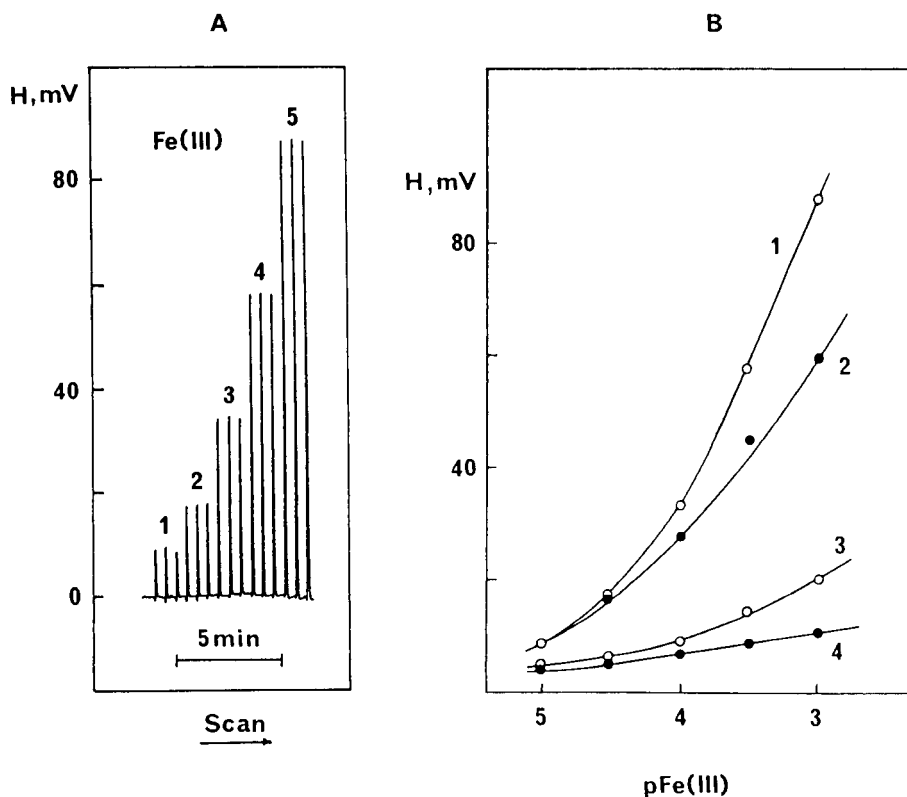


Fig. 8. (A) Peaks recorded in the flow-injection determination of Fe(III) in 0.1 M acetate buffer, pH 4.4, with 1 mM EDTA. Iron(III) concentration in injected solutions: (1) 0.01; (2) 0.03; (3) 0.1; (4) 0.3 and (5) 1.0 mM. (B) Calibration plots obtained in flow-injection determination of Fe(III) with different ligand/buffer streams: (1) 0.1 mM acetate buffer, pH 4.4, with 1 mM EDTA present; (2) the acetate buffer alone; (3) 0.1 M phosphate buffer, pH 6.8, with 1 mM EDTA; (4) the phosphate buffer alone. A flow rate of 3.4 min^{-1} was used in each line of the manifold.

Oxidation mechanism

Larger peak heights were observed for injections of iron(III) ions into acetate buffer stream in comparison with other metal ions. This suggests that a different mechanism controls the electrode response. Figure 8A shows typical peaks obtained; the peaks result from direct oxidation of copper metal rather than from indirect compleximetric response. A similar mechanism has been reported in the chromatographic detection of chlorate, bromate and iodate [15]. The reaction can be attributed to the equilibrium $\text{Fe(III)L} + \text{Cu} \rightleftharpoons \text{CuL} + \text{Fe(II)L}$, where the equilibrium constant increases with an increase in the conditional stability of the CuL and Fe(II)L complexes, but decreases with an increase in stability of the iron(III) complex. In the absence of EDTA, peaks observed in acetate buffer were higher than in phosphate, because of the much higher stability of phosphate complexes of iron(III) compared with those of copper(II).

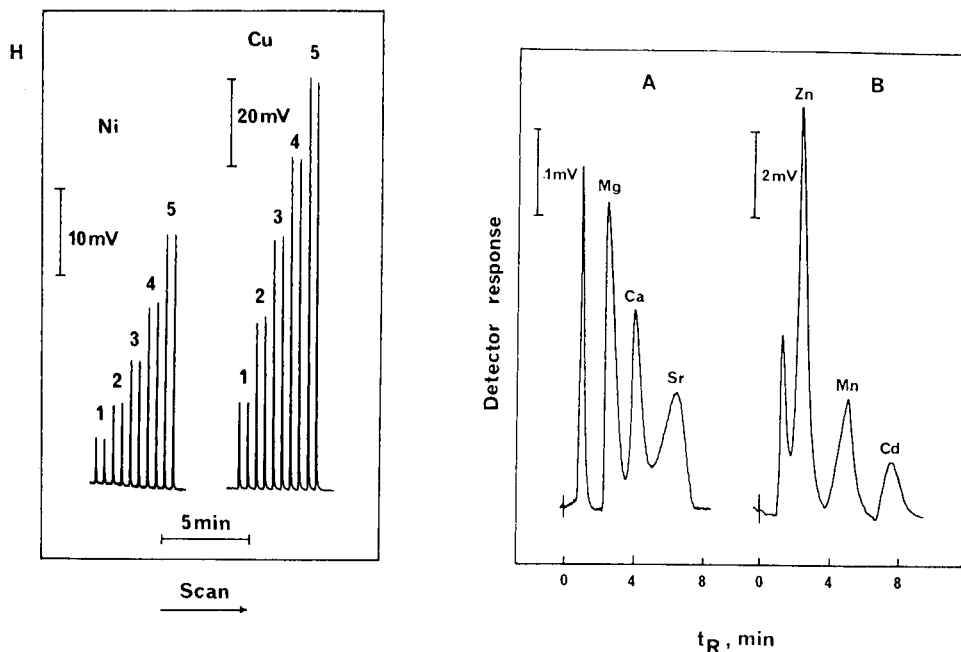


Fig. 9. Peaks recorded for injections of Ni^{2+} and Cu^{2+} , with a solution of 1 mM sodium citrate (pH 6.0) containing 0.1 M NaNO_3 in line B of the manifold shown in Fig. 1. Concentration of metal ions in injected samples: (1) 0.2; (2) 0.4; (3) 0.6; (4) 0.8 and (5) 1.0 mM.

Fig. 10. Chromatograms obtained for tri-component mixtures with a Wescan 269-004 cation-exchange column. (A) Separation of Mg, Ca and Sr with 0.1 M glutamate/1 mM ethylenediamine, pH 7.6, as eluent; flow rate 0.5 ml min^{-1} ; injected volume $20 \mu\text{l}$. (B) Separation of Zn, Mn and Cd with 0.5 mM citrate/0.5 mM ethylenediamine, pH 4.6, as eluent; flow rate 0.4 ml min^{-1} ; injected volume $10 \mu\text{l}$. Injected amounts: 80 nmol Mg, 50 nmol Ca, 25 nmol Sr; 10 nmol each of Zn, Mn and Cd.

Chromatographic applications of indirect detection of cations

The flow-injection measurements described above were usually obtained in buffered media. Such measurements for nickel and copper(II) ions in unbuffered media are shown in Fig. 9; 0.1 M sodium nitrate was added to the citrate carrier solution in order to decrease the noise level observed when 1 mM sodium citrate solution alone was used. Table 3 shows that peak heights from an unbuffered solution of 1 mM citrate were much higher than those from the buffered solution. The observed potential changes may be influenced by local pH changes in the stream, caused by release of hydrogen ions during complex formation and by acidification of the carrier solution from the injected sample (e.g., for Al^{3+}).

A serious disadvantage of indirect flow-injection determinations is their poor selectivity, analogously to indirect compleximetric titrations. For practical analytical application of such a detection system, chromatographic separation of cations seems essential. In chromatography with a single column, a large excess of buffering species generally detracts from resolution. The concentration of ligand must be low and the ligand serves simultaneously as eluent and as the reagent necessary for the indirect detection. In chromatographic measurements, however, the acid effect discussed above influences the size of the void peak but does not affect the peaks for species retained on the column. Sample chromatograms of three-component mixtures obtained with a low-capacity cation-exchange column (Wescan 269-004) are shown in Fig. 10; similar chromatograms have been discussed in detail elsewhere [12].

CONCLUSIONS

The peak heights obtained in indirect flow-injection determinations of cations with a copper electrode depend on the electrode response to the

TABLE 3

A comparison of peak heights obtained for injections of cation solutions (75 μl ; 1 mM) into a stream of distilled water merged with unbuffered 1 mM citrate solution or a buffered solution containing 1 mM citrate and 0.01 M phosphate. The pH of both solutions was 6.0

Metal ion	Peak height (mV)		Metal ion	Peak height (mV)	
	Unbuffered solution	Buffered solution		Unbuffered solution	Buffered solution
Ca^{2+}	12	4.3	Cu^{2+}	97	24
Ba^{2+}	9.0	2.5	Ni^{2+}	30	8.6
Al^{3+}	51	-6.0	Mn^{2+}	16	6.0
Pb^{2+}	31	2.3	Zn^{2+}	30	7.7
Cd^{2+}	26	6.2	UO_2^{2+}	40	3.4
Co^{2+}	27	7.2			

ligand used in the carrier solution and on the stability of the metal complexes formed. In some cases, small potential changes are caused by slow complex formation. The use of ligands which strongly complex copper ions is subject to interference from oxygen; increased peak heights are due to corrosion processes. In measurements with EDTA and Trien it was essential to remove oxygen from both the carrier and injected solutions. Because of the effect of oxygen, the use of moderately complexing ligands is more favourable, although this leads to a decreased sensitivity.

REFERENCES

- 1 E. P. Serjeant, *Potentiometry and Potentiometric Titrations*, Wiley, New York, 1984, Chap. 5.
- 2 J. W. Ross and M. S. Frant, *Anal. Chem.*, 41 (1969) 1900.
- 3 M. Mascini, *Anal. Chim. Acta*, 56 (1971) 316.
- 4 A. Hulanicki and M. Trojanowicz, *Talanta*, 23 (1976) 503.
- 5 A. Hulanicki and M. Trojanowicz, *Talanta*, 16 (1969) 225.
- 6 I. Sekerka and J. F. Lechner, *Anal. Lett.*, A11 (1978) 415.
- 7 G. J. M. Heijne and W. E. van der Linden, *Anal. Chim. Acta*, 96 (1978) 13.
- 8 P. W. Alexander and C. Maitra, *Anal. Chem.*, 53 (1981) 1590.
- 9 P. W. Alexander, P. R. Haddad and M. Trojanowicz, *Anal. Chem.*, 56 (1984) 2417.
- 10 P. W. Alexander, P. R. Haddad and M. Trojanowicz, *Anal. Chim. Acta*, 171 (1985) 151.
- 11 P. W. Alexander, M. Trojanowicz and P. R. Haddad, *Anal. Lett.*, 17(A4) (1984) 309.
- 12 P. R. Haddad, P. W. Alexander and M. Trojanowicz, *J. Chromatogr.*, 294 (1984) 397.
- 13 R. M. Smith and A. E. Martell, *Critical Stability Constants*, Plenum Press, New York, 1976.
- 14 C. Bertin-Natsch, *Ann. Chim.*, 7 (1952) 481.
- 15 P. R. Haddad, P. W. Alexander and M. Trojanowicz, *J. Chromatogr.*, 321 (1985) 363.

Short Communication

EFFICIENT APPLICATION OF NON-LINEAR TRANSFORMATION OF FACTORS IN EMPIRICAL MODELLING BASED ON EXPERIMENTAL DESIGNS

P. KOŚCIELNIAK and A. PARCZEWSKI*

Department of Analytical Chemistry, Jagiellonian University, Kraków (Poland)

(Received 9th May 1985)

Summary. A method is proposed for selecting the best transformation of factors in empirical modelling based on experimental design. Linear, parabolic, power, exponential, hyperbolic and logarithmic transformations were tested. The example used concerns the interference effect of titanium in the flame atomic absorption spectrometry of calcium. Hyperbolic or logarithmic transformation of the titanium concentration provided the closest approximation of the experimental results by linear or second-degree polynomial models. Selection of the best parameter in the transformation functions is also discussed.

It has been shown [1–3] that the efficiency of design of experiments as well as empirical modelling can be improved significantly if the following generalized polynomial model \hat{R} is applied in approximation of the relationship between an analytical signal R (or its function) and the concentration of n sample components, c_1, \dots, c_n :

$$\hat{R} = B_0 + \sum_{i=1}^n B_i \tilde{c}_i + \sum_{\substack{i,j=1 \\ (i \leq j)}}^n B_{ij} \tilde{c}_i \tilde{c}_j + \dots \quad (1)$$

where B is a regression coefficient evaluated on the basis of measurements made on standard samples with compositions selected according to a preset plan, e.g., 2^n factorial [4]. The functions (transformations of concentrations), $\tilde{c}_i = f_i(c_i)$, should satisfy the following coding conditions:

$$\tilde{c}_i = f_i(c_i^{(l)}) = -1, \tilde{c}_i = f_i(c_i^{(u)}) = 1, \tilde{c}_i = f_i(c_i^*) = 0 \quad (2)$$

where $c_i^{(l)}$ and $c_i^{(u)}$ denote the lower and upper levels of concentration c_i in the plan, and $c_i^{(l)} < c_i^* < c_i^{(u)}$. Some examples of functions \tilde{c} (index i has been omitted) are as follows:

linear

$$\tilde{c} = (c - c^{(o)})/\Delta c, \Delta c = (c^{(u)} - c^{(l)})/2, c^{(o)} = (c^{(u)} + c^{(l)})/2 \quad (3)$$

parabolic

$$\tilde{c} = [q(c^{(u)} - c^{(l)})(c - c^{(u)})(c - c^{(l)}) + 2c - c^{(u)} - c^{(l)}]/(c^{(u)} - c^{(l)}) \quad (4)$$

exponential

$$\bar{c} = [2 \exp(qc) - \exp(qc^{(u)}) - \exp(qc^{(l)})] / (\exp(qc^{(u)}) - \exp(qc^{(l)})) \quad (5)$$

hyperbolic

$$\bar{c} = [2c - c^{(u)} - c^{(l)} + q(c^{(u)} - c^{(l)})] / [q(2c - c^{(u)} - c^{(l)}) + c^{(u)} - c^{(l)}] \quad (6)$$

logarithmic

$$\bar{c} = \log_q \{ [(q^2 - 1)(c - c^{(l)}) + c^{(u)} - c^{(l)}] / q(c^{(u)} - c^{(l)}) \} \quad (7)$$

power

$$\bar{c} = [2c^q - c^{(u)q} - c^{(l)q}] / (c^{(u)q} - c^{(l)q}) \quad (8)$$

The parameter q is related to concentration c^* according to the coding condition (2), i.e., the relationship between q and c^* can be obtained by substituting 0 for \bar{c} and c^* for c in formulae 4–8. For these non-linear functions 4–8, the concentration c^* does not correspond to the geometrical centre of the plan applied.

The adequacy of a polynomial empirical model (Eqn. 1) depends strongly on the \bar{c} functions applied as well as on the empirical parameters, q or c^* , in these functions. The aim of the present communication is to show how these two factors influence the quality of approximation of the interference effect, a problem which has already been noted [1–3]. The example chosen concerns the determination of calcium in presence of titanium by atomic absorption spectrometry (a.a.s.).

Experimental

Calcium (4 and 10 $\mu\text{g ml}^{-1}$) was determined in presence of titanium (0–40 $\mu\text{g ml}^{-1}$) with the use of an AAS-1 spectrometer (C. Zeiss-Jena) at 422.7 nm in an air/acetylene flame. The results are presented in Fig. 1.

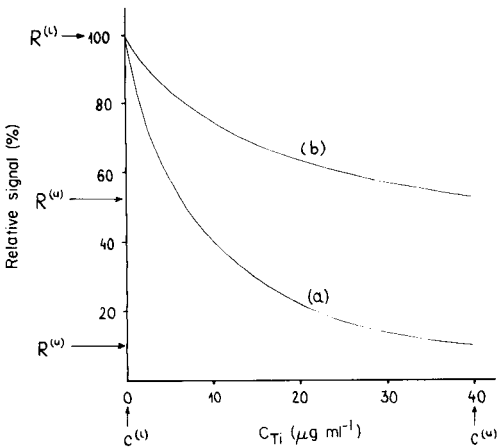


Fig. 1. Experimental effect of titanium on the signal obtained from calcium: (a) 4 $\mu\text{g ml}^{-1}$; (b) 10 $\mu\text{g ml}^{-1}$. R indicates interference (relative signal).

Models

Each curve in Fig. 1 was approximated by the following models (c denotes the concentration of titanium):

$$\hat{R}_1 = B_0 + B_1\tilde{c} \quad (9)$$

$$\hat{R}_2 = B_0 + B_1\tilde{c} + B_{11}\tilde{c}^2 \quad (10)$$

in which functions 3–8 were applied. The coefficients B in these models were calculated on the basis of the experimental results: $R^{(l)}$, $R^{(u)}$ and R^* (read from the curves in Fig. 1) were obtained for $c = c^{(l)} = 0$, $c = c^{(u)} = 40 \mu\text{g ml}^{-1}$ Ti, and $c = c^*$ ($0 < c^* < 40$), respectively. Parameter q in functions \tilde{c} (Eqns. 4–8) was varied and the agreement between the experimental lines in Fig. 1 and the lines calculated from the models was assessed. The mean absolute error was taken as the measure characteristic of model inadequacy:

$$E = \sum_i |R_i(\text{exp}) - R_i(\text{calc})|/39 \quad (11)$$

where the sum covers the experimental, $R(\text{exp})$, and calculated, $R(\text{calc})$, R values obtained for $c = 1, 2, 3, \dots, 38, 39 \mu\text{g ml}^{-1}$ Ti (39 points).

Linear models (Eqn. 9). In this case, only $R^{(l)}$ and $R^{(u)}$ are applied in the calculation of coefficients B ; $c^{(l)} = 0$ and $c^{(u)} = 40 \mu\text{g ml}^{-1}$ Ti make a 2^1 factorial, $B_0 = (R^{(l)} + R^{(u)})/2$, $B_1 = (R^{(u)} - R^{(l)})/2$. Two models were obtained, corresponding to curves (a) and (b) in Fig. 1: $\hat{R}_{1a} = 55 - 45\tilde{c}$ and $\hat{R}_{1b} = 76.25 - 23.75\tilde{c}$, respectively. Figure 2 shows the error (E) of these models, calculated for the various functions \tilde{c} (Eqns. 4–8) as a function of parameter c^* (analogously, E/q curves can be presented because q is explicitly related to c^*). It can be seen that E sharply depends on c^* . Thus without at least some prior knowledge of the shape of curve to be approximated, it is diffi-

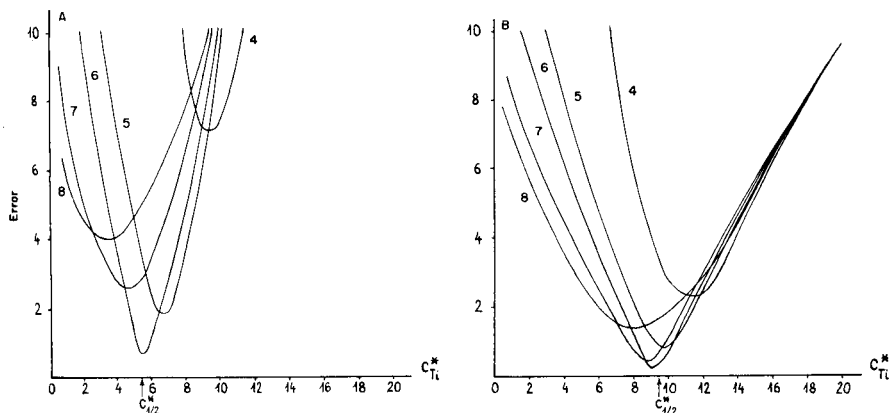


Fig. 2. Dependence of the model error (E) on parameter c^* in functions 4–8 (as indicated by the numbers on the curves) applied to the linear models that approximate curves (a) and (b) in Fig. 1: (A) \hat{R}_{1a} ; (B) \hat{R}_{1b} . $c_{1/2}^*$ is the Ti concentration that corresponds to signal $R = (R^{(u)} + R^{(l)})/2$. The model errors are 26.13 and 9.55 when the linear function 3 is applied in models \hat{R}_{1a} and \hat{R}_{1b} , respectively.

cult to select the optimal parameter c^* (or q). However, this disadvantage can effectively be overcome as follows.

In the case of the linear model (9) just discussed, the following fitting procedure [1] can be applied to select a suitable parameter q in a function \tilde{c} ; the model (9) must fit accurately to a selected experimental point (c', R') , i.e., $\hat{R} = R' = B_0 + B_1\tilde{c}'$, where $\tilde{c}' = f(c', q)$, thus the parameter q is calculated by solving this equation. Figure 3 shows the relationship between the model error and the concentration c' ; the error E does not now depend sharply on c' over a broad concentration interval, especially for the hyperbolic and logarithmic functions (curves 6 and 7) which give the best approximation of the experimental lines (Fig. 1).

Parabolic models (Eqn. 10). The coefficients B in this model were calculated on the basis of the experimental results $R^{(l)}$, $R^{(u)}$, and R^* as follows ($c^{(l)} = 0$, $c^{(u)} = 40 \mu\text{g ml}^{-1} \text{ Ti}$, and $c = c^*$ make an unconventional 3^1 factorial): $B_0 = R^*$, $B_1 = (R^{(u)} - R^{(l)})/2$, $B_{11} = (R^{(u)} + R^{(l)})/2 - R^*$. The following models correspond to the experimental data (a) and (b) in Fig. 1, respectively:

$$\hat{R}_{2a} = R^* - 45\tilde{c} + (55 - R^*)\tilde{c}^2$$

$$\hat{R}_{2b} = R^* - 23.75\tilde{c} + (76.25 - R^*)\tilde{c}^2$$

In this case, both the functions \tilde{c} (Eqns. 4–8) and the coefficients B in these two models depend on c^* . In the exceptional case of the linear function (3), c^* is fixed: $c^* = c^{(o)}$ (see Eqn. 2); in the example given, $c^{(o)} = 20 \mu\text{g ml}^{-1} \text{ Ti}$. Figure 4 shows the model error, E . The parabolic model (10) should not have an extreme in the interval, $c^{(l)}$, $c^{(u)}$, as it is used in approximation of monotonic functions (Fig. 1). This is so if $c_l^* \leq c^* \leq c_u^*$, where c_l^* and c_u^* correspond to $R = (3R^{(u)} + R^{(l)})/4$ and $R = (R^{(u)} + 3R^{(l)})/4$, respectively. In the particular case of the parabolic transformation (Eqn. 4), an additional

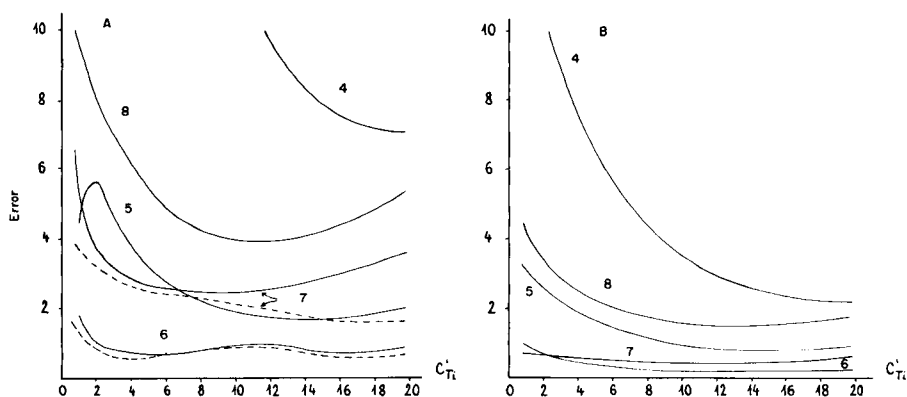


Fig. 3. Dependence of the model error (E) on concentration c' , the abscissa of point (R', c') , to which linear models \hat{R}_{1a} (A) and \hat{R}_{1b} (B) were fitted in order to determine parameter q in functions \tilde{c} . The broken lines correspond to the weighted error E (see Discussion).

condition should ensure that it is monotonic in the interval $(c^{(l)}, c^{(u)})$. Consequently, the interval (c_l^*, c_u^*) becomes quite narrow in this case, e.g., 11.8, 12.6 $\mu\text{g ml}^{-1}$ Ti, if curve (a) in Fig. 1 is considered.

Discussion

Figures 3 and 4 show that the experimental lines which describe typical interference in atomic spectrometry (Fig. 1) can be approximated accurately by a generalized polynomial of low degree if nonlinearly transformed concentration, $\tilde{c} = f(c)$, is applied. The logarithmic and hyperbolic functions \tilde{c} proved to be most suitable. Even the first-degree polynomial seemed much better than the "conventional" parabolic model in which the linear function (3) was applied.

Some practical hints may help in selection of the parameter c^* or q in the applied function $\tilde{c} = f(c; q)$ which should be logarithmic or hyperbolic. In the case of the linear model (Eqn. 9), the determination of q by the fitting procedure described above is recommended. As Fig. 3 shows, the model error is not very sensitive to the point fitted (c') over a broad concentration interval. It should be noted, however, that the minima of the curves in Fig. 2 coincide well with $c_{i/2}^*$, i.e., the parameter $c^* = c_{i/2}^*$ leads to quite satisfactory results, where $c_{i/2}^*$ is the interferent concentration corresponding to $R = (R^{(u)} + R^{(l)})/2$.

In some cases, different parts of the experimental curve to be approximated by the model \hat{R} may have different benefits from the analytical point of view. Then the weighted mean error of the absolute model $E = \Sigma_i w_i |R_i(\text{exp}) - R_i(\text{calc})| / \Sigma_i w_i$, can be applied instead of Eqn. 10. Figure 3 shows E vs. c^* curves which correspond to the hyperbolic and logarithmic functions \tilde{c} : $w_i = 1/\tan \alpha_i$ (reciprocal slope of curve (a) in Fig. 1 at point i). It can be seen that the above hints for selection of parameter c^* are also useful in this case.

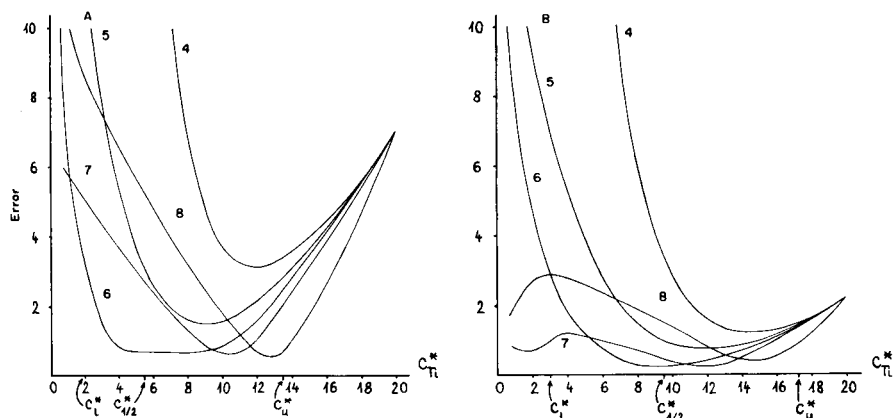


Fig. 4. Dependence of the model error (E) on parameter c^* in functions 4–8 (as indicated on the curves) which were applied in the second-degree models that approximate curves (a) and (b) in Fig. 1: (A) \hat{R}_{2a} ; (B) \hat{R}_{2b} . For c_l^* , c_u^* and $c_{i/2}^*$, see text. The model errors are 7.08 and 2.22 when the linear function 3 is applied in models \hat{R}_{2a} and \hat{R}_{2b} , respectively.

The economy of the approach based on experimental designs should be emphasized; the models considered above were formulated on the basis of only two or three experimental points. The calculation of regression coefficients in the models and the error analysis are simple. These advantages are important, especially when several factors (sample components) have to be taken into account, e.g., when multicomponent systems are considered or multidimensional calibration graphs are prepared [1-3, 5, 6].

The investigations were supported financially within the scope of project M.R.I.32.

REFERENCES

- 1 P. Kościelniak and A. Parczewski, *Anal. Chim. Acta*, 153 (1983) 103.
- 2 P. Kościelniak and A. Parczewski, *Anal. Chim. Acta*, 153 (1983) 111.
- 3 P. Kościelniak and A. Parczewski, *Chem. Anal. Warsaw*, 29 (1984) 685.
- 4 D. L. Massart, A. Dijkstra and L. Kaufman, *Evaluation and Optimization of Laboratory Methods and Analytical Procedures*, Elsevier, Amsterdam, 1978.
- 5 P. Kościelniak and A. Parczewski, *Mikrochim. Acta*, II (1984) 359.
- 6 P. Kościelniak, *Mikrochim. Acta*, II (1984) 369.

Short Communication

**A COMPUTER-CONTROLLED LABORATORY FRACTIONAL
DISTILLATION COLUMN**

J. R. CHIPPERFIELD*, J. R. GREGORY and D. E. WEBSTER

Department of Chemistry, University of Hull, Hull HU6 7RX (Great Britain)

(Received 2nd May 1985)

Summary. A microcomputer (Commodore PET 8032) is used to control a batch mode fractional distillation apparatus, designed for small-scale separations. The column-jacket temperatures, boil-up rate, and reflux ratio are controlled to achieve optimum separation on a 30 theoretical plate column. The system is designed to minimise manual intervention.

Fractional distillation is possibly the most important method for separating liquid mixtures, and large-scale fractional distillation is widely used in the chemical industry. There are two distinct methods of performing fractional distillation [1, 2]. In the continuous process, the liquid mixture is continually introduced into the column and the more volatile component(s) move upwards while the less volatile component(s) move downwards. In batch distillation, the mixture to be fractionated is in a still pot and each component in turn is removed from the head of the column. Continuous distillation is in many ways the simpler of these methods and is widely used industrially. In the laboratory, where small quantities are being distilled, and where the column will probably be used for many different liquid mixtures, the batch method is invariably used. This paper is concerned with such a batch distillation column.

Reports of computer-controlled distillation (see, e.g. [3–5]) concentrate on chemical engineering and large-scale applications. On a laboratory scale, with volumes of feedstock in the 25–100 cm³ range, fractional distillation is not popular, as it is difficult to set up the correct conditions for the fractionation column to operate at a high theoretical-plate efficiency. Three problems arise: (1) it is difficult to control the boil-up rate so that the fractionating column does not flood, and so that the reflux return rate is satisfactory; (2) it is difficult to control the temperature of the heating jacket surrounding the fractionation column so that local boiling or local condensation does not occur, with catastrophic loss of fractionation efficiency; (3) distillation is a slow process and requires continuous attention. All of these problems can be overcome if the column is monitored and controlled by a microcomputer. Here, a Commodore 8032 microcomputer

is used to adjust the boiling rate, the temperatures of the column jacket, and the reflux/take-off ratio for optimum separations over a wide range of temperatures. As well as acting as a controller, the computer also monitors the distillation process and displays a schematic diagram of the distillation apparatus showing the temperatures at the still pot and the condenser.

Equipment and control

Apparatus. A schematic diagram is shown in Fig. 1. The still pot is typically a 250-cm³ three-necked round-bottomed flask. (Extra necks are needed if still-pot sampling is required.) One side-neck is connected to a pressure transducer (SE 21/V range 5D), the centre neck is connected to the fractionation column, and the third neck allows filling and emptying and is also fitted with a temperature sensor to measure the still-pot temperature. The still-pot heater is a 250-W infrared lamp fitted under the pot. This has a very low thermal capacity and allows rapid adjustments in heating rates to be made. The fractionation column is a 1 m × 10 mm i.d. glass tube packed with either 1/16 in. Dixon gauzes or 6-mm diameter glass rings. It is surrounded by a semiconductor glass heating jacket (2.7 cm diameter). The temperature difference between the fractionation column and the heating jacket is monitored by a 15-junction copper/constantan thermopile (Fig. 2).

An automatic vapour-dividing fractionating head is used. The design (Fig. 1) is similar to model FC21C (J. Bibby Science Products). The solenoid which lifts the vapour splitter is controlled from the computer.

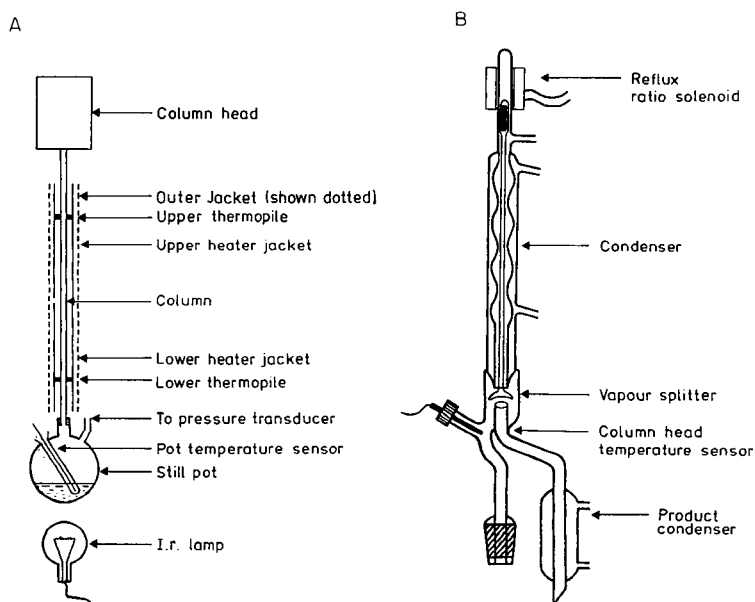


Fig. 1. Schematic diagram of distillation column (A) and column head (B).

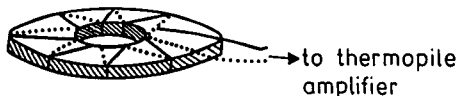


Fig. 2. 15-Junction copper/constantan thermocouple.

Electronics. A block diagram of the electronic circuitry is shown in Fig. 3. The outputs from the various sensors are amplified and passed to an analog/digital converter (ADC). The digital outputs from the ADC's are sent to a series of parallel-in/serial-out shift registers. The outputs from these registers are transmitted in serial form via the CB2 line of the user port of the computer, with the CB1 line supplying the sets of clock pulses required [6, 7]. Similarly, computer output data in serial form is sent on the CB2 line to a series of serial-in/parallel-out shift registers. The user port lines PA0-PA7 are used to control the loading and unloading of these shift registers. The parallel outputs are used to drive digital/analog converters (DAC), and the outputs from these are used to control the column heaters, still-pot heater, etc. To ensure satisfactory control of the still-pot heater and column heaters, the output power must be proportional to the output voltage of the controlling DAC's. This is done by using zero-voltage switches (see sheet 2129, RS Components, Corby, Northants.) which can be used in a proportional control mode. A duty cycle, which can vary from 0.1 s to 100 s according

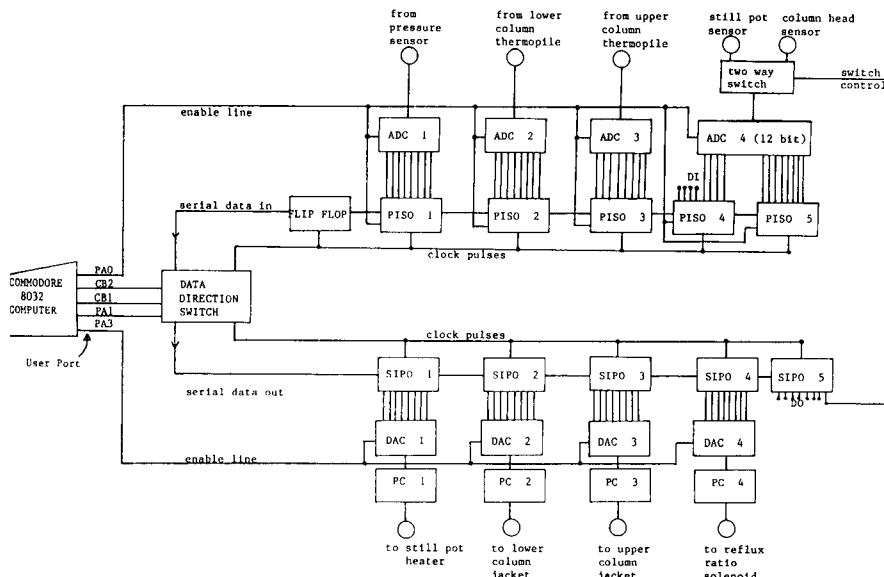


Fig. 3. Block diagram of the electronic circuitry: ADC, analog-digital converter; DAC = digital-analog converter; PISO, parallel-in/serial-out register; SIPO, serial-in/parallel-out register; PC, proportional power controller; DI, spare digital inputs; DO, spare digital outputs.

to the size of a capacitor, is established. During this duty cycle, the mains power is switched off for the first T half-cycles of the a.c. mains; then the power is switched on for the remainder of the cycle. The value of T is set by the size of an analog voltage applied to the zero voltage switch. A duty cycle of about 1 s was chosen. In 1 s the a.c. power is instantaneously at 0 V 100 times. This means the output power can be set anywhere between 0 half-cycle on and 100 half-cycles off to 100 half-cycles on and 0 half-cycle off, giving a resolution of 1 in 100. To use the 1 in 255 resolution available in an 8-bit DAC would require a duty cycle of 255 half-cycles (i.e., 2.55 s). This proportional control also provided a convenient way of controlling the take-off ratio by switching the column-head solenoid on and off for appropriate fractions of a 5-s duty cycle.

Control loops. In this distillation there are three control loops. One uses still-pot pressure as a sensor and controls the still-pot heater. The other two loops sense the temperature difference between the fractionation column and the heating jacket and control the bottom and top jacket heaters. For a control loop, the output is adjusted to produce a minimum value of the difference, E , between the sensor reading and a previously established set point. The output O is best determined by using the three-term or PID control equation:

$$O(\text{new}) = O(\text{old}) + PE + I \int E dt + D dE/dt$$

The constants P , I , and D refer to the proportional, integral and derivative terms in the three-term control [8]. Standard methods are available for setting the optimum values for these three constants [8].

Programming. As far as possible the computer is controlled by BASIC programs. However certain operations, principally the input of serial data, updating the display and scanning the keyboard, must be done quickly and machine-code programs are required. A flow chart for the operational cycle is shown in Fig. 4.

Operation. The operation of the distillation is done automatically as far as possible. For any mixture of components in the still pot, the first action of the computer program is thoroughly to wet the column packing by a rapid boil-up. The still-pot heater is switched to full and rapid boiling is continued until the temperature sensor at the top of the column shows that hot liquid has reached that point. The still-pot heater is then switched off, and then set for control by the pressure sensor. Boil-up rate is controlled by the heater according to the pressure in the still pot. The still-pot heater automatically adjusts its power so that the column pressure corresponds to that for ideal reflux. The whole apparatus is then allowed to equilibrate under total reflux until the temperature at the top of the column has been constant for a suitable period (0.5–2 h). During take-off, the reflux ratio is set to 10 and the fraction is collected until the column-head temperature has risen by a suitable amount (about 1°C). Take-off is then stopped and the operator is requested to change the sampling vessel. (Automatic changing of the collector would be possible, but was not investigated.)

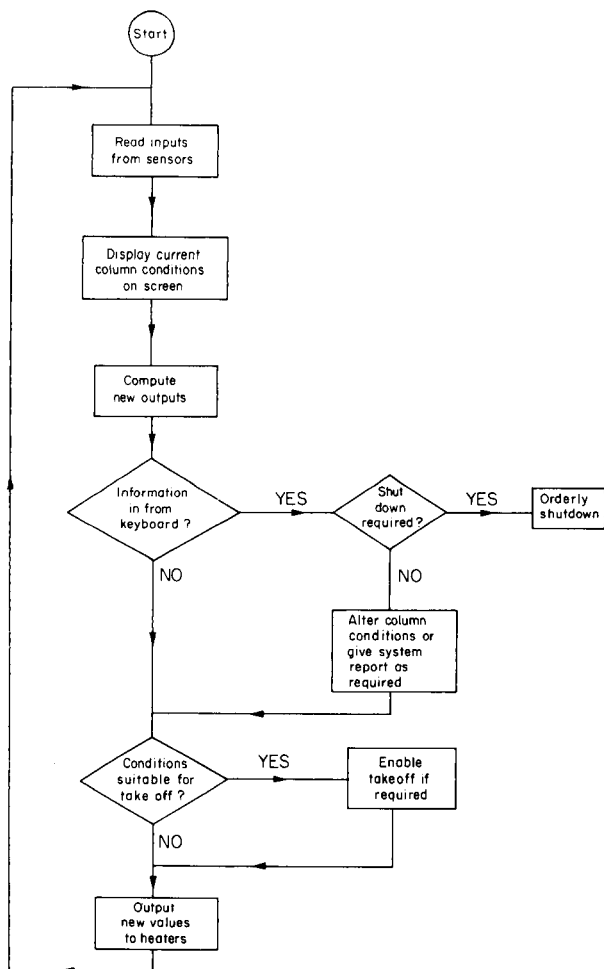


Fig. 4. Simplified flow-chart of operational cycle.

Testing

The system was tested by determination of the number of theoretical plates in the distillation column by the usual method [9]. Two solvent mixtures were used: methylcyclohexane/toluene (boiling range 101–111°C) and chlorobenzene/ethylbenzene (boiling range 132–136°C). The pot and head liquids were examined by gas-liquid chromatography. The column with Dixon gauzes (see above) was shown to have 28 theoretical plates, which is roughly that expected for such a column [1]. The column with glass rings was shown to have 9 theoretical plates. This is in line with the known relative merits of Dixon gauzes and glass rings. The column with glass ring packing was impossible to control by manual adjustment of the heaters, but computer control was so successful that its plate value could be measured readily.

We thank Dr. P. G. Francis (Chemistry Department) for advice on distillation practice, Dr. G. E. Taylor and Dr. P. M. Taylor (Electronic Engineering Department) for advice on control theory, and Mr. M. Bailey for skilled glassblowing.

REFERENCES

- 1 E. Krell, Handbook of Laboratory Distillation Practice, 2nd. edn., Elsevier/North-Holland, New York, 1982.
- 2 E. S. Perry and A. Weissberger (Eds.), Technique of Organic Chemistry, Vol. IV — Distillation, 2nd. edn., Interscience, New York, 1965.
- 3 R. M. Allen and G. Wilson, Nat. Conf. Publ., Inst. Eng. Aust., 79-8 (1979) 46.
- 4 G. A. M. de Bruijn, Polytechnisch Tijdschrift Procestechnik, 36 (1981) 207.
- 5 L. A. Richard and D. B. Greenberg, AIChE Symp. Ser., 75 (1979) 44.
- 6 J. M. Downey and S. M. Rogers, PET Interfacing, Sams, Indianapolis, 1981, pp. 77–88.
- 7 R. C. West, Programming the CBM/PET, Level, London, 1982.
- 8 J. R. Leigh, Applied Control Theory, IEE Control Engineering Series No. 18, Peter Peregrinus, London, 1982.
- 9 E. F. G. Herington, Reference Material for Testing Distillation Columns, NPL Report Chem 55, National Physical Laboratory, Teddington, 1977.

Short Communication

HYDROLYTIC POTENTIOMETRIC TITRATION OF SULPHATE WITH APPLICATION IN THE ANALYSIS OF WATERS

D. DOBČNIK* and D. BRODNJAK-VONČINA

Department of Chemical Engineering, Faculty of Technical Sciences, University of Maribor, Smetanova ul. 17, P.O. Box 24, YU-62000, Maribor (Yugoslavia)

(Received 12th April 1985)

Summary. Sulphate is precipitated with barium ion, and excess of barium is precipitated with chromate, excess of which immediately hydrolyses at the end-point to give a sharp jump in pH, measured with a glass electrode. A 1:1 methanol/water medium is optimal. Application to waters requires pretreatment with a cation-exchange resin. River, potable and mineral waters containing 20–2000 mg l⁻¹ sulphate were analysed accurately with relative standard deviations of 1–2%.

Potentiometric titrations of barium and lead ions with solutions of sodium oxalate and potassium chromate have been reported recently [1, 2]. The general principle of these titrations can be adapted for determining sulphate. Sulphate is precipitated from 1 + 1 water/methanol solution with excess of barium chloride solution, and the excess is titrated with a standard solution of potassium chromate. The initial pH of the solution is 4.0. During the titration, barium chromate precipitates but the pH of the solution is ordinarily unchanged. After the end-point, the excess of chromate hydrolyses: $\text{CrO}_4^{2-} + \text{H}_2\text{O} \rightleftharpoons \text{HCrO}_4^- + \text{OH}^-$. This causes a steep rise in the pH, which can be detected with a glass electrode. The procedure is applicable to samples of mineral, river and drinking waters, after treatment with a cation exchanger.

Experimental

Apparatus and reagents. A digital pH meter (Orion Research; model 701) was used with glass (model 91-01-00) and reference (model 90-01) electrodes. All reagents used were of analytical grade. Solutions of potassium chromate were standardized iodimetrically with sodium thiosulphate, and solutions of barium chloride conductometrically against the chromate solution.

General procedure. The sulphate solution (about 50 ml) in water was heated to boiling with an excess of barium chloride. The cooled solution was diluted with the organic solvent to about 100 ml, the pH was adjusted to the required value, and the excess of barium ions was titrated with a standard potassium chromate solution. The titrant was added at 0.4 ml min⁻¹ from a 10-ml burette (graduated at 0.01 ml intervals). Magnetic stirring was used.

Determination of sulphate in drinking and river waters. The sample of drinking or river water was passed through a column (10 mm diameter, 20 cm high) of Amberlite-120 cation exchanger (H^+ -form) at a speed of 3–4 drops/min. The first 50 ml of effluent was discarded. From the subsequent effluent, 50 ml was transferred to a beaker, heated to boiling, and acidified with 0.1 M hydrochloric acid. Sulphate was precipitated from the hot solution with 5.00 ml of 0.02 M barium chloride. Then 50.00 ml of methanol was added to the cooled solution and the pH was adjusted to 4.0 with 0.1 M hydrochloric acid or sodium hydroxide. The titration was then done, as described above with standard 0.02 M potassium chromate. A blank solution was prepared and titrated in the same way. Calculations were done in the classical manner.

Determination of high contents of sulphate in mineral water. First, carbon dioxide was expelled from the sample by addition of hydrochloric acid. Then 50 ml of sample was evaporated to dryness on a water or sand bath. The residue was dissolved in 3 ml of twice-distilled water and 1 ml of (1 + 3) hydrochloric acid. The solution was filtered through fine filter paper, transferred to a 100-ml volumetric flask and diluted to the mark with distilled water. A 50-ml aliquot of this solution was treated with 10 ml of 0.1 M barium chloride, followed by addition of methanol and adjustment to pH 4.0, all as described above. The solution was titrated with 0.1 M potassium chromate. A blank solution was treated in the same way.

For the determination of sulphate in drinking and river waters, titration of the surplus barium with EDTA [3] was used for comparison. For the determination of high contents of sulphate in mineral water, gravimetry as barium sulphate [4] served for comparison.

Results and discussion

The effects of addition of methanol, acetone and dioxane and the effects of pH, titration speed and diverse ions on the precision of end-point detection were investigated. The effects of methanol, acetone and pH on the titration are shown in Table 1; the 1:1 methanol/water medium with adjustment to pH 4.0 is obviously preferable. When 1,4-dioxane was used, there was no pH jump at the end-point; in the other media, there was a very sharp increase in pH at the end-point, which was evaluated from the intersection of the tangents to the two arms of the curves, as in amperometric titrations. When the methanol/water ratio in the medium was increased from 3:7 to 7:3, the error caused was within 3% (absolute). For precise graphical indication of end-points, the change in slope of the titration curves between the precipitation phase and the hydrolysis phase is important. As the initial pH of the solution titrated increased, the sharpness of the change in slope deteriorated. The maximal change was found in methanolic solutions. On the basis of the results obtained with pure sulphate solutions, the conditions recommended for the titration are a 1:1 water/methanol medium and an initial pH of 4.0.

TABLE 1

The effects of the organic solvent and of the initial pH of the sulphate solution titrated^a

Titration medium	pH	Sulphate found ^b (mg)	Recovery (%)
1:1 Methanol/water	3.0	37.41	82.1
	4.0	45.58	100.1
	5.0	46.34	101.7
1:1 Acetone/water	3.0	37.91	83.2
	4.0	46.24	101.5
	5.0	45.62	101.1
Water	3.0	40.96	89.9
	4.0	49.32	108.3
	5.0	49.06	107.7

^a45.56 mg of sulphate titrated with 0.1 M chromate. ^bMean of 3 runs.

The influence of calcium, nitrate, chloride and orthophosphate ions in the titration of 19.5 mg (0.02 mol) l⁻¹ sulphate was investigated under the optimal conditions. For calcium/sulphate mole ratios > 1, the results for sulphate were low, thus the use of a cation-exchange resin is recommended. At phosphate/sulphate ratios > 0.1, the titration curves were deformed. Nitrate and chloride at mole ratios upto 40 did not affect the titration of sulphate, nor did carbonate pH 4.0.

The results listed in Table 2 show that the proposed method gives good precision and accuracy for a range of waters.

This work was presented at Euroanalysis V, August, 1984, Cracow, Poland.

TABLE 2

Results for sulphate in different types of water

Sample	No. of detns.	Sulphate content (mg l ⁻¹)	
		Proposed method ^a	EDTA titration
River water 1	6	26.0 ± 2.2	25.4
River water 2	6	23.7 ± 1.9	23.1
River water 3	6	37.0 ± 1.7	36.5
Drinking water 1	10	34.6 ± 1.9	34.4
Drinking water 2	10	30.6 ± 1.8	30.5
Mineral water (Donat)	9	2046.4 ± 0.6	2055.6

^aMean with relative standard deviation.

REFERENCES

- 1 D. Dobčnik, *Fresenius Z. Anal. Chem.*, 313 (1982) 411.
- 2 D. Dobčnik, *Croat. Chem. Acta*, 56 (1983) 113.
- 3 R. Sijderius, *Anal. Chim. Acta*, 11 (1954) 28.
- 4 F. P. Treadwell, *Kurzes Lehrbuch der Analytischen Chemie*, 11th edn., F. Denticke, 1943, p. 396.

Short Communication

CONTINUOUS DETERMINATION OF HYDROGEN FLUORIDE IN AIR WITH THE FLUORIDE-SELECTIVE ELECTRODE

KUNIO NAGASHIMA*, YASUTAKA FUJIHIRA and SHIGETAKA SUZUKI

Department of Industrial Chemistry, Faculty of Technology, Tokyo Metropolitan University, Setagaya-ku, Tokyo 158 (Japan)

(Received 5th March 1985)

Summary. Hydrogen fluoride in a standard or sample gas stream at 200 ml min⁻¹ permeates through a teflon membrane (0.8 μm pore size, 0.08 mm thick) into an absorption solution (citrate/acetate buffer at pH 5.4) flowing at 30 ml min⁻¹. The fluoride produced is measured with the fluoride-selective electrode. The response time is about 12 min. The absorption efficiency of hydrogen fluoride is about 70% between 6.5 and 0.25 ppm by volume (5.2 and 0.2 mg m⁻³). In this range, the Nernst equation is valid with a relative standard deviation of less than 1.8%. The lower determination limit for hydrogen fluoride is 0.1 ppm (0.08 mg m⁻³).

In aluminium refining, glass manufacturing and phosphoric acid plants, a lot of hydrogen fluoride is produced as waste. Gaseous hydrogen fluoride is not only harmful to health but also destructive to all materials; the Japanese threshold limit value (time-weighted average) for hydrogen fluoride in working environments is defined as 2.5 ppm (2 mg m⁻³).

Spectrophotometric and ion-selective potentiometric methods are recommended [1] for the determination of hydrogen fluoride in air. The spectrophotometric procedure is based on the conventional reaction of fluoride with eriochrome cyanine R and zirconium in hydrochloric acid. Both methods require the sampling of large volumes of air sample; the recommended sampling time is about 3 h [1]. For poisonous gases in work areas, continuous monitoring based on methods with high sensitivity and selectivity is obviously preferable. The fluoride-selective electrode [2] has very high selectivity for fluoride, and can be considered as providing the best method for the continuous determination [3, 4] of hydrogen fluoride in air [5, 6].

In this study, a membrane permeable to hydrogen fluoride and an absorption solution are used in the continuous determination of hydrogen fluoride with the fluoride-selective electrode.

Experimental

Reagents and equipment. The absorption solution for hydrogen fluoride was prepared by dissolving 4.2 g of trisodium citrate dihydrate in 1 l of water

containing 1.1 ml of acetic acid; the pH of this solution was ca. 5.4. Fluoride standard solutions were prepared by dissolving sodium fluoride, dried for 1 h at 130°C, in the absorption solution. Standard concentrations of hydrogen fluoride (0.1–6.5 ppm) were prepared by using a permeation tube (PD-1B; Gastec Co.; 14, Fig. 1), controlling both the flow rate of nitrogen dilution gas and the temperature of the permeation tube which had an effective length of 5 cm (Gastec Co.). Fluoropore microporous polytetrafluoroethylene (PTFE) membranes (Sumitomo Denko Co.) were used; the pore sizes examined were 0.22, 0.80, 5.0 and 10.0 μm , and the thickness was in the region of 0.06–0.1 mm. The effective surface of the membranes was 38 mm long by 4 mm wide in the filter holder, though the circles were of 47-mm diameter. The fluoride-selective electrode (Denki Kagaku Keiki Co.; Model 7200-IP) was used in combination with a saturated calomel reference electrode. A peristaltic pump (SJ-1211; Atto Co.) was used to pump the absorption solution into the filter holder.

Flow system and membrane filter holder. A schematic diagram of the flow system and the membrane filter holder is shown in Fig. 1. The hydrogen fluoride standard gas mixture prepared with the permeation tube was split in permeation tube 14, one stream being passed into the membrane filter holder and the other being discharged via an absorption tube to remove the hydrogen fluoride waste. The gas containing hydrogen fluoride was introduced into the bottom groove of the filter holder at a constant flow rate of 200 ml min^{-1} . Hydrogen fluoride in the sample gas permeated through the membrane filter into the absorption solution, which was pumped through the top groove of the filter holder at 30 ml h^{-1} . The directions of both

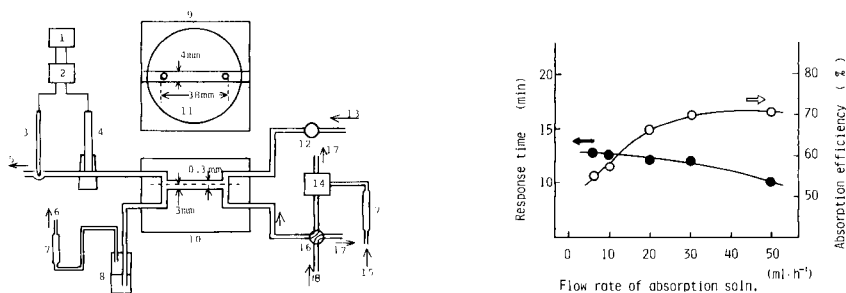
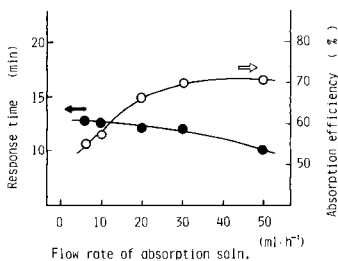


Fig. 1. Schematic diagram of flow system and membrane filter holder: (1) recorder; (2) voltmeter; (3) SCE; (4) working electrode; (5) liquid waste; (6) gas waste; (7) flow meter; (8) absorption tube; (9) top view of filter holder; (10) side view of filter holder; (11) membrane filter; (12) peristaltic pump; (13) absorption solution; (14) permeation tube; (15 and 18) nitrogen; (16) four-way cock; (17) gas waste via absorption tube.

Fig. 2. Effect of flow rate of absorption solution on response time and efficiency for 0.92 ppm hydrogen fluoride. Conditions: sample gas flow rate 200 ml min^{-1} ; membrane pore size 0.80 μm .



flows were the same. The absorption solution containing the fluoride produced then passed to the fluoride-selective electrode and discharged via the SCE. Potentials were measured at room temperature with the voltmeter and recorded. All gas tubing was made of teflon. The membrane filter holder was specially constructed from acrylic resin (Denki Kagaku Keiki Co., Tokyo). The filter holder was made in two parts which were screwed together tightly to hold the circular (47-mm diameter) filter. The groove for the sample gas section was 38 cm long, 4 mm wide and 3 mm deep; the groove for the absorption solution was 38 mm long, 4 mm wide and 0.3 mm deep. At the sample gas flow rate of 200 ml min^{-1} , the mean residence time of the gas in the holder was about 0.14 s. When the absorption solution flow rate was 30 ml h^{-1} , the mean residence time of the solution in the holder was about 5.5 s.

Results and discussion

Relation of solution flow rate to absorption efficiency and response time.

The absorption efficiencies for hydrogen fluoride in the flow stream were calculated from the values obtained from both standard hydrogen fluoride gases and standard sodium fluoride solutions at flow rates of $5\text{--}50 \text{ ml h}^{-1}$ for the absorption solution (Fig. 2). The absorption efficiency increased with increasing flow rates from 6 to 30 ml h^{-1} , probably because the absorption efficiency into fresh absorption solution was larger than that with an absorption solution already containing some fluoride. Figure 2 also shows the relation of flow rate to response time, defined as the time required for the electrode potential to come within 1 mV of its steady-state value. Both the response and the response time decreased with the increasing flow rate of the absorption solution. The selected flow rate of absorption solution (30 ml h^{-1}) is a compromise between these effects.

The relation of flow rate of sample gas to the absorption efficiency and to the response time. Although the absorption efficiency decreased with increasing flow rate of the sample gas (Fig. 3), the response increased and the response time also slightly increased. Because it is difficult to control a high flow rate of sample gas in practice, a flow rate of 200 ml min^{-1} was chosen as the optimal flow rate.

Effect of pore size of membrane filter. The system is based on a non-equilibrium process across the membrane and it is important to transfer as much gas as possible from the gas stream during its brief residence time in the filter holder. Four gas-permeable filters with different pore sizes were tested. Table 1 shows the relation between membrane features and response; the responses obtained agree with each other within experimental error. The response time increased with increasing thickness of the membranes but was virtually unaffected by the pore size. A pore size of $0.8 \mu\text{m}$ was chosen because gaseous fluoride is defined as the substance which can permeate through $0.8\text{-}\mu\text{m}$ pore size filters [1]. The lifetime of the membrane was at least 3 months.

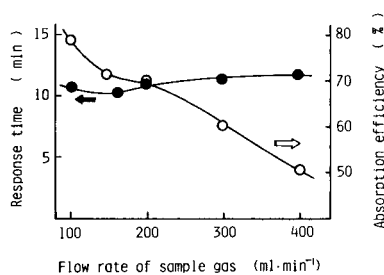


Fig. 3. Effect of flow rate of sample gas on response time and efficiency for 0.92 ppm hydrogen fluoride. Conditions: absorption solution flow rate 30 ml h⁻¹; membrane pore size 0.80 μ m.

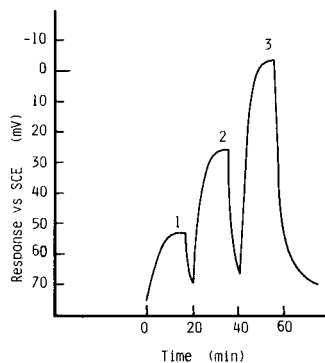


Fig. 4. Response/time characteristics for different concentrations of hydrogen fluoride: (1) 0.7; (2) 2.0; (3) 6.5 ppm. Flow rate of sample gas 200 ml min⁻¹, flow rate of absorption solution 30 ml h⁻¹; pore size of membrane filter 0.80 μ m.

TABLE 1

Relation between membrane features and response to 1.00 ppm hydrogen fluoride^a

Pore size (μ m)	Porosity ^b (%)	Thickness (mm)	Response time (min)	Response vs. SCE (mV)
0.22	65	0.06	10	43.2
0.80	82	0.08	12	42.4
5.00	82	0.10	15	43.0
10.0	84	0.10	15	42.2

^aGas flow rate 200 ml min⁻¹; solution flow rate 30 ml h⁻¹. ^bPorosity means the percentage area occupied by the pores.

Response/time characteristics and calibration curve. The response/time characteristics for three concentrations of hydrogen fluoride obtained under the recommended conditions are shown in Fig. 4. The samples containing hydrogen fluoride were introduced in place of nitrogen alone at times of 0, 20 and 40 min, the pure nitrogen being re-introduced at times of 15, 35 and 55 min.

The calibration graph showed an almost Nernstian response in the range 0.23–6.5 ppm; the relative standard deviation at 1.0 ppm was less than 1.8% ($n = 10$). The plot curved in the usual way below 0.2 ppm, and the lower detection limit was 0.1 ppm hydrogen fluoride.

Influence of carbon dioxide. Hydroxide is the only serious interference with the fluoride-selective electrode. The selectivity coefficient is 0.1 [7]. The pH of the absorption solution is 5.4, thus there is no problem provided

that the gas sample does not contain much alkaline substance. The concentration of carbon dioxide in air is 325 ppm, thus sodium hydrogencarbonate was added to a sodium fluoride standard solution in the molar ratio 650:1. The concentration of fluoride examined corresponded to 0.5 ppm hydrogen fluoride in the gas sample. The response to this mixed solution was 1.7 mV larger than that of the sodium fluoride solution alone, the difference corresponding to a 6.8% error in concentration. For monitoring purposes, this error would not be critical at low concentrations.

The authors are indebted to Mr. Y. Asano of Denki Kagaku Keiki Co. for making the membrane filter holder.

REFERENCES

- 1 Japanese Industrial Standard (Ed.), JIS Hand Book Kogai Kankei, 1982, p. 664.
- 2 D. Midgley and K. Torrance (Eds.), Potentiometric Water Analysis, Wiley, New York, 1978, p. 313.
- 3 W. J. Van Oort and E. J. J. M. Van Eerd, *Anal. Chim. Acta*, 155 (1983) 21.
- 4 M. Sankandas (Ed.), Trace Analysis and Technological Development, Wiley, New York, 1983, p. 369.
- 5 K. A. Phillips and C. J. Rix, *Anal. Chem.*, 53 (1981) 2141.
- 6 J. C. Landry, F. Cupelin and C. Michal, *Analyst (London)*, 106 (1981) 1269.
- 7 M. S. Frant and J. W. Ross, *Science*, 154 (1966) 1553.

Short Communication

DETERMINATION OF SOME AMPHOLYTIC AND CATIONIC SURFACTANTS BY POTENTIOMETRIC TITRATIONS BASED ON ION-PAIR FORMATION

K. VYTRÁŠ*, J. KALOUS and J. SYMERSKÝ

Department of Analytical Chemistry, University of Chemical Technology, 532 10 Pardubice (Czechoslovakia)

(Received 23rd April 1985)

Summary. Ampholytic surfactants of the betaine type are titrated directly with sodium tetraphenylborate in acidic medium, in which they become cationic forms. Generally, ampholytic surfactants and cationic surfactants that contain hydrophilic groups can be determined by precipitation with sodium tetraphenylborate, the excess of which is back-titrated with thallium(I) nitrate. An aluminium wire electrode coated with a plasticized PVC membrane is used for end-point indication. Characteristic data are given for determinations of nine surfactants and applications to textiles are outlined.

Quaternary ammonium ions and cationic surfactants are readily determined by ion-pair titrations [1]. Such cations containing one or more long-chain alkyls are usually of such hydrophobic character that the solubility of their salts depends on the properties of the corresponding anion only. The tetraphenylborates of these cations are sufficiently insoluble in water and are easily extractable into organic solvents (membrane liquids). Direct titrations of the cationic surfactants with sodium tetraphenylborate can be monitored with simple potentiometric sensors of the coated-wire type, however, only if organic cations do not contain further hydrophilic groups [2].

Ampholytic surfactants form bipolar ions which may be cationic or anionic, depending on the pH value. Traditional two-phase titrations such as are used in determinations of cationic and anionic surfactants, are not suitable for ampholytic surfactants [3]. Potentiometric titrations of such materials seem not to have been reported earlier, but are easily achieved by using simple ion-selective plastic-membrane electrodes.

Experimental

Solutions and samples. Sodium tetraphenylborate (NaTPB) solution (ca. 10^{-2} M) was prepared by dissolving about 1.71 g of the substance (VEB Jenapharm Laborchemie, Apolda) in water, adjusting with sodium hydroxide to pH 9, and diluting to 500 ml with water. Solutions were standardized potentiometrically against standard 10^{-2} M thallium(I) nitrate, which was prepared by dissolving 1.3319 g of the recrystallized salt to 500 ml of water.

TABLE 1

List of compounds investigated

Sample	Commercial name	Formula	Molecular mass
I	Flavol BMK	$\text{R}-\overset{\text{CH}_3}{\underset{\text{CH}_3}{\text{N}^+}}-\text{CH}_2\text{COO}^-$; R = C ₁₂₋₁₄ (alkyl)	271
II	Empigen CDR 30	$\text{R}-\overset{\text{CH}_2\text{COO}^-}{\underset{\text{H}_2}{\text{C}}}=\overset{\text{CH}_2}{\text{N}^+}-\text{CH}_2\text{CH}_2\text{OH}$; R = C ₁₂₋₁₄ (alkyl)	353
III	Tego-Betain L7	$\text{C}_{12}\text{H}_{25}\text{CONHCH}_2\text{CH}_2-\overset{\text{CH}_3}{\underset{\text{CH}_3}{\text{N}^+}}-\text{CH}_2\text{COO}^-$	342.5
IV	Reaktocel BA	$\text{C}_6\text{H}_5-\text{CH}_2-\overset{\text{CH}_3}{\underset{\text{CH}_3}{\text{N}^+}}-\text{CH}_2\underset{\text{OH}}{\text{CH}}\text{CH}_2-\text{Cl} \cdot \frac{1}{2}\text{SO}_4^{2-}$	276.8
V	Reaktocel GL ^a	$\text{CH}_2-\text{CH}-\text{CH}_2-\overset{\text{CH}=\text{CH}}{\underset{\text{CH}}{\text{N}^+}}-\text{CH}_2-\text{CH}-\text{CH}_2 \cdot \text{Cl}^-$	216.7
VI	Levogen RS	$\text{CH}_2-\text{CH}-\text{CH}_2-\overset{\text{CH}_3}{\underset{\text{CH}_2}{\text{N}^+}}-\text{CH}_2-\text{CH}_2-\text{CH}_2-\text{O}$	193.7
VII	Glytac A100	$\text{CH}_2-\text{CH}-\text{CH}_2-\overset{\text{CH}_3}{\underset{\text{CH}_3}{\text{N}^+}}-\text{CH}_3 \cdot \text{Cl}^-$	151.6
VIII	Verolan KAF	$\text{CH}_2-\underset{\text{Cl}}{\text{CH}}-\text{CH}_2-\overset{\text{CH}_3}{\underset{\text{CH}_3}{\text{N}^+}}-\text{CH}_3 \cdot \text{Cl}^-$	188.1
IX	Dextrosil KA	As compound VIII	188.1

^aDuring preparation of the manuscript, the compound was introduced into industrial use under the name Apreton BA.

The samples were ampholytic surfactants of the betaine type or cationic compounds containing quaternary nitrogen and either a chlorohydrin configuration or an oxirane ring (Table 1). The samples were dissolved in water to obtain approximately 10^{-2} M solutions. Only the sample of Tego-Betain L7 (III) was analyzed on both 5×10^{-2} M and 1×10^{-2} M levels.

Equipment. For the titrations, a digital pH meter OP-208 (Radelkis, Budapest) was used with a 10-ml burette, or an automatic titrator was used; the latter comprised a universal meter M110, pH meter M120, titration attachment M121, and syringe burette M122 (all Mikrotechna, Prague) connected with an *x-y* recorder (LP-4103; Laboratorní přístroje, Prague). The indicator electrodes were prepared as described earlier [4, 5] by coating an aluminium conductor with a membrane from a solution of poly(vinyl chloride) (0.085 g) and plasticizer (0.2 ml) in tetrahydrofuran (3 ml); the plasticizers used here were 2,4-dinitrophenyl *n*-octyl ether (electrode 181A) and 2-ethylhexyl 4-hydroxybenzoate (electrode 479A). A double-junction calomel electrode (RCE-102; Monokrystaly, Turnov) filled with 10^{-2} M sodium nitrate was used as reference.

General procedures. For direct titrations, the sample (5 ml of about 10^{-2} M solution) was measured into a 100-ml beaker, acidified with 1% hydrochloric acid (1 ml), diluted with water to about 50 ml, and titrated with 10^{-2} M NaTPB, the titration being monitored with the electrode specified below.

For indirect titrations, the sample (5 ml of ca. 10^{-2} M solution) and 10^{-2} M NaTPB (10 ml) were mixed and then left for about 5 min. The precipitate was separated on a fritted disk (S3 or S4) under suction and the filter cake was carefully washed with the minimal volume of water. The filtrate was transferred quantitatively to a suitable beaker and titrated potentiometrically with standard 10^{-2} M thallium(I) nitrate.

Results and discussion

Direct titrations. Ampholytic surfactants I and II (see Table 1) can be titrated directly with sodium tetraphenylborate (NaTPB) in acidic solutions, in which they are cationic; the 181A electrode is best. Sample III can be titrated directly but it is better to use a more concentrated titrant. Some results, and information on the size and steepness of the potential jump at the end-point, are given in Table 2. It should be noted that direct titrations of these compounds by a cationic titrant in alkaline medium were unsuccessful because the compounds cannot be converted to simple anions. Of the other cationic compounds, only sample V could be titrated directly when the 181A coated-wire electrode was used, but the overall potential break and its steepness near the end-point were poor. These observations confirmed earlier experiments with compound IX (3-chloro-2-hydroxypropyltrimethylammonium chloride); the cation was precipitated with tetraphenylborate but the titration with NaTPB could not be followed potentiometrically because of the hydroxy group in the quaternary salt [2].

Direct titrations of samples IV and V could also be followed with the

TABLE 2

Determination of compounds directly titratable with NaTPB

Sample	Indicator electrode	Titration curve		Content (%)		
		Overall potential change (mV)	Steepness near end-point (mV/0.1 ml)	Declared	Found ^a	
I	Flavol BMK	181A	290–350	30–40	20–30?	20.0 ± 0.3(3)
II	Empigen CDR 30	181A	215–250	15–24	20–30?	18.2 ± 1.5(2)
III	Tego-Betain L7	181A	230–240	6–8	30	29.5 ± 3.3(3)
			235–250 ^b	8–10	30	30.5 ± 2.3(3)
V	Reaktocel GL	181A	130–160	8–10	—	76.6 ± 2.6(3)
			479A	85–100	3–4	—
IV	Reaktocel BA	479A	130–140	3–4	—	95.9 ± 1.2(4)

^aGiven as a reliability interval $\bar{x} \pm u_0 R$ for the significance level $\alpha = 0.05$; \bar{x} is the arithmetic mean, R the range, u_0 the critical value for the number of replicates given in parentheses. ^bTitrated with ca. 5×10^{-2} M NaTPB; other data are given for titrations with ca. 1×10^{-2} M NaTPB.

479A electrode, which had a more hydrophilic membrane plasticizer, but the titration curves were not improved (Table 2) and Gran plots were needed to provide reliable evaluation of the end-points.

Indirect determinations. For the determination of samples IV–IX, back-titration was much more convenient. The sample solution was mixed with excess of NaTPB, which was then back-titrated with standard thallium(I) nitrate solution after removal of the precipitate by filtration. The corresponding potential breaks of ca. 300 mV were steep (ca. 50 mV/0.1 ml). The indirect procedure was suitable for samples V–IX in Table 1. The tetraphenylborate of sample IV was difficult to filter, but back-titration could be done without separating the precipitate (Table 3). When this procedure was used for the other samples, the consumption of thallium(I) corresponded to the total addition of NaTPB, indicating that TPB in the precipitates was also titrated.

Applications. Preparations IV–VIII have found use in the textile industry in order to increase the affinity of textiles to acidic dyestuffs. In strongly alkaline medium, the chlorohydrin group of compounds IV and VIII forms an oxirane ring which can attack the cellulose hydroxyl groups to create a stable chemical bond; compounds V–VII contain the oxirane group already. The cationic cellulose can then form ion-pairs not only with acidic dyestuffs, but also with other bulky organic anions including tetraphenylborate.

In the procedure developed, a weighed amount of cotton material (1–2 g) in a 100-ml Erlenmeyer flask was soaked in 20–40 ml of 10^{-2} M NaTPB solution. The flask was stoppered and shaken strongly for about 5 min. The mixture was then filtered on a dry, clean glass frit, which retained the

TABLE 3

Indirect determinations of the textile cationic preparations

Sample		Found ^a
V	Reaktocel GL	75.6 ± 1.2(6)
VI	Levogen RS	84.6 ± 0.5(4)
VII	Glytac A100	80.3 ± 0.5(3)
VIII	Verolan KAF	90.2 ± 0.0(3)
IX	Dextrosil KA	42.1 ± 0.2(4)
IV	Reaktocel BA ^b	95.1 ± 0.5(3)

^aSee footnote (a) in Table 2. ^bTitred without separation of the precipitate; the separation is difficult and results were then significantly lower, 89.3 ± 1.3% (for comparison, see data for IV in Table 2).

cotton fibres. A portion (5–8 ml) of the filtrate was diluted to about 50 ml with water and titrated with 10⁻² M thallium(I) nitrate, the 181A electrode serving for end-point detection. This procedure, tested on samples of cotton skeins and fabrics, provided results which could readily be correlated with the concentrations of the cationic compound in the treatment bath [6].

The authors are obliged, for the donation of samples, to Dr. M. Morák, Spolek pro chemickou a hutní výrobu, Ústí n. L. (samples I, II and IX), Dr. M. Čoupková, VÚTP, Prague (III), and Dr. D. Dvorský, VÚZ, Dvůr Králové n. L. (IV–VIII).

REFERENCES

- 1 K. Vytřas, *Ion-Selective Electrode Rev.*, 7 (1985) 77.
- 2 K. Vytřas, M. Dajková and V. Mach, *Anal. Chim. Acta*, 127 (1981) 165.
- 3 A. Blažej, P. Hodul, E. Markušovská, L. Novák, M. Paulovič and I. Vyskočil, *Tenzidy, Alfa*, Bratislava, 1977, pp. 324–5.
- 4 K. Vytřas, M. Remeš and V. Ríha, *Czech. Pat.*, A0 225 222.
- 5 K. Vytřas, *Mikrochim. Acta*, III (1984) 139.
- 6 K. Vytřas, J. Kalous, J. Symerský, D. Dvorský and M. Šmíd, *Textil*, 40 (1985) 314.

Short Communication

DETERMINATION OF TIN AND LEAD BY DIFFERENTIAL PULSE POLAROGRAPHY WITH ADDITION OF HYAMINE-2389

JOSÉ L. GUINÓN* and JOSÉ GARCÍA-ANTÓN

Departamento de Química, E.T.S.I. Industriales, Universidad Politécnica de Valencia, Valencia (Spain)

(Received 29th January 1985)

Summary. The influence of Hyamine-2389 on the polarographic peaks for tin and lead in hydrochloric acid/oxalic acid electrolytes is described. In 0.5 M hydrochloric acid/0.1 M oxalic acid containing 0.2% (w/v) Hyamine-2389, the peak potentials for lead and tin are about 400 mV apart, which allows simultaneous determination of these elements. Calibration plots are linear up to 5×10^{-5} M for tin and 1.3×10^{-4} M for lead, with detection limits of 8.4×10^{-7} M and 2.4×10^{-8} M, respectively. Simple methods are proposed for the determination of tin in solders and canned fruit juices.

The simultaneous determination of tin and lead by polarography or anodic stripping voltammetry (a.s.v.) is made difficult by the tendency of tin(IV) to hydrolyze and polymerize [1] as well as by overlapping peaks [2, 3]. Even when a.c. and other types of polarography are used [4–6], strongly acidic media are needed and the peak separation of tin and lead is not very good. The addition of methanol [7, 8] or ammonium iodide [9] to 1 or 0.5 M hydrochloric acid, respectively, provides a peak separation of ca. 70 mV in a.c. polarography.

Surface-active agents can change the peak heights and peak potentials of electroactive species so that these agents can be effective as electrochemical masking agents. The influence of surfactants in the polarography of tin [10], lead and other ions [11] and in a.s.v. of tin and/or lead with other ions [12–15] has been described. In the present communication, a study of the polarographic behaviour of tin and lead in presence of the surfactant Hyamine-2389 is reported. The peak potentials of these ions are well separated. The method is applied to the determination of tin in solders and in canned grape juices.

Experimental

Apparatus. A Metrohm E-626 Polarecord and an E-505 polarographic stand were used with an EA-1019/2 dropping mercury electrode (DME), an EA-285 platinum ring auxiliary electrode and an EA-441/5 Ag/AgCl reference electrode (all from Metrohm). The drop time was 0.5 s, the pulse amplitude 50 mV, and the scan rate 10 mV s^{-1} . A Selecta 382 thermostat was used. Dissolved oxygen was removed by bubbling nitrogen for 7 min.

Chemicals. Solutions of lead were prepared from lead nitrate (Merck). Tin metal (UCB) was dissolved in 6 M hydrochloric acid and 30% hydrogen peroxide, the excess of hydrogen peroxide was removed by boiling gently and the solution was adjusted to 2.5 M in hydrochloric acid. Stock solutions (10%) of Hyamine-2389 [alkyl (C_5-C_{15}) benzyltrimethylammonium chloride; Serva] were prepared by dissolution of the commercial product in distilled water. The remaining chemicals were of analytical-reagent grade and were used as received.

Procedures. For the determination of tin in solder, weigh accurately 0.1–0.2 g of the alloy and dissolve in 40 ml of 6 M hydrochloric acid with some drops of 30% hydrogen peroxide, warming gently to aid dissolution. Boil gently to remove the excess of peroxide, transfer to a 100-ml standard flask and dilute to the mark with water. Transfer 1–2 ml of the solution to a 50-ml standard flask, dilute to the mark with 0.5 M hydrochloric acid/0.1 M oxalic acid containing 0.2% (w/v) Hyamine-2389. Record the polarogram under the conditions outlined above, at 35°C.

For the determination of tin in canned grape juices, weigh accurately 0.5–1 g of the juice into a 50-ml standard flask. Add 2 ml of concentrated hydrochloric acid, shake and leave for 5 min. Add 10 ml of 0.5 M oxalic acid, dilute with water, add 1 ml of 10% (w/v) Hyamine-2389 and dilute to the mark with water. Record the polarogram as outlined above.

Results and discussion

As shown in Fig. 1, when the concentration of Hyamine-2389 is increased up to $2 \times 10^{-2}\%$, the tin(IV) peak potential remains constant at -430 mV and the peak height increases slightly. Higher concentrations of Hyamine (4×10^{-2} – $8 \times 10^{-2}\%$) decrease the height of the peak, which may even disappear, while a second peak appears at a much more negative potential

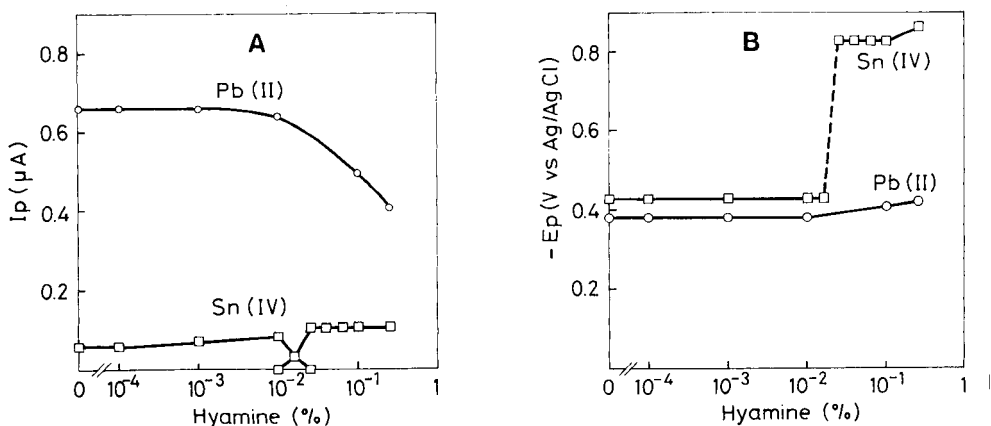


Fig. 1. Effects of Hyamine-2389 on the peak height (A) and peak potential (B) of 10^{-4} M lead and 10^{-4} M tin in 0.5 M HCl/0.1 M $H_2C_2O_4$ (25°C).

(-810 mV). For lead, the peak potential (-380 mV) and peak height are practically unchanged up to ca. $10^{-2}\%$ Hyamine-2389; more surfactant causes a small shift of peak potential to -410 mV, and a progressive decrease in the peak height.

The effect of the hydrochloric acid concentration is shown in Fig. 2. The peak height of lead increases steeply with increasing concentration of the acid up to about 1 M, after which it remains almost constant up to 4 M. In contrast, the peak height of tin(IV) remains constant up to about 0.5 M hydrochloric acid, decreases progressively at higher acidities and disappears in the 3 M acid. This different behaviour can be explained in an analogous way to other aquo and complex ions [16, 17]; the negatively charged tin(IV) complex could be repelled by chloride adsorbed on the layer of cationic surfactant at the mercury electrode, while the positively charged lead is more easily reduced under the same conditions.

Consequently, Hyamine-2389 may be used in two different ways, as an electrochemical masking agent and as a means of peak separation. In 3 M hydrochloric acid/0.1 M oxalic acid, tin(IV) and lead are reduced at almost the same potential, -0.49 and -0.46 V, respectively. Addition of 0.2% Hyamine-2389 completely inhibits the electrode reaction of the tin(IV) complex and only the lead peak is observed on the polarogram. In 0.5 M hydrochloric acid/0.1 M oxalic acid, the addition of 0.2% Hyamine 2389 allows the simultaneous determination of lead and tin, because the peak potentials are then -0.41 and -0.81 V, respectively. A typical polarogram is shown in Fig. 3.

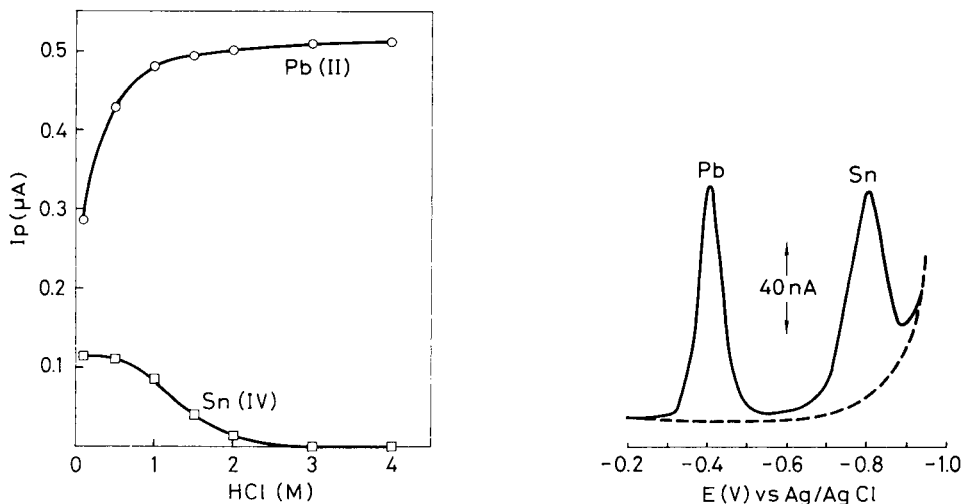


Fig. 2. Effect of HCl concentration on the peak heights of 10^{-4} M lead and 10^{-4} M tin in 0.1 M oxalic acid in the presence of 0.2% Hyamine-2389 (25°C).

Fig. 3. Differential pulse polarogram of 1.93×10^{-5} M lead and 3.36×10^{-5} M tin in 0.5 M HCl/0.1 M $\text{H}_2\text{C}_2\text{O}_4$ in the presence of 0.2% Hyamine-2389 (35°C).

The calibration graph for tin by differential pulse polarography presented two straight-line portions. The first line corresponds to clear solutions while the second line corresponds to somewhat turbid samples. This behaviour may be attributed to the formation of an ion-pair between negatively charged tin(IV) complexes and the cationic surfactant [18]. Analogously, solutions of tin(IV) should not be prepared by dissolving tin in hydrochloric/nitric acid mixtures [19]; some turbidity is produced by interaction between nitrate and Hyamine-2389. The adsorption of the ion-associates formed may account for the oscillations which appear at the tin peak. The range of linearity of the first portion of the graph increased with increasing temperature, with corresponding disappearance of turbidity. The graph was linear at 25°C for the range 0– 3.3×10^{-5} M and up to 5×10^{-5} M at 35°C. A linear least-squares regression on five points gave the equations I_p (nA) = $1.839 \times 10^6 C + 19.1$ ($r = 0.998$) at 25°C and I_p (nA) = $2.731 \times 10^6 C + 21.2$ ($r = 0.999$) at 35°C. The temperature coefficient obtained in the range 20–40°C was 2.6%, typical of a diffusion-controlled process. The detection limit based on twice the magnitude of the observed background current was 8.4×10^{-7} M (0.1 mg l⁻¹).

The calibration graph for the lead was linear over the range of concentration studied, 0– 1.3×10^{-4} M, with I_p (nA) = $5.441 \times 10^6 C - 2.7$ ($r = 0.999$) at 25°C and I_p = $6.211 \times 10^6 C - 3.6$ ($r = 0.999$) at 35°C. The temperature coefficient obtained was 1.45%, which indicates that the electrode process is also diffusion-controlled. The detection limit was 2.4×10^{-8} M (5 µg l⁻¹).

Analyses of synthetic samples containing various concentrations of lead and tin showed that simultaneous determinations were possible for lead/tin (mg l⁻¹) ratios of 20:1 to 1:20, with tin ≤ 7 mg l⁻¹. For higher concentrations of tin some turbidity appeared, and results were then low. For lead, better results were always obtained.

Determination of tin in solder. When the method recommended was applied, antimony in the solder did not interfere because no antimony peaks were observed in the electrolyte used. Table 1 shows the results obtained. The precision, estimated from the standard deviations ($n = 5$) for each sample was 1.1–3%. The agreement with results obtained by a standard method or with certified values is satisfactory, the bias being –2.2 to 1.8%.

TABLE 1

Determination of tin in solder

Sample	A	B	C	D
Sn present (%)	3.53 ^a	4.02 ^a	5.09 ^b	10.51 ^a
Sn found (%) ^c	3.45	3.91	5.18	9.97

^aASTM E-46 determination. ^bCertified value by BCS (177/1) containing 84.5% Pb and 10.4% Sb. ^cMean values of three individually weighed samples.

Determination of tin in canned grape juices. The proposed method was compared with that reported by Dabeka and Mackenzie [20] which involves nitric acid digestion and atomic absorption spectrometry (a.a.s.) with a nitrous oxide/acetylene flame. The results are shown in Table 2. For the four samples analysed, the difference between the two methods was $\leq 5\%$. The poorer agreement, compared to the data for tin in solders, may be attributed to the influence of the organic matrix. The relative standard deviation for five replicate analyses of one sample was 3%. Standard additions of lead to grape juice showed that the d.p.p. method offers a detection limit (based on twice the magnitude of the background current) of 0.01 mg l^{-1} lead in the solution subjected to polarography, which is equivalent to 0.5 mg kg^{-1} in the grape juice. Therefore, the d.p.p. method is also suitable for detecting contamination by lead beyond the limit (0.5 mg Pb/kg juice) allowed by Spanish regulations.

TABLE 2

Determination of tin (mg kg^{-1}) in canned grape juices

Sample	A	B	C	D
Sn found, a.a.s.	73.7	86.0	98.3	110.2
Sn found, d.p.p. ^a	76.6	88.9	95.3	115.3

REFERENCES

- 1 T. M. Florence and Y. J. Farrar, *J. Electroanal. Chem.*, 51 (1974) 191.
- 2 I. M. Kolthoff and J. J. Lingane, *Polarography*, Interscience, New York, 1952.
- 3 A. M. Bond, *Anal. Chem.*, 42 (1970) 1165.
- 4 L. I. Veselago, *Zh. Anal. Khim.*, 24 (1969) 464.
- 5 M. Harrison, C. L. Roughton and B. Surfleet, *Analyst (London)*, 95 (1970) 894.
- 6 L. S. Nadezhina, E. L. Grinzaid and E. G. Novakovskaya, *Tr. Leningrad. Politekh. Inst.*, 304 (1970) 141.
- 7 L. Metzger, G. G. Willems and R. Neebs, *Fresenius Z. Anal. Chem.*, 288 (1977) 35.
- 8 L. Metzger, G. G. Willems and R. Neebs, *Fresenius Z. Anal. Chem.*, 292 (1978) 20.
- 9 A. M. Shafiqul Alam, O. Vittori, H. Tersigni and G. Courtois, *Anal. Chim. Acta*, 91 (1977) 325.
- 10 G. G. Willems and R. Neebs, *Fresenius Z. Anal. Chem.*, 269 (1974) 110.
- 11 J. Hernandez-Mendez, R. Carabias and I. Garcia-Garcia, *Anal. Chim. Acta*, 132 (1981) 59.
- 12 Z. Lukaszewski, M. K. Pawlak and A. Ciszewski, *Talanta*, 27 (1980) 181.
- 13 J. Hernandez-Mendez, R. Carabias and M. E. Gonzales Lopez, *Anal. Chim. Acta*, 138 (1982) 47.
- 14 P. Sagberg and W. Lund, *Talanta*, 29 (1982) 457.
- 15 A. Ciszewski and Z. Lukaszewski, *Anal. Chim. Acta*, 146 (1983) 51.
- 16 E. Jacobsen and H. Lindseth, *Anal. Chim. Acta*, 86 (1976) 123.
- 17 F. C. Anson, J. B. Flanagan, K. Takahashi and A. Yamada, *J. Electroanal. Chem. Interfacial Electrochem.*, 67 (1976) 253.
- 18 K. L. Mittal, *Solution Chemistry of Surfactants*, Plenum Press, New York, 1979.
- 19 S. Glodowski and Z. Kublik, *Anal. Chim. Acta*, 104 (1979) 55.
- 20 R. W. Dabeka and A. D. Mackenzie, *J. Assoc. Off. Anal. Chem.*, 64 (1981) 1297.

Short Communication

LIQUID-JUNCTION POTENTIAL EFFECTS IN MEASUREMENTS OF SODIUM ION ACTIVITY IN UNBUFFERED AQUEOUS SOLUTIONS

JIAN-WEI CHEN and JOSEPH GEORGES*

Laboratoire de Chimie Analytique 3 (UA 04 435), Université Claude Bernard, Lyon I, 69622 Villeurbanne Cedex (France)

(Received 17th May 1985)

Summary. Measurements of pNa with the glass-membrane ion-selective electrode in unbuffered aqueous solutions require care in the constitution of the measuring cell, because of variable liquid-junction potentials at the salt bridge. Of the bridge electrolytes tested, with calomel or silver/silver chloride reference electrodes, 3 M ammonium chloride in agar-agar gel was most satisfactory. Calibration graphs were of almost theoretical slope in the range 10^{-3} – 5×10^{-1} M sodium ion.

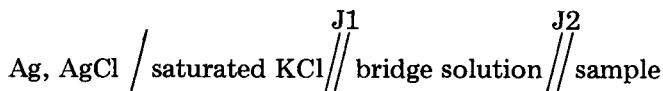
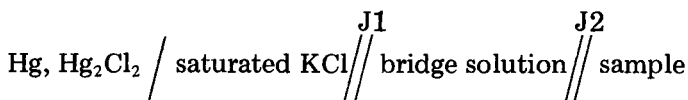
Determinations of the concentration of free sodium ions, in the range of 10^{-3} – 5×10^{-1} M, in sodium dodecylsulfate (SDS) solutions without any supporting electrolyte were required. Setting up a suitable electrochemical cell with a sodium ion-selective electrode and a reference electrode poses problems under these conditions [1, 2], especially with regard to variable liquid-junction potentials at the interface between the reference electrode and the sample solution. A bridge solution is normally used when it is necessary to prevent contamination of the sample solution by species in the reference electrode which would alter the composition of the sample or the response of the electrode. In this communication, it is shown that the composition of the bridge solution is very important in the application mentioned because of interferences with the Na⁺-selective electrode and precipitation of the surfactant in the junction of the reference electrode.

Experimental

For the pNa measurements, a standard solution of sodium chloride was added to the cell from a microsyringe. The cell was thermostatted with a water bath at $25 \pm 0.2^\circ\text{C}$. Potentials were measured with a digital pH/millivoltmeter (Minisis, Solea-Tacussel). The sodium-selective electrode was a Corning glass electrode, the membrane of which (NAS 11-18) exhibits high selectivity for sodium ions in the presence of potassium ions; the apparent Na⁺/K⁺ selectivity at pH 7 is about 1000. However, it was necessary to avoid having potassium ions in the sample solution, because the Na⁺/K⁺ selectivity decreases rapidly at pH <7; no buffering agent could be added to the sample

solutions under test. The electrode response to sodium is unaffected by pH (provided that $\text{pH} - 2 \geq \text{pNa}$).

The pNa electrode was used with two common reference electrodes, an Ag/AgCl electrode (home-made) and a calomel electrode (Solea-Tacussel), both with saturated potassium chloride solution. A salt bridge was inserted between the reference system and the sample solution because of possible interference from potassium ion, especially at the low sodium ion concentrations and to prevent precipitation of potassium dodecylsulfate during the experiments with sodium dodecylsulfate. The reference electrode assemblies used were



The junction structure at J1 and J2 was a ceramic porous plug in the calomel electrode and fritted glass in the Ag/AgCl electrode.

The bridge solutions were made from common electrolytes reported in the literature or recommended by the electrode manufacturers. They were chosen so that leakage of the solution into the sample would produce minimum contamination of the sample by interfering ions, and so that there would be no reaction with the sample to form a precipitate which would block the junction. Usually, the bridges were prepared with agar-agar gels. All chemicals were of analytical grade.

Results

The liquid junction potentials in the cell must be independent of the composition of the sample solution and must remain constant during the series of measurements. This is not easily achieved when sample solutions cannot be buffered. Figure 1 shows the calibration curves obtained with the double-junction calomel electrode with 0.1 M barium chloride as the bridge solution. The presence of the same electrolyte in the sample solution is needed to obtain a good calibration curve (slope, 55 mV/pNa). Without barium chloride in the sample solution, the liquid junction potential changes slowly as the sodium ion concentration is increased, leading to a slope (73 mV/pNa) greater than the theoretical slope for the range 5×10^{-3} – 2×10^{-1} M sodium ion.

When the pNa measurements must be done in pure water, it is clear that other electrolytes must be found. Figures 2 and 3 compare the results obtained with various gel bridges used with the calomel and Ag/AgCl electrodes. Ammonium nitrate caused a serious error in the calibration plot (Fig. 2); at low concentrations, the slope is about 30 mV/pNa whereas at greater concentrations, it approaches the theoretical value. With lithium

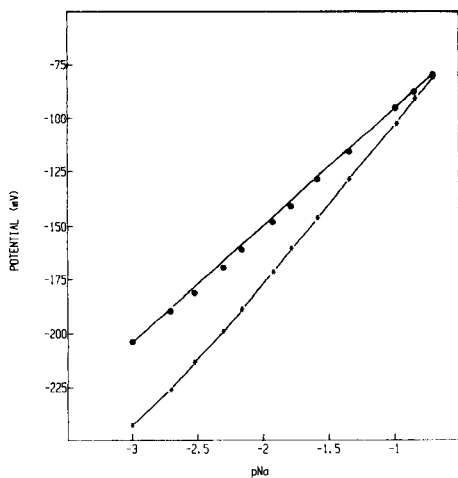


Fig. 1. Plots of potential vs. pNa with a Na^+ -selective electrode and a double-junction calomel electrode as reference. The bridge solution was 0.1 M BaCl_2 . Initial solutions: (*) pure water; (●) water + 0.1 M barium chloride.

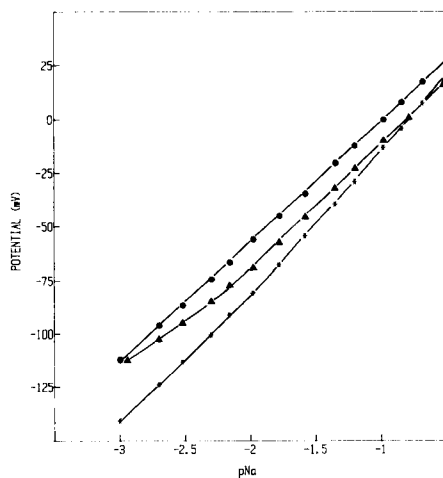
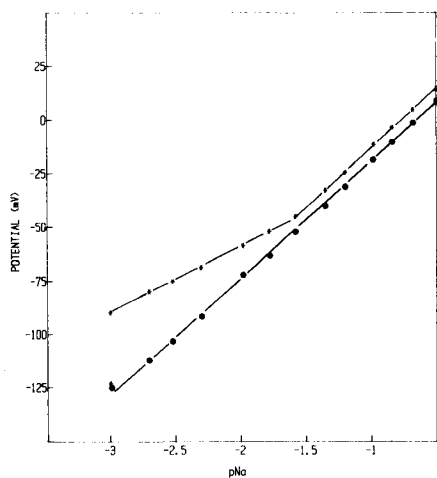


Fig. 2. Calibration graphs with a pNa electrode and a double-junction calomel electrode in pure water without any electrolyte. Bridge solution in agar-agar gel: (*) 1 M ammonium nitrate; (●) ammonium chloride.

Fig. 3. Calibration graphs with a pNa electrode and a double-junction silver chloride electrode in pure water without any electrolyte. Bridge solution in agar-agar gel: (*) 0.1 M tetrabutylammonium hydrogensulfate/0.1 M tetrabutylammonium hydroxide; (▲) 0.1 M lithium perchlorate; (●) 3 M ammonium chloride.

perchlorate, the calibration plot curves in the low concentration range (Fig. 3). The tetrabutylammonium hydrogensulfate/tetrabutylammonium hydroxide buffer (pH \approx 6) gives a good slope at low sodium ion concentrations but the slope is 68 mV/pNa at high sodium ion concentrations. The best results were obtained with ammonium chloride in the bridge solution (Figs. 2 and 3); the electrode response is linear over the whole concentration range studied with a slope (55–56 mV/pNa) close to the theoretical value.

REFERENCES

- 1 P. L. Bailey, *Analysis with Ion-Selective Electrodes*, Heyden, London, 1980.
- 2 W. E. Morf, *The Principles of Ion-Selective Electrodes and of Membrane Transport*, Elsevier, Amsterdam, 1981.

Short Communication

AN AUTOMATED SYSTEM FOR THE DETERMINATION OF FLUORIDE

WAI LENG CHEK^a and R. W. CATTRALL*

Analytical Chemistry Laboratories, Department of Chemistry, La Trobe University, Melbourne, Victoria 3083 (Australia)

I. C. HAMILTON

Department of Chemistry, Footscray Institute of Technology, Melbourne, Victoria 3011 (Australia)

(Received 19th July 1985)

Summary. A procedure is reported for the automated determination of fluoride by the method of standard addition. Additions of standard are made via a peristaltic pump and the amounts of standard added are computed from the change in weight of the standard in its container on a digital electronic balance.

Ion-selective electrodes have found widespread application in analytical chemistry but their use, particularly at low concentrations, can be tedious. A consequence of this is poor accuracy and precision. A major cause is the relatively slow response of electrodes and the need for subjective judgements on when the potential has reached the "equilibrium value". A microcomputer can tackle such work far better than the analyst because it will monitor electrode potentials continuously for long periods. Thus, in most of our work with ion-selective electrodes, a microcomputer is interfaced with a millivoltmeter. The system described in this communication is based on a Southwest Technical Products Corporation M6800/2 machine and an Orion 801A digital millivoltmeter; an Apple IIe interfaced with an Orion Model 901 meter has also been used in other work.

Various automated systems for potentiometry have been reported [1–9] in which both direct and standard addition methods are used. These systems are an improvement over their manual counterparts in that greater accuracy and precision are obtained. In all cases, a microcomputer reads the millivoltmeter and the computer is used also to control other functions such as solution delivery via a burette or peristaltic pump. The proposed system differs from the others in the way in which the amount of solution dispensed is determined.

^aPresent address: Environment Protection Authority of Victoria, Melbourne, Victoria 3001, Australia.

Experimental

Equipment. A Southwest Technical Products Corporation M6800/2 microcomputer interfaced to an Orion Model 801A Ionalyzer was used to monitor the potential. Read-out was to a 43 Teleprinter Basic KSR terminal (Teletype Corporation). A Sartorius 1264-MP electronic top-loading balance with a mass range of 0.01–3000 g and a Gilson Minipuls II peristaltic pump were also interfaced to the computer.

Electrodes. An Orion 94-09 or Radiometer F1052F fluoride electrode was used in conjunction with a Titron double-junction calomel reference electrode. The outer junction contained 10% (w/v) ammonium nitrate.

Reagents. Standard fluoride solutions were prepared from a 1000 $\mu\text{g ml}^{-1}$ stock solution of pre-dried sodium fluoride (Ajax Chemicals; analytical-reagent grade). Acetate buffer (TISAB II) containing CDTA (Aldrich) was added to all solutions (1:1, v/v) before measurement. All fluoride solutions were stored and used in polythene containers.

Description of the system. Figure 1 illustrates the apparatus for the automated determination of fluoride by standard addition. Standard is delivered to the sample from a vessel standing on the electronic balance. The computer records the weight loss and calculates the amount of standard added to the sample. Rice [10] has used an electronic balance for dispensing

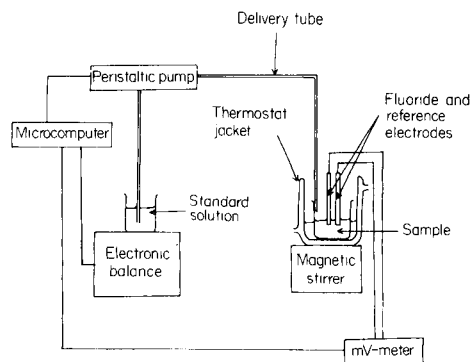


Fig. 1. The automated system.

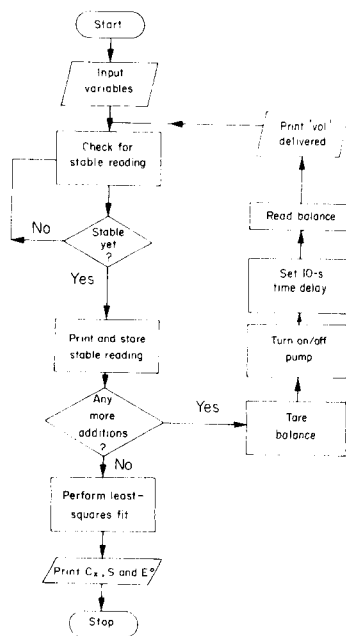


Fig. 2. Program flow chart.

solutions, but only in a manual mode. The delivery tube consists of an isoversinic tube (3.0 mm i.d.) for the pump which is connected to teflon tubing, the diameter of which is not crucial but ends in a tip of 0.64 mm i.d. Care is needed to ensure that the delivery tube is supported clear of the container so that it does not influence the weight of the standard recorded on the balance. The outlet of the delivery tube is adjusted such that it just touches the inner wall of the sample vessel and is high enough not to touch the sample even after all additions have been made. The hydrophobic nature of the polythene vessel used for the sample ensures that standard solution does not cling to the sides and is added quantitatively to the sample solution. A pumping rate of 0.1 ml s^{-1} is used for the standard. Software controls additions of standard so that the overall potential change is at least 30 mV.

Software. The program flow chart is shown in Fig. 2; a copy of the program is available on request from the authors. The assumption is made that the fluoride concentration of the standard before the first addition is at least a factor of ten higher than that of the sample. This, of course, can be established by noting the potential of the sample, estimating its concentration range from previous knowledge of the electrode performance and choosing the concentration of standard accordingly. Addition of standard is noted by the computer to have occurred if the potential changes by more than 5 mV.

The criterion of potential stability can be set by the operator and in the present work a stable potential is defined as one which does not change by more than 0.1 mV over a period of 2 min. Solutions are not stirred during equilibration.

Results

The automated standard addition method was evaluated on one pure fluoride standard ($100.1 \mu\text{g ml}^{-1}$) and two samples (F_1 and F_2) from an inter-laboratory study of fluoride determination conducted by the Environment Protection Authority (EPA) of Victoria. Four standard additions were made in each of the five determinations on each sample. The results are shown in Table 1. The actual values for F_1 and F_2 are those given by the EPA and it

TABLE 1

Automated analysis of fluoride-containing samples

Sample	Concn. of standard ($\mu\text{g ml}^{-1}$)	Fluoride conc. ($\mu\text{g ml}^{-1}$)	
		Actual	Found
Pure std.	1000	100.1	100.1 ± 4.19^a
F_1	10.0	1.32	1.40 ± 0.05
F_2	1000	37.7	37.4 ± 1.53

^aMean deviation.

should be noted that these solutions also contained $1.67 \mu\text{g ml}^{-1}$ aluminium. The results demonstrate that the automated system is capable of providing acceptable accuracy and precision.

We are grateful to the Australian Research Grants Scheme for financial assistance with this work. This paper was presented at the 8th Australian Conference on Analytical Chemistry, Melbourne, April, 1985.

REFERENCES

- 1 I. Sekerka and J. F. Lechner, *Talanta*, 20 (1973) 1167.
- 2 R. T. Oliver, G. F. Lenz and W. P. Frederick, *Technicon Symposium*, Vol. II, Mediad, New York, 1969, p. 309.
- 3 M. Vandeputte, L. Dryon and D. L. Massart, *Anal. Chim. Acta*, 91 (1977) 113.
- 4 A. M. Bond, H. A. Hudson, P. A. Van den Bosch and F. L. Walter, *Anal. Chim. Acta*, 136 (1982) 51.
- 5 J. Slanina, F. Bakker, J. J. Mols, J. F. Ordelman and A. G. M. Bruyn-Hes, *Anal. Chim. Acta*, 112 (1979) 45.
- 6 B. W. Renoe, K. R. O'Keefe and H. W. Malmstadt, *Anal. Chem.*, 48 (1976) 661.
- 7 A. Gustavsson and P. Nylén, *Anal. Chim. Acta*, 125 (1981) 65.
- 8 W. A. Lingerak, F. Bakker and J. Slanina, in E. Pungor (Ed.), *Conference on Ion-Selective Electrodes*, Akademia Kiado, Budapest, 1977, p. 453.
- 9 K. A. Phillips and C. J. Rix, *Anal. Chim. Acta*, 169 (1985) 263.
- 10 T. D. Rice, *Anal. Chim. Acta*, 97 (1978) 213.

Short Communication

PHOTO-CURED POLYMERS IN ION-SELECTIVE ELECTRODE MEMBRANES

Part 2: A Calcium Electrode for Flow Injection Analysis

T. J. CARDWELL, R. W. CATTRALL and P. J. ILES

Analytical Chemistry Laboratories, Department of Chemistry, La Trobe University, Melbourne, Victoria 3083 (Australia)

I. C. HAMILTON

Department of Chemistry, Footscray Institute of Technology, Melbourne, Victoria 3011 (Australia)

(Received 3rd July 1985)

Summary. The preparation of a calcium-selective electrode based on a photo-cured polymer membrane containing a neutral carrier is described. This electrode is suitable for use in flow injection analysis because of its fast initial response and the hardness and mechanical strength of the membrane.

In a recent paper [1], the application of photo-cured polymers in the preparation of ion-selective electrode membranes was described and the advantages of this approach over the use of poly(vinyl chloride) as the membrane matrix material were discussed. The membranes prepared were calcium-selective and were based on the calcium salt of bis-[4-(1',1',3',3'-tetramethylbutyl)phenyl]phosphoric acid as the sensor. These membranes are homogeneous with a low water uptake and most importantly are hard and mechanically strong. These properties make them very suitable for use in "on-line" techniques such as flow injection analysis (f.i.a.).

In this communication, the preparation and use in f.i.a. of a calcium-selective electrode which is based on a neutral carrier ionophore in a photo-cured polymer membrane with a solid contact are reported.

Experimental

Materials. Ebecryl 600 (epoxyacrylate) and Uvecryl P36 (copolymerisable benzophenone photoinitiator) were obtained from UCB Chemical Sector (Belgium), and 1,6-hexanedioldiacrylate from Anchor Chemicals Australia Pty. The neutral carrier was *N,N'*-di[(11-ethoxycarbonyl)undecyl]*N,N'*-4,5-tetramethyl-3,6-dioxo-octane diamide (ETH 1001; Fluka). Di-*n*-decylphthalate (Eastman Kodak Co.), 2-nitrophenyl *n*-octyl ether (Alfa Products) and sodium tetraphenylborate (May and Baker) were also used in the membrane formulation.

Electrode preparation and testing. Ebecryl 600 (39.4% w/w), 1,6-hexanedioldiacrylate (19.7%), Uvecryl P36 (14.7%), di-n-decyl phthalate (23.8%), neutral carrier (1.9%) and sodium tetraphenylborate (0.5%) were mixed in an ultrasonic bath and applied to a platinum disc (7-mm diameter) fixed to the end of a perspex barrel. The electrode was held vertically in a nitrogen-filled glass chamber and the membrane was cured, through a polyethylene film window, for 40 min under a high-intensity (150 W) medium-pressure mercury lamp at a distance of 6–10 cm. After curing, the membrane was slightly cloudy but hard and very hydrophobic in nature.

The response characteristics of the electrode were tested with an Orion Model 901 Ionalyzer, in the differential mode interfaced with an Apple IIe microcomputer. The reference electrode was a Titron double-junction calomel electrode with both compartments containing saturated potassium chloride.

Flow-injection measurements were made in a single-line system with a short line length (5 cm, 0.5 mm i.d.) to minimize dispersion. A Gilson (Minipuls II) peristaltic pump was used at a flow rate of 1.5 ml min^{-1} with a teflon injector (Rheodyne 5020) fitted with a $100\text{-}\mu\text{l}$ sample loop. Samples were injected manually and measurements were made with the Orion 901 meter connected to a chart recorder. A solid-state chloride electrode (HNU) was used as reference to eliminate liquid junction effects and the carrier stream accordingly contained a constant chloride ion concentration (0.15 M NaCl). The detector and reference electrodes were mounted in a FiAtron flow cell.

Results and discussion

After conditioning for 10 min in 5×10^{-2} M calcium chloride, the electrode exhibited logarithmic response to calcium in the activity range 10^{-1} – 10^{-5} M. The slope, however, was 41.8 mV per decade which is in contrast to the solid-contact electrode prepared with the phosphate ion-exchanger which had a slope of 29.9 mV per decade [1]. Such "hyperNernstian" behaviour is a characteristic which occasionally arises with solid contact electrodes [2]. It is formally explicable in terms of an influence of the primary ion on the potential at the interface between the platinum metal and the ion-selective membrane, but there is no experimental evidence on this point. Nevertheless, if the slope is reproducible, as it is in this case, the electrodes can be used with confidence and the advantage of improved analytical sensitivity is obvious.

The electrode was fast in response and reached 95% of the equilibrium potential value instantly for concentrations of 10^{-4} M Ca^{2+} and above. Equilibrium, defined fairly stringently in this work as the potential that is stable to within ± 0.1 mV for 2 min, was achieved in less than 10 min for all solutions except 10^{-5} M (45 min). The response was independent of pH in the range of pH 4–9.5 for 10^{-3} M Ca^{2+} and 2.5–9.5 for 10^{-1} M Ca^{2+} , and the electrode responded in the expected fashion [3] when used in a potentiometric titration of Ca^{2+} with EDTA.

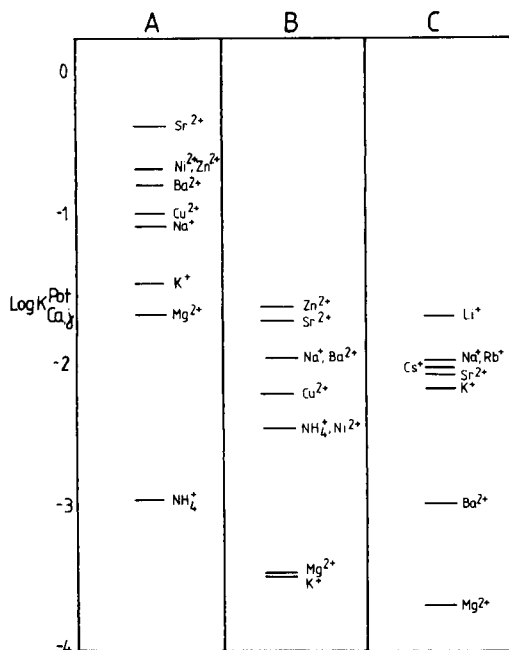


Fig. 1. Selectivity coefficients: (A) photo-cured membrane with phthalate plasticizer; (B) photo-cured membrane with nitrophenyl octyl ether/phthalate plasticizer; (C) PVC membrane with nitrophenyl octyl ether plasticizer [4].

Interferences were measured by the mixed-solution technique and the results are shown in Fig. 1. The $K_{Ca,j}^{Pot}$ values are compared with those of a poly(vinyl chloride)-based electrode with the same neutral carrier [4]. It can be seen that the present electrode is far less selective than the PVC-based one. This is understandable because the di-n-decylphthalate modifier in the membrane is of low polarity whereas the PVC membrane contains the more polar reagent 2-nitrophenyl n-octyl ether; it has been shown [4] that high selectivity for calcium is associated with the more polar modifier. Unfortunately, it is impossible to use a reagent containing a nitro group in the initial membrane mixture because it inhibits the photo-curing process.

This difficulty can be overcome in a very simple way by introducing the ether into the membrane after curing. This is done by applying two drops to the membrane surface and allowing it to permeate into the membrane for 30 min. Excess of ether is then removed with a tissue and the electrode is conditioned in the normal way. The selectivities for the treated electrode are also shown in Fig. 1 and compare very favourably with the PVC-based electrode. The treated electrode could be used for several days without any noticeable change in performance. This technique offers a very simple way of studying the effect of different modifiers on the behaviour of electrodes of this type, particularly with regard to selectivity.

The electrode shows considerable promise for use in flow injection analysis because of its fast initial response and has particular advantages in flow cells of the "wall-jet" design, such as the FiAtron cell, because of the hardness and mechanical strength of the membrane.

A calibration run with a 0.15 M sodium chloride carrier stream containing 10^{-6} M Ca^{2+} gave logarithmic response in the Ca^{2+} concentration range 10^{-1} – 10^{-3} M with a slope of 29.9 mV per decade and an analytically useful range extending to 10^{-5} M. The slope found for the electrode used in the flow-injection mode is lower than that observed in equilibrium measurements. This effect is to be expected when the electrode response time is comparable with the rise time of the sample peaks arriving at the detector cell. Even when electrode response is fast, a reduction in slope will result from the influence of hydrodynamic flow conditions in the cell on the maximum concentration of analyte reached in the boundary layer at the electrode surface. The reproducibility (equivalent to an RSD of 0.3% for 10^{-3} M solutions) and fast response of the electrode in f.i.a. are clearly illustrated in Fig. 2. It is possible to make 120 injections per hour with this system.

We are grateful for the financial support provided by the Australian Research Grants Scheme.

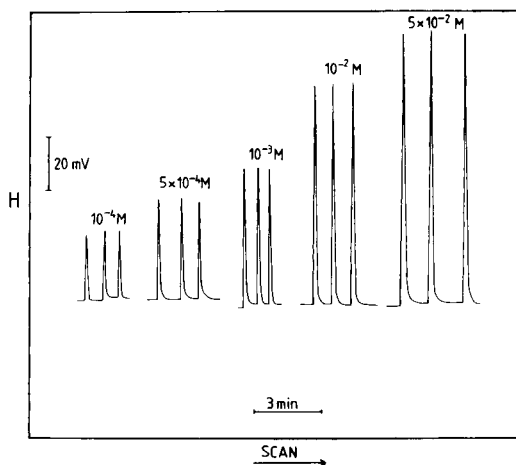


Fig. 2. Measurements in the range 10^{-4} – 5×10^{-2} M Ca^{2+} by f.i.a.

REFERENCES

- 1 R. W. Cattrall, I. C. Hamilton and P. J. Iles, *Anal. Chim. Acta*, **169** (1985) 403.
- 2 R. W. Cattrall and I. C. Hamilton, *Ion-Selective Rev.*, **6** (1984) 125.
- 3 R. W. Cattrall and H. Freiser, *Anal. Chem.*, **43** (1971) 1905.
- 4 D. Ammann, R. Bissig, M. Guggi, E. Pretsch, W. Simon, I. J. Borowitz and L. Weiss, *Helv. Chim. Acta*, **58** (1975) 1535.

Short Communication

THE ACID DISSOLUTION OF SULFIDE MINERAL SAMPLES UNDER PRESSURE IN A MICROWAVE OVEN

F. SMITH* and B. COUSINS

Chemistry Department, Laurentian University, Sudbury, Ontario P3E 2C6 (Canada)

J. BOZIC and W. FLORA

INCO, Ltd.; Copper Cliff, Ontario (Canada)

(Received 21st June 1985)

Summary. A system for the rapid dissolution of sulfide samples from mines, mills and smelters is described. The samples and an acid mixture are placed in sealed teflon-PFA vessels, which are then heated in a microwave oven for 3 min. Following the dissolution, metals of interest (copper and nickel) are quantified by atomic absorption spectrometry. The system described produces significant savings in time and materials and increased output and efficiency in comparison with traditional methods; it is also much cleaner. Results are similar to those obtained with a more conventional dissolution method.

Microwave ovens have been used in chemical laboratories for moisture determinations [1] and wet-ashing procedures of biological and geological materials [2–7] for some years. The pressure dissolution of geological specimens in Parr bombs heated in water baths has also been developed [8–10]. But it is only very recently that the two techniques have been combined, and that the rapid heating capability of the microwave oven has been applied to heat sealed vessels containing the samples for dissolution in an acid mixture [11].

This communication describes the results of attempts to dissolve a variety of mill and smelter sulfide samples by a technique that involves microwave heating of samples in acid in vessels manufactured from a new Teflon-PFA copolymer.

Experimental

Apparatus. The kitchen-model microwave oven (Toshiba model ER-800BTC) had nine power settings starting at 72 W and increasing by 81 W increments to 720 W. The teflon-PFA vessels used for the dissolutions had an approximate volume of 150 ml (Saville Corporation, Minnetonka, MN 55343). Atomic absorption measurements were done with a Perkin-Elmer model 703 spectrometer with an air/acetylene flame.

Reagents. All the chemicals and reagents used were of analytical-reagent grade.

Procedures. The samples examined were control samples used for daily assays. All material was ground to 400-mesh prior to entering a flotation process from which these samples were taken at different stages.

The comparison procedure involved four-acid attack in which 0.5 g of sample was mixed with 15 ml each of concentrated hydrochloric acid and nitric acid, 5 ml of concentrated sulfuric acid, and 2 ml of hydrofluoric acid in a 250-ml beaker covered by a watch glass. The beaker was then heated for 1–1.5 h, after which the residue was dissolved in 10 ml of concentrated hydrochloric acid and the solution was diluted to 1 l with distilled water.

In the new procedure, the sample (0.5 g for feeds and concentrates, 1.0 g for tailings), potassium chlorate (1.5 g), concentrated nitric acid (10 ml) and hydrofluoric acid (5 ml) were introduced into a 150-ml Savillex vessel, and the cap was screwed on tightly with the wrench supplied. Four such vessels at a time were put into the microwave oven, which was then run for 3 min at 477 W. The containers were then cooled in an ice bath for 5 min and opened, and the contents were diluted to 1 l with distilled water.

Results and discussion

Attempts to apply the pressure dissolution technique described by Matthes et al. [11] in the analysis of the present sulfide mill and smelter samples were unsuccessful. The polycarbonate vessels quickly became opaque and brittle with brown and yellow deposits adhering to the walls. Vessels specially machined from teflon rod, with screw caps, worked well, but were too bulky and expensive for multiple simultaneous dissolutions. Several alternatives were tried, of which the most suitable proved to be vessels constructed from the teflon-PFA tube segments and end caps marketed by Savillex. (The company has now made available a range of prefabricated screw-topped vessels which should prove even more appropriate than those used here.) For the particular mill and smelter samples investigated, use of the standard four-acid dissolution procedure in an open beaker on a hot-plate typically takes about 1.5 h to give a solution suitable for atomic absorption spectrometry. In contrast, the microwave technique can give a suitable solution in only 10 min. The results obtained for nickel and copper determinations by the two procedures are shown in Table 1. The values for the percentages of these two metals in the various samples, given by the microwave method, are similar to those obtained by the traditional method, and are within the specification range needed for these routine assays.

Complete dissolution was not achieved for all samples, particularly for the tailings, which have a high silica content. For these, a small amount of white residue settled in the volumetric flasks used for the final dilutions. Subsequent analysis of the combined insoluble residues from a number of experiments showed that they contained virtually no nickel or copper, but had a high silica content. Work is continuing on this problem, but in the meantime, the procedure outlined above yields significant savings in time and materials as well as increased output and efficiency in comparison with the traditional method. The system is also much cleaner, and it is expected that considerable reductions in fume hood requirements and corrosion costs will be additional benefits.

TABLE 1

Comparison of results for nickel and copper by the old and new methods

Sample	Nickel (%) ^a		Copper (%) ^a	
	Old	New	Old	New
<i>Clarabelle Mill</i>				
Feed	1.44 (0.02)	1.47 (0.02)	1.52 (0.02)	1.57 (0.01)
Tailings	0.145 (0.003)	0.148 (0.002)	0.078 (0.003)	0.081 (0.002)
Concentrate	10.36 (0.39)	10.37 (0.11)	14.41 (0.49)	14.47 (0.09)
<i>Frood-Stobie Mill</i>				
Tailings	0.183 (0.009)	0.174 (0.002)	0.102 (0.005)	0.101 (0.002)
Concentrate	6.64 (0.19)	6.52 (0.08)	9.98 (0.23)	10.04 (0.12)
<i>Copper Cliff Mill Concentrates</i>				
Nickel	10.27 (0.18)	10.16 (0.05)	1.51 (0.04)	1.48 (0.05)
Copper	0.927 (0.03)	0.916 (0.004)	26.36 (0.71)	26.62 (0.08)
Pyrrhotite	0.802 (0.044)	0.826 (0.009)	0.083 (0.004)	0.081 (0.002)

^aStandard deviations are given in parentheses; $n = 200$ for the old method and $n = 8$ for the new method.

We thank Dr. Vladimir Zátka (of the Inco J. Roy Gordon Research Laboratory, Mississauga, Ontario) for machining the special teflon vessels, and Heinz Oestreich (of Inco Manitoba), for helpful discussions concerning his own experiences with the adaptation of microwave dissolution techniques to mill and smelter samples. One of us (B. C.) thanks Laurentian University for the award of a Graduate Teaching Assistantship.

REFERENCES

- 1 J. A. Heseck and R. C. Wilson, *Anal. Chem.*, 46 (1974) 1160.
- 2 A. Abu-Samra, J. S. Morris and S. R. Koirtyohann, *Anal. Chem.*, 47 (1975) 1475.
- 3 A. Abu-Samra, J. S. Morris and S. R. Koirtyohann, *Trace Substances Environ. Health*, 9 (1975) 297.
- 4 T. N. Cooley, D. F. Martin and R. F. Quincel, *J. Environ. Sci. Health*, A12 (1977) 15.
- 5 P. Barrett, L. J. Davidowski, K. W. Penaro and T. R. Copeland, *Anal. Chem.*, 7 (1978) 1021.
- 6 S. Matsumura, I. Karai, S. Takise, I. Kiyota, K. Shinagawa and S. Horiguchi, *Osaka City Med. J.*, 28 (1982) 145.
- 7 R. A. Nadkarni, *Anal. Chem.*, 56 (1984) 2233.
- 8 R. T. Rantala and D. H. Loring, *At. Absorpt. Newsl.*, 14 (1975) 117.
- 9 R. T. Rantala and D. H. Loring, *At. Spectrosc.*, 1 (1980) 163.
- 10 R. A. Nadkarni, *Anal. Chem.*, 52 (1980) 929.
- 11 S. A. Matthes, R. F. Farrell and A. J. Mackie, *Tech. Prog. Rep. U.S. Bureau of Mines*, No. 120, 1983.

Short Communication

THE DETERMINATION OF ORGANOCHLORINE PESTICIDES AND POLYCHLORINATED BIPHENYLS BY COMBUSTION TUBE DECOMPOSITION AND MOLECULAR EMISSION CAVITY ANALYSIS

GOCOO PERSAUD, ROHITH B. BOODHOO, DEREK R. BUDGELL and DAVID A. STILES*

Department of Chemistry, Acadia University, Wolfville, Nova Scotia, BOP 1X0 (Canada)

(Received 28th April 1985)

Summary. The determination of microgram quantities of chlorine in polychlorinated biphenyls and organochlorine insecticides by molecular emission cavity analysis is described. Samples either pure, in admixture or mixed with sand were decomposed at $900 \pm 50^\circ \text{C}$ in a quartz combustion tube in a humidified oxygen atmosphere. The products of decomposition were bubbled through water or 1% ammonia and 4- μl aliquots of the solution obtained were injected into a stainless steel indium-lined cavity and heated in a nitrogen/hydrogen flame. The chlorine was quantified by comparing the intensity of the InCl emission at 360 nm with that obtained from hydrochloric acid standards. The effect of potential interferences such as alkali and alkaline earth metals, nitrogen, phosphorus, sulphur, carbon, aluminium and iron were studied. Except for the alkali and alkaline earth elements, the recoveries of the compounds burned were not affected. Where the elements interfered, methods for eliminating the interferences are described. The chlorine recovery was usually >90%.

For many years, organochlorine compounds have been used extensively in a variety of applications including agriculture and the electrical industry. In more recent times, however, their use has been severely curtailed, because of resistance to breakdown in the environment, their bioaccumulation and toxicity to wildlife, as well as their link to various diseases including cancer. Many methods exist for the identification and confirmation of these classes of compounds at trace levels, the most extensively reported being those based on gas chromatography. More recently, however, methods based on high-performance liquid chromatography (h.p.l.c.) or gas chromatography combined with mass spectrometry (g.c./m.s.) have gained prominence [1]. These techniques however, are either time-consuming or costly, and are therefore not well-suited as initial screening procedures.

Molecular emission cavity analysis (m.e.c.a.) has also been used successfully as the basis of methods to determine total halogens at trace levels [2]. The technique is sensitive, requires relatively inexpensive instrumentation and is comparatively rapid. In some earlier m.e.c.a. experiments, organohalogen compounds were extracted from sand and decomposed to

the hydrogen halide by oxygen flask combustion [3, 4]. The decomposition products were dissolved in a minimal volume of either water or aqueous ammonia (5.0 ml) and aliquots (4 μ l) were injected into an indium-lined stainless steel cavity. The cavity was heated in a nitrogen-cooled hydrogen flame and the InCl emission intensity ($\lambda_{\text{max}} = 360 \text{ nm}$) was used to quantify the halogen present. Although the recovery for a variety of fortified samples was over 90%, the detection limit was limited by the halogen blank of the combustion paper used in the decomposition step.

An alternative method for determining organohalogen compounds has been reported by Solomon and Uthe [6] and Ladrach et al. [7]. Organochlorine compounds were decomposed in an atmosphere of humidified oxygen in a quartz combustion tube and the hydrogen chloride produced was dissolved in water, the chlorine being determined microcoulometrically. The method was suitable for determining trace quantities of analyte.

This paper reports experiments in which the combustion tube decomposition is combined with m.e.c.a. to determine organochlorine compounds, as total chlorine, at trace levels. Also discussed are the effects of various potential interferences.

Experimental

Chemicals. Organochlorine insecticide standards were obtained from Velsicol Chemical Corp., Chicago, IL, and polychlorobiphenyl (PCB) compounds from Monsanto Company, St. Louis, MO. All chemicals were used without further purification. Hydrochloric acid standards used in preparing m.e.c.a. calibration graphs were made by serial dilution of aqueous standards of the analytical-grade acid. Standard solutions of organochlorine compounds were prepared in pesticide-grade acetone/hexane (3:2, v/v) solution.

Decomposition of organochlorine compounds. The decomposition chamber used was a quartz combustion tube specially made (Nova Scotia Research Foundation, Dartmouth, Nova Scotia, B2Y 3Z7) to fit inside a Lindberg Hevi-Duty model 167 tube furnace. Quartz combustion boats, 30 \times 5 mm, were obtained from the same company. The m.e.c.a. analyser (Anacon, Ashland, MA) was operated with an indium-coated stainless steel cavity, as reported previously [3]. The gas flow rates were 4.0 l min⁻¹ hydrogen and 7.0 l min⁻¹ nitrogen. The collimating slit was set at 1.4 mm.

Organochlorine standards were prepared either pure, in admixture, or as fortified acid-washed sand samples. For the sand samples, a known amount of organochlorine compound was applied to sand (0.3 g) in the combustion boat, and the solvent was allowed to evaporate. The chlorinated compounds burned included Aroclor 1242, Aroclor 1254, lindane, DDT, dieldrin, 2,4-D, endrin and aldrin, with ranges of 10–1000 μ g chlorine. During combustion, the boat was placed into the combustion tube at point N (Fig. 1), the connection was made at H, and the boat was pushed as quickly as possible into the furnace, with the aid of a stainless steel rod (E) through the 3-way stopcock (G). After pulling out the rod, the stopcock was turned to allow only helium to flow, the rate being maintained at 2–3 ml min⁻¹.

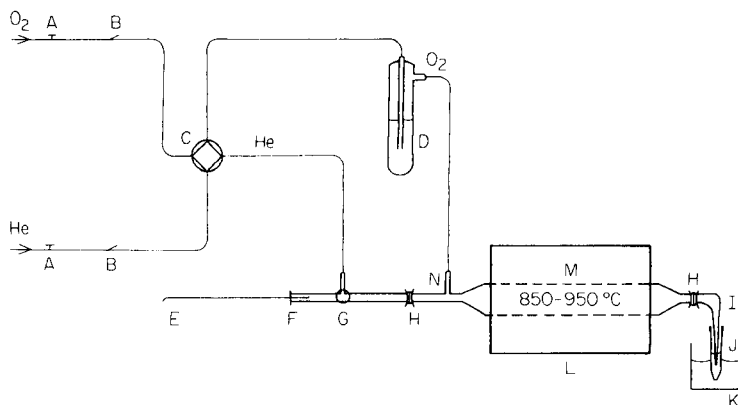


Fig. 1. Schematic diagram of the combustion tube apparatus used to decompose the organochlorine compounds: (A) needle valve; (B) toggle switch; (C) 2-way switch; (D) oxygen humidifier; (E) steel wire; (F) rubber septum; (G) 3-way stopcock; (H) clamps; (I) delivery tube; (J) 5-ml centrifuge tube; (K) ice bath; (L) furnace; (M) quartz combustion tube; (N) entrance end of combustion tube.

Each sample was allowed to evaporate in the helium atmosphere for 30 s, after which the helium flow was turned off, and the oxygen flow turned on. The flow rate of oxygen varied between 5 and 100 ml min⁻¹, the lower flow rates being used in the early stages of combustion. Liquid samples were heated for 10 min while those of fortified sand were heated for 25 min. The gases produced during combustion were blown through 2.5 ml of ice-cold water or aqueous 1% ammonia, contained in a 5-ml calibrated centrifuge tube (J).

After combustion, the oxygen flow was stopped, and the delivery tube (I) was disconnected and washed with 1–2 ml of trapping solvent to remove any acid droplets retained by the tube. These washings were collected along with the other products of combustion. Aliquots (4 μl) of this solution were injected into the cavity, and the cavity was heated in the nitrogen/hydrogen flame. The intensity of the resulting InCl emission was measured and used to obtain the concentration of chlorine, with the aid of a calibration graph prepared from results from the aqueous standards.

Treatment of samples and the removal of interferences

Standard solutions containing each of the potentially interfering species (organic sulphur and phosphorus, and inorganic sulfur, phosphorus, sodium, calcium, magnesium, iron and aluminium) were prepared as shown in Table 1. These were added in known quantities to fortified sand samples, and heated according to the procedure described above.

Alkali and alkaline earth metals. For each of these species, 0.100 ml of the interferent solution was added to sand (0.3 g) and the solvent allowed to

TABLE 1

Potential interferent solutions used

Interfering element	Compound used	Solvent	Concentration of interferent (M)
Na	NaNO ₃	Water	0.430
K	KNO ₃	Water	0.198
Mg	Mg(NO ₃) ₂ · 6H ₂ O	Water	0.780
Ca	Ca(NO ₃) ₂ · 4H ₂ O	Water	8.47 × 10 ⁻³
Fe	Fe(NO ₃) ₃ · 9H ₂ O	Water	0.181
Fe + S	FeSO ₄ · 7H ₂ O	0.025 M Sulphuric acid	0.180
Al	Al(NO ₃) ₃ · 9H ₂ O	Water	0.374
P (organic)	(CH ₃ CH ₂ O) ₃ P	Acetone/hexane	0.350
P and Na	Na ₂ C ₃ H ₅ (OH) ₂ PO ₄ · 5.5H ₂ O	Water	0.318
P	NH ₄ H ₂ PO ₄	Water	1.74 × 10 ⁻³
S	H ₂ SO ₄	Water	0.574
S	(NH ₄) ₂ S	Water	0.352
S (organic)	(CH ₃ C ₆ H ₄ S) ₂	Acetone/hexane	0.312

evaporate. Solutions of the organochlorine compounds were added and, after solvent evaporation, the sample was burned. The aqueous decomposition solutions obtained from calcium- and magnesium-spiked sand were further treated by addition of a solution of 0.10 M EDTA (0.100 ml) to 1 ml of this solution; the pH was adjusted to 8 for the calcium-containing sand and 11 for the magnesium-fortified sand. Aliquots (4 μ l) of the final solution were used for quantification of the recoverable chlorine.

In another method, the chlorinated compounds were extracted after addition of the interferences to soil. A small quantity of soil was fortified with a known amount of one of the interferents, i.e., sodium, potassium, calcium or magnesium, in a glass vial, followed by addition of 3:2 acetone/hexane mixture (0.200 ml; 3:2). After shaking on a Wig-L-Bug, the vial was centrifuged and aliquots (0.100 ml) of the extract were combusted. The percent recovery of the organochlorine compound as total chlorine was determined as described above.

Sulfur. A 1-ml aliquot of the solution obtained in the collection tube after combustion was shaken with 0.05 ml of mercury on a Wig-L-Bug for approximately 1 min and allowed to stand. Aliquots (4 μ l) of the supernatant liquid were injected into the cavity, and the chloride content was determined. This procedure was repeated until the supernatant liquid showed no positive interference from sulphur.

Results and discussion

Preliminary experiments designed to investigate the efficiency of the combustion tube procedure gave recoveries of over 90% for a variety of organochlorine compounds. This compared well with the oxygen flask

method of decomposition utilized in earlier investigations [3]. The limit of detection was not determined by the combustion paper blank, but by the volume of solvent used to trap the exit gases and that required to wash the exit tube.

The flow rate of oxygen through the combustion tube was an important factor governing the extent of conversion of organochlorine compounds to hydrogen chloride. Relatively small quantities of analyte (100 μg) were completely decomposed at an oxygen flow rate of 200 ml min^{-1} , in accordance with the observations of Solomon and Uthe [5]. However, as the amount of organochlorine compound being decomposed increased, the relative recovery decreased. Most likely this is due to the incomplete absorption of hydrogen chloride gas by the trapping solution, as shown by the misty appearance of the vapor above the water in the collection tube as the gases bubble through. Slower oxygen flow rates of 20–40 ml min^{-1} were found to eliminate the formation of mist above the water, and gave increased percent recovery of chlorine. The use of aqueous ammonia (1%) was found to give similar recoveries. The relative standard deviation for a given sample was 5.0%.

Interferences

Sulphur. Sulphur was studied as three different interfering species, sulphate, sulphide and organic sulphur. In all cases, these species are converted to sulphur dioxide or sulphur trioxide in the highly oxidizing atmosphere inside the combustion tube. Inside the m.e.c.a. cavity, the reducing atmosphere produces S_2 and other sulphur-containing emitting species. At normal chart speeds (1.25 cm min^{-1}), these sulphur emission peaks overlap the InCl peaks, causing positive interference. By increasing the chart speed to 12.5 cm min^{-1} , three maxima were resolved. When samples corresponding to 100 μg Cl were heated, these maxima appeared at t_m values (time from insertion into flame to maximum intensity) of 1 s, 2.5 s and 4.5 s, and by using the maximum which corresponds to that of the chloride standards ($t_m = 4.5$ s) the positive interference was removed. Samples containing 10 μg of chlorine were quantified in the presence of 500 μg of sulphur without significant interference.

The alternative method of mercury treatment of the final solution gave similar results to those obtained by using the above procedure. Recoveries after this treatment were over 90%.

Alkali and alkaline earth metal cations. Direct combustion of samples containing these ions decreased the recovery by up to 40%. Alkali metal cations (500 μg) in particular gave variable recoveries (60–100%) with the samples treated first giving the higher recoveries. Also, the organochlorine pesticides, which are more easily broken down than the PCBs, gave more variable results. The percent recovery of chlorine was found to be dependent on the length of time the organochlorine compound and alkali metal ion were in contact, longer periods of contact generally giving lower recoveries.

Alkaline earth cations, however, gave reproducible recoveries of 81%, and attempts to complex these ions with EDTA in the trapping solution only increased the recovery to 85%. This is only slightly above the precision of the method (2%) and can be considered insignificant.

An alternative procedure involving extraction of the chlorinated compounds with acetone/hexane followed by combustion of the extract, gave recoveries when alkali metals were present of over 90% and for the alkaline earth metals of over 80%.

Iron, aluminium, phosphorus, nitrogen and carbon. Iron was added in both oxidation states and phosphorus was added as both organic and inorganic phosphate as well as inorganic phosphite. Nitrogen and carbon were added as nitrates and organic compounds, respectively. Except for sodium glycerophosphate, which gave variable recoveries between 80 and 100%, the other elements did not affect the percent recovery of chlorine. Recoveries for samples containing 10–150 μg of chlorine were over 90%.

Therefore the potential interfering elements studied did not affect the determination of organochlorine compounds with the combustion tube/m.e.c.a. technique and thus this method is suitable for rapid screening for this class of compounds.

Acknowledgement is made to the Natural Sciences and Engineering Research Council for a grant to support this work, and to the Environment Protection Services, Government of Canada, for the award of a contract.

REFERENCES

- 1 J. Sherma and G. Zweig, *Anal. Chem.*, 55 (1983) 57R.
- 2 R. Belcher, S. L. Bogdanski, Z. M. Kassir, D. A. Stiles and A. Townshend *Anal. Lett.*, 7 (1974) 751.
- 3 D. R. Marine, M. E. Peach and D. A. Stiles, *Anal. Lett.*, 9 (1976) 767.
- 4 M. H. K. Abdel-Kader, M. E. Peach, M. H. T. Ragab and D. A. Stiles, *Anal. Lett.*, 12 (1979) 1399.
- 5 J. Solomon and J. F. Uthe, *Anal. Chim. Acta*, 73 (1974) 149.
- 6 W. Ladrach, F. Van de Craats and P. Gouverneur, *Anal. Chim. Acta*, 50 (1970) 219.

Short Communication

SPECTROPHOTOMETRIC DETERMINATION OF CHROMIUM(VI) BY EXTRACTION WITH THE 1-NAPHTHYLMETHYLTRIPHENYLPHOSPHONIUM CATION

D. THORBURN BURNS and S. KHEAWPINTONG

Department of Analytical Chemistry, The Queen's University of Belfast, Belfast BT9 5AG (Northern Ireland)

(Received 16th May 1985)

Summary. Chromium(VI) (0–85 μg) can be determined by spectrophotometric (or spectrofluorimetric) measurement after its extraction as 1-naphthylmethyltriphenylphosphonium dichromate into 1,2-dichlorobenzene. The effects of acidity, diverse ions and masking studies are reported. The system has been applied to the spectrophotometric determination of chromium in a range of highly alloyed steels.

The oxyanions are the least studied group of species which form ion-pairs with onium cations, capable of extraction into organic solvents [1, 2]. For the determination of chromium(VI), spectrophotometric studies with triphenylsulphonium [3], triphenylselenonium [4], tetraphenylphosphonium [5], n-propyltriphenylphosphonium [6] and trioctylmethylammonium [7] cations have been reported. No spectrofluorimetric determination based on onium cation extraction of chromium(VI) has been described and only one basic dye system [8], which uses safranin-T [9]. The present communication reports the first use of 1-naphthylmethyltriphenylphosphonium cation as an ion-pairing extractant for chromium(VI) as dichromate. Determinations on a 1,2-dichlorobenzene extract may be completed spectrophotometrically. Alternatively, the decrease in fluorescence of the extract can be measured, although this gave a less reproducible procedure. The system has been applied to the determination of chromium in steels, after oxidation of chromium(III) to chromium(VI) by permanganate.

Experimental

Apparatus. A Pye Unicam SP8000 spectrophotometer and a Baird Atomic SFR 100 spectrofluorimeter were used for recording absorption and fluorescence (excitation and emission) spectra, respectively. Routine absorbance measurements (at 355 nm) were made with a Pye Unicam SP6-550 digital spectrophotometer, and fluorescence measurements with a Perkin-Elmer 1000 fluorimeter ($\lambda_{\text{ex}} = 342 \text{ nm}$, $\lambda_{\text{em}} = 430 \text{ nm}$) and 1-cm quartz cells.

Reagents. 1-Naphthylmethyltriphenylphosphonium chloride (Lancaster Synthesis) was used as supplied; carbon and hydrogen data proved that it

was pure. A 0.5% (w/v) stock solution was prepared in water. A stock 1000 $\mu\text{g ml}^{-1}$ chromium(VI) solution was prepared by dissolving 2.830 g of potassium dichromate (AnalaR, previously dried for 2 h at 140°C) in 1 l of water. More dilute standard solutions were prepared as required. 1,2-Dichlorobenzene was distilled under reduced pressure, and the fraction with b.p. 30–31°C at 1 mm Hg was collected for use. All other reagents were of analytical grade, and twice-distilled water was used throughout.

Choice of solvent. Various solvents including alcohols, ketones, esters, ethers and chlorinated and aromatic hydrocarbons were examined for extraction efficiency; 5-ml aliquots of 20 $\mu\text{g ml}^{-1}$ dichromate [ca. 10 $\mu\text{g ml}^{-1}$ Cr(VI)] solution, with 10 ml of 0.5 M sulphuric acid and 5 ml of 0.5% 1-naphthylmethyltriphenylphosphonium chloride were extracted with 10 ml of solvent for 1 min. The absorbance of each extract was measured within 5 min at 355 nm against pure solvent. Trichloromethane, chlorobenzene, dichloromethane, tetrachloromethane and 1,2-dichlorobenzene were the most efficient extractants. Dichloromethane and 1,2-dichlorobenzene extracts of the reagent showed the highest fluorescence. Dichloromethane was rejected because of its relatively high volatility and 1,2-dichlorobenzene was used for the rest of the study.

Optimum amounts of reagents. The absorbance of extracts was found to be independent of sulphuric acid concentration over the range 0.1–2.5 M, and 0.5 M was adopted. The absorbance of extracts increased rapidly with addition of up to 3 ml of 0.5% 1-naphthylmethyltriphenylphosphonium chloride solution and thereafter increased slowly, by 1.3% from 3 to 7 ml, therefore 5 ml of reagent solution was adopted for routine use.

Composition of the complex. This was established spectrophotometrically at 355 nm by Job's method of continuous variations [10] and by the mole ratio method [11] to be $(\text{C}_{29}\text{H}_{24}\text{P})_2\text{Cr}_2\text{O}_7$.

Spectrophotometric analysis of steel samples. For samples containing 3–6% chromium, such as high-speed tool steels, dissolve accurately weighed 0.1-g samples in 10 ml of 20% (v/v) sulphuric acid in 250-ml conical flasks by warming. Add 1 ml of concentrated nitric acid and simmer gently until all the carbides are decomposed. Add 2 ml of (1 + 1) sulphuric acid and evaporate carefully to fumes. Cool. Add 50 ml of water and warm to dissolve the soluble salts. Cool and if necessary filter through a Whatman No. 40 filter paper into a 100-ml (or larger or smaller depending on the chromium content) volumetric flask. Wash the residual solids (silica, tungstic acid) with a small volume of hot (1 + 99) sulphuric acid followed by water and make up to volume. Mix well. Transfer a 10-ml aliquot of this solution to a 100-ml beaker, add 1 ml of (1 + 1) sulphuric acid and 1 ml of 1% (w/v) potassium permanganate solution. Heat the solution on a steam bath for 20 min and cool to room temperature. Add 5% (w/v) sodium azide solution dropwise (3–5 drops) with swirling to destroy the excess of permanganate. Boil for a further 5 min and cool in a cold water bath. Transfer quantitatively to a 100-ml volumetric flask and make up to volume with water.

Transfer 5 ml to a 100-ml separating funnel and add 10 ml of 0.5 M sulphuric acid, 5 ml of the 0.5% reagent solution and 5 ml of water, and mix. Add 10 ml of 1,2-dichlorobenzene and shake for 1 min. Allow the phases to separate. Filter the lower phase through a Whatman No. 1 filter paper and measure the absorbance at 355 nm.

Prepare a calibration graph over the range 0–175 μg of dichromate, adding 5 ml of iron solution prepared from pure iron sponge dissolved and treated as for the samples. This is to compensate for the residual effect from the use of permanganate to oxidise chromium(III).

Results and discussion

A linear calibration graph was obtained over the range 0–175 μg of dichromate at 355 nm (apparent molar absorptivity = $2.94 \times 10^3 \text{ l mol}^{-1} \text{ cm}^{-1}$) and the fluorescence calibration was linear over the same range but with a negative slope. For 50 μg of dichromate the relative standard deviations for seven replicate determinations were 0.63% and 0.93% for the spectrophotometric and indirect fluorescence measurements, respectively.

The possible interferences of a number of cations and anions on the extraction of 50 μg of dichromate were examined. Under the optimal conditions, the following ions in a weight ratio of 200:1 were without appreciable effect on absorbance or fluorescence measurements: zirconium(IV), lead, manganese(II), iron(III), nickel, aluminium, vanadate, tartrate, citrate, acetate, phosphate and sulphate. Tin(IV) and chloride were found to increase only the fluorescence readings (by 15 and 16%, respectively) whilst fluoride and nitrate produced negative errors on the absorbance measurements (both -7%) at 200:1 weight ratios. The results of the interference and subsequent masking studies are summarised in Table 1.

As for other dichromate methods, the interferences by manganese(VII), molybdenum(VI), tungsten(VI) and copper(II) were significant but could be masked by addition of 10 ml of 5% sodium azide solution for up to 50 mg of manganese(VII) and 2 ml of 40% (w/v) ammonium potassium tartrate solution for up to 100 mg of copper(II). Tungsten(VI) is removed during dissolution of the steels and molybdenum(VI) may be removed by extraction as its chloro complex into 10 ml of 1:1 (v/v) diethylether/carbon tetrachloride followed by addition of 1 ml of 0.1 M silver sulphate to mask the chloride. For the steels examined, it was not necessary to mask copper(II) or to extract molybdenum(VI).

Peroxodisulphate, cerium(IV) and permanganate were examined for oxidation of chromium(III) to (VI). Permanganate was found to be satisfactory and compatible with the analysis of steels, and the excess of permanganate was selectively decomposed by addition of azide. For 500 μg of permanganate initially added per aliquot taken, slightly increased extraction occurred (0.3 and 1.3% for the absorbance and fluorescence measurements, respectively), which is allowed for in the preparation of the calibration graph.

TABLE 1

Effect of diverse ions on the determination of dichromate (50 μg)

Ion ^a	Ion/ Cr ₂ O ₇ ²⁻ (w/w)	Absorbance change (%)	Fluor. change (%)	Ion ^a	Ion/ Cr ₂ O ₇ ²⁻ (w/w)	Absorbance change (%)	Fluor. change (%)
Sb(III)	200	-50	+30	Oxalate	200	-9	-15
	5	-48	+21		5	0	0
	1	-42	0		WO ₄ ²⁻	200	+80
Cu ²⁺	200	-11	+7		1	0	0
	5	0	0	Cl ⁻	200	0	16
	200 ^b	0	0		5	0	0
Fe ²⁺	200	-67	+19		200 ^c	0	0
	1	-52	+6	ClO ₄ ⁻	200	-100	-100
					1	0	0
Sn(IV)	200	0	+15	NO ₃ ⁻	200	+6	+40
	5	0	0		5	0	0
AsO ₃ ³⁻	200	-51	+22	MoO ₄ ²⁻	200	+70	+40
	5	-46	+20		5	0	0
SCN ⁻	200	+15	-15		200 ^d	0	0
	1	0	0	MnO ₄ ⁻	200	+1650	-98
	200 ^e	0	0		1	0	-43
					200 ^e	0	0

^aCations added as chloride or sulphate; anions added as sodium salt. ^bIn the presence of ammonium potassium tartrate. ^cIn the presence of silver sulphate. ^dAfter extraction of the chloro complex with 1:1 (v/v) diethyl ether/carbon tetrachloride. ^eAfter addition of sodium azide.

TABLE 2

Analysis of high-speed tool steels and a stainless steel

BCS steel no.	Chromium in steel (% w/w)		
	Certified	Certified range	Found ^a
482	4.09	4.06-4.14	4.0 ± 0.08
484	5.17	5.14-5.20	5.19 ± 0.23
485	4.15	4.11-4.18	4.17 ± 0.24
241/2	5.35	5.29-5.40	5.36 ± 0.15
467	18.05	17.97-18.18	18.01 ± 0.30

^aSpectrophotometric method: mean ± 95% confidence limit, 4 replicates.

The results for the spectrophotometric determination of chromium in British Chemical Standard Steels (Table 2) are in excellent agreement with the certificate values. However, the confidence limits with the fluorescence procedure were too wide ($\pm 1.5\%$) to be of practical use and hence are not

reported. Although the reagent has been available since its synthesis by Zander and Franke [12], it has not previously been used as an ion-pairing spectrophotometric reagent although it has been used in Wittig reactions [13-15].

REFERENCES

- 1 A. J. Bowd, D. Thorburn Burns and A. G. Fogg, *Talanta*, 16 (1969) 719.
- 2 D. Thorburn Burns, *Anal. Proc.*, 20 (1983) 595.
- 3 R. Bock and C. Hummel, *Z. Anal. Chem.*, 198 (1963) 176.
- 4 M. Zeigler and K. D. Pohl, *Z. Anal. Chem.*, 204 (1964) 413.
- 5 R. Bock and J. Jainz, *Z. Anal. Chem.*, 198 (1963) 315.
- 6 J. Hala, O. Navratil and V. Nechuta, *J. Inorg. Nucl. Chem.*, 28 (1966) 553.
- 7 J. Adam and R. Pribil, *Talanta*, 18 (1971) 91.
- 8 A. Gomez-Hems and M. Valcarcel, *Analyst (London)*, 107 (1982) 465.
- 9 A. T. Pilipenko, T. L. Shevchenko and A. I. Volkova, *Zh. Anal. Khim.*, 32 (1977) 731.
- 10 P. Job, *Ann. Chim. (Paris)*, 9 (1928) 113.
- 11 J. H. Yoe and A. L. Jones, *Ind. Eng. Chem. Anal. Ed.*, 16 (1944) 111.
- 12 M. Zander and W. Franke, *Chem. Ber.*, 94 (1961) 446.
- 13 K. E. Stensio and U. Ahlin, *Tetrahedron Lett.*, 49 (1971) 4729.
- 14 A. Yasuhara, S. Akiyama and M. Nakagawa, *Bull. Chem. Soc. Jpn.*, 45 (1972) 3638.
- 15 W. J. Archer, R. Taylor, P. H. Gore and F. S. Kamounah, *J. Chem. Soc. Perkin Trans. 2*: (1980) 1818.

Short Communication

DETERMINATION OF PHENYL ISOCYANATE IN A FLOW-INJECTION SYSTEM WITH INFRARED SPECTROMETRIC DETECTION

D. J. CURRAN* and W. G. COLLIER^a

Department of Chemistry, University of Massachusetts, Amherst, MA 01003 (U.S.A.)

(Received 14th February 1985)

Summary. A flow-injection system for the determination of isocyanate moiety, as an example of organic functional groups, is described; infrared detection is used in the transmittance mode. Absorption is measured at 4.40 μm with carbon tetrachloride as the solvent and carrier stream. Injections (25 μl) of 0.100–16.0 mM phenyl isocyanate solutions provide a useful calibration curve with a linear response up to about 1.5 mM. The detection limit for phenyl isocyanate at a signal-to-noise ratio of 2 is about 4 $\mu\text{g ml}^{-1}$ in the sample injected.

Infrared (i.r.) spectrophotometry possesses much better selectivity than ultraviolet-visible methods. Flow-injection techniques of sample handling are very useful for rapid, repetitive determinations. A combination of these two techniques could produce a fast, selective approach to determinations based on organic functional groups. There do not appear to be previous reports on the use of i.r. detection with flow injection analysis. Each complements the other. Phenyl isocyanate was used as a test compound in a carbon tetrachloride flow stream. The absorption of the isocyanate moiety at 4.40 μm was monitored. The method is sensitive and fast.

Experimental

Reagents and solutions. Carbon tetrachloride, used as the carrier stream and for the preparation of solutions, was Omni-solve spectrometric-grade (MCB). Phenyl isocyanate (Eastman White Label) was used as received. Solutions in carbon tetrachloride were prepared in Kimax 50-ml volumetric flasks using a 2.5-ml Gilmont ultra-precision micrometer buret (RGI Industries, Box 732, Vineland, NJ). The stock solution of phenyl isocyanate and solvent were kept in a constant-temperature bath at 19.5°C.

Apparatus. The flow injection system consisted of a Constametric-III pump (LDC-Milton Roy, Riviera Beach, FL) with stainless steel tubing, a Rheodyne model N-60 loop injector valve equipped with a 25.0- μl loop, teflon

*Present address: Department of Chemistry, University of Lowell, 1 University Avenue, Lowell, MA 01854, U.S.A.

flow lines (Altex 0.3 mm i.d. teflon tubing), a circulating constant-temperature bath (P. M. Tamson, N.V. Holland), a flow-through infrared cell, and a MIRAN-1A variable-filter infrared spectrometer (Wilks-Foxboro, South Norwalk, CT). The flow line was equipped with a water jacket placed just before the injection valve. A Varian Model G 2500 strip-chart recorder was used. The length of 0.3-mm i.d. tubing between the injector valve and the detector was 15.4 cm. The entire apparatus was placed in a hood. The flow-through i.r. cell was a modified International Crystal Laboratories (Elizabeth, NJ) cell. The bottom half of this cell holder is threaded so that the top can be screwed down. A new top plate was constructed which served to align the cell window vertically with the light path, and provision was made for inlet and outlet connections. A cavity (2.25-cm length, 0.280-cm width, 0.205-cm depth) was cut in a teflon spacer to provide the flow channel through the cell.

Procedures. All solutions were stored in the constant-temperature bath at 19.5°C for at least 30 min prior to sample injection, and all flasks were sealed with Parafilm. Seven repeated injections were done for each solution. The first injection of each set was used to clean the sample loop, and the next six injections were used for the calculation of mean peak heights. These were converted to absorbance and plotted against their respective injected concentrations. Operating parameters were as follows: flow rate 0.70 ml min⁻¹; injection volume 25 μl; residence time 3 s; slitwidth 0.5 mm; wavelength 4.40 μm; time constant 4 s; recorder chart speed 2.54 cm min⁻¹.

The N=C=O functionality absorbs in the region 4.40–4.46 μm [1]. To select the optimum wavelength, the infrared cell was filled with a solution of 0.200 mM phenyl isocyanate and the wavelength of the spectrometer was scanned from 4.35 to 4.46 μm while the absorbance was monitored. The maximum absorbance occurred at 4.40 μm.

The system dispersion was evaluated as described by Ruzicka and Hansen [2]. The spectrometer was zeroed with solvent in the cell. The solvent reservoir was then filled with a solution of 0.200 mM phenyl isocyanate in carbon tetrachloride. This solution was then pumped through the detector cell until a steady-state signal was obtained. After cleaning the solvent reservoir, pure solvent was added and pumped through the cell until the signal returned to baseline. A set of six repeated injections of the same phenyl isocyanate solution was then made and the absorbance peaks were recorded. The dispersion is the ratio of the steady-state absorbance to the mean absorbance calculated for the six injections.

Results and discussion

The steady-state absorbance for the 0.200 mM phenyl isocyanate solution was 0.0440 while the mean absorbance for six injections of the same solution into the flow stream was 0.00965. These data yield a dispersion of 4.6. According to the classification of Ruzicka and Hansen [2], this is a medium-dispersion system.

Peaks for six injections of 0.600 mM phenyl isocyanate are shown in Fig. 1. Satisfactory baseline separation was achieved at an injection rate of about 1 min^{-1} for all the concentrations tested but there was less noise at higher concentrations. Data obtained for the construction of the working curve are plotted in Fig. 2. For absorbances ranging from 0.005 to 0.41, relative standard deviations were mostly in the range 1.2–4.2% with one value of 8.290. The nonlinear nature of the working curve is clear. Several known solutions of phenyl isocyanate were prepared in carbon tetrachloride and regarded as unknowns. Mean absorbances for three of them are shown as points B–D in Fig. 2. The concentrations found are shown in Table 1. These results show that the nonlinear region of the calibration can be used with reasonable accuracy. The plot of the data for the lowest decade range of concentration is linear. Statistical treatment of the data gave the following results: correlation coefficient, 0.9996; slope, 43.5 absorbance/mol l^{-1} ; Y intercept, 0.00105 absorbance; standard error of the estimate, 0.000446; 95% confidence limits of the slope and intercept, ± 0.00556 and ± 0.000740 , respectively. The concentrations taken for solution A of Table 1 are in the linear region of the working curve, and the results obtained from the plot and from the linear regression line show positive errors as did more concentrated solutions, indicating a systematic error in the procedure. A possible cause of this is atmospheric carbon dioxide absorbing at $4.3 \mu\text{m}$.

There are several factors which contribute to the non-linearity of the working curve. The cavity volume was $129 \mu\text{l}$ which is large enough to make a significant contribution to dispersion, and variable mixing may have been obtained in the 90° turn at the entry to the cell cavity. The volume of the flow line preceding the cell was $462 \mu\text{l}$; the volume occupied by the light beam was much smaller than the cavity volume, and the peak volumes were typically about $370 \mu\text{l}$. For the lowest concentration of phenyl isocyanate investigated, 0.100 mM, the infrared spectrometer was used on its most sensitive full scale range of 0.025 absorbance. The peak-to-peak noise of the

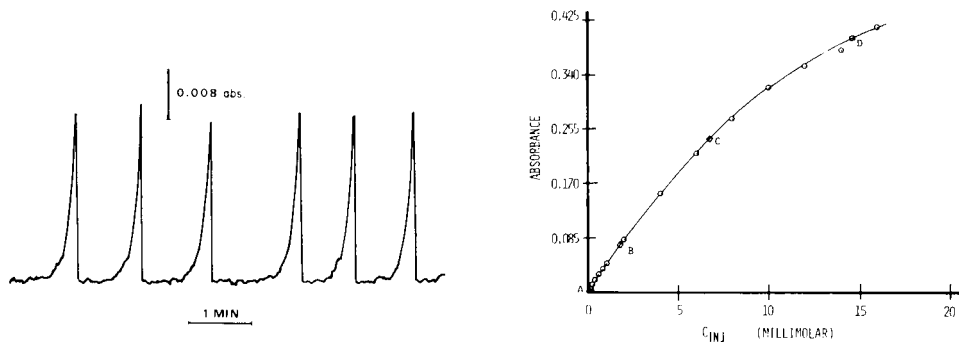


Fig. 1. Recorded output for 0.600 mM phenyl isocyanate in carbon tetrachloride.

Fig. 2. Absorbance vs. concentration curve for phenyl isocyanate in carbon tetrachloride. For explanation of points A–D, see text.

TABLE 1

Results of the determination of phenyl isocyanate solutions

Solution	Concentration (mM)		Rel. error (%)
	Taken	Found	
A	0.240	0.248 ^a	+3.3
		0.246 ^b	+2.5
B	1.80	1.90 ^a	+5.6
C	6.40	6.63 ^a	+3.6
D	13.6	14.2 ^a	+4.4

^aFrom working curves. ^bCalculated from the linear regression line.

background signal was 0.000875 absorbance. From this result and the data in Fig. 2, a signal-to-noise ratio of 5.78 was calculated. Extrapolating to a signal-to-noise ratio of 2 gave a detection limit for phenyl isocyanate of 103 ng, or about 4 $\mu\text{g ml}^{-1}$ in the sample injected.

Ham and Willis [3] reported a value of 1140 for the molar absorptivity of phenyl isocyanate in carbon tetrachloride. Data from the present steady-state experiments indicated a molar absorptivity of 1073, which is in reasonable agreement with the literature value. The absorptivity of isocyanates is at the upper end of the normal range for organic functional groups. However, improvements in the detector cell are possible which would result in lower dispersion so that the results obtained here can be taken as reasonably representative of the capabilities of the overall approach to determinations via organic functional groups.

This work is taken in part from the M.S. thesis of W. G. Collier. We wish to thank the Foxboro Company for the loan of the MIRAN instrument.

REFERENCES

- 1 J. G. Grasselli and W. M. Richey (Eds.), *Atlas of Spectral Data and Physical Constants for Organic Compounds*, 2nd edn., CRC Press, Cleveland, OH, 1975, Vol. 1, p. 346.
- 2 J. Ruzicka and E. H. Hansen, *Flow Injection Analysis*, Wiley, New York, 1981, p. 16, 17.
- 3 N. S. Ham and J. B. Willis, *Spectrochim. Acta*, 16 (1960) 279.

Short Communication

SPECTROFLUORIMETRIC DETERMINATION OF SILICON BY FLOW INJECTION ANALYSIS

P. LINARES, M. D. LUQUE DE CASTRO and M. VALCARCEL*

Department of Analytical Chemistry, Faculty of Sciences, University of Córdoba, Córdoba (Spain)

(Received 15th May 1985)

Summary. The sensitive ($30\text{--}600\ \mu\text{g l}^{-1}\ \text{SiO}_2$), precise (r.s.d. = 0.25%), fast ($120\ \text{h}^{-1}$) and selective method is based on the oxidation of thiamine by molybdosilicic acid to highly fluorescent thiochrome. The method is applied to synthetic water samples.

The determination of dissolved silicate as means of analyzing for silicon requires the prior conversion of other chemical forms of this element to silicate. Silicon is determined in a large variety of samples such as semiconductors, metallurgical products, waste waters, rocks and pottery [1, 2]. The determination of silicon in earthenware is particularly interesting [3]. Commonly used methods for determining silicon are gravimetric (either as an organic molybdosilicate or as potassium hexafluorosilicate) or spectrophotometric based on heteropolyacid formation with molybdate [1, 2, 4]. Other heteropolyacid-based procedures have involved voltammetry [5] and fluorimetry [6, 7].

Flow injection analysis (f.i.a.) has been used to determine silicon. The method proposed by Israel and Barnes [8] for direct determination of silicon involves atomic emission. Other methods involve the formation of molybdosilicate with voltammetric [9, 10] or spectrophotometric [11] detection or monitoring of the molybdenum blue formed by reduction of the heteropoly anion [12, 13]. Fluorimetric detection, however, has not so far been utilized in a flow-injection method for the determination of silicon. The method proposed herein is based on the oxidation of thiamine to highly fluorescent thiochrome by molybdosilicate. This reaction has previously been used for the determination of phosphate [14], in which silica interfered seriously.

Experimental

Reagents. Stock aqueous solutions were 0.06 M ammonium heptamolybdate, 1×10^{-2} M silicate and $1\ \text{g l}^{-1}$ EDTA. Aqueous thiamine solutions of suitable concentration were prepared daily. The buffer solution contained 3.814 g of sodium tetraborate decahydrate and 37.4 ml of 5 M ammonia

adjusted to the desired pH with concentrated hydrochloric acid and diluted to 100 ml with distilled water.

Apparatus. A Perkin-Elmer LS-1 LC fluorescence detector was used with a 1.5-cm square flowcell and a Perkin-Elmer 56 recorder. A Gilson Minipuls-2 or Ismatec S-840 peristaltic pump, a Tecator L100-1 injection valve and a Selecta S-382 thermostat were also used. The manifold and recommended conditions are shown in Fig. 1.

Results and discussion

The reaction sequence yielding the fluorescent product (thiochrome) entails formation of molybdosilicic acid in a perchloric acid medium and oxidation of thiamine in a basic medium. Therefore the manifold designed to implement the method (Fig. 1) consists of a channel of sodium molybdate in an acidic medium into which the sample is injected, with heteropolyacid formation taking place in L_1 . The instability of thiamine in a basic medium requires its mixing with the ammoniacal borate solution almost immediately before the point of confluence with the molybdate channel. Thiamine is oxidized in reactor L_2 .

The chemical variables were optimized by a modified simplex method, and the system variables and the temperature by the univariant method. The values obtained are those shown in Fig. 1. The calibration graph obtained under these conditions was linear in the range $30\text{--}600\ \mu\text{g l}^{-1}$ silica ($5 \times 10^{-7}\text{--}1 \times 10^{-5}$ M) ($r = 0.9997$, 7 points). When 11 identical samples of 4×10^{-6} M silica were injected in triplicate, the relative standard deviation was 0.25%. The sampling rate was 120 samples per hour.

Interferences. Interfering species which may be present in water samples were studied thoroughly. Samples containing $240\ \mu\text{g l}^{-1}$ SiO_2 were used, adding a 100-fold greater weight concentration of the other ion. The results are shown in Table 1. Co(II), Fe(III), Fe(II) and Cu(II) also interfered, but their effect was eliminated by introducing a further channel containing $1\ \text{g l}^{-1}$ EDTA to mix with the molybdate stream before the injection valve. Attempts to remove the serious interference of phosphate and sulphide by adding oxalate, tartrate or citrate to the samples, as in other methods [1, 9]

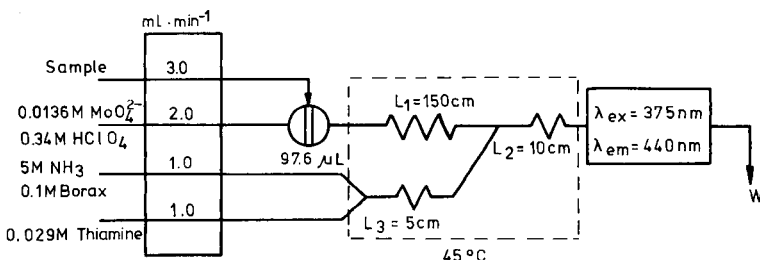


Fig. 1. Manifold used for determination of silicon and optimum values of the variables. The boxed section is thermostatted.

TABLE 1

Study of interferences in the determination of silicon

Tolerated wt. ratio Foreign ion: SiO ₂	Foreign ion
100	Acetate, EDTA, citrate, Cl ⁻ , CO ₃ ²⁻ , oxalate, CrO ₄ ²⁻ , I ⁻ , NO ₂ ⁻ , NO ₃ ⁻ , SO ₄ ²⁻ , tartrate, Br ⁻ , F ⁻ , NH ₄ ⁺ , Na ⁺ , K ⁺ , Ca ²⁺ , Mg ²⁺ , Cd ²⁺ , Cr ³⁺ , Ni ²⁺ , Zn ²⁺ , Hg ²⁺ , Pb ²⁺ , Al ³⁺ , Co ^{2+a} , Fe ^{2+a} , Fe ^{3+a} , Cu ^{2+a}
50	AsO ₄ ³⁻ , SO ₃ ²⁻
15	I ⁻
5	ClO ⁻
<1	PO ₄ ³⁻ , S ²⁻

^aIn the presence of EDTA.

TABLE 2

Synthetic water samples used for method evaluation

Sample No.	Composition (µg ml ⁻¹)
1	5.0 SiO ₂ , 15 Cl ⁻ , 10 CO ₃ ²⁻ , 5 NO ₃ ⁻ , 2 NO ₂ ⁻ , 5 SO ₄ ²⁻ , 100 Ca ²⁺ , 100 Mg ²⁺ , 1 Fe ³⁺ , 2 Cu ²⁺ .
2	20.0 SiO ₂ , 5 PO ₄ ³⁻ , 20 Cl ⁻ , 20 CO ₃ ²⁻ , 10 NO ₃ ⁻ , 5 SO ₄ ²⁻ , 20 Ca ²⁺ , 10 Mg ²⁺ , 5 Fe ³⁺ , 2 Fe ²⁺ , 10 Pb ²⁺ .
3	15.0 SiO ₂ , 40 Cl ⁻ , 50 CO ₃ ²⁻ , 10 NO ₃ ⁻ , 40 SO ₄ ²⁻ , 15 F ⁻ , 5 CrO ₄ ²⁻ , 50 Ca ²⁺ , 20 Mg ²⁺ , 10 Fe ³⁺ , 10 Pb ²⁺ , 20 Cu ²⁺ .
4	20.0 SiO ₂ , 2 PO ₄ ³⁻ , 50 Cl ⁻ , 10 CO ₃ ²⁻ , 10 NO ₃ ⁻ , 10 SO ₄ ²⁻ , 10 SO ₃ ²⁻ , 20 F ⁻ , 20 Br ⁻ , 200 Ca ²⁺ , 100 Mg ²⁺ , 20 Al ³⁺ , 5 Co ²⁺ .
5	10.0 SiO ₂ , 20 Cl ⁻ , 100 CO ₃ ²⁻ , 20 NO ₃ ⁻ , 5 NO ₂ ⁻ , 50 SO ₄ ²⁻ , 50 I ⁻ , 10 Ca ²⁺ , 50 Mg ²⁺ , 10 Fe ²⁺ , 10 Hg ²⁺ .
6	15.0 SiO ₂ , 200 Cl ⁻ , 5 CO ₃ ²⁻ , 10 SO ₄ ²⁻ , 20 SO ₃ ²⁻ , 5 Br ⁻ , 20 I ⁻ , 20 Ca ²⁺ , 20 Mg ²⁺ , 10 Fe ³⁺ , 10 Ni ²⁺ .
7	20.0 SiO ₂ , 5 PO ₄ ³⁻ , 20 Cl ⁻ , 20 CO ₃ ²⁻ , 10 NO ₃ ⁻ , 10 SO ₄ ²⁻ , 20 Ca ²⁺ , 10 Mg ²⁺ , 5 Fe ³⁺ , 5 Fe ²⁺ , 10 Pb ²⁺ , 10 Co ²⁺ .
8	20.0 SiO ₂ , 5 PO ₄ ³⁻ , 40 Cl ⁻ , 10 CO ₃ ²⁻ , 20 NO ₃ ⁻ , 5 NO ₂ ⁻ , 20 SO ₄ ²⁻ , 10 SO ₃ ²⁻ , 50 Ca ²⁺ , 100 Mg ²⁺ , 20 Hg ²⁺ , 10 Cu ²⁺ .

or by adding precipitants such as calcium, mercury(II) or silver were unsuccessful.

Determination of silicon in synthetic samples. In order to test the applicability of the proposed method, a series of synthetic water samples was prepared, containing various amounts of common cations and anions appropriate to several types of waters. The results were compared with those obtained by applying the standard spectrophotometric method based on the formation of molybdosilicic acid in hydrochloric acid medium and monitoring the absorbance at 410 nm [2]. The composition of the samples is shown in Table 2, and the results obtained are given in Table 3. The results indicate the useful

TABLE 3

Comparison of results obtained with the flow injection system and the standard spectrophotometric procedure [2]

Sample (Table 2)	SiO ₂ added ($\mu\text{g ml}^{-1}$)	SiO ₂ found ($\mu\text{g ml}^{-1}$)		Error (%)	
		Standard method	F.i.a.	Standard method	F.i.a.
1	5.0	5.3	5.0	5.4	0.2
2	20.0	21.3	19.9	6.3	-0.5
3	15.0	16.3	16.2	8.8	8.3
4	20.0	19.8	19.9	-1.2	-0.6
5	10.0	11.2	10.0	12.4	0.1
6	15.0	15.3	14.9	1.9	-0.7
7	20.0	23.1	19.7	15.5	-1.3
8	20.0	20.3	20.2	1.7	1.1

ness of the f.i.a. method, which has the following improvements over the standard procedure. The standard method requires the use of 50 ml of sample solution, in addition to another 50 ml of solution for the blank, whereas the f.i.a. method requires only 0.75 ml of test solution, which is diluted with distilled water to 25 ml; blanks are unnecessary. A minimum time of 8 min is needed for complete colour development in the standard method; the flow-injection technique permits determining up to 120 samples per h. Samples containing $<2 \mu\text{g ml}^{-1}$ SiO₂ cannot be determined by the standard method, whereas the flow procedure allows the determination of $\geq 30 \mu\text{g l}^{-1}$. Finally, the flow-injection procedure is more accurate (Table 3).

REFERENCES

- 1 W. J. Williams, *Handbook of Anion Determination*, Ellis Horwood, Chichester, 1977.
- 2 American Public Health Association, American Water Works Association and Water Pollution Control Federation, *Standard Methods for the Examination of Water and Wastewater*, 15th edn., Am. Public Health Assoc., New York, 1980, p. 429.
- 3 H. Bennett, *Analyst* (London), 102 (1977) 153.
- 4 L. G. Hargis, *Anal. Chem.*, 42 (1970) 1494.
- 5 A. G. Fogg, N. K. Bsebsu and B. J. Birch, *Talanta*, 28 (1981) 473.
- 6 K. Krzysztow, *Chem. Anal.*, 14(6) (1969) 1325.
- 7 G. Ellion and J. A. Radle, *Anal. Chem.*, 33 (1961) 1623.
- 8 Y. Israel and R. M. Barnes, *Anal. Chem.*, 56 (1984) 1188.
- 9 A. G. Fogg and N. K. Bsebsu, *Analyst* (London), 106 (1981) 1288.
- 10 A. G. Fogg and G. C. Cripps, *Analyst* (London), 108 (1983) 1485.
- 11 Y. Hirai, T. Yokoma, N. Yoza, T. Tarutani and S. Ohashi, *Bunseki Kagaku*, 30 (1981) 350.
- 12 T. Yokoyama, Y. Hirai, N. Yoza, T. Tarutani and S. Ohashi, *Bull. Chem. Soc. Jpn.*, 55 (1982) 3477.
- 13 J. Thomsen, K. S. Johnson and R. L. Petty, *Anal. Chem.*, 55 (1983) 2378.
- 14 J. Holzbecher and D. E. Ryan, *Anal. Chim. Acta*, 64 (1973) 151.

Short Communication

SIMPLE AND RELIABLE DETERMINATION OF BROMAZEPAM IN HUMAN PLASMA BY HIGH-PERFORMANCE LIQUID CHROMATOGRAPHY

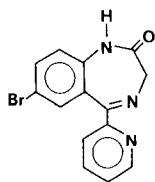
W. D. HOOPER*, J. A. ROOME, A. R. KING, M. T. SMITH, M. J. EADIE and R. G. DICKINSON

Department of Medicine, University of Queensland, Clinical Sciences Building, Royal Brisbane Hospital, Herston, Queensland 4029 (Australia)

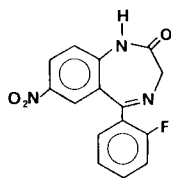
(Received 17th July 1985)

Summary. Bromazepam is extracted into diethyl ether from 1 ml of plasma adjusted to pH10 (carbonate buffer), the extract is evaporated to dryness, and the residue is reconstituted in mobile phase and chromatographed on a C₁₈ radial compression column. The limit of detection is 2 ng ml⁻¹ from a 1-ml plasma sample, for detection at 236 nm. Calibration is linear for 2–100 ng ml⁻¹ ($r^2 \geq 0.999$). More reproducible results were obtained when plastic test tubes and pipettes were used instead of glass.

Since the introduction in 1960 of chlordiazepoxide [1], the number of benzodiazepines in clinical use and their range of therapeutic applications has increased steadily. Thirteen benzodiazepines are currently marketed in Australia, and substantially more elsewhere [2]. Bromazepam is used for the symptomatic relief of tension and anxiety. The compound has two chemical features which are unusual amongst commercial benzodiazepines, viz. the 7-bromo and 5-(2-pyridyl) substituents rather than the typical 7-chloro and 5-phenyl groups.



Bromazepam



Ro 5-4435

Determinations of bromazepam in blood and other body fluids have proven particularly troublesome. Most authors using gas chromatographic (g.c.) procedures without [3–5] or with derivatization [6] or hydrolysis [7] have elaborated on problems with their assays, or on difficulties in reproducing assays published by others. Recently, two high-performance liquid chromatographic (h.p.l.c.) methods have been described. One of these [8] offered several advantages over g.c. procedures, but seemed too

cumbersome for routine use. The other [9] seems quite convenient, but differs in several ways from the procedure described below. An improved h.p.l.c. procedure for bromazepam assay is reported here, with some observations which may help to explain the difficulties encountered previously in assaying this compound.

Experimental

Chemicals. Bromazepam was provided by Alphapharm (Brisbane, Australia) and Ro 5-4435 (*N*-desmethylflunitrazepam) and temazepam by Roche Products (Sydney). Diethyl ether (analytical-reagent grade anhydrous; Mallinckrodt Australia) and acetonitrile (h.p.l.c. grade; J. T. Baker, Phillipsburg, NJ) were used. All other chemicals were of analytical-reagent grade.

Apparatus. The h.p.l.c. system comprised a Tracor model 950 pump, a Rheodyne 7120 injector, a Waters RCM-100 radial compression module fitted with a 5- μ m Novapak C18 cartridge, and a Waters model 481 absorbance detector. The output was displayed on a Shimadzu R-101 strip-chart recorder (10 mV full scale deflection).

Determination of bromazepam in plasma. Stock solutions of bromazepam (1 μ g ml⁻¹ and 0.1 μ g ml⁻¹) and Ro 5-4435 (1 μ g ml⁻¹) were prepared in acetonitrile. Portions (50 ng) of Ro 5-4435 were added to all assay tubes as internal standard, and the acetonitrile was evaporated. Calibration standards were prepared by dispensing the appropriate aliquots of bromazepam solutions to give 20–200 ng of drug in the assay tubes, evaporating the organic solvent, and adding 1 ml of drug-free plasma. All assays were conducted in plastic tubes (polypropylene or polycarbonate), and contact with glass was eliminated wherever possible.

To the 1-ml plasma sample (standard or unknown) was added 1 ml of carbonate buffer (1.0 M, pH 10) and 7.5 ml of diethyl ether. After shaking by hand (1 min) and centrifuging (2 min at 1000g), the diethyl ether was transferred to a polypropylene test tube with tapered bottom, using a polyethylene pasteur pipette. The ether was evaporated under a gentle nitrogen stream at 40°C. The dried residue was reconstituted in 100 μ l of mobile phase, and 50 μ l was injected into the h.p.l.c. from an SGE microlitre syringe.

The mobile phase was prepared by mixing 180 ml of acetonitrile, 0.5 ml of triethylamine and 3.5 ml of 1 M orthophosphoric acid, and diluting to 500 ml with h.p.l.c.-quality water. The mobile phase was degassed in an ultrasonic bath, and then operated with recycling to the reservoir; it was renewed every 48 h. The flow rate was 1 ml min⁻¹, and the detector was set at 236 nm. Under these conditions, bromazepam eluted at approximately 6.4 min and Ro 5-4435 at 9.6 min.

Determination of precision, recovery and detection limit. The precision of the assay was evaluated from six replicate assays of a 50 ng ml⁻¹ standard of bromazepam in plasma. Recovery was also assessed at 50 ng ml⁻¹, by

comparing the peak heights of bromazepam and Ro 5-4435 from samples taken through the extraction procedure with those obtained from unextracted standards. Peak heights in the recovery experiments were measured relative to the peak height of temazepam, 50 ng of which was added just prior to injection onto the column. The detection limit was ascertained by analysing serial dilutions of a plasma standard, to establish the bromazepam concentration which gave a peak height equal to three times the noise level.

Results and discussion

No difficulty had been expected in modifying our extensively tested procedures for benzodiazepine assays to include bromazepam. However, initial attempts to apply h.p.l.c. or g.c. with electron-capture detection (with bromazepam either underivatized or methylated), all gave very poor precision. It is clear from published reports [3–9] that other workers have encountered problems with the determination of this compound. In the face of these difficulties, it was decided to concentrate on developing the h.p.l.c. method, as the chromatographic separations were very satisfactory (Fig. 1).

Early results suggested erratic losses of bromazepam during sample handling. Scatter similar to, and sometimes worse than, that shown by the squares in Fig. 2, was observed. It is well known that weak bases, such as the benzodiazepines, are subject to adsorptive losses onto glass surfaces [10]; for this reason, all glassware is routinely treated with acid washing followed by

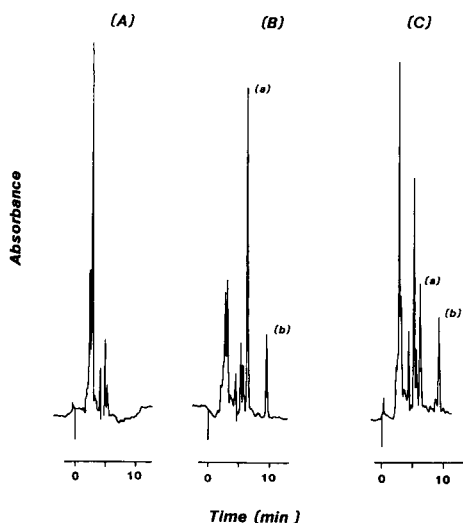


Fig. 1. Liquid chromatograms: (A) an extracted blank plasma; (B) an extracted standard plasma (1 ml) spiked with 100 ng of bromazepam (peak a) and 50 ng of Ro 5-4435 (peak b); (C) an extracted plasma sample from a subject who had taken bromazepam (6 mg) 24 h before sampling (the bromazepam concentration was evaluated as 36 ng ml⁻¹).

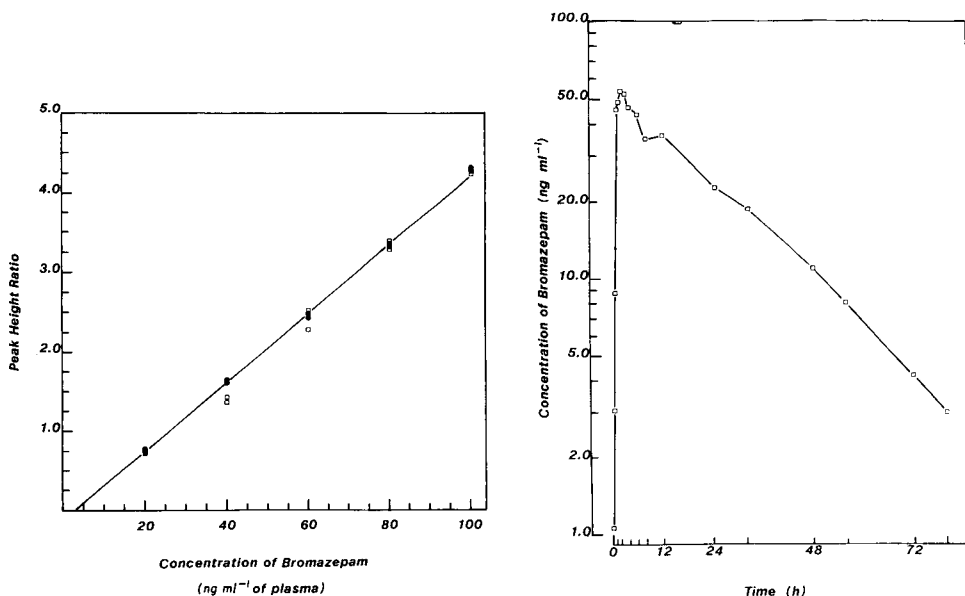


Fig. 2. Calibration standards for plasma samples spiked with bromazepam (5–100 ng ml⁻¹) and analysed in acid washed and deactivated glass test tubes (squares) or in polypropylene test tubes (circles, solid line).

Fig. 3. Plasma concentration—time profile for bromazepam in a subject who took a single 6 mg dose of the drug.

soaking in aqueous cetyltrimethylammonium bromide (50 mg l⁻¹) to deactivate the surface. In order to test whether the variation in bromazepam/Ro 5-4435 peak height ratios resulted from selective loss of bromazepam onto glass surfaces, assays were conducted in polypropylene tubes. A marked decrease in scatter was attained, but precision was still not acceptable. Only when polyethylene pasteur pipettes were substituted for glass was a fully acceptable assay achieved (Fig. 2). Calibration plots were then linear over the concentration range 5–200 ng ml⁻¹; the regression coefficient for sets of standards ($n = 12$) was typically 0.999. The relative standard deviation ($n = 6$) at a bromazepam concentration of 50 ng ml⁻¹ was 3.2%, the recovery was >95%, and the limit of detection was 2 ng ml⁻¹.

This assay offers several advantages over earlier g.c. procedures [3–7], chiefly simplicity, speed, precision and low detection limit. It avoids the tedious evaporation steps described earlier for h.p.l.c. [8], and offers shorter chromatographic run times and improved peak shape, which should improve sensitivity. It differs from another recent method [9] with respect to extraction procedure, chromatographic conditions and internal standard, and offers a slightly lower detection limit which is well suited to assay of plasma levels in single dose studies. The assay has been used in a comparative

bioavailability study following the oral administration of a 6-mg tablet to volunteers. A typical plasma level/time profile is shown in Fig. 3.

The rather surprising observations on the high affinity with which bromazepam binds to glass may help to explain many of the problems encountered previously in the assay of this drug. This may be a consequence of the chemical structure of this compound which is unusual among the clinically used benzodiazepines. The worst aspect of the problem was the unpredictable magnitude of the variability, for reasons which were never established. On occasions, results much more scattered than those in Fig. 2 were obtained. These data also suggest that plastic ware may be generally preferable to glass for work involving trace levels of weak bases.

REFERENCES

- 1 L. H. Sternbach, S. Garattini, E. Mussini and L. O. Randall, in *The Benzodiazepines*, Raven Press, NY, 1973, pp. 1-26.
- 2 M. J. Eadie, *Med. J. Aust.*, 141 (1984) 827.
- 3 J. A. F. de Silva, I. Bekersky, M. A. Brooks, R. E. Weinfeld, W. Glover and C. V. Puglisi, *J. Pharm. Sci.*, 63 (1974) 1440.
- 4 J. A. F. de Silva, I. Bekersky, C. V. Puglisi, M. A. Brooks and R. E. Weinfeld, *Anal. Chem.*, 48 (1976) 10.
- 5 T. Kaniewska and W. Wejman, *J. Chromatogr.*, 182 (1980) 81.
- 6 U. Klotz, *J. Chromatogr.*, 222 (1981) 501.
- 7 J. P. Cano, A. M. Baille and A. Viala, *Arzneim. Forsch.*, 25 (1975) 1012.
- 8 H. Hirayama, Y. Kasuya and T. Suga, *J. Chromatogr.*, 277 (1983) 414.
- 9 P. Heizmann, R. Geschke and K. Zinapold, *J. Chromatogr.*, 310 (1984) 129.
- 10 E. Reid, *Analyst (London)*, 101 (1976) 1.

Short Communication

THE DETERMINATION OF ACETIC, FORMIC, AND PROPANOIC ACIDS IN RAIN WATER BY REVERSE-PHASE HIGH-PERFORMANCE LIQUID CHROMATOGRAPHY

R. W. GILLETT* and G. P. AYERS

Division of Atmospheric Research, C.S.I.R.O., Private Bag 1, Mordialloc, Victoria 3195 (Australia)

(Received 18th June 1985)

Summary. The three organic acids, as well as nitrite and nitrate, are separated on a Spherisorb S3-ODS2 column with a methanesulfonic acid mobile phase containing *n*-octylamine for ion-pairing, after concentration on a Vydac column. Detection is at 210 nm. Retention times are <10 min. Detection limits are in the range $0.45\text{--}1.5 \times 10^{-6}$ M for 1-ml samples.

In recent years, the considerable interest in the composition of precipitation in remote areas has led to the need to determine natural and anthropogenic acid components in the atmosphere [1]. In such areas, organic acids can contribute up to 65% of the total free acidity [2, 3] and so have a controlling influence on the pH. In contrast, the total free acidity in more polluted areas such as north-eastern U.S.A., is controlled mainly by inorganic acids [1, 4]; organic acids account for only 16–35% of the total free acidity of precipitation [4] while the remainder is provided by sulfuric and nitric acids, resulting from SO₂ and NO_x emissions from urban/industrial sources.

Organic acids in rain in remote areas are thought to be of natural origin. Some of the possible sources are aldehyde oxidation in gas and liquid phase, oxidation of olefinic marine compounds, biomass burning, biomass emissions and bacterial processes in clouds [5]. In Australia, the Northern Territory is one sparsely populated region where organic acids have been reported [2, 3], and in order to establish the origin and distribution of these organic acids, a reliable and well documented detection technique is required.

Experimental

The system used consisted of a Laboratory Data Control (LDC) chromatography control module, Constametric III pump, Spectro-Monitor D variable-wavelength detector set at 210 nm and a Rheodyne 7125 injector. The separating column was either a Spherisorb S5-ODS2 (5 μm; 250 × 4.6 mm) or a Spherisorb S3-ODS2 (3 μm; 150 × 4.6 mm) reverse-phase column. The injector sample loop was replaced by a concentrator column (50 × 3.2 mm) containing Vydac 302SC (30–40 μm) pellicular packing material. The typical

injection volume for rain-water samples was 1 ml. The flow rate was 2 ml min^{-1} at a back pressure of about 24 MPa.

Standards were prepared from analytical-reagent grade chemicals and distilled/deionised water obtained from a Milli-Q water purification system. The preferred mobile phase was an aqueous solution which was 8.0×10^{-3} M in methanesulfonic acid (Fluka) and 2.5×10^{-3} M in n-octylamine (Tokyo Kasei) and was filtered through a 0.45- μm filter.

Results and discussion

The analyses of rain and air samples for organic acids has some special problems. It is now well known that organic acids disappear from solution even when stored at 4°C [3, 4]. Apparently bacteria can utilize organic acids as a food source, so chloroform is added as a biocide to prevent organic acid loss. The samples also contain nitrate and nitrite, which can interfere with the determination of organic acids.

Several techniques are currently available for the detection of organic acids. Ion chromatography can be used if the rather specialised equipment is available [3, 6]. The Dionex system provides almost baseline separation between formic and acetic acids and detection limits in the $\mu\text{g l}^{-1}$ range for most organic acids. A disadvantage is that the retention times of about 15, 16 and 19 min for formic, acetic and propanoic acids are rather long. Resin-based ion-exclusion columns such as the Bio-Rad HPX-87H give good separations for organic acids [7]; these columns provide retention times of 8 and 10 min for formic and propanoic acids, respectively, but nitrite and nitrate cannot be determined together with organic acids. Another problem is that the injection volumes typically needed (1 ml) change the ionic strength, thus causing swelling or shrinking of the resin bed leading to pump pulsations and peak broadening. Reverse-phase high-performance liquid chromatography (h.p.l.c.) has been used for organic acid separations [8]. This technique appears to give good separations for organic acids, and the sensitivities for formic, acetic and propanoic acids are 0.2, 0.1 and 0.4 ng, respectively. Although this is a very sensitive technique, it is not suitable for samples which contain a mixture of nitrate, nitrite, chloroform and organic acids. Another reverse-phase technique has also been used for formic acid, acetic acid, nitrate and nitrite [9] but it suffers from lack of sensitivity. Other reverse-phase h.p.l.c. techniques are available [10, 11] but rely on tedious derivatisation of the organic acids. A Vydac ion-exchange column has been used to separate formic acid in rain samples [12] but acetic acid elutes too close to the solvent front peaks for routine work, and the detection limit for formic acid is only 20 ng. Various other ion-exchange methods have been used to separate organic acids [13–15], but these were found to be of insufficient sensitivity for the rather clean rain samples from remote areas under investigation.

In this study, Spherisorb ODS columns were used. It was found that methanesulfonic acid alone in the mobile phase caused co-elution of nitrite

with acetic acid, and also nitrate with propanoic acid. This problem was overcome by adding a small amount of *n*-octylamine which acts as an ion-pairing agent to decrease the polarity of the nitrate and nitrite and so increases their retention times. The *n*-octylamine had little effect on the retention times of the weakly ionised organic acids. Chloroform eluted as a large peak with a long retention time and so did not overlap any other peaks.

The column requirements for separation of organic acids have been reported [8]. The column must be end-capped to minimise absorption effects and must be highly efficient. The 5- μm and 3- μm Spherisorb columns have resolutions of 86 000 and 144 000 plates/metre respectively, and both are fully end-capped. Methanesulfonic acid has previously been used as a mobile phase in ion chromatography [11, 16]. It was used here in preference

TABLE 1

Detection limits and retention times on a Spherisorb ODS2 (3 μm) column for injection volumes of 1 ml

Species	Detection limit (10^{-6} M)	Retention time (min)	Species	Detection limit (10^{-6} M)	Retention time (min)
Formic acid	0.45	1.8	Propanoic acid	1.5	4.7
Acetic acid	0.75	2.3	Nitrate	0.01	9.5
Nitrite	0.01	2.6	Butanoic acid	3.0	13.4

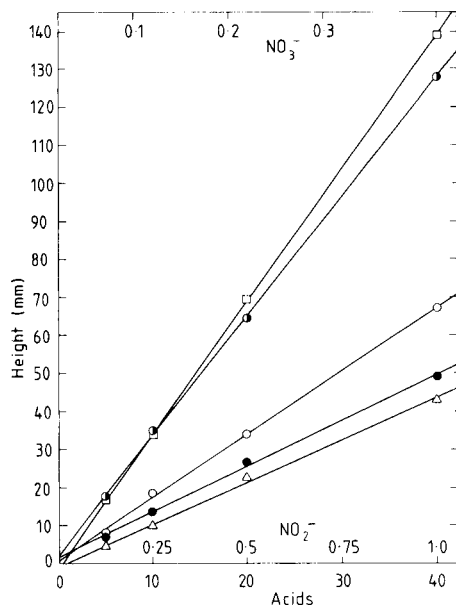


Fig. 1. Calibration plots: (\square) formic acid; (\circ) acetic acid; (Δ) propanoic acid; (\circ) nitrite; (\bullet) nitrate. All concentrations are $\times 10^{-6}$ M.

to sulfuric acid because of its lower absorptivity, thereby giving decreased baselines for species being detected by direct u.v. absorption. In tests with sulfate in the mobile phase, the organic acid peaks were invariably broader than those produced with methanesulfonate, so that sensitivity was further reduced.

Table 1 shows the retention times and the typical detection limits of the compounds of interest. The detection limits were evaluated from the injection of 1 ml of a standard solution, for a signal-to-noise ratio of 3, and a detector range of 0.02 absorbance full scale. These detection limits were sufficient for the present study, but they could easily be improved by using a lower detector range and injecting larger sample volumes. In this context, the use of a concentrator column is essential, because large volumes of sample can be injected while the volume of sample matrix that actually passes into the separating column remains constant. Figure 1 shows plots of peak height

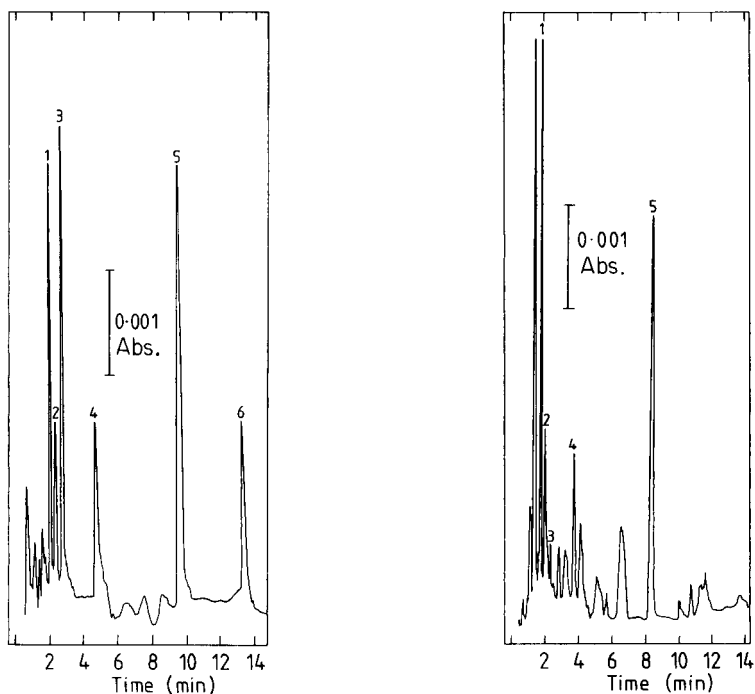


Fig. 2. Chromatogram of a standard solution. Peaks: (1) formic acid ($40 \mu\text{M}$); (2) acetic acid ($40 \mu\text{M}$); (3) nitrite ($1 \mu\text{M}$); (4) propanoic acid ($40 \mu\text{M}$); (5) nitrate ($0.5 \mu\text{M}$); (6) butanoic acid ($40 \mu\text{M}$). Injection volume $250 \mu\text{l}$, wavelength 210 nm , attenuation 4, $3\text{-}\mu\text{m}$ Spherisorb ODS2 column.

Fig. 3. Chromatogram of a typical rain-water sample. Peaks: (1) formic acid ($40.4 \mu\text{M}$); (2) acetic acid ($30.3 \mu\text{M}$); (3) nitrite ($0.05 \mu\text{M}$); (4) propanoic acid ($16.8 \mu\text{M}$); (5) nitrate ($9.8 \mu\text{M}$); other peaks are unknown. Injection volume $500 \mu\text{l}$, wavelength 210 nm , attenuation for nitrate 128 otherwise 4, $5\text{-}\mu\text{m}$ Spherisorb ODS2 column.

against standard concentrations for the species of interest; the calibrations are linear down to low concentrations.

Although the technique was developed particularly for determinations of formic, acetic and propanoic acids, Fig. 2 shows that butanoic acid was also satisfactorily separated. Indeed, preliminary tests indicated that other acids and diacids can also be separated with appropriate adjustments to the mobile phase concentration. Figure 3 shows a chromatogram of a typical rain-water sample in which other, unidentified species are clearly evident.

During this study, three separate Spherisorb ODS columns were used; one was 3- μm and the other two were 5- μm packings. The retention times on all these columns varied slightly (cf. Figs. 2 and 3) although the mobile phase concentrations were identical as was the total number of plates per column. The corollary is that the concentrations of mobile phase and ion-pairing agent should be modified slightly to achieve the optimum resolution for a given column, depending on its age, efficiency and condition. In general, a molar ratio of methanesulfonic acid to ion-pairing agent of about 4:1 has been successful. Moreover, the 3- μm columns appear to give higher sensitivity than the 5- μm columns. For example, a 3- μm column gave a peak height of 48 mm for 250 μl of 40×10^{-6} M acetic acid, i.e., for 1×10^{-8} mol of acetic acid (Fig. 2); in contrast, a 5- μm column gave a peak height of 48 mm for 500 μl of 30.3×10^{-6} M acetic acid, i.e., 1.5×10^{-8} mol (Fig. 3). Thus, for organic acid separations, the 3- μm Spherisorb ODS2 columns are about 50% more sensitive than the 5- μm columns.

REFERENCES

- 1 See, e.g., J. N. Galloway, G. E. Likens and M. E. Hawley, *Science*, 226 (1984) 829.
- 2 J. N. Galloway, G. E. Likens, W. C. Keene and J. M. Miller, *J. Geophys. Res.*, 87 (1982) 8771.
- 3 W. C. Keene, J. N. Galloway and J. D. Holden, Jr., *J. Geophys. Res.*, 88 (1983) 5122.
- 4 W. C. Keene and J. N. Galloway, *Atmos. Environ.*, 18 (1984) 2491.
- 5 J. N. Galloway and A. Gaundry, *Atmos. Environ.*, 18 (1984) 2649.
- 6 L. J. Marlou and P. M. Kabra, *Liquid Chromatography in Clinical Analysis*, The Humana Press, 1981, Chap. 17.
- 7 R. E. Pauls and G. J. Weight, *J. Chromatogr.*, 254 (1983) 171.
- 8 N. E. Skelly, *J. Chromatogr.*, 250 (1982) 134.
- 9 K. H. Sui, K. A. Buckle and M. Wootton, *J. Chromatogr.*, 260 (1983) 189.
- 10 S. Vainiolato, P. Pfaffli and A. Zitting, *J. Chromatogr.*, 258 (1983) 207.
- 11 J. Pempkowiak, *J. Chromatogr.*, 258 (1983) 93.
- 12 G. P. Ayers and R. W. Gillett, *J. Chromatogr.*, 284 (1984) 510.
- 13 H. J. Cortes, *J. Chromatogr.*, 234 (1982) 517.
- 14 P. R. Haddad and A. L. Heckenberg, *J. Chromatogr.*, 252 (1982) 177.
- 15 S. Rokushika, Z. L. Sun, and H. Hatano, *J. Chromatogr.*, 253 (1982) 87.
- 16 J. P. Ivey, *J. Chromatogr.*, 267 (1983) 218.

Short Communication

THE SOLUBILITY OF TRI-*n*-OCTYLAMINE IN WATER AND PHOSPHORIC ACID SOLUTIONS

S. STENSTRÖM*

Department of Chemical Engineering 1, Lund Institute of Technology, Box 124, S-221 00 Lund (Sweden)

M. DALENE

Department of Analytical Chemistry, University of Lund, Box 124, S-221 00 Lund (Sweden)

G. SKARPING

Department of Technical Analytical Chemistry, Lund Institute of Technology, Box 124, S-221 00 Lund (Sweden)

(Received 25th June 1985)

Summary. The solubility of tri-*n*-octylamine (TOA) in water and phosphoric acid is reported. Equilibration is achieved by circulating the solution through PVC pieces saturated with the adsorbed amine in a glass tube. The dissolved TOA is determined by capillary gas chromatography which can detect amine concentrations down to $10 \mu\text{g l}^{-1}$. The solubility of TOA in water is 0.039 mg l^{-1} and in 5.5 M phosphoric acid 0.82 mg l^{-1} ; these values are much lower than those reported in the literature.

Long-chain tertiary amines have been widely used in liquid-liquid extraction technology for many years, particularly for commercial extraction of uranium, vanadium and cobalt. The commercial success of such an extraction process largely depends on small losses of extractant and diluent (kerosenes). Losses are normally caused by solubility in and entrainment to the aqueous phase because of incomplete phase separation. The total loss of tertiary amines has been reported [1] as $10\text{--}40 \text{ mg l}^{-1}$ in extractions of uranium from sulphate solutions. Normally the entrainment loss can be assumed to be the dominating part but not much is known about the actual solubilities of these extractants in various media. During the development of a pollution abatement process for cadmium extraction with tertiary amines from phosphoric acid solutions [2], solubility data of these extractants in water and phosphoric acid were needed.

A literature survey produced some data for the solubilities of the tertiary amines (Table 1). The manufacturer of Alamine-336 (a mixture of tri-*n*-octyl and tri-*n*-decylamine produced by Henkel Corporation, Minneapolis, MN, U.S.A.) states the water solubility to be $<5 \text{ mg l}^{-1}$. Numerous measurements were reported by Nikolaev et al. [3] and Oparin et al. [4]. Solubilities of tri-*n*-octylamine (TOA) were measured in water and in various acids

TABLE 1

Reported values for the solubility of long-chain tertiary amines in various media

Amine	Medium	Conc.	Solubility (mg l ⁻¹)	Ref.
Alamine 336	H ₂ O	—	< 5	— ^a
Tri-n-octylamine	H ₃ PO ₄	40.6% (w/w)	39.2	3
Tri-n-octylamine	H ₂ SO ₄	9.26% (w/w)	24.0	3
Tri-n-octylamine	H ₂ O	—	82.0	3
Tri-n-octylamine	H ₂ O ^b	—	7.25	3
Alamine 336	H ₂ SO ₄	pH 1.8	10	5
Alamine 336	CH ₃ COOH	10% (w/w)	< 10	6
Tri-n-octylamine	H ₂ O ^c	—	0.039 ^d	This work
Tri-n-octylamine	H ₃ PO ₄	5.5 M	0.82 ^d	This work

^aManufacturer's data. ^bWith filtration of water after equilibration. ^cDistilled deionized water. ^dAt 25°C.

and salt solutions. Equilibration of the amine with the aqueous phase was done by shaking the phases for 30 min. Amine concentrations were measured spectrophotometrically after extraction with tetrachloromethane. Filtration of the aqueous phase decreased the values by a factor of more than 10 (see Table 1). Obviously either amine drops were separated by the filter or the amine was adsorbed on the filter material. Solubility in sulphuric acid for 0.1 M Alamine-336 dissolved in a kerosene was reported by Pich et al. [5] as 10 mg l⁻¹. The same magnitude was given by Ricker and King [6] for the solubility in 10% (w/w) acetic acid.

Reported values vary depending on how the equilibration was done, whether the amine was dissolved in a diluent or not, whether or not secondary dispersions were eliminated before measurements and on the method of analysis. Amine determinations at the picogram level can be done by gas chromatography (g.c.) with capillary columns [7]. The aim of this study was to measure the solubility of the long-chain tertiary amine, TOA, in water and phosphoric acid solutions.

Experimental

Chromatographs and detectors. A Varian Model 3700 gas chromatograph equipped with a Carlo Erba on-column injection system and a Varian thermionic specific detector was used. Typical settings for the detector were: gas flow rates 4.0 ml min⁻¹ hydrogen and 180 ml min⁻¹ air; bead heating current, 6.5 scale divisions; bias voltage, -10 V; temperature, 250°C.

Gases. The carrier gas was helium with an inlet pressure of 0.3 kg cm⁻². The make-up gas was nitrogen at a flow rate of 20 ml min⁻¹. These gases were dried over molecular sieve 5A and deoxygenated using an "Indicating Oxytrap" (Chrompak, Middelburg, The Netherlands). Hydrogen and air were used without extra purification.

Chemicals. Tri-*n*-octylamine, toluene and phosphoric acid were of analytical grade (Merck). The stationary phase was PS-255 (Fluka) and 1,3-divinyltetramethyldisilazane was from Pertrach Systems (Bristol, PA, U.S.A.). Solvents used were all of analytical grade. Distilled-deionized water was used throughout.

Equilibration. Initial measurements by equilibration of 50 ml of either water or phosphoric acid with 2 ml of TOA in ordinary separating funnels produced unsatisfactory results; solubility values for TOA in water between 0.010 and 0.65 mg l⁻¹ were measured. This was assumed to be caused by incomplete phase separation and formation of secondary dispersions. Amines readily form salts with acids. Thus, in equilibrations of TOA with phosphoric acid, the amine formed a viscous gelatinous amine salt. In order to avoid the difficulties with formation of secondary dispersions and third-phase formation (amine salt aggregation), a different method was tested. Small (ca. 5 × 5 mm) pieces of PVC were put in a glass tube (25 mm diameter, 350 mm tall) and impregnated with TOA by pouring small amounts of TOA through the tube. Draining the excess of TOA and washing several times with water produced a thin film of adsorbed TOA on the PVC surface. It was assumed that the adsorption equilibrium $\text{TOA (aq)} \rightleftharpoons \text{TOA (PVC)}$ was shifted sufficiently to the left to ensure saturation of the aqueous phase. The solutions were circulated through this tube with a pump at a flow of 2 l h⁻¹. The total volume of solution in the system was 1.5–2 l. Equipment was of glass and all tubes were made of teflon. Solutions were circulated so many times that the tubes and glassware could be assumed to be saturated with TOA. The arrangement is outlined in Fig. 1. Samples were taken for analysis after 1–20 h of circulation.

The samples were normally centrifuged for 10 min at 4800 rpm and then analyzed for TOA. Filtration through filter paper reduced the values by up to 50%; this was considered to be due to sorption of amine in the paper so filtration of the aqueous solution was not used. With this way of equilibration, no secondary droplets were visible and formation of the viscous amine compound with phosphoric acid was avoided.

After equilibration, the samples were made alkaline with potassium hydroxide and, usually, 5 ml was extracted with 2.5 ml of toluene. After phase separation, the organic phase was injected onto the g.c. column.

Column preparation. Duran 50 borosilicate glass capillary columns were drawn on a Carlo Erba GCDM Model 60 drawing machine and handled as described by Grob and Grob [8]. The columns (10 m, 0.23 mm i.d.) were dried by nitrogen purging for 2 h at 250°C. Deactivation was achieved by dynamic coating with a plug of 1,3-divinyltetramethyldisilazane followed by flame-sealing and thermal treatment at 350°C overnight. After rinsing with toluene, methanol and diethyl ether, PS-255 stationary phase was applied by static coating from pentane solutions. The phase was then cross-linked with azo-*tert*-butane [9]. The final film thickness was ca. 0.4 μm.

Linear range and detection limits. Peak heights were used for data

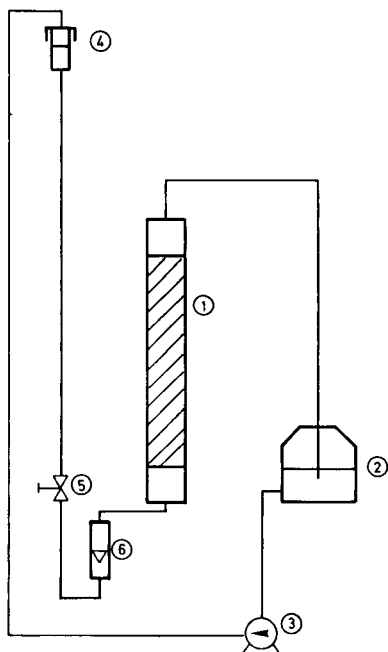


Fig. 1. Arrangement for solubility measurements of TOA in water and phosphoric acid. (1) Tube with PVC pieces; (2) buffer container, 1.5–2 l; (3) membrane pump; (4) reservoir for constant gravity flow; (5) regulating valve; (6) flow meter.

calculation. Calibration plots for TOA were linear in the 20–2000-pg range. The detection limit for TOA was in the order of 10–20 pg for a signal-to-noise ratio of 2:1.

Results and discussion

Solubility. Circulation of the solutions about 7 times over the impregnated PVC pieces was sufficient to reach a steady-state concentration in the solutions, as is seen for water in Fig. 2. Rejecting the outlying data where equilibrium was presumably not reached and where very high values were obtained, presumably because of entrainment of small TOA droplets in the samples (one third of the data were rejected), the concentration of TOA in the water samples varied between 0.024 and 0.055 mg l⁻¹ with a mean of 0.039 mg l⁻¹ (Table 1). For 5.5 M phosphoric acid, the values showed a variation between 0.79 and 0.87 mg l⁻¹ with a mean of 0.82 mg l⁻¹.

Gas chromatography. Figure 3 shows a chromatogram of a cycled water solution of TOA, extracted with toluene after being made alkaline. Because of the selectivity of the detector, a peak is easily obtained for 50 pg of TOA.

Conclusion

The combination of glass capillary columns, on-column injection and the

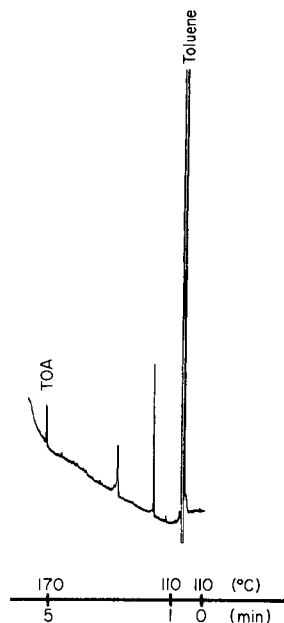
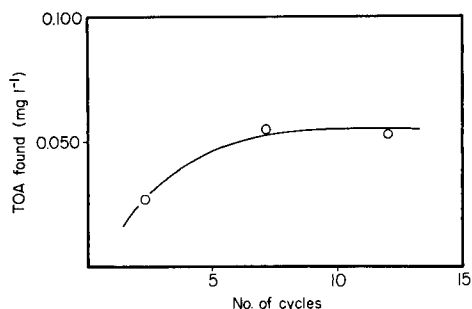


Fig. 2. TOA concentration in water after repeated circulation over impregnated PVC pieces.

Fig. 3. Chromatogram of an aqueous solution containing TOA (50 pg in the 7 μ l injected). Column: see text. Temperature programming from 110 to 170°C at 15°C min⁻¹. Detector parameters, see text; attenuation 2×10^{-12} attenuation full scale.

thermionic detector makes it possible to detect TOA concentrations down to 0.010 mg l⁻¹ in the solution injected. The measured solubility in water is 2–3 orders of magnitude lower than previously reported values (Table 1). For phosphoric acid, the present values are also much lower. The difference could be due to the elimination of secondary dispersions when the amine is adsorbed on PVC pieces and to the use of gas chromatography for the determination of low amine concentrations.

The experimental technique could be modified in terms of selection of the adsorption material in the cycling tube, to allow measurements of the solubility of other substances with very low solubilities for which equilibration is the crucial step.

REFERENCES

- 1 G. M. Ritcey and A. W. Ashbrook, *Solvent Extraction, Principles and Applications to Process Metallurgy, Part I*, Elsevier, Amsterdam, 1984, p. 261.
- 2 S. Stenström and G. Aly, *Proceedings International Solvent Extraction Conference 1983, Denver*, pp. 197–198.

- 3 A. V. Nikolaev, G. M. Grishin, A. A. Koleshikov and G. I. Pogadayev, *Izv. Sib. Otd. Akad. Nauk SSSR*, 2 (1969) 145.
- 4 A. N. Oparin, V. A. Kopylov and V. I. Rodin, *Sov. Chem. Ind.*, 12 (1980) 1186.
- 5 H. C. Pich, C. S. Santos, J. T. Elias, M. F. Alves, E. H. Conceicao and H. X. Vieira, *Proc. Symp. on Recovery of Uranium*, IAEA, Vienna, 1971, IAEA-SM-135/17.
- 6 N. L. Ricker and C. J. King, *Final Report on Grant No. 830733*, U.S. Environmental Protection Agency, 1980.
- 7 M. Dalene and G. Skarping, *J. Chromatogr.*, 331 (1985) 321.
- 8 K. Grob and G. Grob, *J. High Resolut. Chromatogr. Commun.*, 2 (1979) 677.
- 9 B. W. Wright, P. A. Peaden, M. L. Lee and T. J. Stark, *J. Chromatogr.*, 248 (1982) 17.

Short Communication

A FAST PHOTOMETRIC TITRATION FOR THE STANDARDIZATION OF DITHIZONE SOLUTIONS

S. ALEGRET,* M. BLANCO and J. M. PAULÍS

Departament de Química Analítica, Universitat Autònoma de Barcelona, Bellaterra, Barcelona (Spain)

(Received 30th April 1985)

Summary. A simple method is reported for standardizing 10^{-5} – 10^{-4} M dithizone solutions for titrimetric analysis. Dithizone in an anhydrous acetic acid/chloroform (4% v/v) medium is titrated with 2×10^{-4} M mercury(II) acetate in the same medium. The titration takes only a few minutes. The accuracy (+0.2%) and precision (r.s.d. = 0.7%) achieved are similar to those obtained by the classical extractive titration with silver(I).

The instability of dithizone, in solid form but especially in solution, necessitates purification of the solid and standardization of its solutions. The commonest method of standardizing dithizone solutions is based on the application of Beer's law, using a pre-established molar absorptivity. The imprecision of this procedure is 1–3% [1]. However, there is significant disagreement between the reported molar absorptivities in authoritative monographs about dithizone [2, 3], the compiled values in chloroform differing by 3.6%. This discordance still remains in a recent review on dithizone [4]. The most precise and accurate method of standardizing dithizone solutions is based on extractive titration of a standard aqueous silver nitrate solution [3]. The main problems with this method, which is practically used with dithizone only [5], are that it is time-consuming and requires considerable experimental skill [4].

The use of dithizone in homogeneous medium has been described [6, 7]. Photometric titrations have been applied [8, 9] but little was said about standardization of the titrant. A water/acetone medium was proposed by Le Goff and Tremillon [8] but dithizone had to be kept in an alkaline aqueous solution, in which it is not entirely stable [2]. In this communication, photometric titration in a chloroform/anhydrous acetic acid medium is suggested for the standardization of dithizone solutions. This work forms part of a general investigation aimed at extending the use of dithizone in the determination of organometallic compounds, by means of photometric titrations in mixed homogeneous media.

Experimental

The usual cleaning precautions for work with dithizone [3] were taken. All the experiments were done under diffuse light. All solutions were pre-

pared with analytical-reagent chemicals. Twice-distilled water from an all-glass pyrex still was used throughout.

Apparatus. For the titrations, a Coleman Junior II u.v.-visible spectrophotometer was used; the 20-ml photometric cell (path length 21 mm) was modified by attaching a cone (from a glass funnel) to the cell so that its volume was increased to 50 ml and the solution could be stirred. Visible spectra were recorded with a Perkin-Elmer 554 spectrophotometer.

Dithizone solution. A stock solution of pure dithizone in chloroform was obtained by following essentially the purification process recommended by Iwantscheff [3] and using metal-free ammonia obtained by isopiestic distillation [10]. The ratio of the absorbance readings at the two peak wavelengths (605 nm and 440 nm) of dithizone in chloroform (peak ratio index) was used to evaluate the purity of the dithizone solution. The purification process was repeated until the index was ≥ 2.66 [11]. This pure stock solution in chloroform, and the working solutions (10^{-5} – 10^{-4} M), were stored under layers (ca. 1 cm) of 1 M sulphuric acid, and protected from light in a refrigerator (5°C).

The purity test mentioned was also applied as a criterion to check the stability of dithizone solutions before each set of experiments. The working and storage conditions described were found to be satisfactory.

Mercury(II) acetate solution. The solid (0.46 g) was dissolved in 250 ml of anhydrous acetic acid, and standardized potentiometrically against standard sodium chloride solution; an Ag/AgCl electrode was used with a saturated calomel electrode having a potassium nitrate solution salt bridge. The working solution (ca. 2×10^{-4} M) was prepared daily by diluting a portion of stock solution with chloroform until the solution contained about 4% (v/v) anhydrous acetic acid in chloroform.

Organic solvents. The anhydrous acetic acid was checked for heavy metals by adding excess of aqueous ammonia solution and shaking with a solution of dithizone in chloroform; a colorless organic phase indicated the absence of "dithizone metals". Some of the chloroform used was distilled and stabilized with 0.5% (v/v) ethanol. Commercial chloroform lots that gave negative tests based on the peak ratio index were used without further purification.

Titration procedure. Place in the photometric cuvette (path length 21 mm) 25 ml of chloroform, 10 ml of dithizone solution (ca. 6×10^{-5} M) at room temperature, and 1.5 ml of pure anhydrous acetic acid. Then titrate with small portions of mercury(II) acetate solution (2×10^{-4} M) until a constant absorbance reading is attained at 600 nm. Plot the absorbance (corrected for dilution) as a function of the volume of mercury(II) acetate solution, extrapolating the straight branches of the plot to establish the equivalence point.

Results and discussion

In the first attempts to utilize photometric standardization of dithizone in homogeneous medium, a chloroform/ethanol/water mixture was used,

because this medium was successful in the determination of methylmercury(II) salts [9]. For the present problem, in which standardized aqueous solutions of silver nitrate and mercury(II) nitrate (ca. 10^{-4} M) were used, low results were obtained. The water present proved to have a decisive influence on the error. The relative influence of mixing the three solvents in different proportions was studied systematically. The lowest error ($<4\%$) was obtained with a 57% chloroform/40% ethanol/3% water medium. Consequently, different organic solvents capable of dissolving the mentioned salts without water were studied.

The solvents were tested by adding small portions of standard silver(I) or mercury(II) solution in the organic solvent (anhydrous acetic acid or ethanol) to a portion of standard dithizone solution. The reverse order of addition was not examined because secondary dithizonate formation was enhanced. The visible spectra of these systems are shown in Fig. 1. The absorption peaks can be approximately correlated with the peaks described in the literature [2, 12], with due consideration of the displacements caused by the change of medium. In all these systems, except one, it is seen that

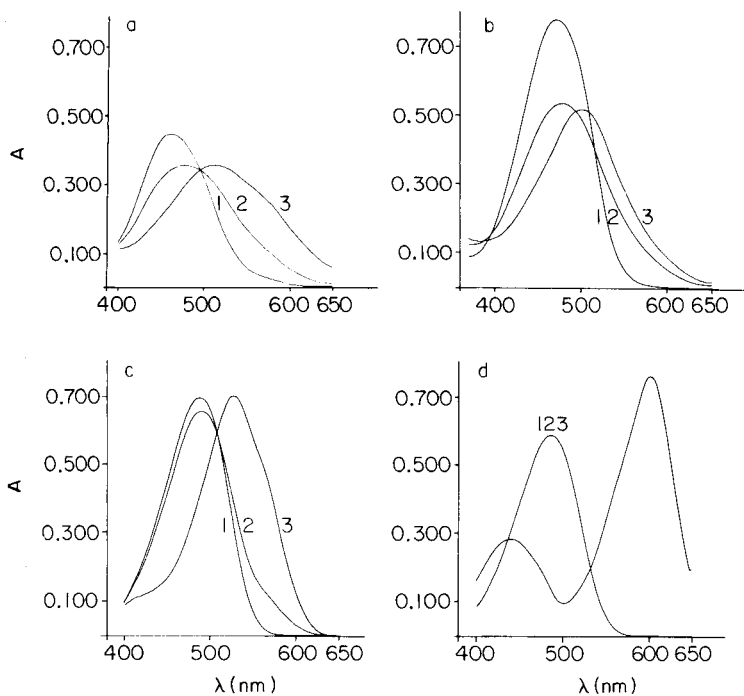


Fig. 1. Absorption spectra for dithizone in chloroform in the presence of different amounts of titrant solutions: (a) silver nitrate in ethanol; (b) silver nitrate in anhydrous acetic acid; (c) mercury(II) acetate in absolute ethanol; (d) mercury(II) acetate in anhydrous acetic acid. Curves: (1) equivalent amounts; (2) twice the equivalent amount of metal ion; (3) large excess of metal ion. In part (d), the spectrum of dithizone in that medium is also shown.

primary and secondary species are formed if an excess of metal ion is added. The absorbance of the secondary dithizonates is less stable than that of primary dithizonates, especially when mercury(II) acetate in ethanol is added. This modifies the titration curve after the equivalence point. When the titrant is mercury(II) acetate in anhydrous acetic acid, new species containing excess of metal are not formed, even with a large excess of metal.

The resulting titration curves were of the kind shown in Fig. 2. These curves confirm that the acidic solutions do not favour the formation of secondary dithizonates [2]. When the acidic mercury(II) titrant is used, formation of the secondary complex is wholly avoided. Given the instability of secondary dithizonates, it was concluded that mercury(II) acetate in anhydrous acetic acid and chloroform provided the best system.

In the final tests, the results obtained for a dithizone solution in chloroform by titration with mercury(II) acetate in anhydrous acetic acid (method A) or in a 4% (v/v) anhydrous acetic acid/chloroform mixture (method B)

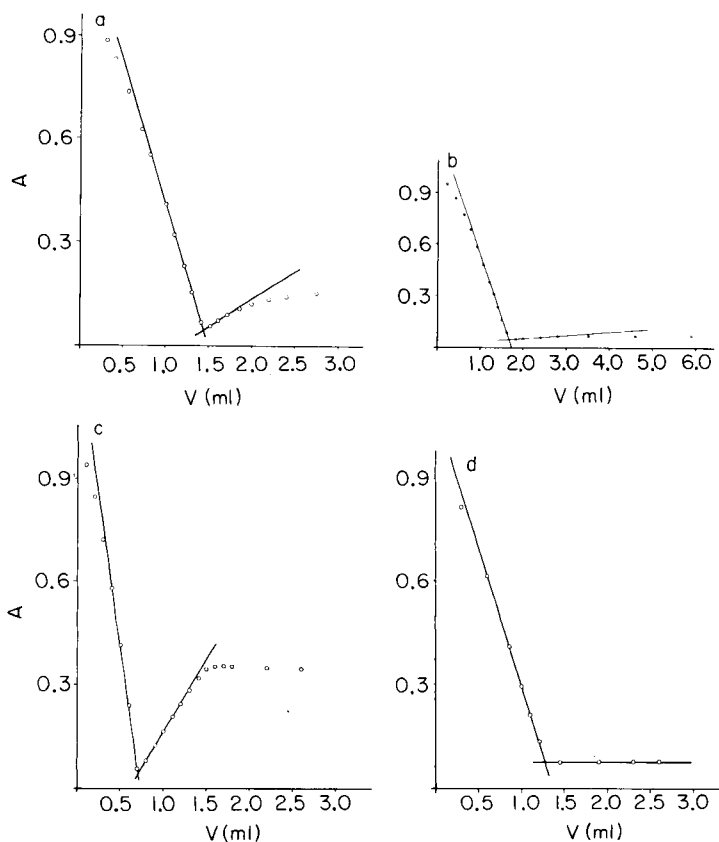


Fig. 2. Photometric titration curves for dithizone in chloroform. Titrant: (a) silver nitrate in ethanol; (b) silver nitrate in anhydrous acetic acid; (c) mercury(II) acetate in absolute ethanol; (d) mercury(II) acetate in anhydrous acetic acid.

were compared with those obtained by the classical extractive titration with standard silver nitrate. When the titrant was in the mixed medium, the dithizone solution was prepared in the same medium. The averages of seven titrations by each of these procedures were 59.4 μM (classical method), 59.0 μM (method A) and 59.5 μM (method B); the error range was 1.8% in all cases, the standard deviation being 0.4 μM and the relative standard deviation 0.67–0.68%. The slight error (–0.7%) in method A becomes negligible in method B (+0.2%). The precision obtained is similar to that of the extractive titration [3] and much better than that of the direct spectrophotometric method [1].

The authors express their sincere thanks to Prof. Folke Ingman, Royal Institute of Technology, Stockholm, for critical comments and valuable discussion.

REFERENCES

- 1 L. Meites and H. C. Thomas, *Advanced Analytical Chemistry*, McGraw-Hill, New York, 1958, p. 287.
- 2 H. M. N. H. Irving, *Dithizone*, Anal. Sci. Monograph. No. 5, Chem. Soc., London, 1977.
- 3 G. Iwantscheff, *Das Dithizon und seine Anwendung in der Mikro- und Spuren-analyse*, 2nd edn., Verlag Chemie, Weinheim, 1972.
- 4 H. M. N. H. Irving, *CRC Crit. Rev. Anal. Chem.*, 8 (1980) 321.
- 5 Yu. A. Zolotov, *Extraction of Chelate Compounds*, Ann Arbor-Humphrey Science Publishers, London, 1970, p. 195.
- 6 C. Buisson and M. Breant, *Anal. Chim. Acta*, 56 (1971) 197.
- 7 M. E. Makovskii, *J. Anal. Chem. USSR*, 25 (1970) 1059.
- 8 P. Le Goff and B. Tremillon, *Bull. Soc. Chim. Fr.*, (1964) 350.
- 9 F. Ingman, *Talanta*, 18 (1971) 744.
- 10 H. M. N. H. Irving and J. J. Cox, *Analyst (London)*, 83 (1958) 526.
- 11 H. M. N. H. Irving and A. T. Hutton, *Anal. Chim. Acta*, 128 (1981) 261.
- 12 T. Nowicka-Jankowska and H. M. N. H. Irving, *Anal. Chim. Acta*, 54 (1971) 489.

Book Reviews

R. Pribil, *Applied Complexometry*. Pergamon Press, Oxford, 1982 (ISBN 008-026-2775). xv + 410 pp. Price U.S. \$75.00.

One of the most delightful experiences in analytical chemistry has been to watch Dr. Pribil demonstrating intricate and imaginative reaction sequences that can be used in EDTA titrations. One colour succeeds another in rapid succession; counting drops replaces the use of the burette. The result is an enthusiastic encapsulation of the important principles of EDTA titrations, and of the masking, demasking and indicator reactions on which the titrations are strongly dependent. Much of this enthusiasm has found its way into the present text. The earlier chapters deal with the basic chemistry involved in compleximetric titrations: the chelating properties of complexans, useful indicators, masking and demasking agents, separation methods, and standardization. The treatment is as descriptive as the subject allows, but the use of stability constants and α -coefficients is essential. There follow chapters dealing with individual metal ions, grouped according to whether they form very strong, moderately strong, or weak complexes with EDTA, and a discussion of indirect methods for anions. The remaining 160 pages are devoted to a most useful compilation of procedures and discussion concerning the applications of compleximetric titrations to the analysis of alloys, rocks, slags, cements, glasses, ores, electroplating solutions and many other types of sample. The information is comprehensive and detailed, and bears the stamp of authority of the scientist who has contributed at least as much to this subject as anyone. There are few criticisms. The book is directly reproduced from typescript, and, although this has been excellently done, it does detract from the presentation. Reversion to the term "volumetric" after patient endeavours to encourage the use of "titrimetric" is unfortunate, as is the suggestion that masking agents might also be called screening agents. But these are very minor comments in a book that will be of great practical value to analytical chemists, and should serve them well through this decade.

A. Townshend

R. Caulcutt and R. Boddy, *Statistics for Analytical Chemistry*. Chapman and Hall, London, 1983 (ISBN 0-412-23730-X). Price £22.50.

Statistics is a discipline that is generally badly taught and regarded with unjustified suspicion, and most practising analytical chemists must wish that they had a better appreciation of its principles and applications. The present volume is designed to fill that gap, and is based on the material for a well-

known series of short courses offered by the authors over several years. Its thirteen chapters are accompanied by tutorial problems (with solutions) and are followed by a summary of useful formulae and abbreviated forms of the most commonly used statistical tables. Individual references are not provided in the text, but there is a short general bibliography. The whole book is clearly produced with remarkably few errors, but the reviewer's ritual complaint about the price seems particularly justified in the case of a text of moderate length that presumably seeks large volume sales.

The book is very clearly aimed at the practising analyst. This is reflected in the extensive and very practical discussions of precision, calibration and bias, and the repeated references to advisory publications such as British Standard monographs. There can of course be no complaint about such an approach, but the layout of the book is such that it might not be altogether suitable for higher education students of analytical chemistry, or for chemists using statistical methods to evaluate research results. Much of the subject matter is introduced with the aid of a small number of fictional examples. This approach might well be viable in a taught course, but is much less suited to a written text: I found it increasingly irritating when the same example was used in later chapters, making frequent back references necessary. The almost total absence of statistical theory will disappoint only a few readers, but the omission of two other aspects of statistics might limit the usefulness of the book. There is no discussion of non-parametric methods, which do find a good deal of everyday use because of the simplicity of some of the calculations. And there is no hint of the modern chemometric methods (optimization, pattern recognition, etc.) that are now within the range of every laboratory with a microcomputer. The book satisfactorily covers the backbone of statistical methods most useful to the analyst, however, and many chemists will find it valuable.

J. N. Miller

R. R. Smardzewski, *Microprocessor Programming and Applications for Scientists and Engineers*. Elsevier Science Publishers, Amsterdam, 1984 (ISBN 0-444-42407-5). xiv + 353 pp. Price Dfl. 98.00.

Microprocessors today affect nearly all aspects of our daily life to one extent or another. This includes, of course, the chemical laboratory. Today microprocessors are used to process data and control laboratory instruments ranging from simple thermostats and single-pan balances to very complex and sophisticated spectrometer systems. However, before a microprocessor can be of any use in the laboratory, it must be properly programmed and interfaced to the outside world. There is an increasing number of standard programs available on the market, which are adequate for many standard applications. However, there is often no over-the-shelf system available for

research applications, and a fully optimized solution of an individual standard problem often requires extensive modifications and adjustments. Furthermore, even for standard routine applications meaningful results can be expected only if the microprocessor system is operated within its design limits, which consequently have to be known by the user. Critical evaluation of the data acquired and of the behaviour of the system controlled by a microprocessor absolutely requires understanding of the microprocessor and of the program that controls its operation. The "black box" philosophy if pushed to extremes will invariably lead to disaster. This book attempts to teach the minimum basic knowledge about microcomputer programming and interfacing that any chemist should have. It is written by a chemist for chemists.

Concepts and principles are explained by many well-chosen examples and experiments, based on the AIM-65 microcomputer, which is built around the popular 6502 MPU, as are many other microcomputers, including the Apple II/IIe, the Commodore Pet (VC-20) VC-64, and the Atari. It is not essential to have access to an AIM-65 for working through this book, but some elementary know-how is required to transfer the programs to other systems. This know-how can be acquired by working through the book without actually doing the experiments.

The first part gives the basic facts about microprocessors and their associated circuitry: computer organization, number systems, code conversions, and logic gates. Then follows an introduction to instructions and addressing modes of the 6502 microprocessor unit (MPU), with many instructive experiments. The 6522 Versatile Interface Adapter (VIA), the most widely used chip for connecting the microprocessor to the outside world, is described next, with well designed experimental programs to demonstrate the various capabilities of this rather complex chip. A short chapter is devoted to the monitor program of the AIM-65; this is where users of other microcomputer systems will probably experience most difficulties. However, as the monitor programs for most simple microcomputers are designed along the same general principles, even a beginner can solve the associated problems within a reasonable time.

The section on data acquisition deals extensively with the various approaches to analog-to-digital and digital-to-analog conversion. The potentials and limitations of the different systems are nicely demonstrated as are the control and communication interfaces. This reviewer particularly liked the chapter on program development, which includes an excellent introduction to the general structure of assembler programs. The only high-level language covered is FORTH, which unlike other high-level languages does not isolate the user from the microprocessor. A section on structured programming introduces the reader to system analysis and to well organized program development. Useful appendices complete the book.

Its clear and linear structure makes this book an excellent introduction to microcomputer applications in the chemical laboratory. It is, however, not a

bed-side book; the reader is required to contribute a fair amount of work, particularly in familiarising himself with new terminology. The book is rather similar to the well known "Bugbooks" by Larsen, Rony and Titus, which during the late seventies were the standard introduction to microprocessors for chemists. The present book is more compact and is based on more up-to-date technology. To every chemist who wants an introduction to this field, the book can be recommended, with the reservation that success will depend to a large extent on his own incentive.

J. T. Clerc

R. B. King (Ed.), *Chemical Applications of Topology and Graph Theory*. Elsevier Science Publishers, Amsterdam, 1983 (ISBN 0-444-42244-7). xii + 494 pp. Price Dfl. 275.00.

Many molecular properties are determined largely by the connectivity of the respective molecules, and in many cases the detailed structure of the compound is of secondary importance only. This empirical fact is the motivation behind most chemical applications of topology and graph theory. A large proportion of the papers presented at a symposium held at the University of Georgia, Athens, Georgia, USA in 1982 and collected in this book use basically the same approach. Structural aspects of a series of chemical compounds are represented as a graph, i.e., a set of nodes connected by edges. The familiar structural diagrams used to represent the connectivity of the atoms in a molecule lend themselves quite naturally to such a transformation. Then, one or more suitable mathematical properties that can be expressed as a number are evaluated for the abstract graph. Such a number is generally referred to as an (topological) index. An early topological index used in chemistry is the Wiener path number $W(G)$ suggested in 1947. Since then, many topological indices have been proposed. Their original purpose was to obtain correlations with a wide variety of physicochemical properties, but they have found numerous other applications, the currently most important ones being bibliographic species classification and pharmaceutical drug design.

Many other chemical systems can be represented by abstract graphs and are thus amenable to analysis by graph theory. Among others, chemical reaction networks and the molecular lattice of liquid water are treated in this book. From a mathematical point of view, the papers presented are clearly written; the subjects are treated on a rather advanced level. The language and style of presentation are definitely mathematical. A chemist with an above average interest in mathematics encounters considerable difficulties in working through the book, whereas the average chemist will probably put the book back to the shelf for good after just browsing. This is unfortunate, as graph theoretical and topological methods may well open new means of solving many chemical problems. For the general chemist this book is of very

little value, but for the specialist and for those chemists willing to invest considerable time and effort into learning the terminology of the field, it may be worth the money.

K. Humbel

Paul E. Mix, *The Design and Application of Process Analyzer Systems (Vol. 70 in Chemical Analysis)*. Wiley-Interscience, New York, 1984 (ISBN 0-471-86518-4). 312 pp. Price £56.25.

This volume is intended to provide basic guidelines for the design and operation of process analyzer systems, and as such it is directed more towards the production engineer and technical personnel than towards the analytical chemist. One of the attractions of the book, however, is that it pays particular attention to sampling procedures and emphasises their crucial role within the overall analyzer design.

After a discussion of sampling systems and safety procedures, there are chapters dealing with various types of detector: pH and conductivity meters, moisture and corrosion monitors, oxygen analyzers, photometric analyzers, digital analyzers (e.g., automatic titrators) and on-line process chromatographs. Each chapter covers the theory of operation of the detector, the calibration techniques used, important design features and applications and other general comments. The information provided is therefore extremely useful for anyone considering the possibility of introducing a process analyzer into an industrial environment, but the text would have been more stimulating if the performance of process analyzers had been critically assessed in some real-life situations, e.g., specific data on cost of installation and operation, precision and reliability, and improvements in plant productivity and quality control.

There is a list of process analyzer manufacturers (predominantly in the U.S.A.), a comprehensive set of references and a glossary of process-analyzer jargon for the reader who wishes to find out more about the subject. Design data and sketches of various process analyzers are included, but photographs of such systems, particularly within an industrial environment, are sparse. As with other books in the series, this volume provides an easy-to-read text that covers the practical aspects of the subject very well. However, the contents could have been made more appealing to the reader with only a peripheral interest in process analyzers.

P. J. Worsfold

Friedrich Oehme und Martin Jola, *Betriebsmesstechnik unter Einsatz von In-line und On-line Analysatoren*. (Reihe: ABC der Mess- und Analysetechnik) Dr. Alfred Hüthig Verlag, Heidelberg, 1982 (ISBN 3-7785-0782-6). xi + 167 S. Preis (kart.) DM 38,00.

Das vorliegende Büchlein behandelt in kurzen, nach Stichworten alphabetisch geordneten Abschnitten Themen aus der industriellen Betriebsmesstechnik. Dabei werden allgemeine Grundbegriffe (z.B. Ist-Wert, Querempfindlichkeit, Spurenanalyse), Instrumenten-Komponenten (z.B. Bezugselektrode, Messumformer, Tauchgeber), Methoden (z.B. Amperometrie, Brechungsindex, Thermometrische Analyse) und industrielle Prozesse (z.B. Bleichen von Textilien, Phosphatieren, Zellstoff-Aufschluss) vorgestellt. Der Text der einzelnen Abschnitte geht in der Regel so tief, dass sich auch der nicht im betreffenden Gebiet spezialisierte Fachmann ein Bild der Anforderungen, der Problematik und der heute üblichen Lösungen machen kann. Auf eine erschöpfende Behandlung wird verzichtet, doch vermitteln zahlreiche Hinweise auf Monographien oder auf Artikel in Fachzeitschriften den Zugang zur weiterführenden Literatur. Das ganze Werk ist ausgesprochen praxisorientiert aufgebaut, die langjährige Erfahrung der Autoren auf dem Gebiet der industriellen Betriebsmesstechnik schlägt immer wieder durch. Dem Referenten erscheint das Büchlein für Anfänger wenig geeignet. Wer aber über eine auch nur minimale Vorbildung in Analytik und/oder Messtechnik verfügt, dem gibt das Buch einen raschen, kompakten und breiten Ueberblick über die Praxis der heutigen Betriebsmesstechnik.

J. Kwiatkowski, *FORTRAN in 8 Lektionen für Anfänger*. Frech-Verlag, Stuttgart, 1983. 216 S. Preis DM 29,80.

J. Kwiatkowski und B. Arndt, *BASIC. Eine Einführung in 10 Lektionen*. Springer-Verlag, Heidelberg 1983. x + 180 S. Preis DM 39,00.

Mit der weiten Verbreitung billiger Kleincomputer hat sich auch ein gesteigertes Bedürfnis nach zum Selbststudium geeigneten Einführungen in die meistverbreiteten Programmier-Sprachen ergeben. Die beiden Bücher versuchen, dieses Bedürfnis für BASIC und FORTRAN zu erfüllen, was weitgehend gelungen ist. Der Stoff ist gut gegliedert und äusserst systematisch und klar dargestellt. Jedem Kapitel sind die anvisierten Lernziele vorangestellt. Dann folgen der Lerninhalt, illustriert mit zahlreichen Beispielen, und eine Zusammenfassung. Am Ende jedes Kapitels finden sich Übungsaufgaben, deren Schwierigkeitsgrad einen weiten Bereich überspannen. Für sämtliche Übungsaufgaben sind im Anhang Musterlösungen angegeben.

Im Vorwort des Buches über BASIC findet sich der folgende Satz: "Bei konsequentem Durcharbeiten des Buches sollte es dem Leser möglich sein, sich je nach Vorbildung und gewünschter Eindringtiefe in die Materie in 1 bis 5 Tagen mit BASIC vertraut zu machen". Eigene Versuche mit (zugegebenermassen oft eher musisch als mathematisch begabten) Studenten ohne jede

Vorbildung lassen vermuten, dass der angegebene Zeitbedarf als eher optimistisch zu beurteilen ist. Andererseits war der Lernerfolg bei beiden Büchern durchaus erfreulich. Sie haben sich in der Praxis gut bewährt und können ohne Vorbehalte empfohlen werden.

J. T. Clerc

Y. Paker, *Multi-Microprocessor Systems*. (Vol. 18 in *A.P.I.C. Studies in Data Processing*). Academic Press, London, 1983 (ISBN 0-12-543980-6). xii + 204 pp. Price £16.50.

These days many analytical instruments contain a microprocessor to control the instrument and assist with data collection and data processing. More sophisticated instruments may have several microprocessors, or an instrument containing a microprocessor may be used with a data station or data-processing network. When more than one microprocessor is involved, digital data have to be passed to and fro between the various microprocessors, and this has to be done in an orderly way. In *Multi-Microprocessor Systems*, the author discusses the design and functioning of such systems and presents an up-to-date account. This is not a book for beginners, nor is it particularly addressed to chemists, but anyone with a fair appreciation of the make-up of a single microprocessor system will be able to gain an insight into the design of these more complex systems. In the first six chapters the author discusses both electronic (hardware) and programming (software) aspects of the subject. The final chapter deals with the thorny problem of designing systems which will recognise when they are not working properly, and are able to make appropriate corrections so that the fault does not cause the system to break down. The book has many clear flow diagrams which are helpful in assisting understanding, but to get a full appreciation of the subject the reader needs to be familiar with the specialised language of the world of computers.

J. R. Chipperfield

Alan G. Marshall (Ed.), *Fourier, Hadamard and Hilbert Transforms*. Plenum Press, New York, 1982. xii + 562 pp. Price \$65.00.

This book seems likely to suffer because of its misleading title. "Methods for Fourier-Transform Spectroscopy (with other transforms)" would be a better description of the subject matter, as there are 13 articles on Fourier-transform spectroscopy, one on Hilbert transforms, one on Hadamard transforms and one on general transforms. Although some of the articles are mathematical, and one contains a FORTRAN program for a fast Fourier

transform on a minicomputer, there is much descriptive material which could be read with profit by a chemist happy to leave mathematics to others.

The types of spectroscopy covered are: ion-cyclotron resonance, nuclear quadrupole resonance, dielectric, microwave, two-dimensional and paramagnetic nuclear magnetic resonance, electron nuclear double resonance, muon spin rotation, infrared, and visible-ultraviolet. There are also articles on faradaic admittance measurements and optical diffraction by electrodes. The volume is dedicated to the memory of W. H. Flygare who has contributed the article on microwave spectroscopy.

It is impossible to comment on all of such a diverse series of topics, but mention may be made of a particularly clear introduction by Morris to two-dimensional Fourier-transform n.m.r. spectroscopy with some excellent diagrams, and a stimulating article by Klainer, Hirschfeld, and Marino on the bright future for Fourier-transform n.q.r. spectroscopy. Overall, the book is a valuable survey of the field and deserves to have a place in any library that caters for research in chemistry.

D. W. Davies

G. A. Webb (Ed.), *Annual Reports on NMR Spectroscopy, Vol. 11B*. Academic Press, London, 1981. x + 502 pp. Price £48.40.

This volume which is compiled by M. Witanowski, L. Stefaniak and G. A. Webb, is completely devoted to a review of nitrogen n.m.r. involving ^{14}N and ^{15}N nuclei. The literature coverage is for the period 1977–1980 subsequent to a previous review in this series, and the 340 pages of tables in this Volume are a measure of the current popularity of nitrogen n.m.r. The tables are clearly presented and cover both experimental and calculated nitrogen shieldings and coupling constants for a wide spectrum of organic, inorganic and biological compounds. About one third of the review is devoted to a discussion of experimental techniques and nitrogen n.m.r. parameters from both experimental and theoretical standpoints.

This is a thorough review which should be a most useful reference source for any laboratory interested in nitrogen n.m.r. There are several other books or reviews available on this topic; the present one compares well on content and presentation, and it covers ^{14}N as well as ^{15}N . However, the literature coverage is largely restricted to a four-year period and the reader would also need Volume 7 for a more complete account.

G. A. Webb (Ed.), *Annual Reports on NMR Spectroscopy, Vol. 14*. Academic Press, London, 1983. vii + 406 pp. Price £54.60.

This volume is entirely devoted to a tabulation of fluorine-19 n.m.r. data compiled by V. Wray. The survey covers the period January 1979–June 1981

and updates a previous compilation by the same author in Vol. 10B. The tables are clearly presented and give ^{19}F chemical shifts and coupling constants. Structural formulae are depicted for all compounds. Most entries are concerned with organofluorine compounds, but there are also sections concerned with fluorine bonded to other elements. Short sections are devoted to ^{19}F -n.m.r. studies of polymers, liquid crystals, solid-state samples, biological applications and theoretical studies.

Volume 14 of this highly regarded series of reviews will be of interest to research groups working with fluorine compounds and to analytical n.m.r. laboratories offering ^{19}F facilities.

W. B. Jennings

Jaroslav Šesták, *Thermal Analysis, Part D, Thermophysical Properties of Solids, Their Measurements and Theoretical Thermal Analysis*, (Vol. XII, Wilson and Wilson's *Comprehensive Analytical Chemistry*, G. Svehla, Ed.), Elsevier Science Publishers, Amsterdam, 1984, 440 pp. Price \$67.50.

Dr. Jaroslav Šesták is a scientist with a deep understanding of the basic theories and concepts of physics and chemistry. Also he realizes the importance of the application of these basics to the development of experimental techniques. Therefore it is not surprising that this book is unique among thermal analysis texts. It is the first real effort to present a coherent development of thermoanalytical theory and practice based on fundamental principles of thermodynamics.

Šesták set for himself a formidable task in this undertaking and has achieved a considerable degree of success. However, it is not a book for light reading although mathematical developments are not included as it is stated in the introduction that specialized knowledge of mathematics is not required. This reader found that many sections required deep thought, and occasionally referral to the original sources given in the well chosen reference lists was necessary for a good understanding of the assumptions and approximations made in a particular development. This is not a criticism but an illustration of the difficulty in presenting a reasonably terse but rigorously developed compendium of the wide spectrum of phenomenological equations which are needed to describe the very large number of cases encountered in treating the physics and chemistry of heterogeneous systems under nonisothermal and nonequilibrium conditions.

A reading of the first chapter is essential for intelligent and productive utilization of the remainder of the book. It serves both as a "study outline" and as a *modus operandi* for the succeeding chapters, for it describes Šesták's basic philosophies for linking theory and experiment. The second chapter covers sample selection and pretreatment, a neglected area in most books. It stresses the importance of atmospheric and thermal control in the mixing,

grinding, sampling, etc., of specimens. The part dealing with preparation of metastable states is of particular interest. The third chapter includes the general definitions and applications of methods of thermal analysis, and the fourth is on measurement, calibration, and temperature control and regulation. Subsequent chapters include thermodynamic principles, thermodynamics of phase equilibria, phase diagrams, theory of phase transitions, mechanism and kinetics of both chemical and physical reactions, calorimetric methods, and measurement of non-thermal properties. A logical sequence is followed in most of these chapters; experimental sample preparation and property measurement are described followed by the theoretical background and the treatment of results. These sections include much work that is not found in other texts. The emphasis is on inorganic systems, especially metal oxide glasses, and includes extensive work done in this latter area which has not appeared before in the English language. The book concludes with sections on computational techniques, algorithms, statistical treatment, regression and curve-smoothing methods, and an appendix containing many useful tables.

The theory and techniques of thermal analysis transcend mere differences in substrates, and I recommend the book both as a reference text and as a means of obtaining a better understanding of thermoanalytical theory and practice.

J. H. Flynn

S. S. M. Hassan, *Organic Analysis using Atomic Absorption Spectrometry*. Horwood/Wiley, Chichester, 1984 (ISBN 0-8531-2559-7). 384 pp. Price £35.00.

At first sight, this book might appear to be a collection of fringe topics concerning indirect methods of atomic absorption spectrometry (a.a.s.), a subject of minor academic interest and of no practical importance. In reality, it is much more. It covers not only the determination of organic compounds but organometallic compounds, and compounds involving some metalloid elements, as well as analyses of pharmaceutical and biological samples and of other organic materials for metals and other species. The book begins with an up-to-date account of the theory and instrumentation of a.a.s., followed by a collection of practical information (e.g., control of interferences, sample handling). Individual chapters deal with the determination of compounds containing nitrogen, phosphorus, arsenic, oxygen, sulphur and halogens. They describe direct and a multiplicity of indirect a.a.s. procedures, not to mention occasional forays into molecular absorption and emission spectrometry. The methods illustrate the great ingenuity of analytical chemists. After a chapter on organometallic compounds (Pb, Hg, Sn, Se, Te, Sb, etc.), which includes their speciation, there follows an impressive and ingenious collection

of indirect methods for the determination of drugs and vitamins, and procedures for determination of metals and non-metals, in a variety of pharmaceutical products. The chapter on determination of trace metals in biological materials is a compact account of a very topical subject, and includes topics such as metal/protein binding and immunoassay. The remaining chapters are devoted to the analysis of organic products such as foods, petroleum products and polymers, and to a range of working procedures.

This is a well researched, comprehensive and unique book. The wealth of information it contains is indicated by the very large number of references: many chapters have more than 400. It should be a valuable source of knowledge for many years to come, and testifies to a continuing feature of modern analytical chemistry, that although it is the instrument that provides the final measurement, it is a wide knowledge of chemistry that allows such measurements to be carried out on such a diversity of compounds and samples.

H. Müller, M. Otto and G. Werner, *Katalytische Methoden in der Spurenanalyse*. Akademische Verlagsgesellschaft, Geest und Portig K.-G., Leipzig, 1981. 168 pp. Price RM 45.00.

Catalytic reactions remain a fascinating aspect of analytical chemistry. Their importance for highly sensitive detection systems for inorganic species, however, has declined with the increasing array of instrumental techniques available. The exception to this general statement has been enzymatic catalysis, but this occupies only a minute portion of the text. With the advent of new automatic analysis systems (flow injection, centrifugal and stopped-flow analyses in which catalytic reactions can readily be used), it is likely that interest in catalytic reactions will be rekindled. And this book could well catalyze that interest.

It begins with a few, probably unnecessary, pages on general aspects of trace analysis before embarking on discussions of basic reaction kinetics, the effect of conditions (including catalysts) on reaction rates, and the methods for measurement of these rates. This is followed by good descriptions of the various types of catalytic reactions, including mechanistic aspects, of activation effects, and of the selectivity of determinations based on catalytic reactions. The section on mechanisation and automation is very useful, as is the selection of detailed methods which follows it. The book concludes with a survey of the fields of application of catalytic analysis, 338 references and a subject index. Overall, this is a comprehensive and authoritative account, that greatly deserves the production of an English translation.

Ferrites. Transition Elements. Luminescence, (Vol. 47, *Structure and Bonding*). Springer-Verlag, Berlin, 1981 (ISBN 3-540-10788-6). v + 126 pp. Price DM 64.00.

This slim volume contains articles by Grenier, Pouchard and Hagenmuller on vacancy ordering in oxygen-deficient perovskite-related ferrites and by Fidelis and Mioduski on the double-double effect in the inner transition elements. Of most interest to analytical chemists, however, is the review by Golovina, Zorov and Runov on "Chemical Luminescence Analysis of Inorganic Substances" (68 pp.). This covers the basic theory of luminescence processes of all types, before considering analytical applications to elements based on the fluorescence and phosphorescence of their complexes with organic reagents, on their native luminescence, on chemiluminescence, and by titrimetric luminescence methods. The treatment is comprehensive, with much of the information provided in tabular form. The review is timely in view of the rapidly increasing interest in analytical applications of luminescence, and especially valuable in that the 746 references include a considerable number to the Russian literature.

A. Townshend

David F. S. Natusch and Philip K. Hopke (Eds.), *Analytical Aspects of Environmental Chemistry*, (Vol. 64, *Chemical Analysis*). Wiley-Interscience, New York, 1983 (ISBN 0-471043249). ix + 267 pp. Price £35.50.

This is not the book to purchase if a manual of the methods used in environmental analysis is required. Rather it is a collection of six chapters on specific topics by authors who are experts in their respective fields. Although no attempt has been made to give an exhaustive literature survey for each of the chosen topics, the chapters are nevertheless well organised with sections on instrumentation and techniques, and selected examples chosen to illustrate each method. A major criticism which must be levelled is the almost total lack of reference to recent publications in most chapters. Scientists interested in following developments in analytical methods, their application to environmental problems and their limitations will, however, find these chapters interesting reading.

Chemical speciation is rightly gaining considerable attention as research workers recognise that not only is the total quantity of an element important, but also the form in which it exists can be quite critical. This is well illustrated in the examples provided by R. S. Braman in the initial chapter. The next two chapters are related in that they deal with capillary gas chromatography (M. Novotny) and gas chromatography/mass spectrometry (P. W. Ryan). Again, instrumental techniques are briefly reviewed with appropriate illustrations of the methods drawn from the analysis of environmental

materials. The chapter by R. W. Linton, D. T. Harvey and G. E. Cabaniss on the applications of the surface analysis techniques of photoacoustic spectroscopy, x-ray photoelectron spectroscopy, Auger electron spectroscopy and secondary-ion mass spectroscopy is a useful survey of the application of these techniques in particulate characterisation and the study of surface reactions. The use of x-ray photoelectron spectroscopy is further expanded by T. Novakov and his associates. Multivariate analysis is another rapidly-developing field in which the environmental analyst must take an interest; and the chapter by P. K. Hopke provides useful illustrations of the application of these statistical techniques to environmental problems.

N. A. Dyson

John Harvey, Jr. and Gunter Zweig (Eds.), *Pesticide Analytical Methodology*. (ACS Symposium Series 136). American Chemical Society, Washington, DC, 1980 (ISBN 0-8412-0581-7). x + 406 pp. Price \$38.00.

This book is based on the papers delivered at a symposium held at a 1979 meeting of the American Chemical Society. As is generally the case with such publications, style and quality of the individual contributions is somewhat inhomogeneous. However, no chapter falls clearly below the standard. The twenty papers deal with a wide range of problems and methods in pesticide analysis. High emphasis is placed on h.p.l.c., this technique having made the greatest advances in recent years. This section includes chapters dealing with new detectors, with procedures for fluorogenic labelling, mobile phase selection, column characterization, and automation. Recent developments in t.l.c. techniques are also dealt with. A further part is concerned with sampling and clean-up methods, both of which are of utmost importance for avoiding artifacts in trace analysis. The applications described include less commonly used techniques, such as g.c./m.s. studies on organotin pesticides, Fourier-transform infrared spectroscopy, negative-ion mass spectroscopy, immunochemical techniques, and computer data processing. The book seems to be well suited to give the reader a broad overview over many aspects of this important area of analytical chemistry.

J. T. Clerc

Arthur E. Martell and Robert M. Smith, *Critical Stability Constants (Vol. 5: First Supplement)*. Plenum Press, New York, 1982 (ISBN 0-306-410052). xvii + 604 pp. Price \$69.50.

The first four volumes in this series are a compilation of critically selected constants and associated thermodynamic parameters for metal complexes of

G. G. Leppard (Ed.), *Trace Element Speciation in Surface Waters and its Ecological Implications* (Vol. 6, NATO Conference Series 1 Ecology). Plenum Press, New York, 1983 (ISBN 0-306-41269-1). 320 pp. Price \$45.00.

This volume in the NATO Conference Series on Ecology takes its title from a NATO Advanced Research Workshop held in Nervi (Genoa), Italy, in November, 1981 and is a compendium of papers presented at the meeting. Its publication comes at a time of increasing interest in the relative toxicity of various physicochemical forms of elements such as mercury, cadmium, lead and arsenic, which has in turn stimulated interest in the development of species-selective analytical techniques.

There are 17 papers in total; one is a summary of the discussions that took place at the meeting, 5 are concerned with analytical approaches to the problem of trace element speciation, 6 deal with the impact of trace element species on aquatic life and 5 discuss new perspectives and future actions in the area. The contents therefore reflect the interdisciplinary nature of the meeting and contain useful background information for the analytical chemist on biological aspects of speciation and on the complex chemical equilibria in surface waters. Of the papers discussing analytical approaches to speciation studies, the current scene is well reviewed by Batley and the various approaches are then discussed in more detail. The use of hybrid chromatography/spectrometry techniques for the study of metal/organic compounds is particularly well presented by Chan and Wong.

This volume is a useful reference for those working in environmental toxicology and marine biology but material of direct interest to analytical chemists constitutes only a small percentage of the text. However, in view of the limited number of publications dealing with analytical aspects of speciation, it is a welcome contribution to the literature.

P. J. Worsfold

A. Maehly and L. Strömberg, *Chemical Criminalistics*. Springer-Verlag, Berlin, 1981 (ISBN 3-540-10723-1). 322 pp. Price DM 162,00.

Modern forensic science relies heavily on analytical science, a feature that is strongly underlined by the present text. The main part of the book claims to present state-of-the-art accounts of a variety of topics, such as drugs, explosives, polymers, fibres, paints and documents. Each section has a similar format, with introductory remarks on the relevance and basic properties of the materials considered, discussions of the more important analytical techniques used in the area, a wide range of well-illustrated examples, and a good collection of references. In addition, there are small chapters on reference collections, "the forensic expert", sources of scientific information and the organization of a forensic laboratory. Overall, the book demonstrates the

amazing power of detection of forensic science, and the extent to which it has made use of most current analytical techniques. It will provide interesting reading, not only to forensic scientists, but to all those who are interested in the applications of analytical science.

A. Townshend

AUTHOR INDEX

- Akagi, T.
—, Fuwa, K. and Haraguchi, H.
Simultaneous multi-element determination of trace metals in sea water by inductively-coupled plasma atomic emission spectrometry after coprecipitation with gallium 139
- Alegret, S.
—, Blanco, M. and Paulís, J. M.
A fast photometric titration for the standardization of dithizone solutions 285
- Alexander, P. W.
—, Haddad, P. R. and Trojanowicz, M.
Response characteristics of a potentiometric detector with a copper metal electrode for flow-injection and chromatographic determinations of metal ions 183
- Ayers, G. P., see Gillett, R. W. 273
- Bartels, J. H. M.
—, Janse, T. A. H. M. and Pijpers, F. W.
Classification of the quality of surface waters by means of pattern recognition 35
- Bartels, J. H. M.
—, Janse, T. A. H. M., Pijpers, F. W. and Thijssen, P. C.
Improvement of the representation of water quality by application of information theory 47
- Blanco, M., see Alegret, S. 285
- Boodhoo, R. B., see Persaud, G. 247
- Bozic, J., see Smith, F. 243
- Brodnjak-Vončina, D. see Dobčnik, D. 209
- Budgell, B. R., see Persaud, G. 247
- Burke, M. F., see Frazer, S. 15
- Burns, D. T.
— and Kheawpintong, S.
Spectrophotometric determination of chromium(VI) by extraction with the 1-naphthylmethyltriphenylphosphonium cation 253
- Cardwell, T. J.
—, Cattrall, R. W., Iles, P. J. and Hamilton, I. C.
Photo-cured polymers in ion-selective electrode membranes. Part 2. A calcium electrode for flow injection analysis 239
- Cattrall, R. W., see Chek, W. L. 235
- Cattrall, R. W., see Cardwell, T. J. 239
- Chek, W. L.
—, Cattrall, R. W. and Hamilton, I. C.
An automated system for the determination of fluoride 235
- Chen, J.-W.
— and Georges, J.
Liquid-junction potential effects in measurements of sodium ion activity in unbuffered aqueous solutions 231
- Childers, A. G., see Freeman, J. E. 121
- Chipperfield, J. R.
—, Gregory, J. R. and Webster, D. E.
A computer-controlled laboratory fractional distillation column 203
- Collier, W. G., see Curran, D. J. 259
- Cousins, B., see Smith, F. 243
- Curran, D. J.
— and Collier, W. G.
Determination of phenyl isocyanate in a flow-injection system with infrared spectrometric detection 259
- Dalene, M., see Stenström, S. 279
- Dickinson, R. G., see Hooper, W. D. 267
- Dobčnik, D.
— and Brodnjak-Vončina, D.
Hydrolytic potentiometric titration of sulphate with application in the analysis of waters 209
- Eadie, M. J., see Hooper, W. D. 267
- Flora, W., see Smith, F. 243
- Frazer, S.
— and Burke, M. F.
Extraction of nonstationarity information from correlation noise 15
- Freeman, J. E.
—, Childers, A. G., Steele, A. W. and Hieftje, G. M.
A fiber-optic absorption cell for remote determination of copper in industrial electroplating baths 121

- Fujihira, Y., see Nagashima, K. 213
 Fuwa, K., see Akagi, T. 139
- Garcia-Anton, J., see Guiñón, J. L. 225
 Georges, J., see Chen, J.-W. 231
 Gillett, R. W.
 — and Ayers, G. P.
 The determination of acetic, formic and propanoic acids in rain water by reverse-phase high-performance liquid chromatography 273
- Gregory, J. R., see Chipperfield, J. R. 203
 Guiñón, J. L.
 — and Garcia-Anton, J.
 Determination of tin and lead by differential pulse polarography with addition of Hyamine-2389 225
- Haddad, P. R., see Alexander, P. W. 183
 Hamilton, I. C., see Chek, W. L. 235
 Hamilton, I.C., see Cardwell, T. J. 239
 Haraguchi, H., see Akagi, T. 139
 Hieftje, G. M., see Freeman, J. E. 121
 Honda, K.
 —, Miyaguchi, K. and Imai, K.
 Evaluation of aryl oxalates for chemiluminescence detection in high-performance liquid chromatography 103
- Honda, K.
 —, Miyaguchi, K. and Imai, K.
 Evaluation of fluorescent compounds for peroxyoxalate chemiluminescence detection 111
- Hooper, W. D.
 —, Roome, J. A., King, A. R., Smith, M. T., Eadie, M. J. and Dickinson, R. G.
 Simple and reliable determination of bromazepam in human plasma by high-performance liquid chromatography 267
- Huber, J. F. K.
 —, Welte, S. and Reich, G.
 Prediction of partition coefficients in ternary liquid-liquid systems as a function of the phase system composition by factor analysis for chromatography 1
- Iles, P. J., see Cardwell, T.J. 239
 Imai, K., see Honda, K. 103, 111
- Janse, T. A. H. M., see Bartels, J. H. M. 35, 47
 Janssen, N. J. M. L., see Thijssen, P. C. 57
- Kalcher, K.
 Voltammetric determination of trace amounts of gold with a chemically modified carbon paste electrode 175
- Kalous, J., see Vytfas, K. 219
 Kateman, G., see Thijssen, P. C. 57
 Kheawpintong, S., see Burns, D. T. 253
 King, A. R., see Hooper, W. D. 267
 Kościelniak, P.
 — and Parczewski, A.
 Efficient application of non-linear transformation of factors in empirical modelling based on experimental designs 197
- Kvalheim, O. M.
 Scaling of analytical data 171
- Lee, M.
 —, Nohta, H., Ohkura, Y. and Yoo, B.
 Assay for aromatic L-amino acid decarboxylase based on fluorescence derivatization with 1,2-diphenylethylenediamine 93
- Linares, P.
 —, Luque de Castro, M. D. and Valcarcel, M.
 Spectrofluorimetric determination of silicon by flow injection analysis 263
 Luque de Castro, M. D., see Linares, P. 263
- MacDonald, R. W.
 — and O'Brien, M. C.
 Extending the use of certified reference sediments for assessment of accuracy in determinations of trace metals 81
- Miyaguchi, K., see Honda, K. 103, 111
 Mizutani, F.
 —, Yamanaka, T., Tanabe, Y. and Tsuda, K.
 An enzyme electrode for L-lactate with a chemically-amplified response 153
- Nagashima, K.
 —, Fujihira, Y. and Suzuki, S.
 Continuous determination of hydrogen fluoride in air with the fluoride-selective electrode 213
- Nohta, H., see Lee, M. 93
 Novič, M.
 — and Zupan, J.
 Hierarchical clustering of carbon-13 nuclear magnetic resonance spectra 23
- O'Brien, M. C., see MacDonald, R. W. 81
 Ohkura, Y., see Lee, M. 93
 Olofsson, B. R.
 Determination of elemental sulfur in jet fuel by differential pulse polarography 167

- Parczewski, A., see Kościelniak, P. 197
- Paulfs, J. M., see Alegret, S. 285
- Persaud, G.
- , Boodhoo, R. B., Budgell, B. R. and Stiles, D. A.
The determination of organochlorine pesticides and polychlorinated biphenyls by combustion tube decomposition and molecular emission cavity analysis 247
- Pijpers, F. W., see Bartels, J. H. M. 35, 47
- Reich, G., see Huber, J. F. K. 1
- Roome, J. A., see Hooper, W. D. 267
- Sedykh, E. M., see Volynsky, A. B. 129
- Skarping, G., see Stenström, S. 279
- Smit, H. C., see Thijssen, P. C. 57
- Smith, F.
- , Cousins, B., Bozic, J. and Flora, W.
The acid dissolution of sulfide mineral samples under pressure in a microwave oven 243
- Smith, M. T., see Hooper, W. D. 267
- Spivakov, B. Ya., see Volynsky, A. B. 129
- Steele, A. W., see Freeman, J. E. 121
- Stenström, S.
- , Dalene, M. and Skarping, G.
The solubility of tri-n-octylamine in water and phosphoric acid solutions 279
- Stiles, D. A., see Persaud, G. 247
- Suzuki, S., see Nagashima, K. 213
- Symerský, J., see Vytřas, K. 219
- Tanabe, Y., see Mizutani, F. 153
- Thijssen, P. C., see Bartels, J. H. M. 47
- Thijssen, P. C.
- , Janssen, N. J. M. L., Kateman, G. and Smit, H. C.
Kalman filter applied to setpoint control in continuous titrations 57
- Trojanowicz, M., see Alexander, P. W. 183
- Tsuda, K., see Mizutani, F. 153
- Valcarcel, M., see Linares, P. 263
- Volynsky, A. B.
- , Sedykh, E. M., Spivakov, B. Ya. and Zolotov, Yu. A.
Minimizing the effect of organic matrices in the analysis of tin-containing extracts by electrothermal atomic absorption spectrometry. Determination of tin in rocks 129
- Vytřas, K.
- , Kalous, J. and Symerský, J.
Determination of some ampholytic and cationic surfactants by potentiometric titrations based on ion-pair formation 219
- Webster, D. E., see Chipperfield, J. R. 203
- Welte, S., see Huber, J. F. K. 1
- Yamanaka, T., see Mizutani, F. 153
- Yoo, B., see Lee, M. 93
- Zolotov, Yu. A., see Volynsky, A. B. 129
- Zupan, J., see Novič, M. 23

(continued from outside back cover)

A computer-controlled laboratory fractional distillation column J. R. Chipperfield, J. R. Gregory and D. E. Webster (Hull, Gt. Britain)	203
Hydrolytic potentiometric titration of sulphate with application in the analysis of waters D. Dobčnik and D. Brodnjak-Vončina (Maribor, Yugoslavia)	209
Continuous determination of hydrogen fluoride in air with the fluoride-selective electrode K. Nagashima, Y. Fujihara and S. Suzuki (Tokyo, Japan)	213
Determination of some ampholytic and cationic surfactants by potentiometric titrations based on ion-pair formation K. Vytřas, J. Kalous and J. Symerský (Pardubice, Czechoslovakia)	219
Determination of tin and lead by differential pulse polarography with addition of Hyamine-2389 J. L. Guiñón and J. García-Antón (Valencia, Spain)	225
Liquid-junction potential effects in measurements of sodium ion activity in unbuffered aqueous solutions J.-W. Chen and J. Georges (Villeurbanne, France)	231
An automated system for the determination of fluoride W. L. Chek, R. W. Cattrall and I. C. Hamilton (Melbourne, Vic., Australia)	235
Photo-cured polymers in ion-selective electrode membranes. Part 2. A calcium electrode for flow injection analysis T. J. Cardwell, R. W. Cattrall, P. J. Iles and I. C. Hamilton (Melbourne, Vic., Australia)	239
The acid dissolution of sulfide mineral samples under pressure in a microwave oven F. Smith, B. Cousins (Sudbury, Ont., Canada), J. Bozic and W. Flora (Copper Cliff, Ont., Canada)	243
The determination of organochlorine pesticides and polychlorinated biphenyls by combustion tube decomposition and molecular emission cavity analysis G. Persaud, R. B. Boodhoo, B. R. Budgell and D. A. Stiles (Wolfville, Nova Scotia, Canada)	247
Spectrophotometric determination of chromium(VI) by extraction with the 1-naphthylmethyltriphenylphosphonium cation D. T. Burns and S. Kheawpintong (Belfast, Northern Ireland)	253
Determination of phenyl isocyanate in a flow-injection system with infrared spectrometric detection D. J. Curran and W. G. Collier (Amherst, MA, U.S.A.)	259
Spectrofluorimetric determination of silicon by flow injection analysis P. Linares, M. D. Luque de Castro and M. Valcarcel (Córdoba, Spain)	263
Simple and reliable determination of bromazepam in human plasma by high-performance liquid chromatography W. D. Hooper, J. A. Roome, A. R. King, M. T. Smith, M. J. Eadie and R. G. Dickinson (Herston, Qld., Australia)	267
The determination of acetic, formic and propanoic acids in rain water by reverse-phase high-performance liquid chromatography R. W. Gillett and G. P. Ayers (Mordialloc, Vic., Australia)	273
The solubility of tri-n-octylamine in water and phosphoric acid solutions S. Sternström, M. Dalene and G. Skarping (Lund, Sweden)	279
A fast photometric titration for the standardization of dithizone solutions S. Alegret, M. Blanco and J. M. Paulís (Barcelona, Spain)	285
Book Reviews	291
Author Index	307

CONTENTS

(Abstracted, Indexed in: *Anal. Abstr.*; *Biol. Abstr.*; *Chem. Abstr.*; *Curr. Contents Phys. Chem. Earth. Sci., Life Sci.*; *Index Med.*; *Mass Spectrom. Bull.*; *Sci. Citation Index*; *Excerpta Med.*)

Computer Methods and Applications

- Prediction of partition coefficients in ternary liquid-liquid systems as a function of the phase system composition by factor analysis for chromatography
J. F. K. Huber, S. Welte and G. Reich (Vienna, Austria)
- Extraction of nonstationarity information from correlation noise
S. Frazer and M. F. Burke (Tucson, AZ, U.S.A.)
- Hierarchical clustering of carbon-13 nuclear magnetic resonance spectra
M. Novič and J. Zupan (Ljubljana, Yugoslavia)
- Classification of the quality of surface waters by means of pattern recognition
J. H. M. Bartels, T. A. H. M. Janse and F. W. Pijpers (Nijmegen, The Netherlands)
- Improvement of the representation of water quality by application of information theory
J. H. M. Bartels, T. A. H. M. Janse, F. W. Pijpers and P. C. Thijssen (Nijmegen, The Netherlands)
- Kalman filter applied to setpoint control in continuous titrations
P. C. Thijssen, N. J. M. L. Janssen, G. Kateman (Nijmegen, The Netherlands) and H. C. Smit (Amsterdam, The Netherlands)
- Scaling of analytical data
O. M. Kvalheim (Bergen, Norway)

General Analytical Chemistry

- Extending the use of certified reference sediments for assessment of accuracy in determinations of trace metals
R. W. MacDonald and M. C. O'Brien (Sidney, B.C., Canada)

Spectrometric Methods

- Assay for aromatic L-amino acid decarboxylase based on fluorescence derivatization with 1,2-diphenylethylenediamine
M. Lee, H. Nohta, Y. Ohkura (Fukuoka, Japan) and B. Yoo (Chungnam, Korea)
- Evaluation of aryl oxalates for chemiluminescence detection in high-performance liquid chromatography
K. Honda, K. Miyaguchi and K. Imai (Tokyo, Japan)
- Evaluation of fluorescent compounds for peroxyoxalate chemiluminescence detection
K. Honda, K. Miyaguchi and K. Imai (Tokyo, Japan)
- A fiber-optic absorption cell for remote determination of copper in industrial electroplating baths
J. E. Freeman, A. G. Childers, A. W. Steele and G. M. Hieftje (Bloomington, IN, U.S.A.)
- Minimizing the effect of organic matrices in the analysis of tin-containing extracts by electrothermal atomic absorption spectrometry. Determination of tin in rocks
A. B. Volynsky, E. M. Sedykh, B. Ya. Spivakov and Yu. A. Zolotov (Moscow, U.S.S.R.)
- Simultaneous multi-element determination of trace metals in sea water by inductively-coupled plasma atomic emission spectrometry after coprecipitation with gallium
T. Akagi, K. Fuwa and H. Haraguchi (Tokyo, Japan)

Electrometric Methods

- An enzyme electrode for L-lactate with a chemically-amplified response
F. Mizutani, T. Yamanaka, Y. Tanabe and K. Tsuda (Ibaraki, Japan)
- Determination of elemental sulfur in jet fuel by differential pulse polarography
B. R. Olofsson (Umeå, Sweden)
- Volatammetric determination of trace amounts of gold with a chemically modified carbon paste electrode
K. Kalcher (Graz, Austria)
- Response characteristics of a potentiometric detector with a copper metal electrode for flow-injection and chromatographic determinations of metal ions
P. W. Alexander, P. R. Haddad (Kensington, N.S.W., Australia) and M. Trojanowicz (Warsaw, Poland)

Short Communications

- Efficient application of non-linear transformation of factors in empirical modelling based on experimental designs
P. Kościelniak and A. Parczewski (Kraków, Poland)